UNIVERSITY OF SOUTHAMPTON

DISPENSER PRINTED ACTIVELY ACTUATED COLOUR-CHANGING SMART FABRICS

by Zeeshan Ahmed

A thesis submitted in partial fulfilment for the degree of Doctor of Philosophy

in the

Faculty of Physical Sciences and Engineering

Department of Electronics and Computer Science

University of Southampton

26th October 2017

This page is intentionally left blank

ABSTRACT

The thesis reports the development of all-printed actively actuated colour-changing fabrics for creative and smart fabric applications. The colour changing fabrics consist of thermochromic materials and track heaters dispenser printed on fabrics. Thermochromic materials change colour in response to a change in temperature and the heaters actuate the colour change function by controlling the temperature of the fabric.

Dispenser printing is a direct-write process where a material is additively deposited on digitally defined locations of the substrate. It is a novel process for printing active and functional materials on fabrics. State of the art thermochromic fabrics use heaters based on conductive yarns, printed circuit boards (PCBs), Peltier semiconductors, conductive coatings and commercial heating foils. These heater technologies have one or more of the four major limitations: inflexibility, limited design freedom, poor integration with fabrics and unreliability. The novel all-dispenser printed approach overcomes the limitations of existing methods by offering flexibility, complete design freedom, good integration with fabrics and reliability.

The thermochromic devices are fabricated on 65/35 blend polyester cotton which has a porous and high variation surface. The surface variation of the fabric is numerically characterised and its adverse effect on the electrical properties of printed conductors is experimentally demonstrated. Printing an interface layer on the fabric surface is used as a method of reducing the fabric surface variation. The four evaluated interface inks DuPont 5018, Electra EFV4/4965, Fabinks-IF-UV-1004 and FB-20 reduced the fabric surface variation by more than 95%. This improved the performance of the printed heaters and electrical interconnections on fabrics.

This thesis also presents design, modelling, fabrication and characterisation of track heaters. Track heaters are modelled in COMSOL Multiphysics software as a tool to determine the output of a heater design. It is used to derive design rules for printing track heaters. It is demonstrated that dispenser printed track heaters offer complete control of the shape and size of their heat profile. In addition to silver and carbon conductive inks, four custom conductive inks were formulated for printing heaters. The conductive inks achieved a broad range of printed resistivity from 2.43×10^{-7} Ω.m to 1.11×10^{-03} Ω.m. This allows the resistance of an application specific heater design to be varied to suit the requirements of an application.

Thermochromic ink development, formulation and characterisation using commercially available materials is discussed. A UV curable thermochromic ink which changed from an opaque black state to a colourless state was achieved. It produced black colour concentration of 90-100 % before colour change and a peak transmittance value of 34% after colour change. It was demonstrated that the optimum ink formulation can be altered to produce a range of colour changing effects such as multiple colour changes which increases the options for thermochromic fabric applications. Fabrication and characterisation of dispenser printed thermochromic devices is also detailed in this thesis.

Four demonstrator applications of the thermochromic devices on polyester cotton 65/35 fabric were achieved: a shutter display, a 7-segment display, a matrix display and a proximity controlled interactive thermochromic device. These demonstrators illustrated the freedom of design and versatility offered by the dispenser printed approach. These dispenser printed thermochromic devices can be used in creative applications to produce dynamic art, in smart fabric systems as actuators to communicate data and as non-emissive displays.

This page is intentionally left blank

DECLARATION OF AUTHORSHIP

I, Zeeshan Ahmed declare that this thesis and the work presented in it are my own and has been generated by me as the result of my own original research.

I confirm that:

1. This work was done wholly or mainly while in candidature for a research degree at University of Southampton;

2. Where any part of this thesis has previously been submitted for a degree or any other qualification at this University or any other institution, this has been clearly stated;

3. Where I have consulted the published work of others, this is always clearly attributed;

4. Where I have quoted from the work of others, the source is always given. With the exception of such quotations, this thesis is entirely my own work;

5. I have acknowledged all main sources of help;

6. Where the thesis is based on work done by myself jointly with others, I have made clear exactly what was done by others and what I have contributed myself;

7. Either none of this work has been published before submission, or parts of this work have been published as:

    - Z. Ahmed, R. Torah and J. Tudor (2015, April). Optimisation of a novel direct-write dispenser printer technique for improving printed smart fabric device performance. In *Design, Test, Integration and Packaging of MEMS/MOEMS (DTIP), 2015 Symposium on* (pp. 1-5). IEEE.
    - Z. Ahmed, Y. Wei, R. Torah, and J. Tudor (2016). Actively actuated all dispenser printed thermochromic smart fabric device. *Electronics Letters*, *52*(19), 1601-1603.
    - Z. Ahmed, R. Torah, K. Yang, S. Beeby, and J. Tudor (2016). Investigation and improvement of the dispenser printing of electrical interconnections for smart fabric applications. *Smart Materials and Structures*, *25*(10), 105021.
    - Y. Wei, Z. Ahmed, R. Torah, and J. Tudor (2016) Dispenser printed actively controlled thermochromic colour changing device on fabric for smart fabric applications At *CIMTEC 2016: 5th International Conference Smart and Multifunctional materials Structures and Systems 2016, Italy. 05 - 09 Jun 2016.*

ACKNOWLEDGEMENTS

I would like to express my deep gratitude to my supervisors Dr John Tudor and Dr Russel Torah for their patient guidance, support and encouragement. Over the course of my research they have helped me grow and have greatly contributed to my development as a researcher. Their comments and critiques have been invaluable for this research.

I would like to thank Dr Abiodun Komolafe and Dr Yang Wei for their assistance and support during my PhD. I appreciate all the present and past members of the smart fabric group and bay 5, Ahmed, Monika, Nhan, Olivia, Yi, Zihao and Nur for making my PhD experience enjoyable.

I would like to thank my parents for their constant support, endless love and encouragement. They have always provided me with inspiration, emotional and moral support without which I would not be able to pursue this PhD degree. I really appreciate all the effort and sacrifices they have made for me from the bottom of my heart. I am grateful to my grandparents, my brothers and my family in London for supporting me throughout the period of my PhD and providing the essential distractions.

Last but not the least, I would like to thank my wife for her patience and understanding. Aatirah has been a constant source of support and encouragement during the last four years. I appreciate all her efforts in helping me pursue this PhD degree. This thesis is dedicated to my parents and my beloved wife.

TABLE OF CONTENTS

LIST OF FIGURES

LIST OF TABLES

GLOSSARY OF TERMS

Activation temperature:

Temperature at which a leuco dye thermochromic pigment, ink or print starts to change colour.

Active actuation:

Raising the temperature of a thermochromic ink, print, fabric or device using a heater to bring about a colour change.

Actuation response time:

The time it takes for a thermochromic fabric, print or device to achieve complete colour change.

Average surface displacement:

The mean difference in the vertical displacement of a surface from the first point of measurement.

Bitmap mode:

A printing mode of the dispenser printer used in this research which allows printing of patterns.

Colour strength:

The concentration of a colour which achieves a particular shade of that colour.

Continuous mode:

A printing mode of the dispenser printer used in this research which prints an ink in the form of filaments.

Creative applications:

Applications of thermochromic fabrics developed to communicate artistic expressions or to achieve specific aesthetic effects.

Dispenser printing:

A direct-write process which additively deposits a material on digitally defined locations of a substrate.

Droplet mode:

A printing mode of the dispenser printer used in this research which prints an ink in the form of droplets.

Interface:

A dielectric ink layer printed on a fabric to reduce its surface variation.

Leuco dyes:

A type of thermochromic material which changes from one colour to another in response to a temperature change.

Liquid crystals:

A type of thermochromic material which produces multiple colour changes in response to temperature changes.

Nozzle height:

The gap between a printing nozzle and the substrate.

Operating temperatures of a thermochromic ink:

A set of temperatures of a leuco dye thermochromic ink at which it starts to produce colour change, completes colour change, start to revert back to its original colour and completely regains its original colour.

Peak to peak surface displacement:

The difference in vertical displacement between the lowest and the highest points of a surface.

Polyester cotton fabric:

Klopman International woven polyester cotton 65/35 blend.

Print pass:

A single deposition of the ink in a designated print area using a specific set of print settings.

Re-colouration:

A thermochromic pigment, print, fabric or device returning to its initial state.

Refresh time:

Time it takes a thermochromic fabric, print or device to return to its initial state.

Resistance distribution:

The electrical resistance experienced in various parts of a printed conductive layer.

Selective heating:

Heating specific parts of a conductive track arrangement.

Sensory indicator applications:

Applications of thermochromic fabrics which use the colour change function as an output for sensors.

Sequential actuation:

Colour change in parts of a thermochromic print or device in a specific order.

Shutter display:

A device which is able to exhibit two distinct states; a default and an actuated state.

Smart fabrics:

Fabrics that can sense and respond to various stimuli, and have communicative, interactive and computing capabilities.

Surface topography:

The physical features of a surface.

Temperature distribution:

The temperatures experienced by various parts of a body.

Thermochromic materials:

Materials that produce colour change in response to a change in temperature.

Track lines:

Consecutive printed conductors in a meander pattern.

This page is intentionally left blank

This page is intentionally left blank

CHAPTER 1 INTRODUCTION

1.1 Research background

Fabrics find applications in many distinct areas of everyday life which include clothing, furnishings, architecture and art. A fabric is any cloth knitted or woven from fibres. Advances in the fields of materials, electronics and fabrics has generated enormous interest in the area of smart fabrics. The concept of smart fabrics is based on fabrics that can sense and respond to various stimuli [1]. It extends to integration of added functionality in fabrics such as communicative, interactive and computing capabilities [2]. Smart fabrics have a wide range of applications such as healthcare, sports and wellness, safety and security, automotive and transport, geo-textiles, architecture, energy, telecommunication, home and interior fabrics, defence and fashion [3]. The following presents some examples of smart fabrics and their applications.

The ProeTEX project [4], focused on protective smart fabrics, produced garments containing sensors which monitor the physiological parameters of wearer and the environment. The ProeTEX suit is specifically designed for health monitoring of emergency operators working in harsh environments such as firefighters. The Life shirt system [5], a healthcare smart fabric garment, continuously collects information on cardiopulmonary parameters and posture data of the wearer using embedded sensors; Optional peripheral devices can be connected to measure additional physiological parameters such as blood pressure, EEG, temperature and blood oxygen saturation. The Klight dress [6] is an example of smart fabrics in fashion industry; incorporating LEDs and electronics to produce various lighting effects in response to wearer's motion adding interactive capability and aesthetic value to the dress. An example of smart fabrics in home and interior is the intelligent carpet [7] which can detect presence, location and displacement of people on the carpet using embedded pressure sensors. It can display the location and displacement of a person by activating embedded luminescent fibres. Textile switches in car seats, sensors in the safety belts and heating in car seats are all smart fabric devices currently employed in the automotive industry [3]. Smart fabrics are increasingly finding more applications as research and development continue to improve underlying technologies.

Smart fabrics can be realised by combining smart materials with fabrics. The smart material group focused on in this research are chromic materials. Chromic materials exhibit a colour change in response to a range of stimuli such as changes of temperature, pressure and mechanical force [8]. Research and development of chromic materials has highlighted their commercial potential and broadened their applications. Some common applications of these materials include spectacle lenses that darken in sunlight, smart windows, temperature indicators and e-ink displays. Temperature and UV light sensitive chromic materials have a broad commercial adoption which can be attributed to the maturity of the two technologies. The group of chromic materials used in this research are temperature sensitive chromic materials.

Thermochromic materials change colour in response to a change in temperature [8]. Thermochromism was first investigated in 1871 by Edwin James Houston [9]. Further research and development since then has led to discovery of more thermochromic materials [10] which enabled commercial utilisation. One of the first commercial applications of these materials was the mood ring in the 1970s; since then they have found a number of applications ranging from thermal mapping to displays. The first commercial application combining thermochromic and fabric materials emerged in the 1990s in the form of Hypercolor™ T-shirts, which would change colour in response to body heat. These materials have not had a considerable commercial impact in the textile industry although they have widespread interest in the creative industries.

Colour is one of the most important features of a fabric; being able to actively actuate the colour change property adds value and dynamic feature to fabrics. Colour change can be considered as an actuator and can be used to incorporate communicative and interactive capabilities in fabrics. Its non-emissive and unobtrusive attributes have made the technology particularly attractive for smart fabric research as it can be employed in multiple smart fabric application areas.

Recent research on thermochromic materials for fabric applications has had a two-fold primary focus. Firstly, design of heating mechanisms for active actuation of the colour change function which include use of the printed circuit boards (PCBs) and Peltier semiconductors [11,12]. Secondly, exploitation of colour change as an output in conjunction with various inputs which include electrical signals and touch to embed added-value functionality such as display capabilities [12] in fabrics.

Printing is commonly used in the textile industry for applying colours to fabrics. It can be used to apply thermochromic materials on fabrics to create smart fabrics. This research introduces dispenser printing as a versatile method of combining smart and functional materials with fabrics to create actively actuated colour-changing smart fabrics. Dispenser printing, a direct-write technology is process in which a material is directly deposited on digitally defined areas of a substrate.

1.2 Research aims

The primary aim of this research is to develop printed colour changing smart fabrics using direct-write dispenser printing technology as the sole fabrication process. Within the main theme, this research aims to achieve the following.

- **Fabrication and characterisation of dispenser printed thermochromic devices on fabrics:** This should provide fabrication details and understanding of the thermochromic device parameters.
- **Demonstrator applications of dispenser printed thermochromic devices on fabrics:** This should provide fabrication details and demonstrate the versatility of the dispenser printing and the thermochromic technology for fabric applications.
- **Optimisation of commercially available thermochromic materials to formulate dispenser printable inks:** This should provide an insight into the performance of the materials and various colour changing options.
- **Development of dispenser printed heaters on fabrics:** This should provide technical details and relevant materials to achieve control over the parameters and the output of a heater.

Achieving the aims of the research should reduce the technical barriers to the use of thermochromic technology in fabric applications by reducing the fabrication to a single print process. It should provide comprehensive technical knowledge of the development of dispenser printed thermochromic devices on fabrics to allow the technology to be used in smart fabric applications.

1.3 Statement of novelty

The core novelties of this research are the all-printed fabrication of actively actuated thermochromic devices and the investigation of dispenser printing as the method of developing these devices on fabrics. Although dispenser printing is not a novel process, dispenser printing on fabrics in general and dispenser printing of thermochromic materials and heaters in particular are novel. The following presents the novelties originated from this research.

- The first all dispenser printed actively actuated thermochromic devices are achieved on fabric and Kapton. In order to fabricate the thermochromic devices the first dispenser printed track heaters are also achieved on fabric and Kapton. The all printed structure of the thermochromic devices and the direct-write fabrication method improve the previously reported

thermochromic fabrics by offering a combination of flexibility, design freedom, reliability and good heater integration with the fabrics. The fabrication, characterisation and development details of the thermochromic fabrics offer a comprehensive insight into their functions and potential applications. Dispenser printed colour changing 7-segment display, matrix display, shutter display and an interactive thermochromic fabric are achieved for the first time on fabric. These devices demonstrate the versatility and design freedom offered by the novel all dispenser printed approach of fabricating the actively actuated thermochromic fabrics.

- The effect of varying track heater fabrication parameters on its output is demonstrated using COMSOL model simulations. This provides an understanding of the influence of each fabrication parameter on the temperature output and cost of fabrication of a track heater. The evaluation of track heater fabrication parameters has not been reported previously. This knowledge allows a heater designer to make informed choices for fabricating application specific printed track heaters.

- The effect of surface variation of a substrate on the geometrical uniformity of printed conductors is experimentally demonstrated for the first time. A thermal imaging method is introduced to assess the resistance distribution of a printed conductive layer. Dispenser printing a dielectric ink on the fabric surface is presented as a novel method of overcoming the surface variation. Four dielectric inks are investigated and optimised for reducing the surface variation of a fabric. The optimisation details and the evaluation of the inks have guiding significance for printing conductive tracks on fabrics which are essential for incorporating electronic functions in a fabric.

1.4 Publications arising from this work

- Z. Ahmed, R. Torah and J. Tudor (2015, April). Optimisation of a novel direct-write dispenser printer technique for improving printed smart fabric device performance. In *Design, Test, Integration and Packaging of MEMS/MOEMS (DTIP), 2015 Symposium on* (pp. 1-5). IEEE.
- Z. Ahmed, Y. Wei, R. Torah, and J. Tudor (2016). Actively actuated all dispenser printed thermochromic smart fabric device. *Electronics Letters*, *52*(19), 1601-1603.
- Z. Ahmed, R. Torah, K. Yang, S. Beeby, and J. Tudor (2016). Investigation and improvement of the dispenser printing of electrical interconnections for smart fabric applications. *Smart Materials and Structures*, *25*(10), 105021.
- Y. Wei, Z. Ahmed, R. Torah, and J. Tudor (2016) Dispenser printed actively controlled thermochromic colour changing device on fabric for smart fabric applications At *CIMTEC 2016: 5th International Conference Smart and Multifunctional materials Structures and Systems 2016, Italy*. *05 - 09 Jun 2016.*

1.5 Thesis structure

Chapter 2 contains a literature review which discusses thermochromism in terms of materials, their working principles and applications. It also presents the existing applications of actively actuated thermochromic fabrics. Finally, it describes and discusses the state of the art actuation technologies for fabrication of actively actuated thermochromic fabrics.

Chapter 3 describes dispenser printing technology, its background and details the dispenser printing setup used in this research. It presents a comparison of dispenser printing with screen and inkjet printing technologies. It characterises the fabric surface variation and experimentally demonstrates the adverse effects of high surface variation on the printed conductors. It investigates four dispenser

printable interface inks as a method of overcoming the surface variation and highlights the improvements in printed conductors.

Chapter 4 presents the development of dispenser printed heaters. It presents a COMSOL model of track heaters used for simulating heater designs. It also presents fabrication and characterisation of dispenser printed heaters. It details the formulation of custom conductive inks suitable for dispenser printing of heaters. Finally, it demonstrates methods of achieving selective heating in a track heater design.

Chapter 5 presents development of dispenser printable thermochromic inks using commercially available materials. It details fabrication and characterisation of dispenser printed actively actuated thermochromic fabrics. It discusses the thermochromic ink formulations required to achieve various colour changing effects such as multiple colour changes and demonstrates these effects in printed devices. Finally, it presents demonstrator applications of thermochromic devices which include a shutter display, a 7-segment display, a matrix display and an interactive colour changing smart fabric.

Chapter 6 summaries the research work done in this study and presents suggestions for future work.

CHAPTER 2 LITERATURE REVIEW: ACTIVELY ACTUATED THERMOCHROMIC FABRICS

2.1 Introduction

This chapter covers the literature review on actively actuated thermochromic fabrics. Active actuation of a thermochromic fabric refers to heating the thermochromic fabric to bring about a colour change. This chapter discusses the state of the art actuation technologies used for active actuation of thermochromic fabrics. It describes the applications of the actively actuated thermochromic fabrics. It presents the background of thermochromic technology in terms of the thermochromic materials, their working principles and applications.

2.2 Thermochromism

2.2.1 Introduction to chromic phenomena

Chromic phenomena refers to a change in colour of a material produced by an external stimulus. Different chromic materials change colour in response to various physical and chemical stimuli. These colour changing effects have been named after the colour changing stimulus; Photochromism refers to colour change stimulated by light, electrochromism is colour change in response to electric current, piezochromism is colour change caused by pressure and thermochromism is colour change caused by the temperature change [8]. This research work will concentrate on thermochromism because it is the most mature chromic technology in terms of existing applications and it is commercially available in suitable physical forms (powders and slurries) to be used in printable paste formulation.

2.2.2 Types of thermochromic materials

Thermochromic behaviour is exhibited by individual materials and in some cases a group of materials; henceforth referred to as thermochromic systems. Colour change associated with these systems can be reversible or irreversible depending on the type and constituents of the system. These systems can be divided into organic and inorganic categories. Temperature can be regarded as directly responsible for colour change by altering the physical properties of the colour causing material, or indirectly causing colour change by altering the chemical environment of the colour causing material. The change in chemical environment of the colour causing material brings about a change in its physical structure.

Inorganic and organometallic thermochromic materials have not been widely investigated for use in fabric applications because a majority of these materials produce irreversible colour changes and they offer limited temperature and colour options [13]; therefore Inorganic and organometallic compounds are not discussed any further in this study. In comparison organic thermochromic materials offer reversible colour changes, broader range of colours and transition temperatures which makes them more suitable for fabric applications.

Leuco dyes and liquid crystal thermochromic materials are the most suitable organic thermochromic materials for printing applications on fabric. They are the only thermochromic materials commercially available, in printing compatible forms of pigments and slurries. They are also available as ready to use printable inks. They offer a variety of colour and temperature options which allow a wide range of choice for the relevant applications. Therefore, only leuco dyes and liquid crystals are further discussed in this thesis.

2.2.3 Leuco dye thermochromic system

2.2.3.1 Leuco dye composition

A leuco dye system uses temperature change as an indirect stimulus. It can be formulated to change colour reversibly or irreversibly. Typically they change from a coloured state to a colourless/translucent state. These systems are composed of a colour former, a developer and a co-solvent [8]. This mixture is microencapsulated to maintain a specific stoichiometry of the three constituents and to protect the mixture from the environment which makes it suitable for a range of applications.

- Colour formers are pH sensitive dyes which, are responsible for the colour in leuco dye systems. The molecular arrangement of these dyes take two forms: either a closed ring form which is attributed to colourlessness or the open ring form which causes the compound to become coloured.
- A developer is a proton donor, often a weak acid. The interaction of the developer with the colour former and the solvent is central to the colour changing principle as explained in subsection 2.2.3.2.
- Organic hydrophobic solvents are used as co-solvents for the composite. The most commonly used co-solvents are the low-melting fatty acids, amides and alcohols. In the coloured form of the leuco dye system the co-solvents exist as solids. Melting of the co-solvent causes the mixture to lose colour. The activation temperature of the leuco dye system is the temperature at which the co-solvent melts and the system changes colour.

2.2.3.2 Leuco dye thermochromic system colour changing principle

Below the leuco dye activation temperature, the co-solvent is a solid and the microcapsule is coloured. The colour former and the developer form a charged complex which leads to the colour former taking the open ring form (coloured) [14]. Above the activation temperature of this system the co-solvent melts causing the interaction between the colour former and the developer to break down. The breakdown of interaction between the colour former and the developer leads to interactions between the developer and co-solvent [15]. This causes the molecular arrangement of the colour former to take the closed ring form which is responsible for the loss of colour [15]. As the temperature drops below the activation temperature of the system, the co-solvent becomes a solid again and the microcapsule regains colour.

An example of the above explained principle is the leuco dye system consisting of a colour former: crystal violet lactone (CVL), a developer: lauryl gallate (LG) and a co-solvent: 1-octadecanol (OD). It is shown in [15] that below the activation temperature of the system CVL forms a charged complex with LG responsible for the coloured state of the system. Above the activation temperature LG forms interactions with OD which leads CVL to its colourless state.

2.2.3.3 Features of the leuco dye thermochromic system

Thermochromic leuco dyes can be formulated in a wide choice of colours and temperatures ranging from -100 °C to 100 °C [16]. Figure 1 below shows the heating and cooling curves of a commercial leuco dye themrochromic ink (Chromazone from LCR hallcrest [17]).

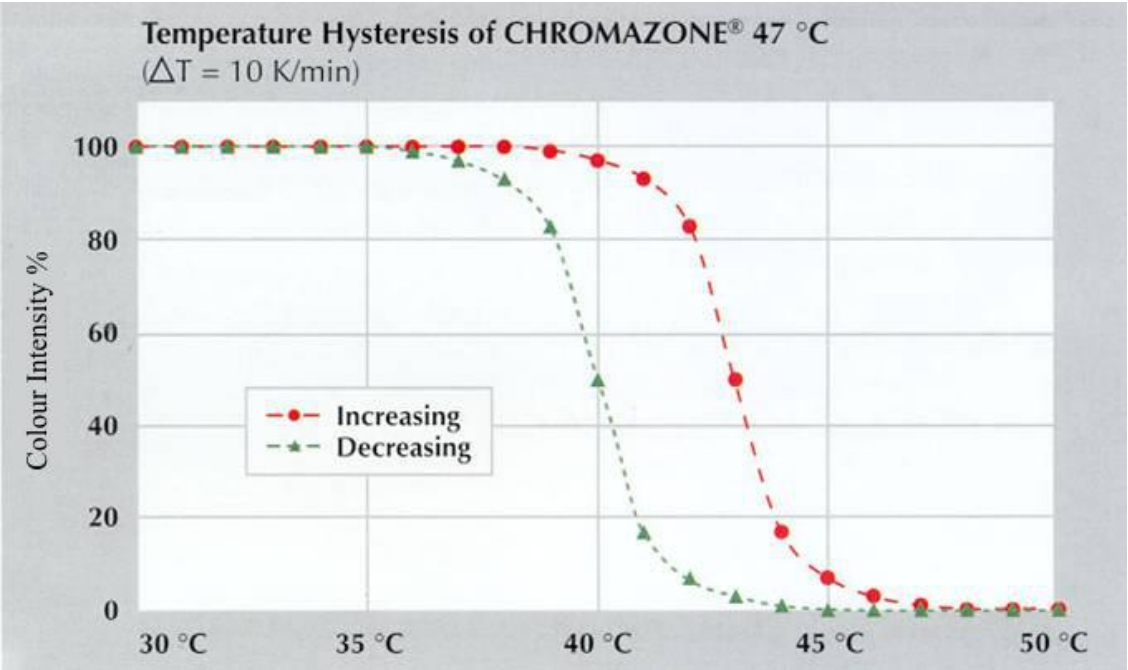

Figure 1: Illustration of change in colour intensity with temperature for a leuco dye thermochromic system showing hysteresis [17]

The colour transition of a leuco dye occurs over a range of temperatures instead of a binary switch at a specific temperature, as shown in figure 1 above. The range of temperature varies with the composition; generally the colour changes occur over an approximate temperature change of 5°C [17]. In that range, the colour changes from the initial colour to lighter shades of the colour before finally going colourless. Leuco dyes exhibit thermal hysteresis, shown in figure 1, as heating and cooling curves do not produce the same colour outputs at specific temperatures [18].

2.2.4 Liquid crystals

Liquid crystal materials are able to attain intermediate phases between the solid and liquid states as they change from crystalline solids to isotropic liquids [19], with increasing temperature. In the intermediate phases, they exhibit structural properties between those of solids and liquids. They show physical behaviour of crystals by retaining a degree of order in the structural arrangement of molecules and mechanical behaviour of liquids as they flow like viscous liquids. Not all liquid crystals exhibit thermochromism, only thermotropic liquid crystals are able to show thermochromism.

The molecules of thermochromic liquid crystals in the intermediate phases are arranged in a helix structure. These helical structures are able to reflect light as well as vary the wavelength of the reflected light in response to the temperature change [19]. The wavelength of light reflected depends on the length of the helix which varies with changes of temperature, giving rise to the thermochromic behaviour.

Thermochromic liquid crystals when heated change from a colourless state to a coloured state and exhibit all the visible spectral colours, colours represented by wavelengths between 400nm to 700nm. These materials are very sensitive to temperature changes and often produce the range of colours in a very small temperature range generally 3 to 5°C. When light is incident on thermochromic liquid crystals some of it is reflected and some of it passes through. The liquid crystals exhibit the range of colours comprehensively only on black backgrounds because the black background absorbs the wavelengths transmitted through the liquid crystals.

Thermochromic liquid crystals are commercially available as unsealed oils and in the microencapsulated form. The liquid crystals are very sensitive to organic chemicals such as fats and common solvents such as acetone. Contact with a very small quantity of these materials can adversely affect their thermochromic properties as they alter the helical structure of the liquid crystals [19]. The microencapsulation reduces this sensitivity but it does not make them insusceptible to the effects of organic chemicals, because the walls of the microcapsules are partially permeable allowing some chemicals to pass through [20].

2.2.4.1 Discussion – leuco dye compared with liquid crystal

A detailed market survey was carried out to identify commercially available thermochromic materials. It was found that leuco dye thermochromic materials are more commonly available compared to the liquid crystals which are offered by only a few suppliers. Leuco dye materials are cheaper to source compared to the liquid crystals due to less cost per kilogram and flexible minimum order quantity. They are available in a wider range of actuation temperatures than the liquid crystals offering more options. Table 1 below compares the feasibility of the two types of thermochromic materials.

Type of TC material	Leuco Dye	Liquid Crystals
Price/kg (£)	~ 210	323
Minimum Quantity	Flexible	1 kg
Actuation Temperature Range	-150 to 150 °C	• 20 -25 °C • 25-30° C • 29 -33° C

Table 1: Feasibility comparison of leuco dyes and liquid crystals

In addition to the above mentioned factors, microencapsulated leuco dyes are not sensitive to organic chemicals like the liquid crystals, which allows the leuco dyes to be used in combination with a wider range of chemicals. Therefore, the leuco dye thermochromic materials were judged to be more suitable for this study than liquid crystals.

2.2.5 Applications of thermochromic materials

Thermochromic materials find applications in a number of areas. The most common application of these materials is their use as temperature indicators for industrial and medical applications [21]. Organic systems enjoy a wider range of applications than the inorganic and organometallic systems. Inorganic and organometallic systems offer limited colour and temperature choices which has restricted their commercial adoption.

Inorganic systems are mainly used in crayons and paints which are applied to various areas on industrial equipment to indicate hot spots to alert the user to potential thermal damage [8]. They have found applications in the area of smart windows which help regulate the temperature of a building. They darken as the direct exposure to sunlight warms the building and increase transparency when the sun is not directly shinning on the window when the temperature drops to a specified level [22].

Organic systems form an integral part of the medical thermometer strips. They are used as temperature indicators on cold drink cans, food containers, mugs and utensils. They are being increasingly used as security inks to verify a document's authenticity. The documents are printed using thermochromic inks which can be slightly heated to verify the authenticity of documents [8].

They are used in novelty products such as colour changing jewellery, cosmetics [23], wallpapers [24] and t-shirts [25]. They are used in batteries as battery usage indicators. They have also been used to produce highway signs which display weather (temperature) dependent warnings to drivers [26].

These systems are also employed in the field of architecture. They are used in building interiors for their aesthetic qualities and as temperature indicators. They also find applications as colour changing interior decorations and to indicate information like thermal hot spots which could emerge from spillage of hot liquids [8].

2.3 Applications of actively actuated thermochromic fabric devices

Colour is a fundamental and ubiquitous property of fabrics, thermochromic materials provide the ability to change this property to add value to fabrics. Recent research has focused on actively controlling the colour change function so it is carried out in a predictable and predetermined manner. Actively actuated thermochromic fabrics have been used for a range of applications which can be broadly categorised in three application areas; Creative applications, sensory indicator applications and display applications. This section discusses the three application areas and presents the associated devices as examples to show the widespread interest in the actively actuated thermochromic fabrics. The actuation technologies of the presented devices are discussed in detail in section 2.4.

Creative applications use the colour change function to manipulate the patterns of fabric devices for aesthetic effects and communicating artistic expressions. Some examples of the thermochromic devices used for creative applications include shimmering flower [27], costume and a wall hanging [28], and blip [29]. Shimmering flower, shown in figure 2, is an actively controlled thermochromic fabric wallpaper which uses a conductive yarn based heater. The leaves in the wallpaper change colour from either brown to yellow or yellow to brown when actuated to exhibit an animation.

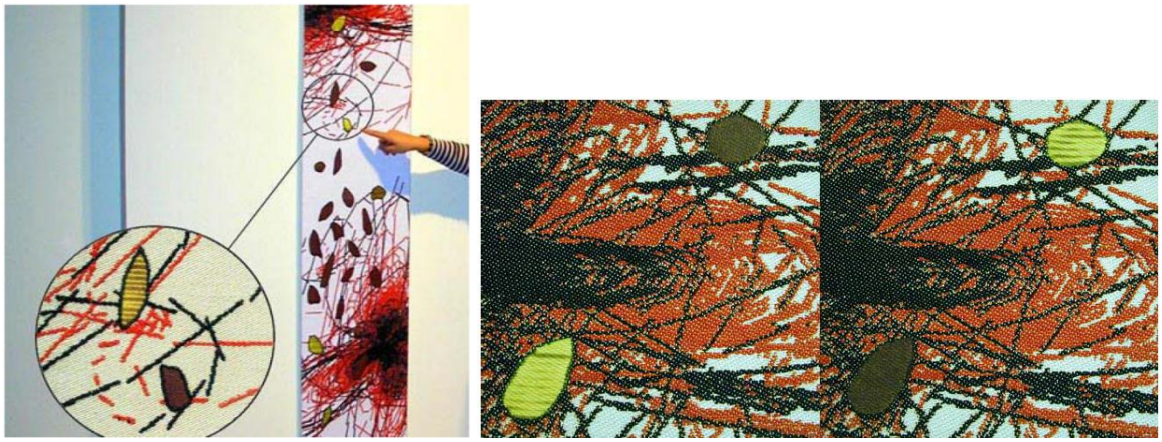

(a) (b)

Figure 2: Shimmering flower – an actively actuated thermochromic fabric wallpaper [27]

Costume and wall hanging, a two part colour changing fabric also uses conductive yarn heater for actuation. Pattern on the wall hanging changes in response to certain movements of the costume wearer such as touching the upper arm to the lower leg. Touching two parts of the costume together results in a wireless signal to the control circuit of the wall hanging, this triggers the colour and pattern change.

Blip is a dynamic fabric artwork which uses thermochromic materials and conductive yarn heater to change the patterns of the fabric. The thermochromic prints on various parts of the fabric are actuated

in different combinations to produce different patterns; the pattern changes are used for communicating artistic expressions.

Sensory indicator applications use the colour change function as an indicator or actuator often linked with a sensor to communicate information or data. The information or data could represent a physical quantity such as distance or an input for further processing such as augmented reality markers. Fabrication bag [30], huggy pajama [31], warning signs [32] and dMarkers [12] are some examples of thermochromic fabrics used in the sensory indicator applications. Fabrication bag is a handbag that undergoes changes in fabric patterns in response to mobile phone activity. The bag was designed to provide unobtrusive alerts as a mobile phone receives calls and text messages while placed in the bag. The pattern consists of dots in shades of grey colour, it changes to colourful dots as a result of mobile phone activity. It uses conductive thread heaters for actuation.

Huggy pajama is a wearable interactive system designed to replicate aspects of physical interaction in remote communication between parents and children. It consists of an interface (doll) and a garment connected via internet. The thermochromic print on the garment produces a colour change as a function of distance between the two parts of the system; it uses a conductive thread heater. A microcontroller combined with a temperature sensor was used to produce two colour changes to represent distance, brown to orange and orange to yellow at 31°C and 38° C respectively. The garment also incorporated colour changing patterns as expression of emotions, the patterns changed as the parent and child communicated remotely.

Warning signs is a line of garments which produce colour change in response to high levels of carbon monoxide. It consists of a thermochromic display, MQ-7 gas sensor for measuring carbon monoxide levels and conductive wires as heaters. The colour change occurs in the print on the front of the garment; it is made using a combination of fabric colours and thermochromics ink. Figure 3 below shows the colour of the warning sign prototype sweatshirt when activated; the blue lines appear on red lung print.

Figure 3: Warning sign sweatshirt in high levels of carbon monoxide [32]

dMarkers are dynamic quick response (QR)/ augmented reality (AR) tags based on thermochromic fabrics which use Peltier semiconductor heaters. The thermochromic prints were arranged on the fabric in the form of multiple squares which were actuated in various combinations to produce different patterns. The QR tag patterns were scanned using the mobile phone camera and processed in a QR/AR software. The software displayed pre-programmed information on the phone screen associated with the scanned QR tag pattern. The displayed information could range from text, images

to animation. The use of thermochromic fabric allowed the QR tag patterns to be dynamically changed.

The display applications use the colour change function for its non-emissive, unobtrusive and ubiquitous properties. The non-emissive nature of the colour change offers an alternative and allows the thermochromic displays to be used as ambient displays that are able to blend in the environment. Ambikraf [33], mosaic textile [34] and a heating foil textile display [28] are examples of thermochromic displays. Ambikraf is a wearable thermochromic display which uses Peltier semiconductor heaters for actuation. Multiple thermochromic inks are printed on a shirt to form a coloured pattern which changes to produce simple animations. Various parts of the pattern are controlled by multiple Peltier semiconductor modules which allow selective actuation of the pattern. Two Ambikraf shirts were programmed to interact with each other where the patterns on the shirt changed as a function of distance between the shirts. The pattern changes were programmed to display graphics as interactive messages.

Mosaic textile is a modular thermochromic display which uses conductive yarn heater for actuation. It consists of nine display elements called fabcells arranged in a 3x3 matrix each of which is individually addressable and is able to produce multiple colour changes. Actuation of various combinations of the fabcells exhibits different graphics.

The heating foil textile display consists of thermochromic ink printed on a cotton fabric and 25 commercial heating foils enclosed in a wooden frame. The heating foils formed modules of the display and could be individually actuated. Heating a foil caused the part of fabric connected to it to turn white, different combinations of the foils could be actuated to form distinct white patterns on the display. It was developed for communicating information in the form of graphics. Figure 4 shows the textile display before actuation and exhibiting two different patterns.

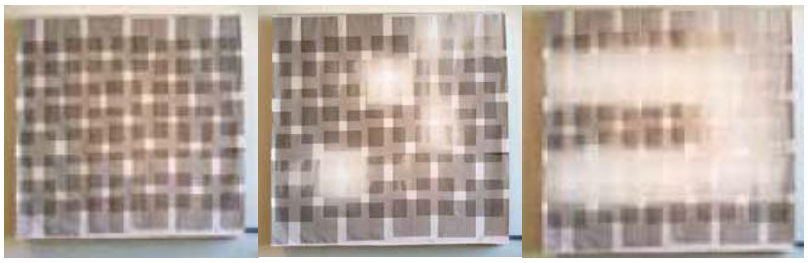

(a) (b) (c)

Figure 4: (a) The heating foil textile display before actuation, textile display exhibiting (b) pattern 1 (c) pattern 2 [28]

The review of applications of actively actuated thermochromic fabrics showed that the colour change function offers an actuator which can be embedded in a fabric in an unobtrusive manner. All the actuation methods of thermochromic fabrics are electronically controlled which allows the colour change to be linked with various sensors and control electronics. It showed that the actively controlled thermochromic fabrics have been used for a broad range of dynamic applications.

2.4 Technologies for active actuation of thermochromic fabrics

The fabrication of state of the art actively actuated thermochromic fabrics has used screen printing and coating as the two methods of application of thermochromic materials on fabrics. This section details the state of the art heating technologies that have been used for active actuation of thermochromic fabrics. Heaters consisting of conductive yarns/threads, Printed Circuit Boards (PCB),

Peltier semiconductors, heating foils, conductive tracks and conductive coating have been used. Each actuation technology is mainly assessed on the following three criteria.

- **Flexibility**: Essential for use in fabric applications as it is a fundamental property of fabrics.
- **Design freedom**: Provides control of the heat profile and fabrication parameters of a heater such as resistance.
- **Integration with the fabrics**: Refers to the attachment of a heater with a thermochromic fabric.

2.4.1 Conductive yarns/threads

Electrical heaters consisting of conductive yarns/threads are the most commonly used actuation technology for actively actuated thermochromic fabrics [28,31,32,35,36]. Conductive yarns are very thin conductive wires mostly consisting of metals such as silver. Conductive threads are typically a combination of conductive yarns twisted with normal fabric yarns [36]. A heater consisting of conductive yarns/threads generates heat due to resistive heating, whereby an electric current experiencing an electrical resistance converts electrical energy into thermal energy.

A conductive yarn based heater consists of a fabric substrate created by weaving or knitting the conductive yarns with non-conductive fabric yarns. Power supplied to the conductive yarns produces resistive heating. This approach of fabricating a heater allows direct integration of the heater within the fabric structure whilst being flexible. However, the conductive yarn heaters offer limited design freedom as the conductive path follows the physical location of these yarns on fabric mostly along the length or width (warp or weft) of the fabric as presented diagrammatically in figure 5.

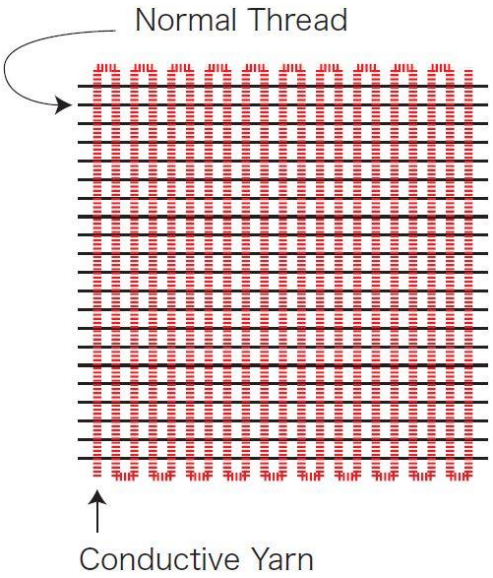

Figure 5: A schematic fabric heater developed by weaving conductive yarns with normal fabric yarns [34]

A conductive yarn fabric requires the substrate to be insulated to avoid short circuits, and to avoid electric shocks if used as a wearable; the metallic conductive yarns make the fabric uncomfortable to wear. Another limitation of the conductive yarn heaters is that they cannot be fabricated on off the shelf fabrics or non-woven fabrics. It is also difficult to connect the conductive yarns with a power supply because individual conductive yarns have to be found among the normal yarns in the fabric structure.

Heaters consisting of conductive threads have been developed by sewing or embroidering these threads on a fabric substrate [37]. The advantage of this approach over the conductive yarn heaters is that the conductive path can be laid out in more complex patterns. The conductive thread heaters are directly attached to the fabric and are flexible. However, the conductive threads are not reliable to use as they are prone to breaking and damage during the sewing or embroidery process which can adversely affect the conductive path and the heater [36].

Most of the reported thermochromic fabrics consisting of conductive yarn and thread heaters do not provide sufficient technical details. An example where some technical details are reported is [37], the thermochromic fabric heated a rectangular area 20 cm x 2 cm in size using a 20 cm long stitched conductive thread; the thread was stitched in the middle of the fabric along its length. It required 1.9 W to achieve a complete colour change in 42.5 seconds, reaching a peak temperature of 65°C.

2.4.2 Printed circuit board heaters

Sara Robertson of Dundee Univerity [11] developed a PCB heater for thermochromic fabrics which used heat generated via a resistor. The resistors were soldered between two copper conductors laid out on the PCB in specific shapes. Heat developed in the resistor flowed into the copper shapes due to copper being a better thermal conductor than the surrounding materials on the board. The thermochromic fabric was placed on the PCB surface in contact with the copper conductors for actuation. Figure 6 below shows a heat sink circuit with a flower patterned copper conductors actuating white leuco dye thermochromic ink.

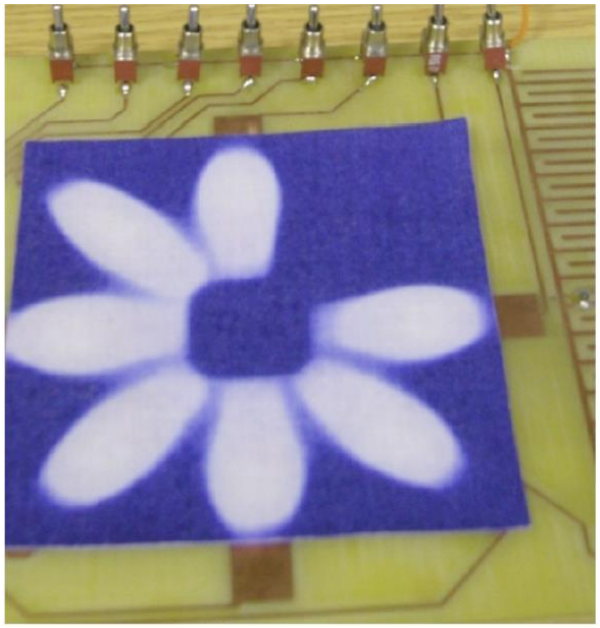

Figure 6: Heat generating PCB circuit activating a printed leuco dye fabric in flower pattern (one petal is missing due to a fault in the circuit) [11]

The PCB heaters offer good design freedom but they are rigid which is a major limitation that restricts their use in fabric applications. The PCB heaters are not integrated with the thermochromic fabrics and require the fabric to be placed on top of the PCB board for actuation. A fabric is required to make good contact with the board for an efficient heat transfer. Another disadvantage of PCBs is that its manufacturing uses chemicals that are hamful for the environment such as lead and formaldehyde and it also produces high material wastage. A PCB heater actuated a cotton thermochromic fabric from 25°C to 36°C in 5 minutes; a 150 Ω resistor was used for the heater and it was supplied 6V for

actuation [11]. Further technical details such as the size of the heater and the area of the fabric heated are not mentioned in the literature.

A flexible alternative to the PCB heater deveoped by Robertson used self-adhesive copper sheets applied directly to the back of the fabric [11]. Resistors were soldered between two copper shapes and wires attached to complete the circuit. In addition to being flexible, this method provides freedom of design as the copper sheets could be cut into any shape. Unlike the PCB heater, this method allows the heater to be directly integrated with the thermochromic fabric. Figure 7 below shows the flexible heat sink circuit actuating thermochromic liquid crystals. The liquid crystals in the image display a range of colours which shows that the heat distribution of the heater in uneven. Temperature at the centre of the circle is higher than at the periphery as the resistor is soldered in the middle and heat flows outwards from the centre.

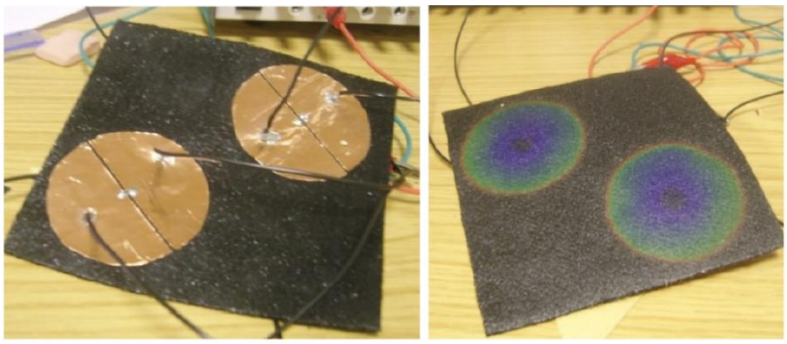

Figure 7: Flexible heat sink circuitry (left) activating liquid crystals (right) [11]

Each flexible heater required two wires to be directly attached to the copper tapes. A design with multiple heaters would require a number of individually attached wires affecting the flexibility of the colour changing fabric. Multiple wires in a design potentially restricts the ability to move the thermochromic fabric. The copper tape heater method is not reliable because the tape is not designed for fabrics and its attachment to the fabrics can be non-uniform as shown in figure 7.

2.4.3 Peltier semiconductors

Joanna Berzowska of Concordia University and Roshan Lalintha Peiris of National University of Singapore have used Peltier semiconductors for actuation of thermochromic fabrics [12,38]. The Peltier modules use the thermoelectric effect which is conversion of temperature difference to electric voltage and vice versa. Peltier semiconductors are bi-directional in terms of temperature which means they can heat up and cool down as well. The heating or cooling function depends on the polarity of the voltage so current flow in one direction heats up one surface of the Peltier module and cools down the other. Change in current flow direction alternates the hot and cool surfaces.

Peltier modules used for thermochromic fabrics were rigid and inflexible which is a major limitation of this actuation technology. The thermochromic fabrics were required to be in contact with the Peltier modules for actuation as they were not integrated or attached with the fabric. They offer limited design freedom as the Peltier modules used for thermochromic fabrics and a majority of the commercially available are square shaped [12]. Peltier semiconductors are expensive and therefore increase the cost of production of thermochromic fabrics. Roshan used a 2.25 cm^2 Peltier element to actuate a thermochromic fabric by producing a temperature difference of 12°C; it required 3.5W power and produced a temperature changing rate of 3-4°C/s.

2.4.4 Heating foils and conductive tracks

Linda Worbin of University of Boras Sweden has used commercial heating foils as an actuation technology for thermochromic fabrics [28]. Custom made metallic foils supplied by BakerCalesco, shown in figure 8 were used; they are flexible resistive heaters. The commercial heating foils were not integrated with the thermochromic fabric and required to be attached with it which is a major limitation. The fabrication process of the foils is not mentioned in the literature and therefore any design limits are unclear. The heating foils measured 25 x 25 cm, required 48 V and 30 W power to reach a temperature of 40°C. It took the heater 3 minutes to get to 40°C from an initial temperature of 20°C.

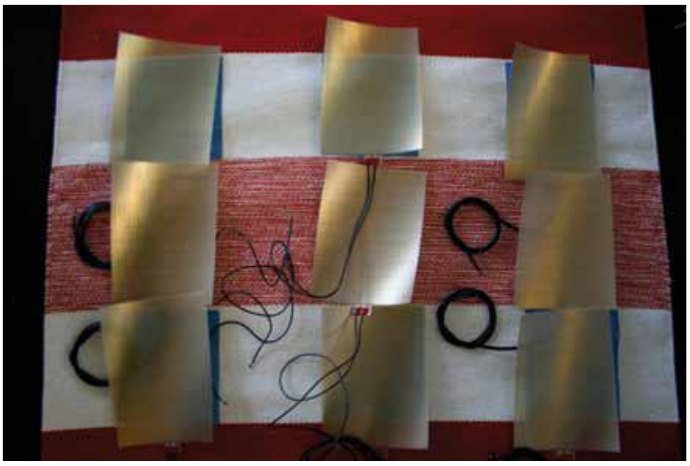

Figure 8: Calesco heating foils used for heating thermochromic fabrics [28]

Roberton used commercially available Minco Polyamide/ULA heat pad (HK5950P) and custom made stainless steel track heater on Mylar film for heating thermochromic fabrics [11]; both generate heat via resistive heating. The fabrication method of the heaters and the steel track heater supplier are not mentioned in the literature. Both the heaters offered same merits of flexibility and uniform heating for the thermochromic fabrics. Their limitations include lack of integration with the fabric as they are required to be attached to the thermochromic fabrics. Minco heat pad was off the shelf heater with a fixed shape and heat profile.

2.4.5 Conductive coating

Guangxi Huang et al [39] coated a commercial polyester covered cotton fabric with polypyrrole, which is a conducting polymer. One side of the fabric is woven using cotton fibres and the other side using polyester fibres. As part of the coating process the fabric was completely immersed in solutions of the reagents used which caused the entire cotton surface of the fabric to be coated with the conductive polymer. The polypyrrole was used as a resistive heater to actuate a thermochromic print on the reverse side of the fabric. The merits of the coated heater includes direct integration with the thermochromic fabric and flexibility. A major demerit of this approach is limited design freedom owing to the coating process used. This coating method is not suitable for laying out the conductive polymer in patterns which restricts the design freedom. The coated heater measuring 3.6 x 3.5 cm achieved a temperature of 70°C when it was heated for 60 seconds using a current of 120 mA.

2.4.6 Summary and discussion

Table 2 summarises the merits and limitations of the actuation technologies used for thermochromic fabrics. The summary presents each technology in terms of integration with fabric substrate, freedom of design, flexibility and other technology specific limitations such as reliability.

Heater technology	Integration with fabric substrate	Design freedom	Flexibility	Other limitations
Conductive yarns	Yes	Limited by the fixed layout of the conductive path	Flexible	- Cannot be used for off the shelf fabrics
Conductive threads	Yes	Yes	Flexible	- Unreliable as conductive path is prone to damage during fabrication
PCB – Heat sink	Requires contact with fabric for actuation	Yes	Inflexible due to PCB boards	
Flexible heat sink	Yes	Yes	Flexible	- Requires attachment of two wires per heater which can affect mobility and flexibility of the fabric; - Unreliable as the copper tape is not designed for fabrics
Peltier elements	Requires contact with fabric for actuation	Limited by the shape of the modules	Rigid due to the modules	
Heating foils	Requires contact with fabric for actuation	Limited by the commercially available designs	Flexible	
Track heaters	Requires contact with the fabric for actuation	Limited by the commercially available designs	Flexible	
Coated heaters	Yes	Limited as coating method is not suitable for patterning	Flexible	

Table 2: Summary of the features of actuation technologies used for thermochromic fabrics

The performance of the heating technologies reviewed could not be compared as the literature does not provide technical details such as the input power, target temperature, area to be heated, environmental temperature, time it took the heater to attain the target temperature and the testing conditions. The performance of two heating technologies can only be effectively compared if factors such as input power, area to be heated, environmental temperature and testing conditions are similar for both heaters which is not the case for the reviewed technologies. In some cases there are no

technical details provided about the heaters [27,29,30,34] and in some cases the provided details are not sufficient for comparison [37,38]. A conclusion commonly drawn about the heater performances in the literature is that a higher input power increases the final temperature reached by a heater for the same environmental temperature [11,37,38].

The review of state of the art heating technologies for thermochromic fabrics showed that they are rigid (PCB and Peltier semiconductors), unreliable (conductive threads and flexible heat sink), offer limited design freedom (conductive yarns, coating and commercial heaters) and are typically not well integrated with the thermochromic fabrics. The review has highlighted that none of the technologies provided a combination of integration with the fabric substrate, flexibility, reliability and design freedom. The technical details of fabrication of the heaters were not provided in sufficient depth to clearly identify an optimum approach using these technologies for thermochromic fabrics. The dispenser printed heaters proposed in this research will provide a step beyond the state of the art and alleviate a number of the issues highlighted.

2.5 Conclusions

This literature review has presented the background of thermochromism in terms of materials, applications and its commercial adoption. Thermochromic materials are commercially available in microencapsulated form which means they can be formulated as dispenser printer inks. Leuco dye thermochromic materials were found to be more suitable for this research due to their wider commercial availability, relatively lower cost, more temperature options and less sensitivity to chemicals compared to liquid crystals.

The state of the art heater technologies for the thermochromic fabrics were found to have one or more of the following four major limitations for fabric applications.

- Poor integration with fabrics
- Limited design freedom
- Inflexibility
- Unreliability

PCB and Peltier heaters were inflexible and required contact with the thermochromic fabrics for actuation. Conductive yarn heaters, coated heaters and commercial heaters offered limited design freedom whereas conductive thread and flexible heat sink heaters were unreliable. Most of the heating systems used in the literature have not been quantified and do not provide sufficient technical details which makes it difficult to assess or replicate them. The different heating technologies were not compared as the comparison require the heaters to have the same heating area, input power, environmental temperature and testing conditions as each of these factors directly affect the heater performance. Although several heating mechanisms were reviewed none of them offered the combination of integration with fabrics, freedom of design, reliability, flexibility and control over the generated heat profile.

The actively actuated thermochromic fabric devices find use in creative, sensory indicator and display applications. Creative applications use the colour change function for enhancing aesthetic effects and for expressing artistic expressions. Sensory indicator applications use the colour change function as an actuator and often electronically link it to sensors to communicate information. Display applications rely on the non-obtrusive qualities of the colour change function to use it as ambient display units.

The state of the art actively actuated thermochromic fabrics were fabricated using screen printing or coating for application of thermochromic materials and combined with one of the above mentioned heating technologies for actuation. These thermochromic fabrics required a minimum of two fabrication processes one for application of thermochromic materials and the other/others for the heater. Dispenser printing offers greater design freedom than screen printing and coating and therefore offers an improvement over the existing methods of application of thermochromic materials on fabric. A comparison of dispenser printing and screen printing technologies is presented in chapter 3.

To go beyond the state of the art, this research proposes to fabricate actively actuated thermochromic fabrics using dispenser printing as the sole fabrication process. The thermochromic materials and heaters will both be dispenser printed on a fabric substrate. The use of a single process for fabrication only requires expertise and equipment for that specific process thus reducing the technical barriers for fabricating thermochromic fabrics. The proposed dispenser printed heaters provide a flexible heating option which can be directly fabricated on the fabrics whilst offering freedom of design and fabrication reliability. In the literature none of the thermochromic fabric systems use an all printed approach thus increasing processing requirements. Therefore, this thesis pursues an all printed design approach for development of an actively actuated colour changing fabric. To demonstrate this process and provide a comparison to complex systems within the literature, fabrication of multifunctional devices incorporating colour changing fabrics, such a digital display and an interactive colour changing fabric, is also pursued.

CHAPTER 3 DISPENSER PRINTING

3.1 Introduction

This chapter introduces the dispenser printing process and discusses the background of the technology. It compares dispenser printing technology with screen and inkjet printing technologies. It presents the dispenser printing equipment used in this research and details the dispenser printing parameters. It describes the operating software of the dispenser printer and details the programmed printing modes. It discusses the adverse effects on prints of variation in the gap between the printing nozzle and the substrate and characterises the variation in the printer stage surface. It also characterizes the surface variation of the polyester cotton 65/35 blend fabric and presents a method of overcoming the fabric surface variation. The surface variation is overcome by dispenser printing dielectric inks on the surface of the fabric. The effect of substrate surface variation on the performance of printed conductors is experimentally analysed. The chapter also discusses the improvement in the performance of the printed conductors achieved by overcoming the substrate surface variation

3.2 Introduction to dispenser printing

Dispensing technology uses pressure control to force out a material from a container outlet to deposit it in an additive manner on a substrate. It is a drop on demand technology which is used for precise and repeatable deposition of a material in controlled quantities. Dispensing technology is not to be confused with dispenser printing technology which refers to digital dispensing of a material, on digitally defined locations of a substrate, to reproduce an image from a digital template. Dispensing technology is used in many industries such as electronics manufacturing, medical, bio-medical, automotive, solar cell and chemical industries. It is used in the industry to dispense a wide variety of materials such as solder pastes, lubricants, adhesives, medical media and sealants [40]. Industrial use of dispensing technology is aimed at repeatable and precise deposition of materials to achieve consistency in an industrial process such as electronic assembly [40]. The pressure used in dispensers can be generated using mechanical or pneumatic systems. In systems that use mechanical pressure, positive displacement of a mechanical part such as a rotor or a plunger is used to force the material out of the container outlet whereas in pneumatic systems compressed air/gas is used for dispensing the material. The materials dispensed are in the form of suspensions, slurries and solutions. A suspension is a heterogeneous mixture in which the mixed materials separate and settle out after a period of time. A slurry is a mixture of insoluble materials with water. A solution is a homogenous mixture of two materials.

Dispenser printing is a direct write process; direct write technology can be described as a group of processes which are used for deposition of functional/structural materials on to a substrate in specific digitally defined locations [41]. The dispenser printing technology combines the dispensing technology with the ability to precisely define locations on a substrate and reproduce an image from a template. A dispenser printer comprises a digitally controlled dispenser and a multidimensional stage. The stage is used to move the substrate in the defined area of printing. Dispenser printing offers custom patterning of materials using digitally defined printing templates. It is a rapid prototyping process which can print a material without the need for extra tooling. Being a drop on demand process, dispenser printing ensures minimum wastage of materials. It can be used to deposit a wide array of materials such as metals, coloured dyes and polymers as inks on a variety of substrates which include PCB, glass and silicon wafers [42,43,44]. Dispenser printing can be used to print inks in a viscosity range of 1 mPa.s to 100 Pa.s [45] depending on the size of nozzle used and the pressure mechanism. It allows printing of single-layered and multi-layered structures which can be composed of a single material or

multiple materials. The dispenser printer used in this research work is based on pneumatic pressure therefore only the pneumatic dispenser printer is described further in this study. Figure 9 below represents schematic of a pneumatic dispenser printer.

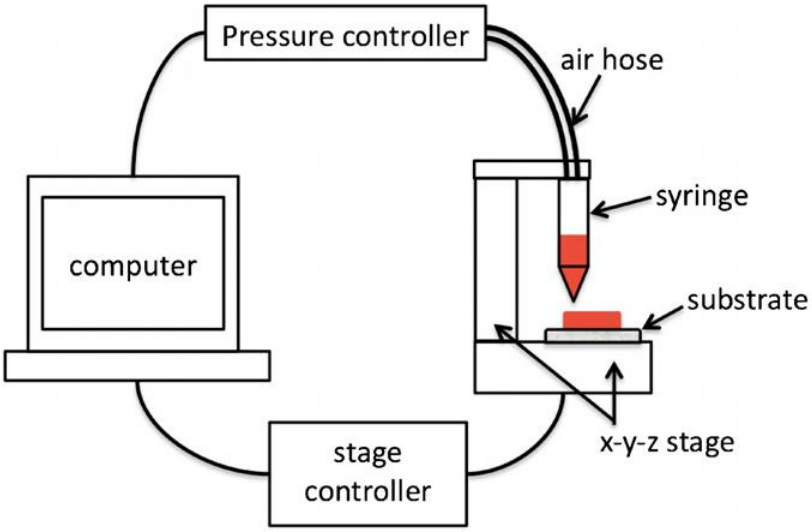

Figure 9: Diagrammatic representation of a pneumatic dispenser printer [44]

A pneumatic dispenser consists of a syringe, an air hose, a movement stage, a stage controller, a pressure controller and a computer. The following text briefly describes the function of each element of the dispenser printer.

- Syringe:
  A syringe contains a reservoir of the ink to be printed. One end of the syringe is connected to a hose; compressed gas reaches the syringe through the hose from the pressure controller. The other end of the syringe has a nozzle which allows the ink to be dispensed on the substrate.

- X-Y-Z movement stages:
  The movement stage consists of multiple stepper motors which control the movement of the substrate in the x-y directions and the dispenser head in the z-direction. The stage movements allow inks to be dispensed in specific patterns to deposit materials in specified designs. The smallest distance a movement stage can move and the nozzle diameter influence the maximum resolution of a dispenser printer. The printing speed is determined by the maximum stage speed.

- Stage controller:
  The stage controller controls the motors driving the stages to translate a software specified pattern into a print by movement of either the dispenser head (z-direction) or the substrate (x and y direction).

- Pressure controller:
  The pressure controller controls the pressure applied to the syringe and the length of time it is applied, thus controlling the amount of ink deposited on to the substrate. It also generates vacuum in the syringe when not printing to prevent dripping of ink when not dispensing.

- Computer:
  The computer coordinates the control of the pressure controller and the stage controller. Co-ordination between the two functions is important to ensure that the material to be printed is deposited in the digitally defined locations. The computer provides a user interface to select the parameters associated with dispenser printing such as the pressure, dispense time, speed and direction of stage movement and area for printing.

3.3 Dispenser printing background

This section discusses the previous work which has used dispenser printing as the fabrication method. It highlights the range of devices that were dispenser printed in terms of the inks, substrates and the dispenser printing equipment used.

Dispenser printing has been previously used at the University of California, USA for fabricating electrochemical energy storage devices [42,43,44], energy harvesting devices [46,47,48,49] and an AC current sensor [50]. The electrochemical energy storage devices were a multi-layered capacitor [42], a multi-layered lithium ion battery [43] and a micro-battery [44]. The three devices were dispenser printed in a multi-layered structure consisting of two electrodes and an electrolyte. The capacitor was fabricated on a stainless steel foil, the lithium ion battery was fabricated on a glass substrate and the micro battery was printed on a nickel foil substrate. The lithium ion battery was printed using a 100 µm nozzle in a 5x5 cm area with dispensing pressures in the range of 40-70 kPa. The micro battery was printed in a 5x5 mm area on the nickel foil. The electrodes of the device were printed using inks with a 90-95% solid content. These devices benefit from the ability of dispenser printing process to print varying ink rheologies and multi-layered structures.

The dispenser printed energy harvesting devices fabricated at University of California, USA consist of thermoelectric energy harvesters [46,47,48] and vibration energy harvester [49]. The thermoelectric devices were printed on a Kapton substrate using inks consisting of active thermoelectric powders mixed with polymer binders. In addition to printing the thermoelectric inks, the silver interconnections were also dispenser printed [48]. The dispenser printer used at the University of California consists of Newmark systems NLS4 series stages and Musashi ML-808FX dispenser unit. This setup offers a resolution of 1 µm and a pressure range of 20-500 kPa [48]. Dispenser printing has been used for fabrication of proof masses on the cantilevers of vibration energy harvesters to modify the frequency responses of the harvesters [49]. The proof masses were printed at ambient temperature using zinc slurry consisting of 85% solid content. Dispenser printing has also been used in fabrication of MEMS AC current sensor [50], it was used for printing permanent magnets on aluminium nitride cantilevers using magnetic powder mixed in a polymer.

Dispenser printing has been used at University of Illinois, USA to fabricate a li-Ion micro-battery [51], electrical interconnections [52,53], electrodes [52,54], an antenna [55] and 3-D bio scaffolds [56]. The li-Ion micro-battery architecture consisted of interdigitated electrodes dispenser printed on a glass substrate. The architecture was printed with gaps between the electrodes so an electrolyte could be poured into the assembly which was then sealed with glass covering. The electrode inks consisted of 57-60 % solid content. The inks were dispensed continuously in the form of filaments through a 30 µm diameter borosilicate micro nozzle at a speed of 250 µm/s using 4136 kPa pressure. Dispenser printing has also been used at University of Illinois to fabricate electrical interconnections in planar and 3-D motifs on glass, a silicon wafer and a Kapton substrate. The electrical interconnections were dispensed using a custom silver-nanoparticle ink consisting of 78%-85% solid content. The printer used for dispensing the electrical interconnections offers dispensing pressures in the range 70-690 kPa, printing speeds in the range 20-500 µm/s and a printing resolution down to 2 µm [52]. The

nanoparticle silver ink was also dispenser printed in various arrangements to form electrodes for electronic devices such as LED arrays [52]. Custom sol-gel inks consisting of 22%-28% solid content were dispenser printed in single layered and multi-layered arrays to form microelectrodes [54]. The electrodes were printed using 1 µm and 4 µm nozzles on a silicon wafer and silicon micro ribbons to demonstrate that the electrodes can be dispenser printed in custom patterns. An antenna was dispenser printed at University of Illinois using bespoke silver nanoparticle ink [55] on a 1.2 mm diameter glass hemisphere. The antenna consisted of meander patterned conductive tracks. The fabrication of the antenna showed that the dispenser printing process is not limited to printing on flat surfaces and can print on concave and convex surfaces. Dispenser printing has been used for fabrication of 3-D bio scaffolds at University of Illinois [56] on a glass substrate. The scaffolds were dispensed using a 200 µm nozzle at a speed of 2 mm/s using pressures in the range of 275-350 kPa. The fabrication of the scaffolds makes use of the custom patterning and the ability of the dispenser printing process to print multi-layer structures.

Dispenser printing has been used at Harvard University to fabricate strain sensors [57] and cellular composites [58]. The strain sensors were fabricated by dispenser printing a carbon based resistive ink into a reservoir of elastomeric material. The resistive ink gets enclosed in the elastomeric material when it cures constituting the sensor. The cellular composites are bio inspired structures dispenser printed using fibre-filled epoxy based inks on glass substrates. The reported cellular composites were printed as multi-layered structures to mimic mechanical and structural properties of balsa wood. The epoxy based inks were dispenser printed using Nordson Ultimus™ V pressure controller which can produce output pressures in the range of 0-700 kPa.

3.3.1 Discussion

The background on dispenser printing showed that the dispenser printing process can be used to print a wide variety of materials with varying ink rheologies. It has been used for printing active, functional and structural materials using inks with a broad range of solid content: 22% to 95%. Dispenser printing has been shown to be compatible with a range of substrates such as glass, Kapton, stainless steel foil, nickel foil and silicon wafers. It was shown that dispenser printing process is not limited to printing on flat surfaces and can print on concave and convex surfaces as well. The reported dispenser printed devices made use of the custom patterning and the ability of the dispenser printing process to print multi-material and multi-layered structures. All the dispenser printer setups mentioned in the background are bespoke, the research on dispenser printers is at an early stage therefore no commercial machines are available. The reported dispenser printer setups offer printing pressures in the range of 0 – 700 kPa, printing resolutions down to 1 µm and a maximum printing speed of 2 mm/s.

3.4 Alternative printing technologies

This section presents inkjet printing and screen printing as alternative printing technologies to dispenser printing. It describes the working principles of the two technologies and discusses the features and limitations of the two technologies. A comparison of dispenser printing with the screen and inkjet printing processes is also presented in this section.

3.4.1 Inkjet printing

Inkjet printing like dispenser printing is a direct-write technology. An ink is deposited directly on a substrate in digitally specified areas. It can be divided into two categories: continuous inkjet and drop on demand inkjet. Continuous inkjet uses an ink pump to move a stream of ink from a reservoir to a nozzle where the ink is broken down into a continuous stream of drops. The drops are charged and then deflected by electrodes for deposition on a substrate in a computer defined pattern [59]. The drops of ink that are not deposited on a substrate during printing are directed back to the ink reservoir

for reuse. Drop on demand only produces ink drops when required by the pattern being printed. Two processes are used for production of droplets on demand: thermal and piezoelectric [60]. The thermal process uses a heater to generate a bubble within the ink reservoir which creates pressure and forces an ink droplet out of the nozzle. Piezoelectric membranes generates a pressure pulse in response to an electrical signal which forces the ink droplets out of the ink chamber and out through a nozzle on to the substrate.

Inkjet technology offers custom patterning and minimum wastage of material. It can print resolutions down to 5 µm [61]; however it can only print low viscosity inks in the range of 1 to 20 mPa.s [62]. The inks have a high solvent and low solid content. The layers produced by inkjet printing are thin, usually less than 1 µm [63] therefore multiple layers are needed for a thicker print. A typical size of a thermochromic leuco dye microcapsule is 6 µm which makes it larger than the typical layer thicknesses produced by inkjet printing.

3.4.2 Screen printing

In screen printing an ink is deposited on a substrate through a mesh, in a pattern defined by the screen. Figure 10 shows the screen printing process steps. The mesh on the screen is made impermeable to ink using an emulsion. The pattern to be printed is defined by permeable regions on the screen. A squeegee forces the screen to come into contact with the substrate and forces the ink through the permeable regions on to the substrate.

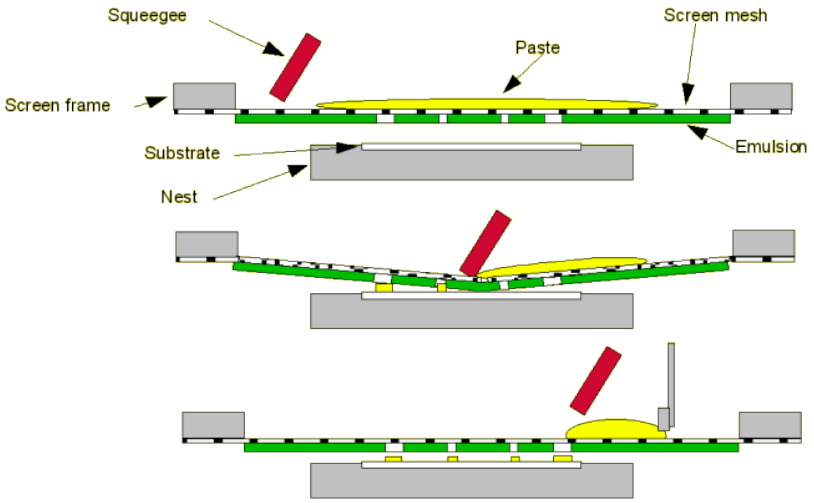

Figure 10: Diagrammatical representation of screen printing process [64]

It is a versatile process which can be used to deposit a wide array of materials on a range of substrates. It is suitable for mass production as it can print large identical batches faster than inkjet and dispenser printing. Screen printing offers print resolutions down to 50 µm and can print ink viscosities in the range of 1 – 10 Pa.s [65]. Screen printing requires a specific screen for each design. Screens are ink specific therefore multiple screens are required for a multi-material design. A single material multi-layered design may also require multiple screens if the layers are non-identical. The other disadvantages of screen printing include wastage of material and long lead times as screen manufacturing requires time which delays the printing process. In addition, any modification to the design requires new screens, further increasing the costs for prototyping or design upgrades.

3.4.3 Comparison of the printing technologies

Dispenser printing offers several advantages over inkjet printing and screen printing technologies. Firstly, dispenser printing can print a wider range of ink viscosities (1 mPa.s – 100 Pa.s) than inkjet

printing (1 m - 20 mPa.s) and screen printing (1 – 10 Pa.s). This allows dispenser printing to print a wider array of materials compared to the other two technologies. It can also produce prints with higher resolutions, down to 1 µm, compared to inkjet printing, 5 µm and screen printing, 50 µm.

Inkjet printable inks generally contain a high solvent content which results in thinner printed layers, less than 1 µm. Thin printed layers of functional materials can adversely affect their electrical/functional performance although printing multiple layers may improve the performance. Comparatively, dispenser printing can be used to print inks with high solid content and therefore can achieve required print thickness in a single layer. Screen printing, although a versatile and faster printing process compared with dispenser printing, has the limitations of requiring a physical design template, wastage of ink and long lead times for design changes. Dispenser printing provides several improvements to the screen printing process. It offers digital custom patterning as the ink can be directly deposited on the substrate in a pattern limited only by the stages. As a drop on demand process it reduces material wastage compared to screen printing. It can print complex multi-layered and multi-material structures without the need of extra tooling. It allows a substrate to be printed with minimum lead times and is therefore suited to rapid prototyping. A dispenser design can be potentially mass produced by either using multiple nozzles or by screen printing. Table 3 below presents the summary of comparison of the three printing technologies.

Printing process	**Printable ink viscosities**	**Resolution**	**Printing template**	**Custom patterning**	**Multi-material structures**	**Multi-layered structures**
Dispenser	1m – 100 Pa.s	1 µm	Digital	Yes	Yes	Yes
Inkjet	1 – 20 mPa.s	5 µm	Digital	Yes	Yes	Yes
Screen	1 – 10 Pa.s	50 µm	Physical	Requires design specific screens	Requires material specific screens	Requires layer specific screens

Table 3: Summary of the comparison of dispenser printing, inkjet printing and screen printing processes

This research aims to fabricate an actively controlled thermochromic devices on fabrics consisting of printed thermochromic materials and printed heaters. The devices require a multi-material and multi-layered approach which is facilitated by the capabilities of dispenser printing. The features of custom patterning is suitable for laying out thermochromic materials and printing heaters in various designs to customise the colour change patterns and heat profiles. The wide range of compatible viscosities offers extensive choice of thermochromic, conductive and resistive material formulations which can be used to print actively actuated thermochromic fabric devices.

3.5 The dispenser printer used in this study

Figure 11 shows the dispenser printer used in this research. The nozzle is typically moved within a distance of 50-200 µm from the substrate for printing. The camera is used to image the printing nozzle relative to the substrate and set the gap between the nozzle and the substrate manually.

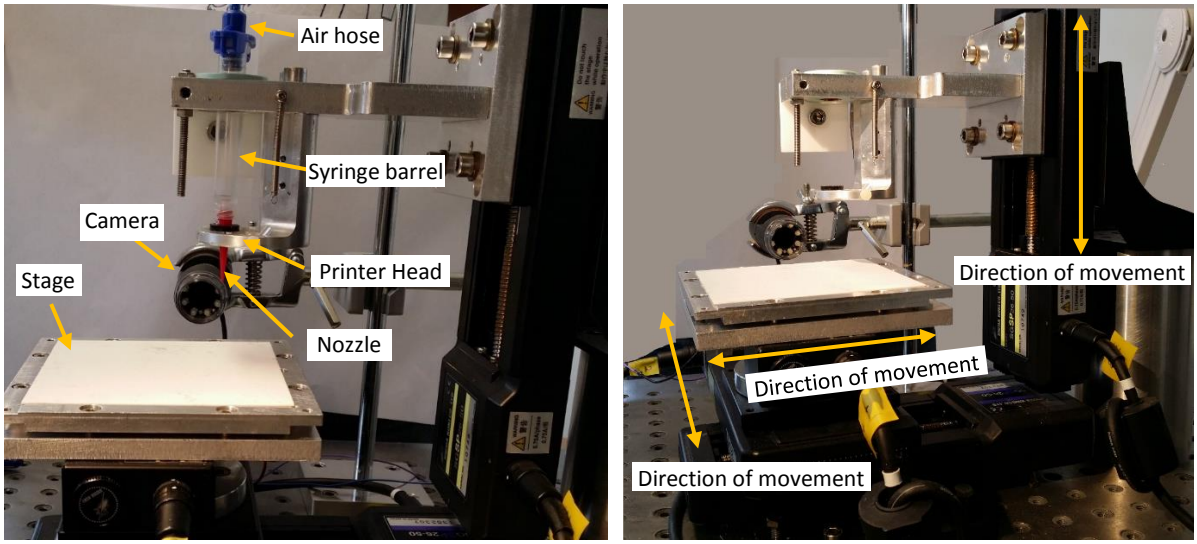

Figure 11: Images of the Dispenser Printer stages used in this research

The printer head used in this setup is only compatible with 3cc syringes due to its small size. A syringe barrel can be transparent or ultra violet blocking; UV blocking syringe barrels are used for UV sensitive inks.

A nozzle is attached to the outlet of the syringe barrel to direct the flow of the ink out of the syringe when pressure is applied. Different types of nozzles are available in a range of sizes down to 1 µm inner diameter [52]. Figure 12 below shows a 25 gauge (250 µm inner diameter) smooth tapered nozzle and a 30 gauge (150 µm inner diameter) blunt end nozzle. Nozzle types are selected to suit the ink; tapered nozzles are used for high viscosity inks as they allow smooth flow whereas blunt end nozzles are used for low viscosity inks to improve flow control. Nozzle sizes influence the speed and resolution of the printing process. Larger nozzle sizes dispense larger droplets/quantity of an ink which reduces the number of droplets/filaments required to fill a designated print area. This reduces the resolution of the print while increasing the speed of the process as fewer droplets/filaments cover a specified area compared to smaller nozzle sizes.

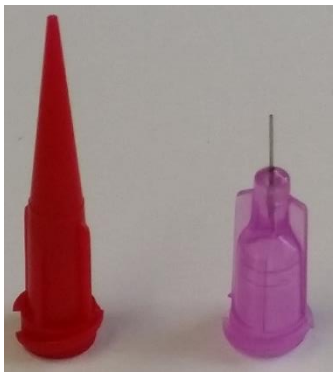

Figure 12: Dispenser printing nozzles 25 gauge smooth tapered (left) and 30 gauge blunt end (right)

The University of Southampton dispenser uses Sigma Koki SGSP26-50 stages, controlled by a Sigma Koki SHOT-204MS four axis stage controller. Table 4 below shows key information about the dispenser printer stages. This work makes use of a Nordson Ultimus™ V digital dispenser as the pressure controller. Table 5 shows the specification of the Nordson dispenser.

Printing Area	Maximum Speed	Resolution
27 cm^2	30 mm/s	2 µm

Table 4: Key information of the movement stages used in this research [66]

Parameters	Nordson Ultimus™ V
Output Pressure Range (kPa)	0-700
Dispense Time Range (s)	0-9.9999
Vacuum Range (kPa)	0-4.5
Vacuum Control	Digital

Table 5: Specification of the Nordson dispenser used in this research [67]

3.5.1 Dispenser printing parameters and modes of operation of the dispenser printer

The following parameters govern dispenser printing:

- **Resolution:** Resolution of the print is characterised by the gap between consecutive droplets/filaments in the x and y axis. The smaller the gap the higher the resolution and vice versa.
- **Nozzle height:** Nozzle height is the gap between the substrate and the printing nozzle.
- **Pressure:** The pressure applied to the contents of a syringe to force the ink out of the nozzle.
- **Dispensing time:** The time duration for which the pressure is applied on the ink to dispense it.
- **Vacuum:** A vacuum can be created in the syringe, providing a back pressure on the ink to avoid dripping between consecutive dots.
- **Dispensing speed:** This represents the speed of movement of the stage and time duration between consecutive dispensed shots of ink (frequency of shots).

The current iteration of the dispenser printer software can be operated in the following three modes:

1. **Droplet printing:** In this mode the ink is deposited on the substrate in the form of droplets. Successive droplets are deposited on the substrate in a straight line to form a print. The print pattern in the droplet mode is limited to squares and rectangles.
2. **Continuous printing:** In this mode the ink is deposited on the substrate continuously in the form of a straight lines/filaments.
3. **Bitmap printing:** This mode allows printing of patterns in the form of droplets. A bitmap image of the pattern is loaded into the software and the printer dispenses a single droplet for each pixel marked on the bitmap pattern.

Figure 13 presents diagrammatic representation of the three printing modes of the current University of Southampton dispenser printer.

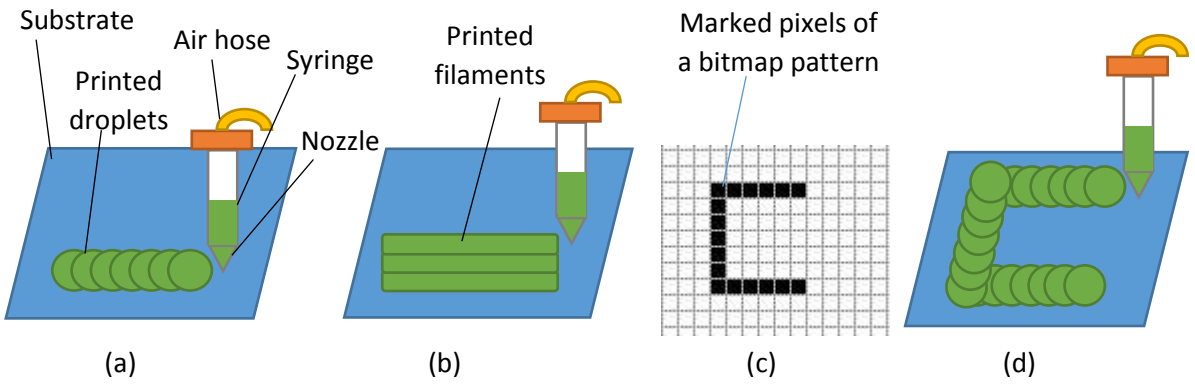

Figure 13: Diagrammatic representation of (a) droplet printing mode, (b) continuous printing mode, (c) digital bitmap template for bitmap printing mode (d) bitmap printing mode

The droplet mode is useful for dispensing a carefully controlled volume of an ink on the substrate. It is slower than the continuous mode and faster than bitmap mode. It is specifically suitable for dispensing low viscosity inks which would overflow by application of continuous pressure as in continuous mode. The overflow of an ink refers to dispensing a larger quantity of ink than that required to achieve a target print.

Continuous mode is the fastest printing mode; the ink is continuously dispensed as the nozzle moves from one point to another in a straight line as opposed to the droplet and bitmap mode where the nozzle stops and dispenses at every point defined by the resolution of the print. The X-Y stage is programmed to move at a fixed speed of 5 mm/s in continuous mode which makes it unsuitable for low viscosity inks as explained earlier.

Bitmap mode offers the ability to print patterns defined by a bitmap image. It is the slowest mode in this iteration of the software as the nozzle stops at every pixel defined on the bitmap image whether a droplet is required to be dispensed or not.

All three modes have been utilised in this research work. The first choice mode has been continuous as it is the fastest mode. It has been used for inks with a tendency to bleed that is spreading out of the designated print area. It reduces the time duration for which the uncured inks are present on the substrate which reduces bleeding. Most of the inks in this work were found to be incompatible with continuous mode as they overflowed even on the minimum dispense pressure because the maximum stage speed is too slow. They were therefore printed using droplet mode.

When an ink is dispenser printed on a substrate, either in the form of droplets or filaments, it coalesces to form a continuous print. The resolution of a print depends primarily on the X resolution, Y resolution, the nozzle diameter, dispensing pressure and the time the pressure is applied. The maximum dispenser printing speed is much slower than the maximum stage speed because of the time delays introduced during communication between the pressure controller, stage controller and the computer. The current dispenser printer does not have a mechanism to accurately measure the gap between the printing nozzle and the substrate. The gap or the nozzle height, in this study, is measured by lowering the nozzle until it touches the surface of the substrate and then this is considered the starting zero position. The distance by which the nozzle is moved away from the substrate in z-axis is the nozzle height. It is an estimated value as it is judged by observation since the nozzle can be just touching the surface or pressing into a substrate by 20 µm. The printer settings for an ink are influenced by the ink rheology and the required print morphology. The settings for each ink used in this study are determined by carrying out preliminary printing trials till the required output was achieved. The dispenser printer used in this work offers similar printing pressures 0-700 kPa,

comparable resolution down to 2 µm and a higher maximum printing speed of around 30 mm/s to the dispenser printers reported in the literature.

3.6 Effect of nozzle height variation on the flow rates of a dispensed ink

The flow rate of a dispensed ink is sensitive to the gap between the printing nozzle and the substrate [68]. An ink being dispensed through a nozzle on to a substrate experiences flow resistance due to the presence of the substrate. This flow resistance leads to a drop in pressure in the printing nozzle which affects the volume of the ink dispensed. Li et al [68] used a computational fluid dynamic model to study the effect of the gap between the nozzle and the substrate (nozzle height) on the pressure drop in the nozzle and the flow rates of a dispensed ink. Figure 14 below represents pressure drop in the printing nozzle as the nozzle height is increased from 5 µm to 30 µm.

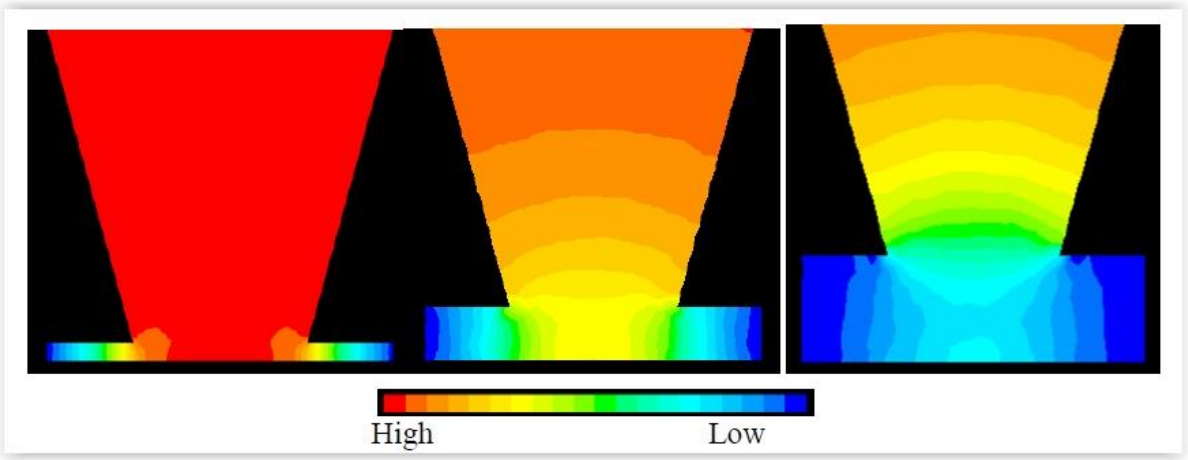

Figure 14: Pressure drop in the nozzle vs. the nozzle height, the nozzle height is 5 µm in the left most image, 15 µm in the centre image and 30 µm in the right image [68].

Figure 14 shows that the pressure drop in the printing nozzle reduces as the nozzle height is increased. A higher pressure drop in the printing nozzle leads to a lower flow rate of the ink which reduces the volume of an ink dispensed. Figure 15 shows the plot of nozzle height vs the flow rate of an ink at three different dispensing pressure values.

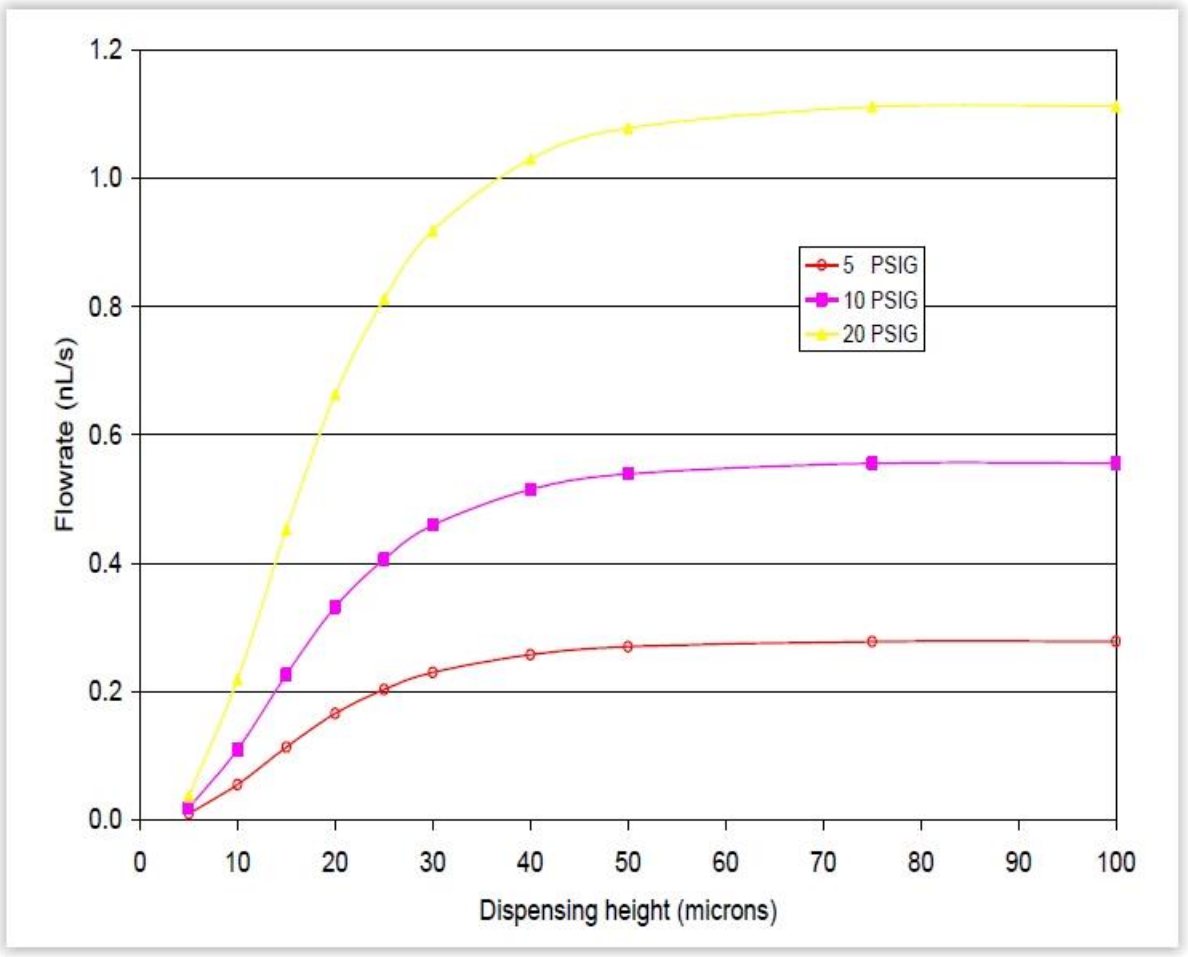

Figure 15: The effect of nozzle height (dispensing height) on the flow rate of a dispensed ink at three different dispensing pressures [68]

The plot shows that the flow rate of an ink is sensitive to the nozzle height at micron resolutions. It shows that, above a certain nozzle height value, a steady flow rate can be achieved. The flow rate is sensitive to a wider range of nozzle heights at higher pressures than at lower pressures. This shows that, during the dispenser printing process, variation in the nozzle height can lead to variation in the volume of an ink being dispensed in a printed design. Variation in the volume of the dispensed ink can lead to non-homogeneous printed structures where the thickness of the prints is non-uniform. In some cases the non-uniform printed structures may not affect the function of the print however in the case of functional inks, such as conductive and resistive inks, the non-uniformity affects their electrical properties such as electrical resistance. The variation in the gap between the printing nozzle and a substrate can be introduced by the variation in the surface of a dispenser printer stage and the substrate. Any surface variation in the printer stage can affect the geometrical homogeneity of a print; therefore it is important to assess the stage surface variation of the printer.

3.6.1 Surface variation of the dispenser printer stage

The stage surface variation of the dispenser printer used in this study was measured using LM-10 ANR1251 micro laser displacement sensor. The displacement sensor has a measurement range of 20 mm and resolution of 1 µm [69]. The sensor was mounted on a retort stand using a clamp directly above the X-Y movement stage by removing the Z movement stage as shown in figure 16. The x-y movement stage and the displacement sensor were programmed for the stage variation measurement using the National Instruments Lab View software. This arrangement for measuring

stage surface variation is directly relevant to the dispenser printing process as the displacement sensor's position is fixed and the x-y stage is moved for surface scanning.

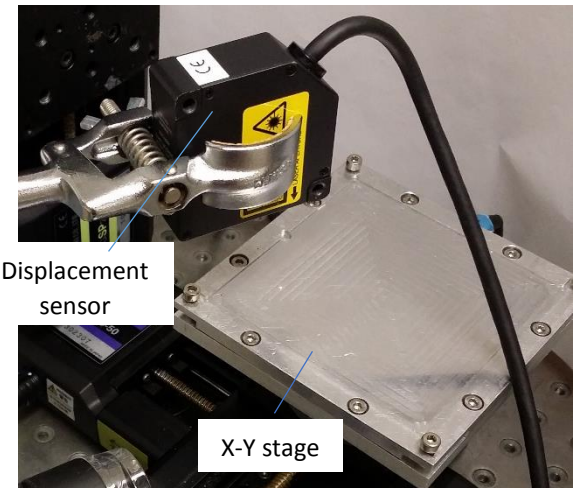

Figure 16: The laser displacement sensor mounted over the dispenser printer X-Y movement stage for measurement of stage surface variation

The output voltage of the sensor was fed into a computer using NI USB 6008 data acquisition device (DAQ). The DAQ device introduced electrical noise in the sensor output causing the output voltage signal to vary by 6 mV peak to peak. The noise was introduced due to the limited accuracy of the DAQ device in measuring the input voltage. The effect of the noise was reduced in the measurements by filtering the high frequency components in the Lab View software using a low pass filter and obtaining an average of the filtered voltage signal. This combination of the software and the hardware setup reduced the accuracy of the displacement sensor to ±5 µm. The accuracy of the setup was determined by measuring twenty known heights ranging from 2 µm to 1 mm. Each measurement is taken after the displacement sensor is positioned at a specific measurement spot for 30 seconds to allow consistent readings.

The dispenser printer stage surface was scanned five times at a scan resolution of 2 mm. The selected scan resolution measures 729 points on the printer stage which provides a reasonable estimation of the stage surface variation. The five scans are averaged, the average of the five scans is presented as a 3-D graph and surface variation map in figure 17 and figure 18 respectively.

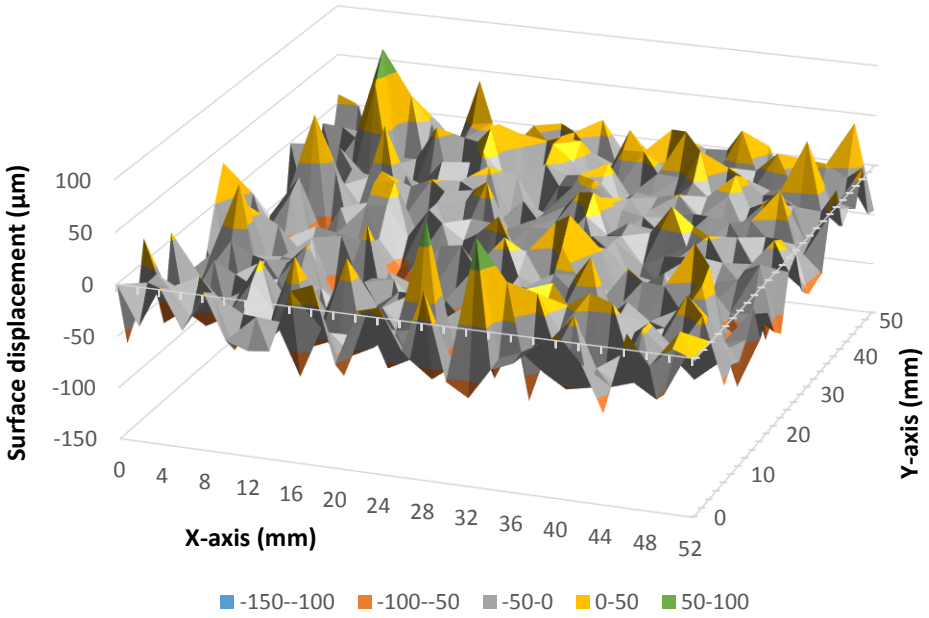

Figure 17: The surface variation 3-D graph of the dispenser printer stage scanned at a resolution of 2 mm

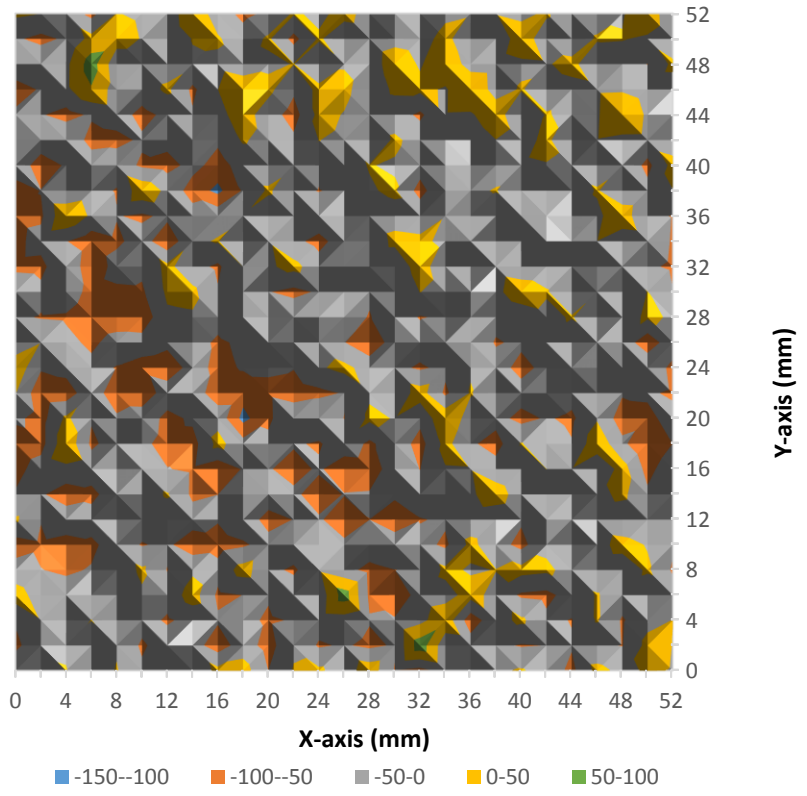

Figure 18: The surface variation map of the dispenser printer stage scanned at a resolution of 2 mm

The two surface variation graphs presented in the figures above show that the dispenser printer stage surface varies significantly with a peak to peak variation in the range of -150 µm – 100 µm. The starting point of the scan is the zero reference point, the surface displacement of every other point in the scan is measured with respect to the zero reference point. The graphs show that the stage surface

displacements do not show any specific pattern and are randomly distributed. Table 6 below shows the average surface displacement and the peak to peak surface displacement of the printer stage with respect to the zero reference point.

Average surface displacement (µm)	32 ± 5
Peak to peak surface displacement (µm)	194 ± 10

Table 6: The average surface displacement and the peak to peak surface displacement of the dispenser printer stage surface

The stage surface data shows that it has an average displacement of 32 µm and a peak to peak variation of 194 µm. The stage surface displacement is of the order of microns which shows that the printer stage to a large extent is flat however generally the nozzle height used is also of the order of microns making the surface variation significant. This shows that the current dispenser printer stage in the absence of a nozzle height measuring and adjusting mechanism is prone to introducing variation in the nozzle height. A substrate placed directly on the stage can lead to geometrically inconsistent printed structures.

In this study a substrate is prepared for dispenser printing by gluing it to an alumina tile to avoid folding or creasing the fabric during the printing process and then placed on the dispenser printer stage for printing. The alumina tiles used are 635 µm thick with a thickness tolerance of ± 60 µm and average surface displacement of 0.8 µm; the tiles and the associated data are supplied by Hybrid Laser Tech ltd. The use of alumina tiles for dispenser printing helps reduce the effect of printer stage surface variation as the average surface displacement is reduced to 0.8 µm and the highest expected peak to peak variation is 120 µm estimated from the thickness tolerance of the tiles.

3.7 Fabric selection for dispenser printed thermochromic devices

Woven polyester cotton 65/35 blend fabric supplied by by Klopman International is selected as the fabric substrate for fabrication of dispenser printed thermochromic devices. Polyester cotton blends combine the durability and tear resistance of polyester with the breathability and comfort of cotton. They are common fabrics used in a wide variety of applications such as garments, furnishings and exhibition canvases. Traditional printed electronic substrates such as Kapton and FR4 present a smooth and low porosity surface where an ink can be uniformly deposited. The polyester cotton 65/35 blend has a loose and porous structure with high surface variation which makes printing on it very challenging. There are two major advantages of using polyester cotton 65/35 fabric in this study. Firstly, due to the loose porous structure and high surface variation, the optimisation of dispenser printed heaters and thermochromic devices on the polyester cotton fabric can be replicated on most fabrics with similar or lower surface variations. Secondly, the use of polyester cotton 65/35 blend for fabricating thermochromic devices can help integrate the thermochromic technology into the wide variety of applications which make use of polyester cotton fabrics.

3.7.1 Fabric surface topography characterisation

Surface topography can be characterised by measuring the roughness and waviness of a surface. Surface roughness can be defined as fine irregularities of a surface compared to its ideal form [70]. Waviness is widely spaced deviations of a surface compared to its ideal form [70]. Figure 19 represents surface roughness and waviness. A surface topography is represented by its primary form which is the combination of the roughness and waviness of a surface.

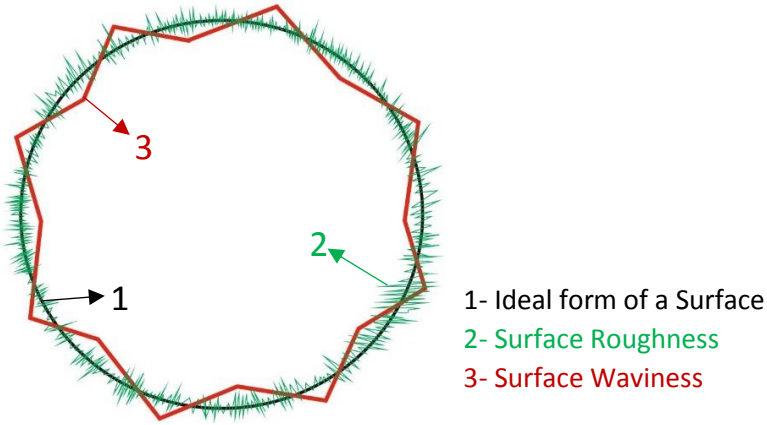

Figure 19: Diagrammatic explanation of surface roughness and waviness

The surface topography characterisation in this work has been performed using two types of profiler: a KLA Tencor P-11 contact profiler and an Alicona infinite focus microscope (IFM) non-contact profiler. The P-11 Tencor has a stylus that moves laterally across a sample. It measures the vertical displacement of the surface through displacement of the stylus as a function of position. The start point of the scan serves as the zero reference and displacement is measured with respect to it. It produces 2-D graphs of the scanned samples which show surface deviations and correlated with lateral displacement. The Alicona infinite focus is an optical profiler that relies on focus variation to produce 3-D scans of a sample. It combines a small depth of focus with vertical scanning to obtain a set of images where parts of the sample are in focus and combines this data to produce a 3-D data set. The surface deviations in the Alicona are measured with respect to a reference plane instead of a zero reference point. The reference plane is selected by the software based on the plane where most points of the data set fall on zero displacement.

The non-contact optical profiler is an improvement over the contact profiler as the topography measurements are not affected by the lay of a print because it can measure a surface as a 3-D dataset. Lay refers to the direction of the dominant pattern of a surface, it is diagrammatically presented in figure 20. The optical profiler also allows measurement of larger surface areas compared to the contact profiler. Alicona is a more modern profiler compared to P-11 with a better support software which offers several post processing features such as 3-D images of the scans and filtering roughness and waviness data from the primary form. This shows that Alicona is the more suitable profiler for surface topography measurement of the fabric therefore the results of the contact profiler are not presented in this thesis.

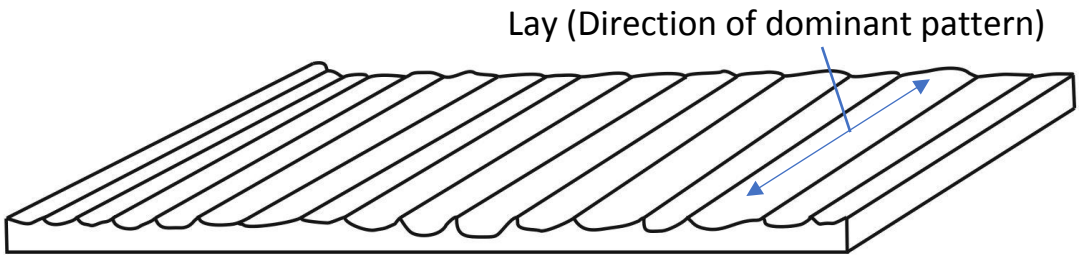

Figure 20: Diagrammatic representation of lay

A surface topography parameter ‘Sa or Pa’ can be used to quantify surface variations. Sa and Pa parameters are the arithmetic mean of absolute values of surface variations as shown by equation 1 and equation 2. Sa represents areal 3-D surface measurements where Pa represents 2-D profile measurements.

Equation 1 [12]: $Sa = \frac{1}{A}\iint_A |z(x,y)|dxdy$ where A = measurement Area, z = surface displacement

Equation 2 [71]: $Pa = \frac{1}{l}\int_0^l |z(x)|dx$ where l = measurement Length, z = surface displacement

The Sa and Pa measurements represent the primary form of the measured surface which includes the variations due to both roughness and waviness.

The fabric surface was scanned three times at a magnifications of 5x and vertical resolution of 410 nm using the Alicona infinite focus microscope. 5x magnification was found to be the most suitable magnification level for scanning the fabric surface as a lower magnification of 2.5x compromised the detail which was obtained using 5x magnification. A higher magnification of 10x was unable to completely scan the fabric surface due to the high variation of surface topology. The fabric was first glued to an alumina tile to hold it flat during the scanning process to avoid measurement error due to folding and creasing. The surface of the fabric was shaved to remove any fabric pills so that the fabric pilling doesn't affect the scanning process. This gluing and shaving process is also followed for the same reasons when printing and therefore scanning the same way produces a more directly relevant result. The scans produced an average Sa value of 34 µm; figure 21 below shows the 3-D image obtained from the scans.

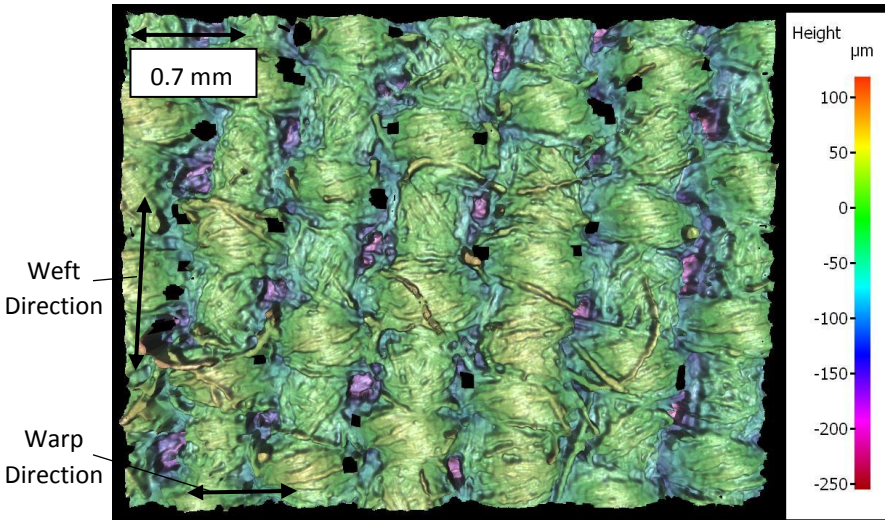

Figure 21: 3-D image of polyester cotton 65/35 blend surface at 5x magnification

Figure 21 shows that the polyester cotton 65/35 fabric has a high surface variation with a peak to peak variation of about 270 µm. It shows that the fabric surface has a dominant pattern in one direction labelled as the weft direction. The black spots in the middle of the scanned 3-D image indicates missing data points; missing data points can arise due to unsuitable illumination at those specific points which in this case are caused by steep variation in the surface topology.

An ink deposited directly on the surface of the fabric is highly likely to conform to the fabric surface and form a geometrically inconsistent structure due to the high fabric surface variation. Inconsistent geometry can adversely affect the performance of printed conductive tracks. The electrical properties of printed conductive tracks are important to consider in the context of this research as dispenser printed heaters are based on printed conductive tracks. In the context of the wider smart fabrics field conductive tracks are essential to form electrical interconnections to embed any electronic functionality in fabrics. It is therefore critical to investigate the effect of fabric surface variation on the printing of conductive tracks.

3.8 Effect of the fabric surface variation on the printing of conductive tracks

Ten 30 mm x 2 mm silver conductive tracks were dispenser printed on Kapton and the fabric substrate to analyse the impact of surface variation on the electrical resistance of the tracks. Kapton, a traditional printed electronics substrate, is used as a reference because it has a non-porous structure with considerably lower surface variation of 1.30 µm compared to the fabric. The surface variation of the Kapton was measured using the Tencor P-11 contact surface profiler because it could not be scanned using the optical profiler due to its glossy and reflective surface. It was glued to an alumina tile to hold it flat during the profiling process and to make the result directly relevant to the practical printing process. The Kapton surface Pa value of 1.30, ± 0.59 µm was calculated by averaging scans of five different sheets of Kapton glued to alumina tiles. AFM measurements, from the literature, of Kapton films without the glue produced root mean square (RMS) surface roughness values of 1 nm [72]. Therefore, the majority of the variation in the Kapton surface measured here is introduced by the layer of glue. The standard deviation of ± 0.59 µm of the Kapton surface Pa values is therefore believed to represent variation in the gluing process.

The printing of conductive tracks required a silver ink which was flexible once cured, screen printable and has a low curing temperature of ≤ 150°C. DuPont 5000 was selected as the suitable silver ink as it fulfils the three requirements. Table 7 below shows the properties of DuPont 5000 silver ink. Several preliminary dispensing trials were carried out to determine the suitable dispenser printer settings for printing the silver ink. The aim of the trials was to achieve a set of dispenser printer settings which completely covered a defined printed area. The ink was printed in droplet mode so that the settings were compatible with the bitmap mode which was required for printing the heaters using this silver ink. The dispenser printer settings used for printing the silver ink is presented in table 8.

Resistivity (Ω.m)	≤ 3.81 E-07
Viscosity (Pa.S)	3.5-16.0
Curing Temperature (°C)	120
Curing Time (mins)	8-10

Table 7: Properties of DuPont 5000 silver ink

Pressure (kPa)	52.5
Dispense Time (ms)	11.0
X-resolution (mm)	0.50
Y-resolution (mm)	0.40
Nozzle Height (µm)	150
Vacuum (kPa)	1.5
Speed (mm/s)	1

Table 8: Dispenser printer settings for printing the DuPont 5000 silver ink in droplet mode

Figure 22 shows the dispenser printed silver tracks on Kapton and the fabric substrate. The ink droplet coverage was more consistent and uniform on Kapton which is shown by the more even deposition of silver on Kapton than fabric.

(a) (b)

Figure 22: Silver conductive tracks on (a) Kapton (b) Untreated polyester cotton fabric

Track thickness was measured using a Mitutoyo micrometer which can measure thickness down to 1 µm. Track width was measured down to 1 µm using Nikon Eclipse microscope. Each track was measured at five equidistant points along its length and the result was averaged. Track resistance is measured using a Wayne Kerr 6500 B precision impedance analyser. It offers a four point probe measurement method and the probe spacing is not fixed. Resistance of each track is an average of five resistance measurements at room temperature. Table 9 below shows the average track thickness, average track widths and the resistance of the 10 tracks printed on Kapton and the fabric each along with the Sa/Pa values of the two surfaces.

	Kapton Plastic Film	**Polyester Cotton Fabric**
Avg. Sa/Pa Value (µm)	1.30	34.00
Avg. Track Thickness (µm)	14.5	18.6
Avg. Track width (µm)	2211	1945
Avg. Track Resistance (mΩ)	483	2036

Table 9: Average Sa/Pa values, track thickness and track resistance of tracks on Kapton and polyester cotton fabric

The results show that tracks printed on the fabric have about 322 % higher average resistance than the tracks on Kapton. The tracks on fabric, on average, are 28% thicker and 12% narrower. The resistance of a printed track is a function of the resistivity of the constituent material and the physical dimensions of the track as in equation 3.

Equation 3: $R = \rho \frac{l}{A}$ R = Resistance, ρ= resistivity, l= length, A = Crossectional area

According to equation 3 thicker tracks of the same width are expected to produce lower resistance. For the fabric experimetal results shown in table 9, the larger thickness is partially compensated by the narower width for the same volume of dispensed material. For constant silver volume the area of the printed tracks should also be constant, but, in case of fabric, the irregular deposition caused by the surface variation means it is not. If the silver layer on fabric was uniform, as in case of Kapton, the thickness difference would be fully compensated by the width difference.

The tracks were further analysed to confirm if the electrical resistance was uniformly distributed throughout the physical geometery of the tracks. A novel method based on the concept of resistive heating was developed for analysing the resistance distribution in a printed conductor. An electrical current passing through an electrical resistance produces heat directly proportional to the resistance. The resistance distribution in a printed track is analysed by assessing the heat distribution of the tracks upon passing an electrical current through the tracks for fixed amount of time. The regions with higher resistance attain a higher temperature. A non-uniformly heated track indicates non-uniform resistance distribution. The tracks printed on Kapton and the fabric are assesed by passing 0.50 A

current through each track for 50 seconds which produces resistive heating. A thermal image is then captured using a Testo 875 thermal imager to acquire heat distribution data. Figure 23 below shows the heat distribution from 10 separate thermal images of five tracks on Kapton and fabric. The 10 assessed silver tracks produced varying amounts of resistive heating due to their different overall resistances and achieved different maximum temperatures. Therefore, the 10 thermal images could not be represented using the same scale; the scale shown in figure 23 indicates relative temperature within a track for assessing heat distribution rather than the absolute temperature.

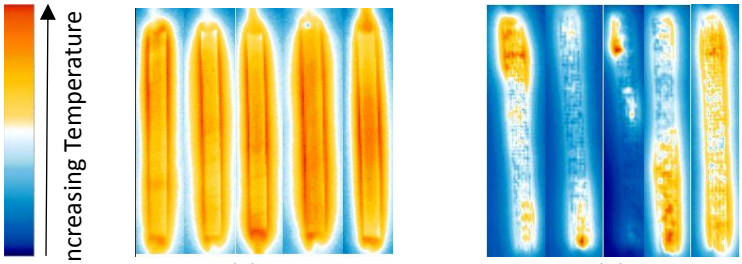

Figure 23: Heat distribution of silver conductive tracks on (a) Kapton and (b) polyester cotton fabric

It can be seen that the heat is relatively uniformly distributed for the tracks on Kapton whereas the heat is concentrated in specific regions for the fabric tracks which show non-uniform resistance distribution within the tracks. The printed tracks were further analysed using cross-sectional SEM images of the silver tracks printed on Kapton and the fabric which is shown in figure 24.

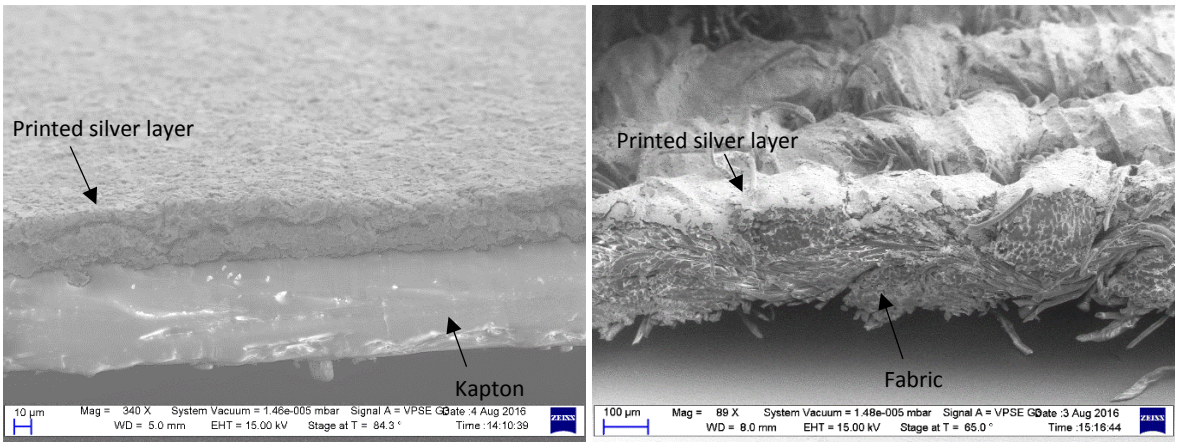

Figure 24: Cross-section of silver track printed on (a) Kapton (b) untreated polyester cotton fabric

The SEM images show that silver ink particles conformed to the surface pattern of the substrate on which they were printed. The printed silver layer on Kapton formed a geometrically consistent structure whereas the printed silver layer on fabric produced a non-uniform structure. Variation in geometry and thickness of the silver layer on fabric caused resistance variation within the tracks. The inconsistent printing of silver tracks on fabric can be attributed to high surface variation and the loose porous structure of the fabric. By comparison, the tracks printed using the same printing parameters and method on Kapton resulted in a uniform silver layer, significantly lower average resistance and a uniform resistance distribution. This result confirms that the printing process produces fairly uniform prints and that it is the substrate which dominates any variation seen in the final printed layers.

3.8.1 Impact of fabric structure orientation on printed conductive tracks

The polyester cotton fabric surface has a dominant pattern in one direction as shown in figure 21 which is called the weft direction with the warp direction being orthogonal. This makes it vital to

analyse if the orientation of the fabric structure geometrically affects the printed conductive tracks. Two sets of five 30 mm x 2 mm DuPont 5000 silver tracks were dispenser printed on the fabric using the settings shown in table 8 to assess the impact of fabric orientation on the printed tracks. The first set of tracks was printed with print direction along the dominant weft pattern and second set of tracks was printed with print direction orthogonal to the dominant pattern. Table 10 below shows the average thickness and resistance of both sets of tracks along with their standard deviation.

Print Direction	**Weft**	**Warp**
Avg. Track Thickness (µm)	27.8 ± 4.2	26.0 ± 1.6
Avg. Track Resistance (mΩ)	1658 ± 375	2045 ± 322

Table 10: Average track thickness and track resistance of tracks printed in fabric weft and warp directions

The results show that tracks printed in the fabric weft direction produce about 19 % lower resistance than tracks printed across the weft direction. The two sets of tracks resulted in a similar resistance variation, shown by the standard deviation, however the thickness variation was higher in tracks printed in the weft direction. The impact of the fabric structure orientation was further analysed using planar SEM images of tracks printed in the weft and warp directions as shown in figure 25.

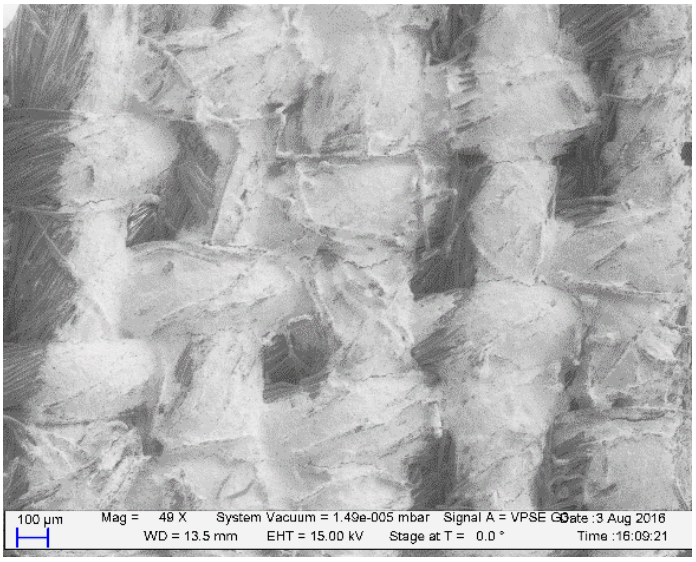

(a)

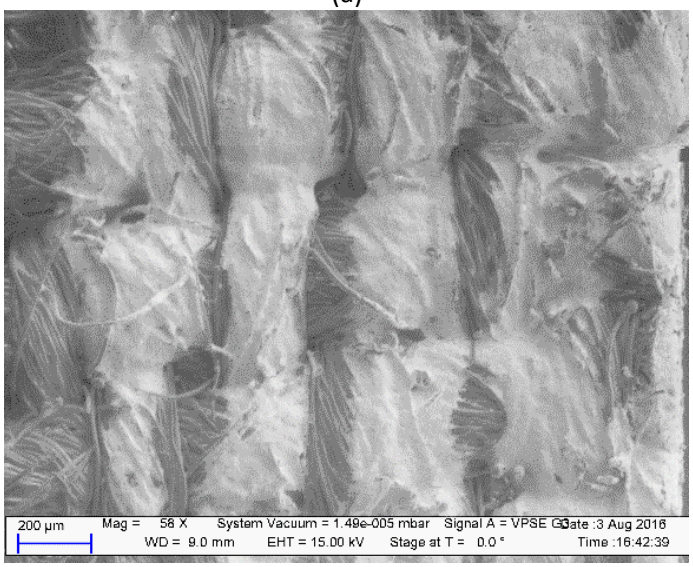

(b)

Figure 25: Planar view of a printed silver track (a) following the weft direction (b) following the warp direction. Lighter regions represent silver layer, darker regions show the original fabric surface

The SEM images show that the track printed in the weft direction has a larger section of surface covered with silver than the track printed in the warp direction. The fabric surface profile varies more across the dominant pattern than along it which leads to a higher thickness variation in the printed silver layer causing the tracks to a produce higher average resistance.

3.8.2 Conductive tracks consisting of multiple print passes on the fabric

The conductive tracks printed in the previous sections do not completely cover the fabric surface using a single deposition/pass of the silver ink. A print pass can be defined as a single deposition of the ink in a designated print area using a specific set of print settings. This section investigates if printing multiple passes of the ink reduces the overall resistance of tracks and makes them comparable to tracks printed on Kapton. Five 30 mm x 2 mm DuPont 5000 silver tracks were printed directly on the fabric surface using the settings shown in table 8. Each of the five tracks was printed with an increasing number of print passes starting from one pass up to five passes; this was repeated 3 times. Each print was cured once the required number of print passes was reached. Figure 26 shows one set of tracks

consisting of increasing number of print passes alongside its thermal image and figure 27 relates the number of print passes with track thickness and resistance.

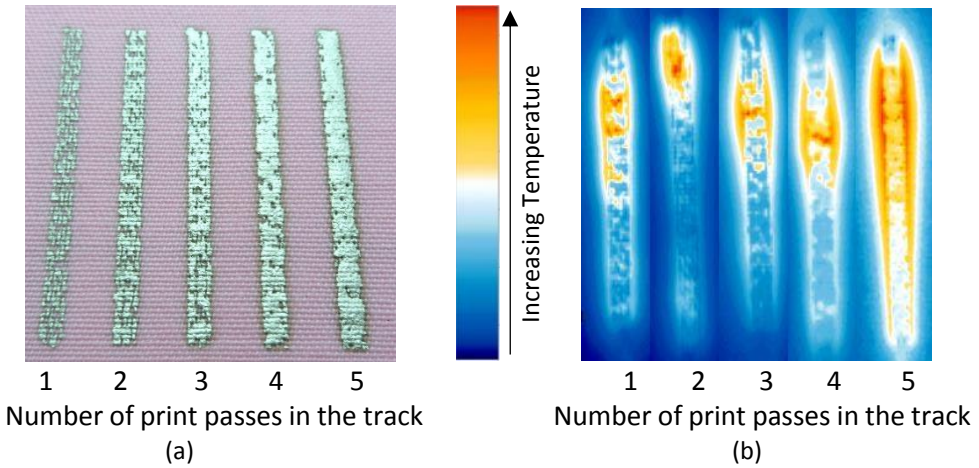

Figure 26: Tracks printed directly on fabric consisting of multiple print passes (a) image (b) thermal image

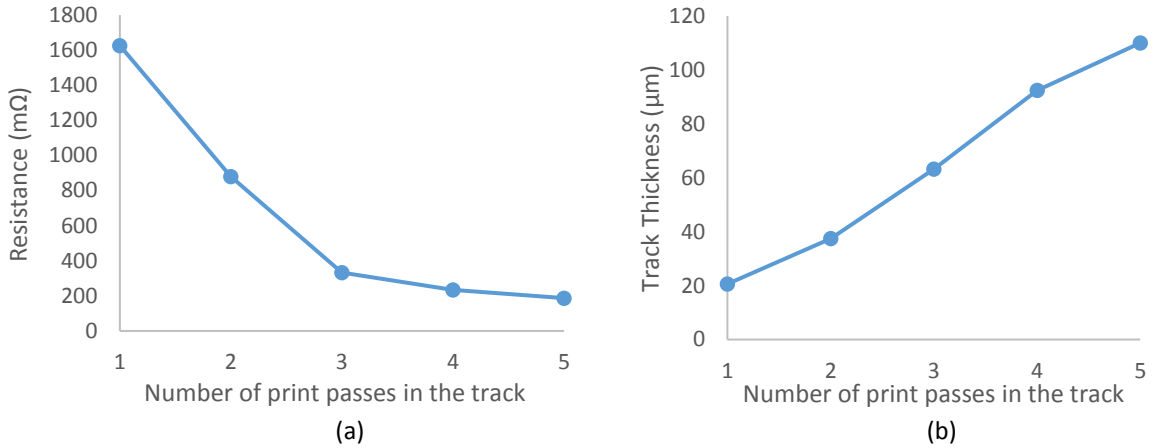

Figure 27: Change in average (a) resistance (b) thickness of tracks with increasing number of print passes

The results show that increasing the number of print passes increases the thickness of the tracks which reduces the resistance of the tracks. The reduction in resistance is attributed to increased thickness and improved silver coverage instead of improved uniformity, which is shown by the heat distribution of non-uniform resistance of the tracks in figure 26. The heat distribution does not show any specific relationship with the number of print passes although the track consisting of five passes produced more even heat distribution than the other tracks. The results also show that approximately three passes of silver are required on the fabric to achieve a similar resistance to the average resistance of the tracks on Kapton. Three times the quantity of expensive silver ink is required on fabric, as defined by the number of print passes, to produce a track with similar resistance to that on Kapton. Despite printing three times the quantity of the silver ink directly on fabric the heat distribution of the tracks remain largely non-uniform unlike the Kapton tracks.

The results show that printing the silver tracks directly on the fabric surface is unsuitable for printed heaters as it would produce heaters with a significantly non-uniform heat distribution. In the wider context of smart fabrics, an increased focus on low powered electronics requires the electrical interconnections to dissipate the minimum of power. Any amount of current passing through a resistance would dissipate power as resistive heating; therefore it is important to fabricate and design

the interconnections with the lowest possible resistance. This shows that it is vital to reduce fabric surface variation to improve the uniformity and consistency of printed electronic layers to produce heaters with more uniform heat distribution. Overcoming the fabric surface variation would also enable printing of low resistance electrical interconnections for general smart fabric applications.

3.9 Dispenser printable method of overcoming fabric surface variation

This section presents a dispenser printable method of overcoming the fabric surface variation to improve the geometrical consistency of printed structures and especially printed conductors. The dispenser printable method consists of printing an interface layer on the fabric surface to form a low variation surface and to strengthen the loose fabric structure to provide a platform for subsequently printed layers.

Previously researchers have used lamination, screen printing of dielectric inks and coating as methods of reducing the fabric surface variation. Karaguzel et al [73] used thermoplastic urethane lamination as a method of overcoming fabric surface variation. Lamination completely covers a fabric surface reducing the breathability and flexibility of the fabric and adds to the number of processes required for producing electrical interconnections. A fabric can be selectively laminated by cutting individual pieces of laminating material and applying it; however it is difficult to align individual pieces in a pattern and this method is less suitable for mass production. A screen printed polyurethane based ink (Fabinks-IF-UV-1004) developed at the University of Southampton has been used previously as an interface between a fabric surface and conductive tracks. The interface layer reduced fabric surface variation for the printing of conductive tracks [74,75]. The interface ink can be selectively printed in a specific pattern, however, each design requires a specific screen and two different screens would be required to print the interface and the subsequent electronic layer. Suh et al [76] coated fabric surfaces with polyurethane, silicone and acrylic resin using brushing to improve surface quality for printed antennas. Brushing as a coating method offers limited control of the coating pattern and the amount of a material coated on a surface. Although [73, 74, 76] mention that lamination, screen printing and coating can be used to improve the fabric surface for printing conductive tracks, they do not characterize the fabric surface variation before or after treatment so the effectiveness of the employed approaches cannot be analysed. In [75] the fabric surface has been characterised which shows the extent of improvement in surface variation but the significance of the improvement in fabric surface is not shown.

Four dielectric inks DuPont 5018, Electra EFV4/4965, Fabinks-IF-UV-1004 and FB-20 are identified as suitable interface inks for the dispenser printing process. DuPont 5018 and Electra EFV4/4965 were shortlisted as suitable interface inks during the EU FP7 MICROFLEX project [77] by the University of Southampton. Fabinks-IF-UV-1004 dielectric ink was specifically developed as a screen printable interface ink to overcome fabric surface variation. FB-20 ink was developed as part of this research and its development is discussed in section 5.2.2. All four inks are UV curable, compatible with fabrics, produce flexible dielectric films and are suitable for screen printing. An ink suitable for screen printing can also be dispenser printed as dispenser printing is able to print a broader range of ink viscosities compared to screen printing. PVC and silicone based inks were considered as interface inks but when cured these materials produce very low surface energy films, which do not allow subsequently printed inks to properly wet their surface leading to incomplete printing and this presents a significant challenge for subsequently printing additional inks on top of films of PVC or silicone. Therefore, the four inks were investigated as potential dispenser printed interface materials.

The investigation of the four inks is based on an assessment of surface consistency, thickness consistency, repeatability, flexibility and thermal stability. The five criteria represent parameters that

would directly affect the printing of electrical interconnections on a fabric substrate. The best interface ink would have the most consistent surface, lowest thickness variation, and highest repeatability to provide a reliable platform for printing of electronic layers. It would also be most flexible to avoid the fabric becoming rigid. The interface is also required to have a high thermal stability to suit thermally curable inks such as the silver ink. However none of the evaluated inks may be the best in every category, in which case the best interface ink can be selected based on requirements of a specific smart fabric application.

The first step in this investigation was to find the optimum print settings for the four dielectric inks. The target parameters for the optimisation process are as follows.

- Sa between 0.71 µm to 1.89 µm
- Thickness of print ≤ 300 µm

The target Sa was chosen for the printed interface to produce a similar surface to that of a Kapton film glued to an alumina tile as this presents the ideal surface for printed electronics. The target thickness was chosen to be more than the peak to peak variation of the fabric structure which is 250 µm as shown in figure 31. All of the interface inks were printed in continuous mode as it is the fastest printing mode. The fastest option was chosen to reduce the amount of time an interface ink deposition remained uncured on the fabric surface which reduced the bleeding of the printed pattern via wicking into the fabric. All of the dielectric inks are UV curable and prints were cured using a Panacol-Elosol UV-P 280 ultraviolet point source with a 400 W Hg Bulb. The prints were exposed to the UV radiation of 2000mW/cm^2 for 60 seconds to cure.

The optimisation scheme used for the prints consisted of the following steps.

- Firstly a set of printer settings that result in the thinnest layer of ink completely filling the designated print area was obtained through varying the dispense pressure and resolution parameters. Pressure was varied in the range of 5 kPa to 80 kPa whereas Y-axis resolution was varied between 0.2 mm to 0.4 mm.
- The layer thickness was then increased by increasing the pressure and resolution in steps of 0.5 kPa and 0.01 mm till the Sa target was met.
- The first layer was visually examined for ink absorption in the fabric structure. If parts of the print were absorbed in the fabric a second layer was printed on top of the cured first layer to improve surface homogeneity.
- The second layer was initially printed using the same settings as the first layer. The layer thickness was then increased or decreased based on the Sa and thickness of the prints till the Sa value and thickness targets were reached.

Table 11 below shows optimum settings and number of layers for each of the four interface inks.

	DuPont 5018		**Electra 4965**	**Fabinks-IF-UV 1004**		**FB-20**
Layer Number	1	2	1	1	2	1
Pressure (kPa)	6.0	6.0	20.0	17.5	15.0	40.0
Y-resolution (mm)	0.20	0.38	0.20	0.40	0.25	0.26
Nozzle height (µm)	100	100	200	200	200	150
Vacuum (kPa)	0.5	0.5	1.5	0.4	0.4	1.0
Speed (mm/s)	5	5	5	5	5	5

Table 11: Optimum dispenser printer settings and number of layers for the four interface inks

Twenty 20 mm x 20 mm samples of each ink were printed using the optimised settings shown in table 11 for assessment as interface prints. The volume of ink in the syringe was maintained throughout the printing process by regularly refilling it after each print. All of the interface prints for each ink were printed on the same 20 mm x 20 mm area of the printer stage to keep the printer stage variation constant for each print. Figure 28 below shows each of the four interface inks printed on the fabric. The following subsections present the evaluation of prints of each of the four inks in terms of surface consistency, thickness consistency, repeatability, flexibility and thermal stability.

(a) (b) (c) (d)

Figure 28: Interface prints on polyester cotton (a) DuPont 5018 (b) Electra EFV4/4965 (c) FB-IF-UV-1004 (d) FB-20

3.9.1 Surface consistency evaluation of the interface prints

The surface consistency evaluation of the four inks was carried out to determine the degree of variation in the surface of the prints. The surface topography of all the prints was measured at 10x magnification using the Alicona optical profiler. Each print was scanned at the four corners (2mm from the boundaries of the print) and at the centre of the print. The five spots were chosen to maintain consistency of the measurements across the 20 prints of each of the four inks. The surface topography measurement of each print (Sa_1) was obtained by averaging the five Sa measurements. Surface consistency of the dispenser printed output of each ink was assessed in terms of the following.

- Average Sa_1 across the 20 prints of each interface ink.
- Average Sa variation per print for the 20 prints of each interface ink (Sa_{sd}).

Average Sa variation per print (Sa_{sd}) is calculated by first calculating the standard deviation of the five Sa measurements for each print and then averaging it for the 20 prints. Smaller Sa_1 and Sa_{sd} values show that a surface has a smoother topography with lower deviations.

3.9.2 Thickness consistency evaluation of the interface prints

An interface print is not entirely uniform and can have thickness differences within it. Thickness of each interface print (T_1) is calculated as the average of five thickness measurements taken at the same positions on the printed layer as the surface topography scans. Thickness is measured using a Mitutoyo micrometer. Thickness consistency is measured by calculating the average of T_1 for the 20 prints and average thickness variation per print for the 20 samples of each ink (T_{sd}). It is calculated by first calculating the standard deviation of the five thickness measurements per print and then averaging it for the 20 prints of an ink. It reflects the degree of thickness variation within each interface print on average.

3.9.3 Repeatability of surface topography and thickness of the interface prints

The repeatability of the process analyses surface topography and thickness variation across the 20 interface prints of each ink when the printing parameters are kept constant. It is defined by calculating the following.

- Standard deviation of Sa_1 for 20 prints of each ink
- Standard deviation of T_1 for 20 prints of each ink

The higher the value of the two parameters the lower the repeatability and vice versa.

3.9.4 Flexibility comparison of the interface prints

A fabric cantilever test is used to measure the flexibility of the interface prints of the four inks. Flexibility of the prints was assessed by measuring the bending angles produced by a cantilever structure consisting of a strip of fabric with a printed interface when a mass was attached to them. Figure 29 below shows a schematic of the fabric cantilever test.

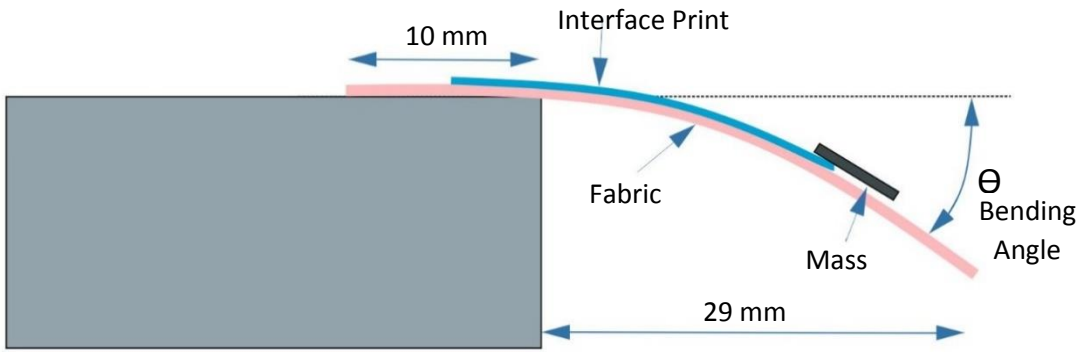

Figure 29: Schematic of the fabric cantilever test

Ten prints of each ink were used for these flexibility tests. The fabric containing the interface prints was cut into strips of 39 mm x 20 mm in the format shown in figure 30 below. One end of the fabric was taped to an aluminium stand and the other end was suspended with two 4.7 g magnets attached to it. The suspended prints would flex producing a bending angle which was recorded; the higher the bending angle the more flexible the printed layer.

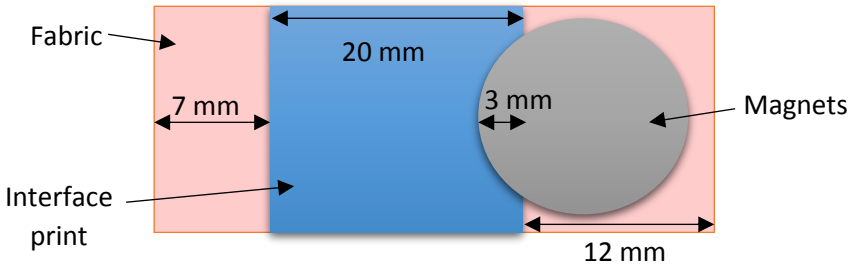

Figure 30: Format of the fabric strips containing the interface prints for flexibility testing

3.9.5 Thermal stability evaluation of the interface prints

The aim of the thermal stability evaluation of the interface prints is to establish the response of the interface prints to heating. Five prints of each of the four inks were cut into the strips shown in figure 30. Thermal stability of the prints was analysed by heating the prints on a hotplate at 100°C for 10 minutes and measuring any change in mass using an Ohaus Voyager Pro balance which can measure mass down to 1 mg. The prints didn't produce any change in mass although the prints twisted when heated as shown in figure 31. When heated to 120°C for 8 minutes, to represent the DuPont 5000 silver ink curing conditions, the prints twisted to varying degrees with three corners of the strips in contact with the hot plate and one corner rising which can be observed in figure 31 (b). The displacement of the highest corner was measured and is presented in the results section as a reflection of thermal stability of the prints. The prints returned to their initial state after they were cooled down to room temperature.

(a)

Fabric strips with interface prints

Hot plate

(b)

Figure 31: Interface prints of the four inks (a) before being heated (b) heated to 120°C for 5 minutes

3.9.6 Results of the interface inks evaluation

The results of the interface evaluation are shown in table 12 below. The results table in addition to surface consistency, thickness consistency, repeatability, flexibility comparison and thermal stability includes viscosity and a percentage fabric surface improvement comparison of the interface inks. Viscosity of the inks was compared to identify any correlation it has with the above mentioned parameters. It was measured using a Brookfield CAP1000+ viscometer. The fabric surface improvement parameter defines the improvement in fabric surface topography characterised by the Sa values of fabric and interface surfaces.

	DuPont	**Electra**	**Fabinks 1004**	**FB-20**
Number of Layers of Optimum Print	2	1	2	1
Viscosity of the Inks (Pa.s)	2.24	11.02	6.00	14.32
Spindle	1	1	1	2
Surface Consistency				
Average Sa_1 for 20 prints (µm)	0.96	1.12	1.28	1.42
Sa_{sd} (µm)	±0.27	±0.16	±0.29	±0.24
Thickness Consistency				
Average T_1 for 20 prints (µm)	262	232	199	194
T_{sd} (µm)	±13	±14	±08	±11
Repeatability				
Standard Deviation S_1 (µm)	±0.20	±0.13	±0.18	±0.20
Standard Deviation T_1 (µm)	±33	±10	±19	±07
Flexibility				
Avg. Bending Angle of optimum print (°)	13.6	13.7	19.9	44.0
Thermal Stability				
Displacement of highest corner (mm)	02	03	07	10
Fabric Surface Improvement (%)	97.2	96.7	96.2	95.8

Table 12: Results of the interface ink evaluation

The results show that all the interface prints significantly improve the fabric surface. DuPont 5018 prints have the least surface variation but its surface has comparatively lower consistency both within

a print surface and across the 20 prints shown by the higher Sa_{sd} and standard deviation of Sa_1 respectively. The Electra prints have the most consistent surface with the best repeatability. Fabinks IF-UV-1004 shows the least thickness variation within a print despite having a higher thickness variation across the 20 prints. FB-20 has the most repeatable thickness and its optimum prints were the most flexible but the least thermally stable. The results showed the following two trends.

- The higher the viscosity of the ink the better the thickness repeatability of an ink.
- The higher the flexibility of prints the lower the thermal stability.

Although all the interfaces significantly improve fabric surface topography none of the four inks produced an interface layer with the best results in each category. Therefore an interface ink can be selected using the results of this evaluation to suit the requirements of an application e.g. for high flexibility FB-20 can be used and, for a highly uniform surface, Electra can be used. Figure 32 shows the 3-D Alicona scans of one of the prints of each of the four interface inks scanned at 10x magnification.

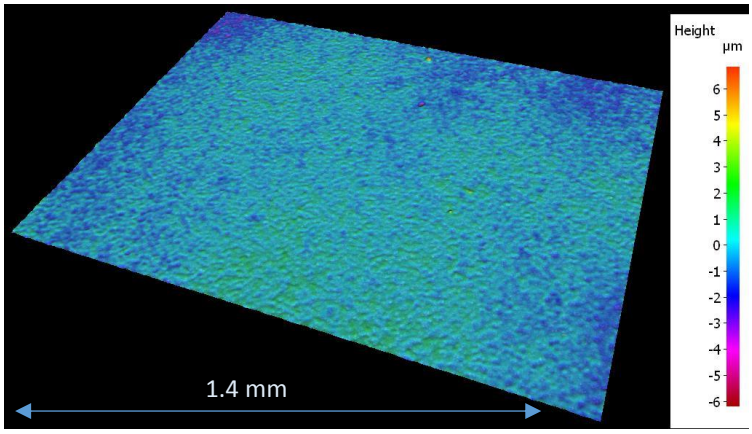

DuPont 5018

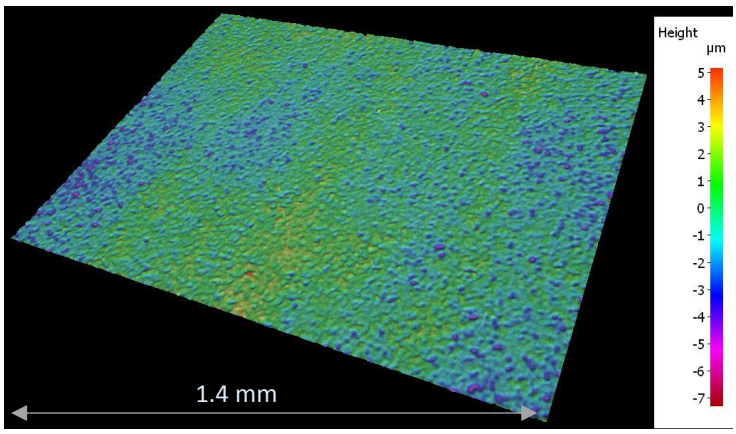

Electra EFV4/4965

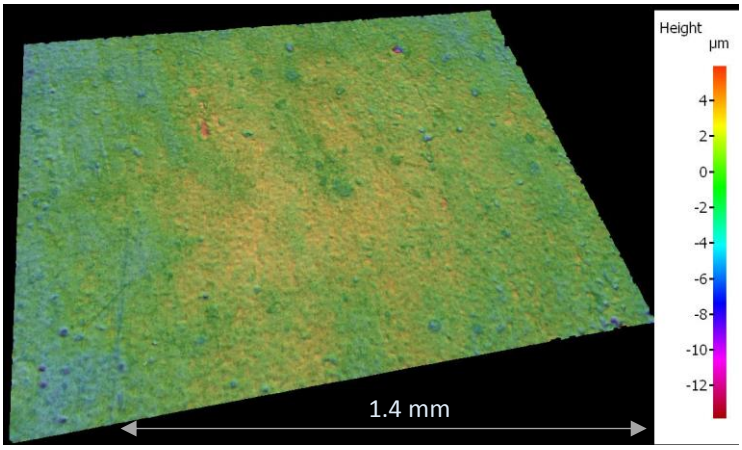

Fabinks-IF-UV-1004

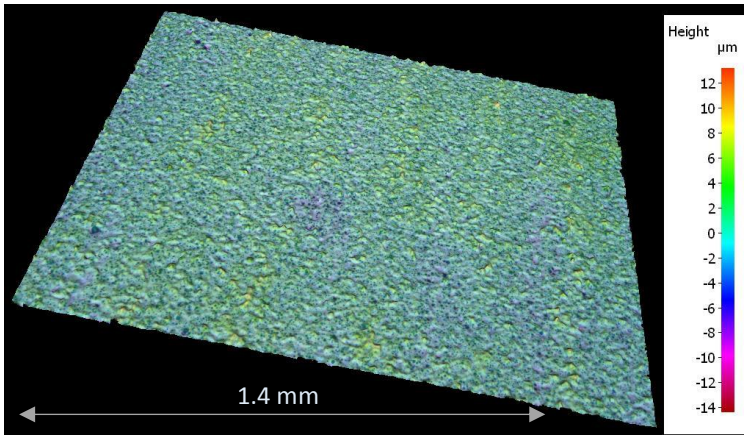

FB-20

Figure 32: 3-D scans of the four interface inks print on polyester cotton 65/35

The Alicona results show that majority of the peak to peak variation with the prints is 3-5 µm for DuPont, Electra and IF-UV-1004 and 10-12 µm for FB-20 which is a considerable improvement over fabric surface variation of 250-300 µm. The interface layers were printed using continuous mode where the printing nozzle continuously moves in a straight line as the ink is dispensed. The dispensed ink often trails the printing nozzle so it is possible to print slightly thicker layers than the nozzle height. However it should be noted that 2 layers of DuPont 5018 were printed to achieve a thickness of 262 µm. The first layer was cured before printing the second layer and the nozzle height for the second layer is set off the surface of cured first layer so there is already an offset of 100 -140 microns. The results and the 3-D images show that the four printed interface inks substantially reduce the fabric surface variation; however it is important to analyse how these results translate into consistent printing of electronic layers on fabrics.

3.10 Conductive tracks printed on interface print surfaces

The printed interface layers provide a low variation surface as a reliable platform for printing electrical interconnections. The impact of the fabric surface improvement on the electrical properties of the printed conductive tracks was assessed by dispenser printing ten 30 mm x 2 mm DuPont 5000 tracks on the interface prints of four inks and a PVC coated fabric (Mehler Frontlit II Standard FR). The PVC coated fabric was chosen as an alternative to interface printed fabric as it offers a non-porous surface with significantly lower surface variation than polyester cotton fabric. Figure 33 shows the 5x magnification Alicona 3-D scan of the PVC coated fabric.

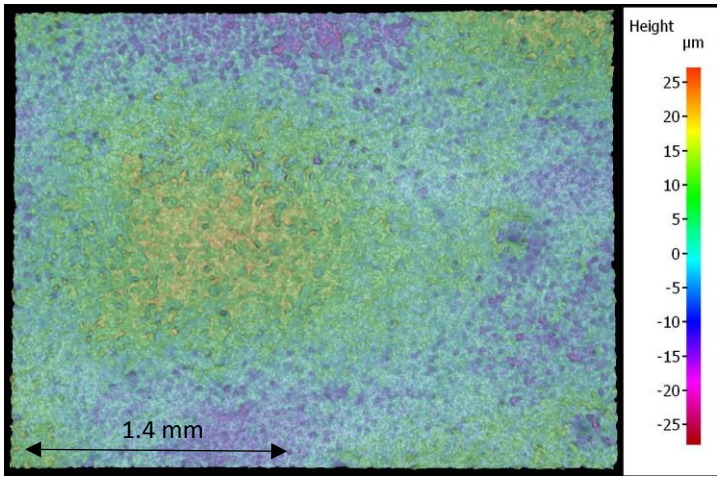

Figure 33: 3-D image of the PVC coated fabric at 5x magnification

It can be seen from figure 33 that the PVC coated fabric has a lower surface variation than the polyester cotton and higher variation than the printed interface coated fabric. Table 13 below shows the average Pa of Kapton and Sa of polyester cotton fabric, prints of four interface inks and the PVC coated fabric.

Substrate	Poly Cotton	Kapton	Dupont	Electra	IF-1004	IF-TC0233	PVC coated fab.
Avg. Sa/Pa (µm)	34.00	1.30	0.96	1.12	1.28	1.42	2.85

Table 13: Sa/Pa values of the substrates used for conductive track printing

Two 37 mm x 40 mm interface prints of the four inks were printed on the polyester cotton fabric to print multiple tracks on each interface print. The conductive tracks were printed on the interfaces using the settings shown in table 8; however these settings did not produce a complete print on the PVC coated fabric. A different set of printer settings with a higher Y-resolution, shown in table 14, were used for printing conductive tracks on the PVC coated fabric. The settings were determined by carrying out dispensing trials of the DuPont 5000 ink on the PVC coated fabric.

Pressure (kPa)	40.0
Dispense Time (ms)	10.0
X-resolution (mm)	0.50
Y-resolution (mm)	0.30
Nozzle Height (µm)	150
Vacuum (kPa)	1.3
Speed (mm/s)	1

Table 14: Dispenser printer settings used for printing conductive tracks on PVC coated fabric

Figure 34 below shows conductive tracks printed on the four interface prints and the PVC coated fabric.

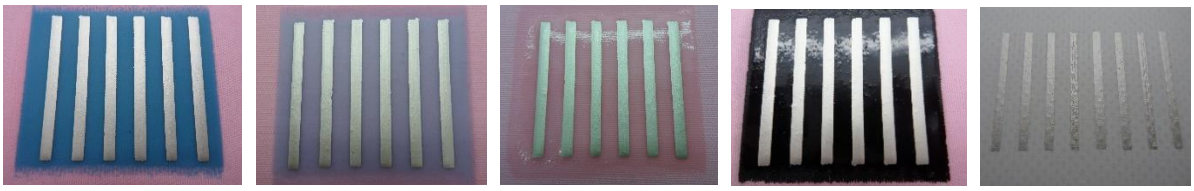

(a) (b) (c) (d) (e)

Figure 34: Silver tracks printed on (a) DuPont 5018 (b) Electra 4965 (c) Fabinks IF-UV-1004 (d) FB-20 (e) PVC coated fabric

The resistance and the thickness of the tracks was measured using the methods described earlier. Comparing the track resistivity is a more suitable way of comparing the tracks as the resistance and thickness of the tracks vary on the same surface and across the different surfaces. The resistivity of each track was calculated using equation 3. The tracks printed on the five surfaces were compared by comparing average resistivity of the 10 tracks printed on each surface. Figure 35 below shows the comparison of conductive tracks printed on polyester cotton fabric, Kapton, DuPont, Electra, IF-1004, FB-20 and PVC coated fabric.

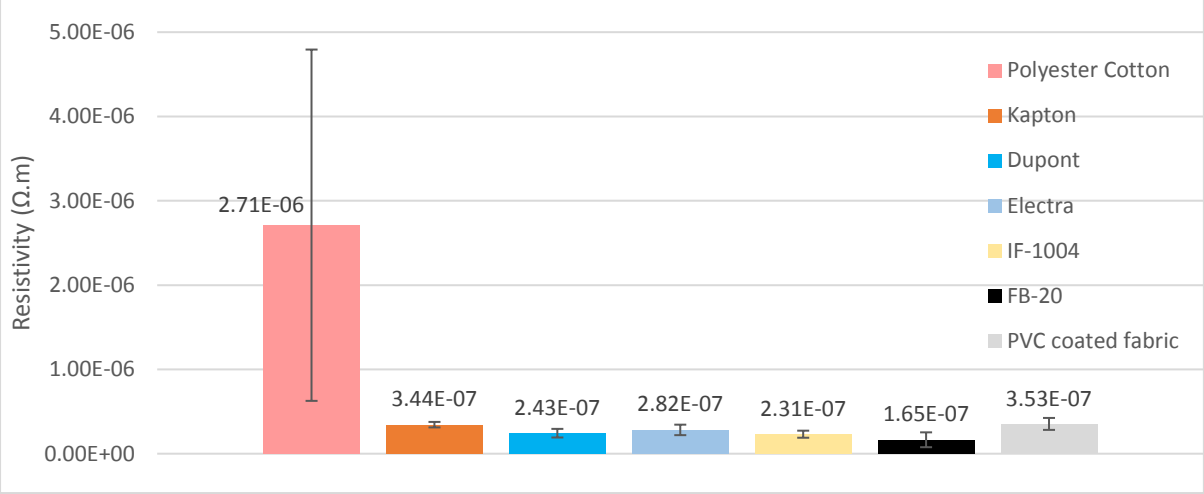

Figure 35: Average resistivity of conductive tracks on seven different surfaces

The error bars in the bar chart represent ± 1 standard deviation of the resistivity of tracks. The results show that tracks printed directly on the fabric surface have significantly higher resistivity and variation compared to tracks on other surfaces. It is assumed in the resistivity calculation that the track thickness is uniform and is represented by the average track thickness. A track with a higher thickness variation would therefore produce a higher resistivity value and vice versa. The higher resistivity of the fabric tracks is caused by non-uniform thickness of the printed tracks due to high fabric surface variation. Figure 36 shows a cross-section SEM image of silver tracks printed on PVC coated fabric and DuPont 5018 interface layer on polyester cotton fabric. The track printed on DuPont 5018 interface layer is a representative of the tracks printed on an interface layer as all the interface inks produced similar low variation surfaces.

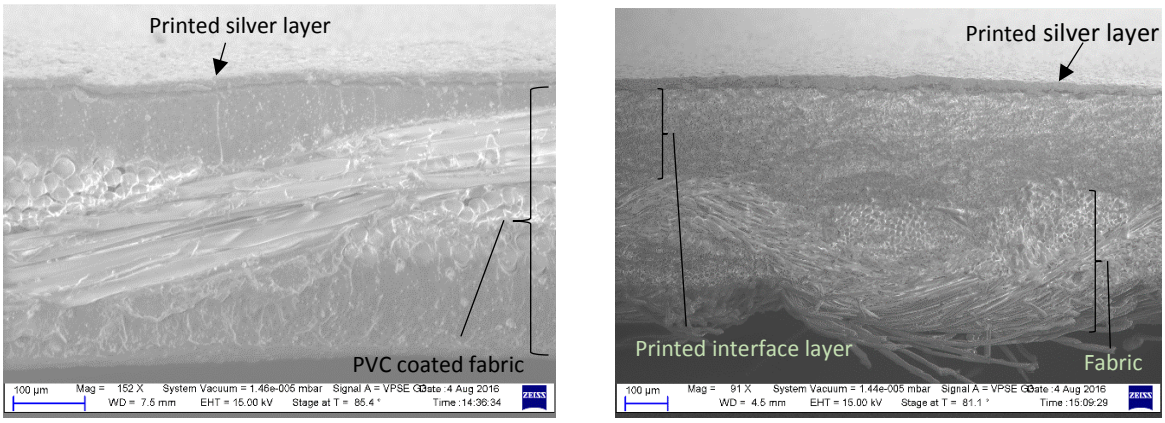

(a) (b)

Figure 36: SEM image cross-section of silver track printed on (a) PVC coated fabric and (b) an interface layer (DuPont 5018) on polyester cotton fabric

Figure 36 shows that the tracks printed on the PVC coated fabric and the fabric printed with interface layer produced a uniform deposition of silver ink as was the case with Kapton. The SEM images also show that the PVC coated fabric provides a sufficiently smooth platform for directly printing silver ink whereas an interface layer is necessary on the fabric surface to overcome the fabric surface variation. The interface ink deposition can be seen in the SEM image to conform to the fabric surface variation forming a smooth homogenous platform for the silver ink layer. Resistance distribution of the tracks printed on the four interfaces and the PVC coated fabric was analysed using thermal imaging. These tracks, like the printed tracks on Kapton, shown in figure 23, produced a fairly uniform heat distribution. The thermal imaging technique can easily differentiate between uniform and non-uniform tracks, however is less suited to a comparison of the degree of uniformity between two uniform tracks especially if the difference in uniformity between the tracks is very small as is the case in this experiment. A more suitable method is to analyse the resistivity of the individual tracks and present it as average resistivity on each surface as used in this experiment. Figure 37 below shows the resistivity of the tracks on all the surfaces omitting the polyester cotton tracks so the results of the remaining surfaces can be compared more easily.

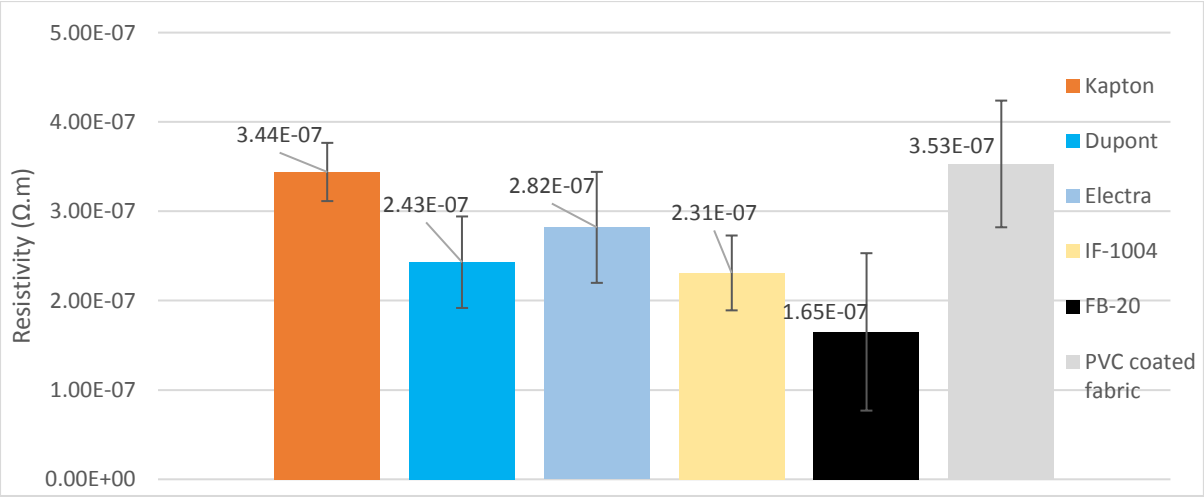

Figure 37: Average resistivity and variation of conductive tracks on Kapton, four interface materials and PVC coated fabric

Figure 37 shows that the tracks on Kapton, the four interfaces and the PVC coated fabric have very similar resistivity although the tracks on Kapton show the least variation in the resistivity. PVC coated fabric tracks show a higher resistivity than the four interface inks which confirms the hypothesis that it is due to the higher surface variation established by the average Sa values. The difference between the average Sa values of the four interfaces and the Kapton is very small which shows they have very similar surface variation; therefore the track resistivity of tracks printed on these surfaces do not produce an accurate reflection of their Sa values. The resistivity of the tracks on all the surfaces, except the fabric, matches the expected resistivity shown in table 7. The results have proved that reducing the surface variation is vital for consistent printing of electronic layers especially if the electrical properties of the layers are dependent on the homogeneity of their physical geometry. It has also been shown that the improvement in fabric surface translates to improvement in the uniformity and resistance of printed conductive tracks.

The results highlight that it is essential to dispenser print an interface layer on the fabric surface for printing track heaters to achieve a consistent and uniform heater output. This makes the interface layer a first and vital component of the actively controlled thermochromic fabric devices. The results of this investigation can be generally applied to all smart fabric applications incorporating any electronic functionality as printing the electrical interconnections is fundamental to integrating electronics with fabrics.

3.11 Conclusions

This chapter introduced dispenser printing in terms of the dispenser technology and the fundamental elements of a dispenser printer. It discussed the features and capabilities of the dispenser printing process such as rapid prototyping, design freedom, the ability to print multi-layered and multi material structures and minimizing waste of printing material. A comparison of dispenser printing with screen and inkjet printing process is presented in this chapter. It was shown that dispenser printing can print a wider array of materials than the other two processes as it can print a broader range of ink viscosities (1 mPa.s – 100 Pa.s) than inkjet printing (1 m - 20 mPa.s) and screen printing (1 – 10 Pa.s). It was also shown that dispenser printing can print higher resolutions, down to 1 µm, compared to inkjet printing, 5 µm and screen printing, 50 µm.

The background of dispenser printing was also presented in this chapter which showed that all the dispenser printers used in the literature are bespoke setups. It was highlighted that dispenser printing is a novel process for printing active and functional material on fabrics as it has not been previously used for printing on fabrics. This chapter presented the bespoke dispenser printer developed at the University of Southampton, used in this research. It discussed the features of its operating software including the printing modes offered. It was shown that the dispenser printer used in this research is comparable to dispenser printers used in the literature.

It was highlighted that the current dispenser printer does not have a mechanism to accurately set up and adjust the gap between the printing nozzle and the substrate (nozzle height) during the printing process. It was shown that the variation in the nozzle height can lead to variation in the flow rates of the dispensed ink leading to geometrically inconsistent structures. The surface variation of the printer stage measured using an LM-10 ANR1251 micro laser displacement sensor showed that the stage has an average surface displacement of 32 µm and a peak to peak variation of 194 µm. The effect of stage variation was effectively reduced by gluing the substrates to alumina tiles for the printing process. The gluing process avoided creasing and folding of substrates during the printing process in addition to reducing the average variation to 0.8 µm and the highest expected peak to peak variation to 120 µm.

The selection of polyester cotton 65/35 blend as the fabric substrate for development of the dispenser printed actively controlled thermochromic devices was also discussed in this chapter. It was concluded that, due to high surface variation and a loose and porous structure, the use of the polyester cotton fabric would allow the development of thermochromic devices to be replicated on most other fabrics with similar or lower surface variation. The surface topography of the fabric characterised using an Alicona optical profiler resulted in Sa value of 34 µm and a peak to peak variation of 270 µm. The fabric surface variation was correlated with the geometrical inconsistency of the printed conductive tracks. It was shown that printed conductive ink tended to conform to the fabric surface producing high resistance tracks with a non-uniform resistance distribution. A novel method of assessing resistance distribution in a printed structure based on thermal imaging was also introduced in this chapter.

A dispenser printable method of reducing surface variation by printing an interface layer on top of the fabric surface was demonstrated. Four suitable dielectric inks DuPont 5018, Electra EFV4/4965, Fabinks-IF-UV-1004 and FB-20 were evaluated as interface materials for dispenser printing. It was shown that printing an interface layer on the fabric surface reduced its variation by more than 95%, forming flexible low variation surfaces. It was shown that the improvement in fabric surface translated into printing of conductive tracks on the four interface materials resulted in ~90% lower resistivity compared to tracks printed directly on fabric and showed similar resistivity to tracks on Kapton, a traditional low variation printed electronics substrate. By printing an interface layer between the fabric surface and the conductive tracks a network of electrical interconnections with substantially lower resistance and improved performance can be fabricated. It was also shown that tracks printed directly on fabric required about 3 times more silver to produce comparable resistance to tracks printed on the four interfaces and Kapton. Therefore, in addition to better performance, printing conductive tracks on an interface layer instead of the fabric surface saves the silver ink thus reducing the cost of fabrication.

Chapter 4 DISPENSER PRINTED HEATERS

4.1 Introduction

This chapter presents design, modelling, fabrication and characterisation of dispenser printed track heaters. It presents a COMSOL model of track heaters which was used to simulate various heater configurations to obtain a set of design rules for a track heater. A test heater based on the derived design rules was designed, simulated, dispenser printed and characterised in terms of the temperature distribution and its uniformity. It also details the formulation of custom conductive inks suitable for dispenser printing of heaters. The chapter also discusses methods of producing localised heating within a printed conductive path.

4.2 Design and modelling

This section details a COMSOL model of track heaters to simulate dispenser printed heaters. Firstly, a general analysis of a track based heater is presented in terms of energy inputs, losses and transfer from the track to the substrate. Materials selected for the fabrication of dispenser printed heaters are discussed followed by details of the development of the COMSOL model. Two designs of simulated track heaters are compared with the printed heaters to validate the model. A series of heater configurations are simulated to determine the effect of fabrication parameters on the heater output. Finally, a test heater is designed and simulated using the design rules determined from the previous simulations.

4.2.1 Track heater energy balance analysis

A track heater consists of an electrically conductive path on a substrate, which produces resistive heating when electrical current is passed through it. The heat is transferred from the conductive path to the substrate by thermal conduction. The thermal energy from the conductive path and the substrate is lost to the surroundings by convection. The heating of a track heater is a time dependent process where at steady state the rate of input energy supply equals the rate of energy losses and a constant temperature is achieved. Figure 38 presents energy balance diagram of a track heater.

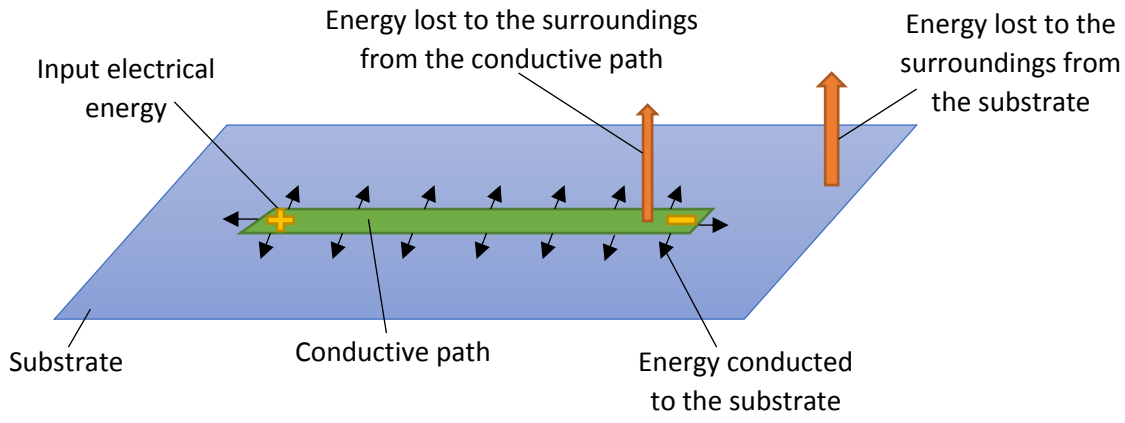

Figure 38: Energy balance diagram of a track heater

Heat transfer from the conductive path to the substrate is in three dimensions (x,y,z). Equation 4 presents a mathematical description of the energy balance of a track heater. It is assumed that the spatial distribution of the temperature is uniform and the resistance of conductive path does not change with temperature change. Energy loss to the environment by radiation can be ignored as it is

likely to be very small compared to energy loss through convection. The thermal radiation equation derived from Stefan Boltzmann's law is dominated by Stefan Boltzmann constant, which is a very small number (5.67 x 10^{-8}) and unless the temperature difference between the track heater and the environment is substantial the energy loss due to radiation will be very small compared to convection.

Equation 4: $$I^2R = m_1C_1\frac{dT_1(t)}{dt} + m_2C_2\frac{dT_2(t)}{dt} + hA_1(T_1(t) - T_0) + hA_2(T_2(t) - T_o)$$

Where I = Current, R = Resistance, m_1 = Mass of conductive track, C_1 = Specific heat capacity of constituent material of the conductive track, $\frac{dT_1(t)}{dt}$ = Rate of temperature change of the conductive track at time t, m_2 = Mass of substrate, C_2 = Specific heat capacity of constituent material of the substrate, $\frac{dT_2(t)}{dt}$ = Rate of temperature change of the substrate at time t, h= Convective heat transfer coefficient, A_1= Area of conductive track, T_1=Temperature of conductive track at time t, A_2= Area of the substrate, T_2=Temperature of substrate at time t, T_0 = Environmental temperature.

The terms in the equation 4 represent that the rate of input electrical energy supply equals the rate of thermal energy transfer to the conductive track, the rate of thermal energy transfer to the substrate and the rate of thermal energy loss from the conductive track and substrate to the environment.

The equation highlights the factors that influence the performance of a track heater. The resistivity and specific heat capacities of the constituent materials of the conductive path and substrate are important to consider from a materials selection perspective. A higher specific heat capacity material will increase the thermal energy transfer rate of the conductive path/substrate provided the other factors are constant. Physical dimensions of the conductive path and substrate are important to consider in fabrication as they affect the resistance and the mass. The environmental temperature influences the maximum temperature of a heater provided the other factors are constant. A higher environmental temperature would result in the heaters achieving a higher maximum temperature.

4.2.2 COMSOL model of track heaters

A conductive path for a heater can be dispenser printed on a substrate in a number of configurations. Variation in independent fabrication parameters such as track width, gap between printed tracks (track gap) and geometric pattern (spiral or meander) can produce printed heaters with different outputs. A comprehensive analysis of a track heater output requires assessment of the spatial temperature distribution including the area of substrate heated and temperature uniformity. Equation 4 cannot predict the spatial temperature distribution because it assumes that the temperature distribution across the entire substrate is uniform. A COMSOL model was therefore developed to provide the spatial temperature distribution of track heater configurations to aid in heater design.

The heater development uses polyester cotton 65/35 blend fabric and Kapton as substrates, DuPont 5018 ink for the interface layer and DuPont 5000 silver ink for printing the conductive tracks. The fabric is used because of its selection as the substrate for dispenser printed thermochromic devices as discussed in section 3.7; an interface layer is required to be printed on the fabric surface to overcome the surface variation. Kapton is used as a substrate in the COMSOL model because the COMSOL material library does not contain polyester cotton blends and printing of DuPont 5000 ink produced similar output on Kapton and interface layer on the fabric as discussed in section 3.9. Kapton is used as an approximation for interface layer printed on fabric as they both have non-porous structures and similar surface variation. The heater printing tests are carried out on both Kapton and the fabric; their output is compared. It is expected that the results of simulated and printed Kapton heaters would be applicable to the printed fabric heaters, however the printed Kapton heaters are expected to produce

a more uniform temperature distribution compared to printed fabric heaters. DuPont 5018 is chosen as the interface ink because it produced lowest average surface variation and highest thermal stability compared to the other interface inks tested in section 3.9.6. The selection of DuPont 5000 silver ink is detailed in section 3.8. The silver ink in the represented in the COMSOL model by pure solid silver.

The COMSOL model consists of two physics modules: electric current shells and heat transfer in solids, and two mapping modules: boundary electromagnetic heat source and temperature coupling. The following provides a brief description of each of the four modules.

- The electric current shells module computes electrical fields, current and potential distribution within the conductive path.
- The heat transfer in solids module accounts for transfer of the thermal energy from the conductive path to the substrate and energy loss to the environment.
- Boundary electromagnetic heat source deals with the conversion of electrical energy to thermal energy and feeds the results into the heat transfer in solids module.
- Temperature coupling inputs the temperature results from the heat transfer in solids module to the electric current shells so temperature dependent resistance of the conductive path can be computed in the simulation results.

Physical properties of Kapton used in the model such as density, thermal conductivity and specific heat capacity are obtained from the COMSOL material library. A 75 microns thick 10 x 10 cm Kapton substrate is used for simulation and printing tests. Similarly density, thermal conductivity, specific heat capacity and temperature coefficient of resistivity for the silver used in the model are acquired from the COMSOL material library. The resistivity of silver in the model was replaced by the measured average resistivity of the silver ink on the DuPont 5018 interface layer (2.43E-07 Ω.m) on the fabric substrate to replicate printed silver ink on the interface layer on fabric. The experiments detailing measurement of resistivity of the silver ink on the interface layer are described in section 3.5.5. It is assumed that the material properties of pure silver with the exception of resistivity is representative of the DuPont 5000 printed silver ink. A room temperature of 22°C was used as the air temperature in the model because the printed heaters were tested at room temperature. A convective transfer coefficient of 15 W/(m^2.K) was used in the model for simulations. It was determined by comparing printed heater results with simulated heaters and varying the convective transfer coefficient in the simulation from 8-15 W/(m^2.K).

4.2.3 Validation of the COMSOL model of track heaters

The COMSOL heater model was validated by comparing the output of the simulated heaters with the dispenser printed heaters. The aim of the comparison was to determine the accuracy of the model in predicting the output of the printed track heater configurations. Two different silver heater track patterns, shown in figure 39, were used for the comparison.

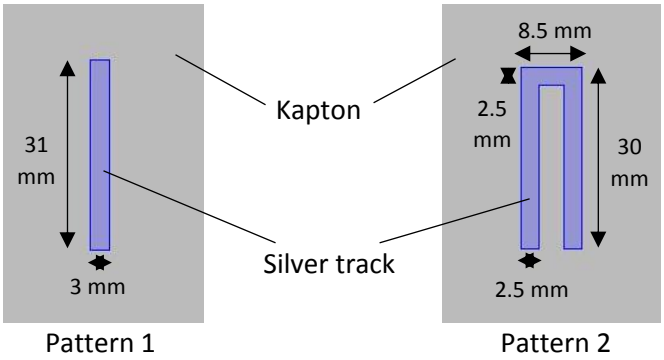

Figure 39: Patterns of silver track used for comparing modelled heaters with dispenser printed heaters

The two heater patterns were dispenser printed on Kapton and the interface layer on the fabric in the same physical dimensions as the modelled heaters; this was repeated thrice to fabricate three samples of each pattern on the two substrates. The interface layer was 37 mm x 15 mm in size for pattern 1 and 35 x 23 mm in size for pattern 2. The interface layer size was chosen to provide sufficient area for printing the two patterns. The print settings used for printing the interface layer and silver are mentioned in table 11 and table 8. Figure 40 below shows the two heater patterns dispenser printed on Kapton and the interface layer on fabric. As discussed in section 3.5.1, the current dispenser printer equipment does not have the capability of measuring and mainting nozzle height during printing. The variation in the nozzle height set up caused the printed heaters of same pattern to obtain different thickness to each other. The thickness differences between the heaters in turn caused the resistance of the heaters to vary. The printed heaters were compared with the simulated heaters in terms of temperature distribution at steady state and their temperature-time relationship.

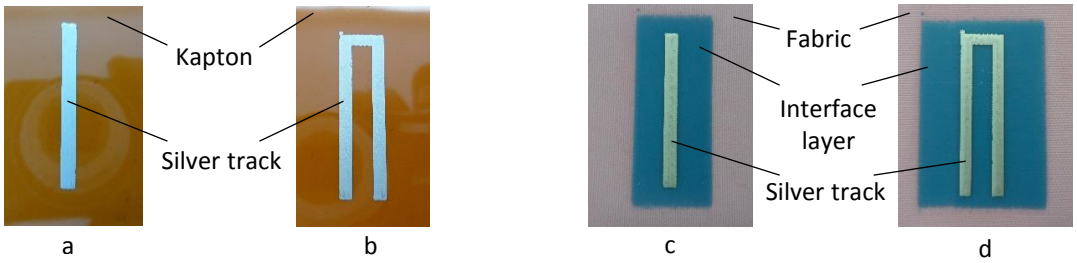

Figure 40: Silver tracks dispenser printed in two different patterns on (a) (b) Kapton and (c) (d) interface layer on polyester cotton 65/35 blend for comparison with simulated heaters

4.2.3.1 Temperature distribution comparison

One printed sample each was selected from the two heater patterns for temperature distribution comparison; samples were selected from both Kapton and fabric heaters. The resistance of the simulated track heaters was matched to the selected printed samples by choosing a suitable thickness. The thickness of the simulated tracks directly affected the resistance because the length, width and resistivity of the heater tracks were the same for simulated and printed samples. Resistance matching ensured that the same input power was supplied to both the printed and the simulated heaters for the comparison. 0.75 A of current was passed through the heaters for the temperature distribution test. The temperature distribution of the printed heaters was measured by capturing its thermal image 300 seconds after the power supply was switched on; this time duration ensured that the heater had reached steady state. The thermal image was taken using a Testo 875 thermal imager. The printed heaters were suspended in air using retort stands for the tests as shown in figure 41.

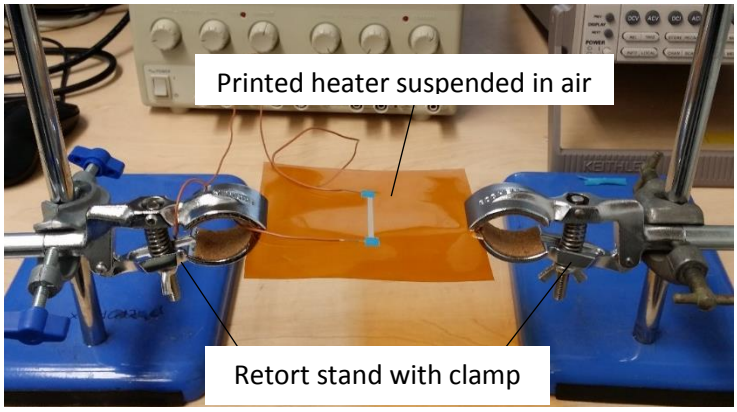

Figure 41: Arrangement used for measuring temperature distribution and temperature time relationship of the printed heaters

Figure 42 shows temperature distribution of printed heaters on Kapton and the simulated heaters of equivalent resistance. The results of the printed Kapton heaters are presented first to establish a benchmark for the printed fabric heaters.

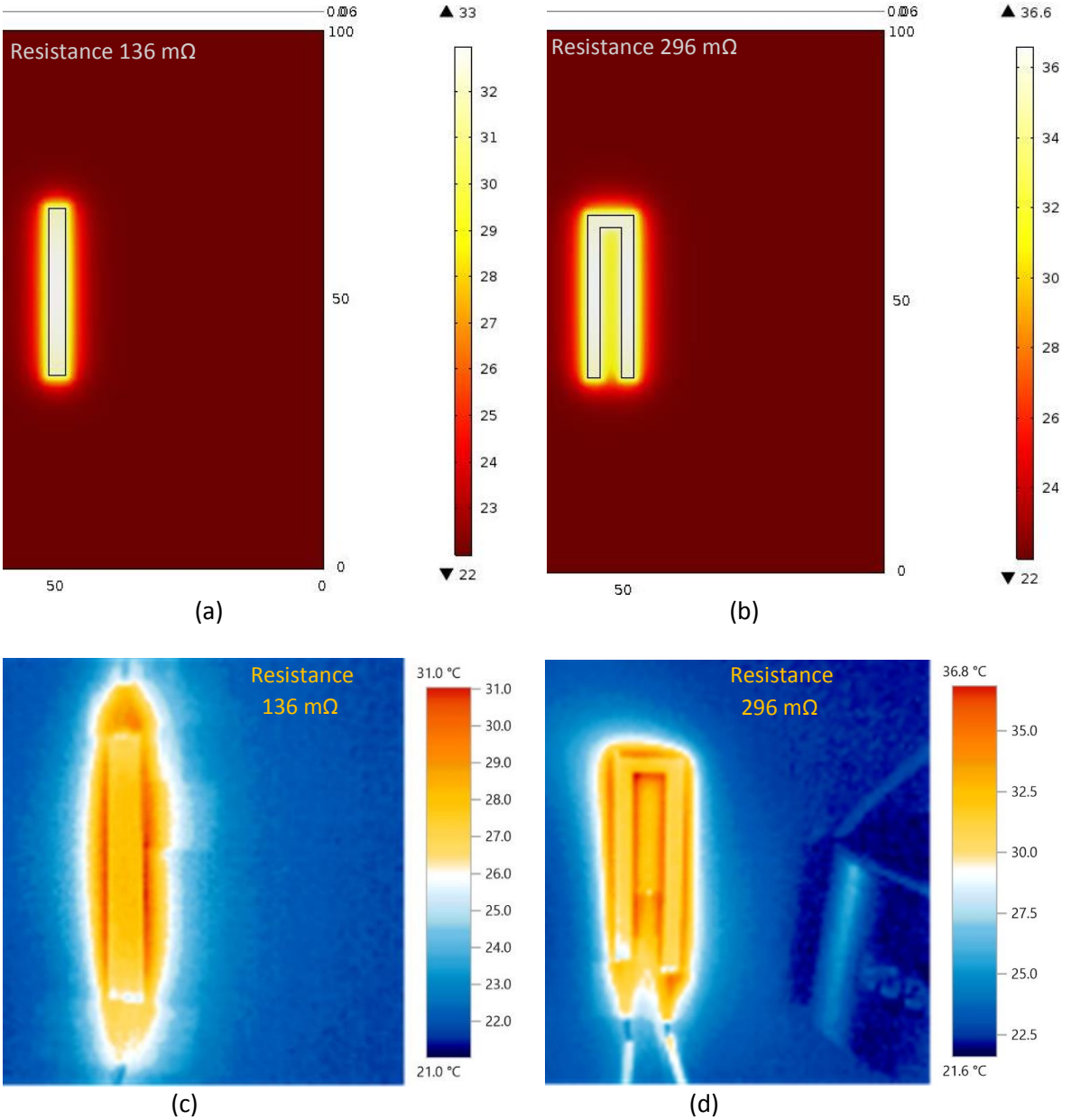

Figure 42: Temperature distribution of the simulated heater (a) pattern 1 (b) pattern 2 and equivalent printed heaters (c) pattern 1 (d) pattern 2 on Kapton

The images show that the overall shape of temperature distribution and the highest temperature attained by the printed heaters is similar to the simulated heaters. Pattern 1 simulated heater achieved a 2°C higher peak temperature and pattern 2 simulated heater achieved a 0.2°C lower peak temperature than their equivalent printed heaters.

The thermal images of the simulated heaters show that their peak temperature is located on the silver tracks whereas for the printed tracks the peak temperature is located on the substrate outlining the tracks. Heat always travels down a temperature gradient from a higher temperature region to a lower temperature region, so it is unlikely that the silver tracks are at a lower temperature to substrate. This was confirmed by a thermal image of the heater from the non-printed side of the Kapton substrate, which showed the peak temperature of the heaters was located on the silver tracks. This suggests that the temperature within the printed silver tracks was not uniform, it was found to be lower at the surface and higher at the bottom. This can be explained by considering thermal conductivity of the printed silver ink. Pure solid silver, used in the simulation has a high thermal conductivity, the heat

loss at the surface of the tracks is quickly compensated by the fast heat flow within the track. The silver ink is expected to have a lower thermal conductivity compared to pure silver because in addition to silver flakes it contains binders, solvents and additives. Due to lower thermal conductivity, the heat flow within the printed silver tracks is relatively slow so the heat loss at the surface is not compensated as quickly as pure silver, thus the surface is at a lower temperature than the rest of the tracks at steady state.

Figure 43 below compares the temperature distribution of the two patterns, printed on the interface layer on the fabric and their resistance equivalent simulated heaters.

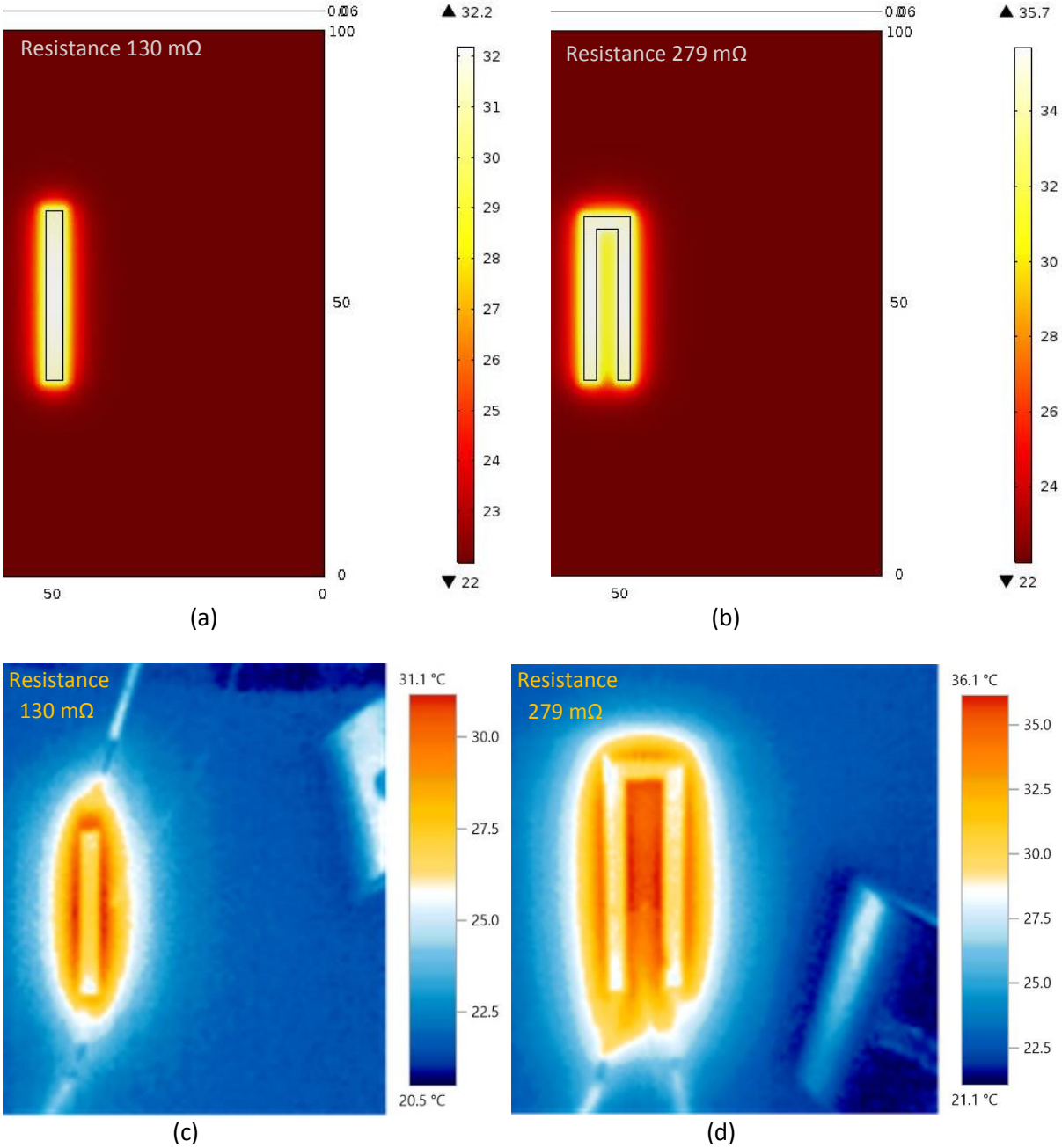

Figure 43: Temperature distribution of simulated heaters (a) pattern 1 (b) pattern 2 on Kapton and their equivalent printed heaters (c) pattern 1 (d) pattern 2 on interface layer on polyester cotton 65/35 blend fabric

The thermal images show that the printed fabric heaters produced a broader heat spread and similar highest temperature compared to the simulated heaters. Pattern 1 and pattern 2 printed heaters achieved a 1.1 °C and 0.4°C higher peak temperature to their equivalent simulated heaters. Like the printed Kapton heaters, the peak temperature of the fabric heaters is also located on the substrate around the tracks.

The printed fabric heaters have a broader heat spread than the printed and simulated Kapton heaters as shown by their thermal images. This can be explained by considering the rate of heat transfer in the two substrates, Kapton and interface on the fabric. Faster heat transfer in Kapton causes the thermal energy to be dissipated to a larger area compared to the interface layer on fabric per unit time. This increases the effective area of convective heat transfer, which causes Kapton to lose heat at a higher rate to the surroundings than the interface on fabric. The interface on fabric achieves a higher temperature at steady state because it loses heat at a lower rate to Kapton.

4.2.3.2 Temperature-time relationship comparison

The temperature time relationship of the heaters was measured using a Keithley 2001 multimeter. A thermocouple was attached to the heaters at the specific spots shown in figure 44. A current of 0.75 A was passed through the heaters and temperature data was recorded over a time of 300s. All six printed samples of each pattern were used for temperature-time tests, this included both the Kapton and the fabric printed heaters.

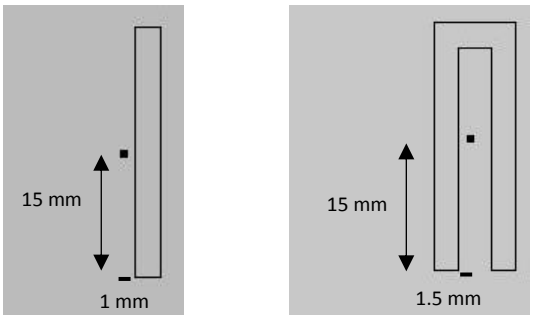

Pattern 1 Pattern 2

Figure 44: Temperature measurement spots of the two heater patterns represented by black dots

Figure 45 and figure 46 show the temperature vs. time graphs of the pattern 1 and pattern 2 heaters respectively. Each of the two figures contain temperature-time data of three heaters printed on Kapton, three heaters printed on the interface layer on fabric and two simulated heaters. The resistances of the two simulated heaters were chosen to represent the upper and lower limit of the range of resistance values attained by the printed heaters.

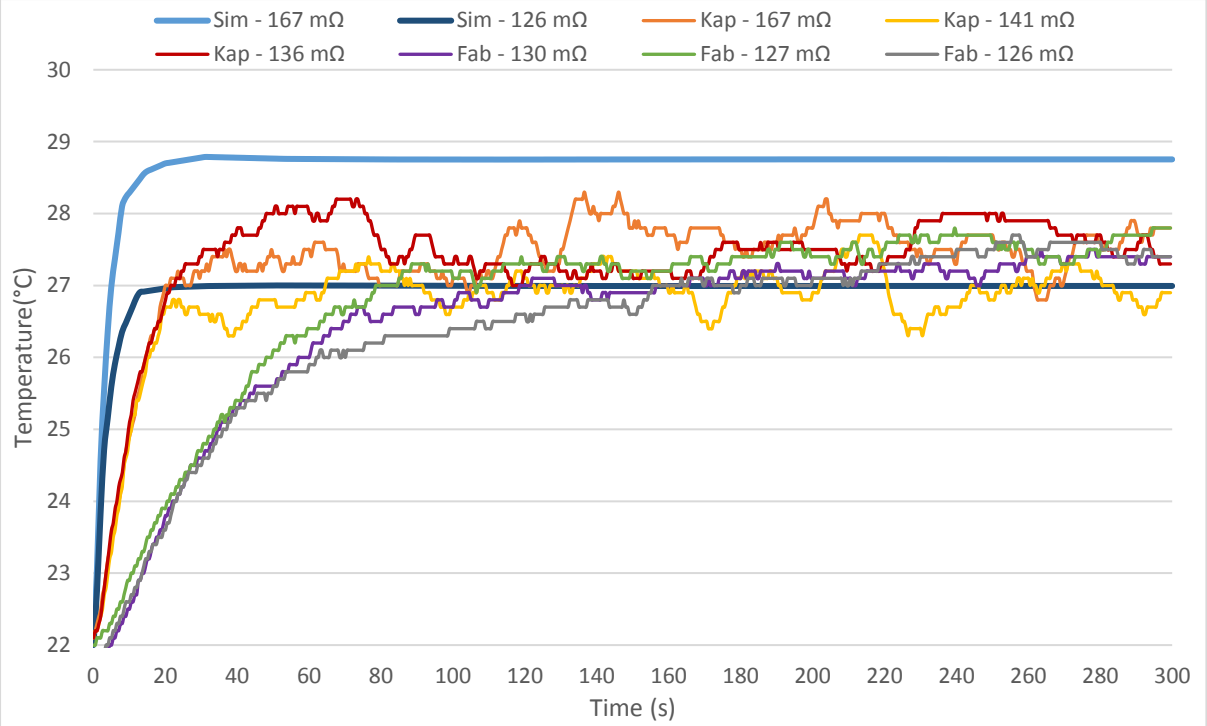

Figure 45: Temperature-time relationship of pattern 1 heaters simulated in COMSOL and printed on Kapton and polyester cotton 65/35 fabric

Figure 45 shows that the temperature-time graph of all the heaters have a similar shape. Initially the rate of change of temperature is high and then reduces as the heater approaches its final temperature before reducing to 0. The rate of increase in temperature is highest for simulated Kapton heaters followed by printed Kapton heaters and fabric heaters respectively. The printed heaters do not maintain a constant final temperature instead the temperature varies in a narrow temperature range. The temperature variation is lower in fabric heaters compared to the Kapton heaters. The final set of temperatures of all the heaters are within a narrow range of 3°C between 26°C and 29°C.

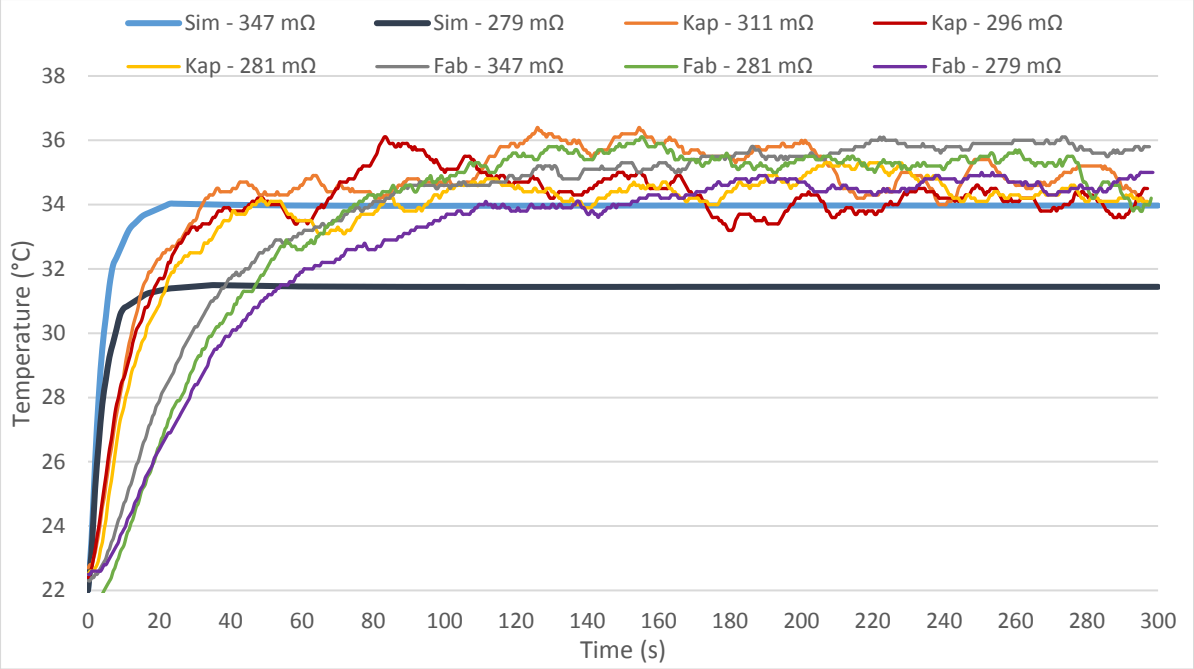

Figure 46: Temperature-time relationship of pattern 2 heaters simulated in COMSOL and printed on Kapton and polyester cotton 65/35 blend

Temperature vs. time graphs of the pattern 2 heaters show similar results to the pattern 1 heaters with all the graphs producing similar general shape. Unlike the pattern 1 heaters, the final set of temperatures of the pattern 2 printed heaters do not lie in the temperature range defined by the two simulated heaters; however they are very close to the higher limit simulated heater. The final set of temperatures of all the heaters with the exception of the 279 mΩ simulated heater lie in a narrow range of 3°C between 33.3°C to 36.3°C; the 279 mΩ simulated heater achieved a final temperature of 31.5°C.

The printed Kapton heaters have a higher rate of temperature increase than fabric heaters which shows that the heat transfer is faster in Kapton than interface layer on fabric, as the substrate is the only difference between the printed heaters. The simulated heaters produced a higher rate of temperature increase than the printed Kapton heaters because the model uses thermal conductivity of pure silver which is higher than the printed silver ink as discussed earlier. The higher thermal conductivity of pure silver allows faster heat transfer from the tracks to the substrate.

Unlike the simulated heaters, the printed heaters did not maintain a constant final temperature, instead the temperature varied in a narrow range. This temperature variation is caused by changes in air movement or air temperature. Any small change to the two factors affects the temperature gradient between the printed heaters and their immediate surroundings, which causes the heater to lose or gain heat. Kapton has a higher heat transfer rate so responds faster to small changes in temperature gradient than the interface layer on fabric resulting in a higher variation in the final set of temperatures.

4.2.3.3 Discussion

The temperature distribution and temperature-time results of the printed and simulated heaters showed that the COMSOL model is a reasonable approximation for the printed heaters. The two test patterns, when simulated, produced similar temperature distributions to the printed heaters on Kapton and a similar shaped narrower heat spread to the printed heaters on fabric. The peak temperature of the simulated heaters was located on the conductive tracks whereas it was located

around the outline of the tracks for the printed heaters. The maximum difference between the peak temperatures of the simulated and printed heaters is 2°C which shows the model produced a fairly accurate estimation of the printed heaters. The temperature-time graphs of the simulated heaters showed similar general shape to the printed heaters. The rate of temperature gain was highest for the simulated heaters followed by the printed Kapton heaters then the printed fabric heaters. However the final set temperatures of printed and simulated heaters were found to be within a narrow 3°C range with only one exception. It can be concluded that the COMSOL model described in this section can be used as an effective tool in determining the output of dispenser printed heaters on Kapton and the interface on fabric using DuPont 5000 silver ink.

4.2.4 Heater design simulation tests

This section investigates the effect of track heater fabrication parameters on its output. The fabrication parameters includes the conductive track's width, length, thickness, geometrical layout, and the gap between two consecutive track lines. These fabrication parameters also influence the heater resistance and the amount of silver ink required for the heater fabrication. The heater resistance is important to consider to determine the input power and choice of power source for an application. The amount of silver used affects the cost of fabrication.

The effect of the heater fabrication parameters is investigated using COMSOL simulation tests. The tests consist of varying each of the following parameters: heater track width, gap between consecutive track lines and geometrical layout, while keeping other parameters constant and simulating the heater designs. The heater output is assessed by measuring the uniformity of the temperature distribution and the area of heater layout covered in silver. Uniformity of temperature distribution evaluates temperature along a straight line across a heater design in the form of a graph to determine the variation in temperature.

4.2.4.1 Heater track width

Four meander track heater layouts with track widths 0.5 mm, 1 mm, 2 mm and 3 mm were simulated in COMSOL to assess the impact of track width on the heater output. The track thickness, the track length, the gap between two consecutive track lines and the input power per unit fabrication area are kept constant. The fabrication area of a heater design is defined as the area covered in silver and the gap between the consecutive silver track lines. Input power per unit fabrication area is kept the same so different sized heaters can be compared. Table 15 below lists the values of the parameters that are kept constant for the track width simulation tests.

Parameter	Value
Thickness of silver tracks (µm)	20
Length of track pattern (mm)	123
Gap between track lines (mm)	1
Input power per unit area (mW)	0.4

Table 15: List of parameters that are kept constant for the track width simulation tests

Figure 47 shows the temperature distribution of the four simulated heaters with tracks widths varying from 0.5 mm and 3 mm. Figure 48 below shows the temperature variation graphs of the four heaters measured along a straight line drawn at length 15 mm across the width of the heaters. The temperature variation is measured across the width of the heaters instead of the length as the temperature variation is minimal along the length of the heaters.

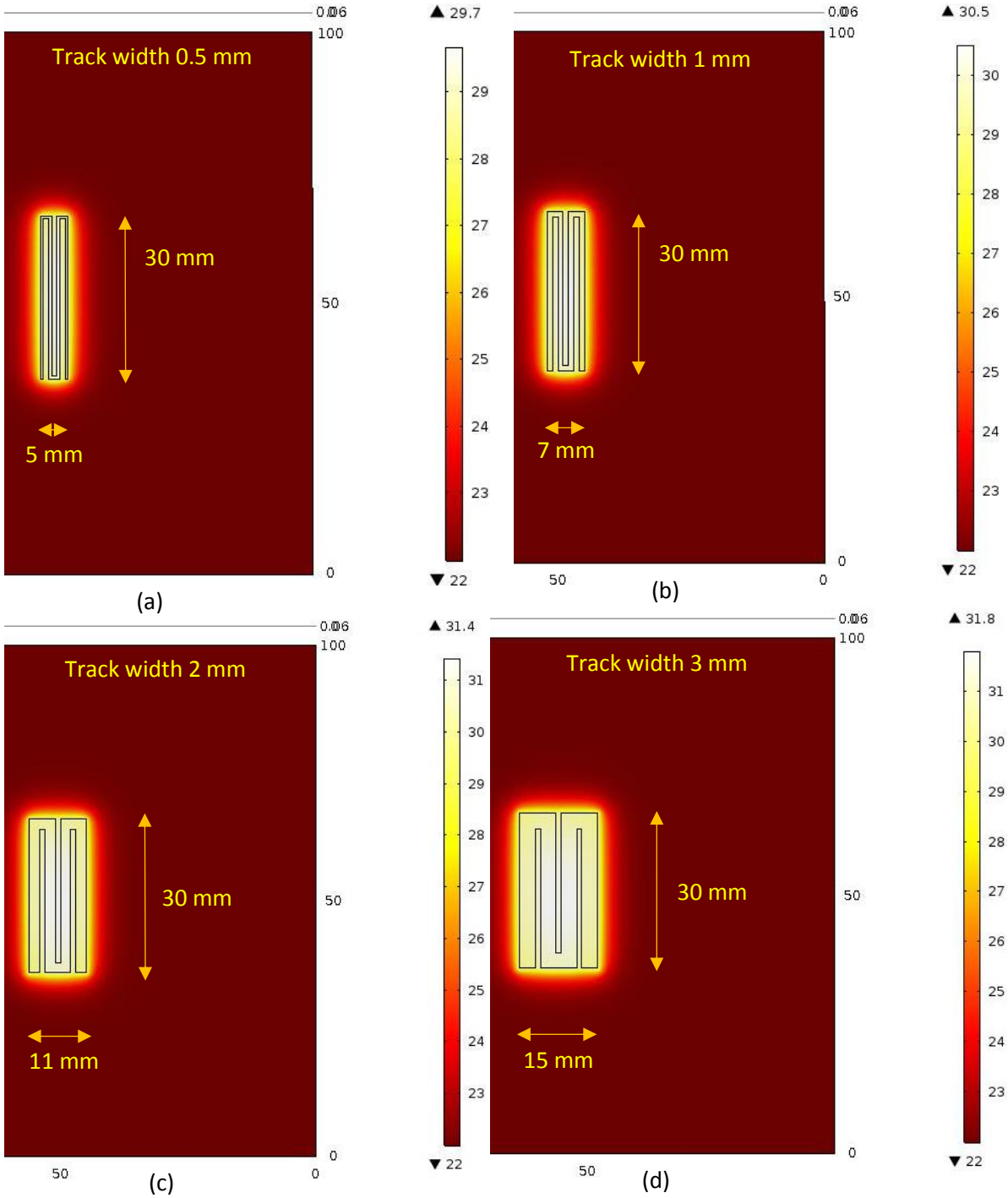

Figure 47: Temperature distribution of heaters with track width (a) 0.5 mm (b) 1 mm (c) 2 mm (d) 3 mm

The temperature distribution of the heaters show that the shape of heat spread conforms to the layout of the tracks. The four heaters have comparable peak temperatures despite the differences in track widths; the peak temperature of the all four heater lie within a range of 2.1°C.

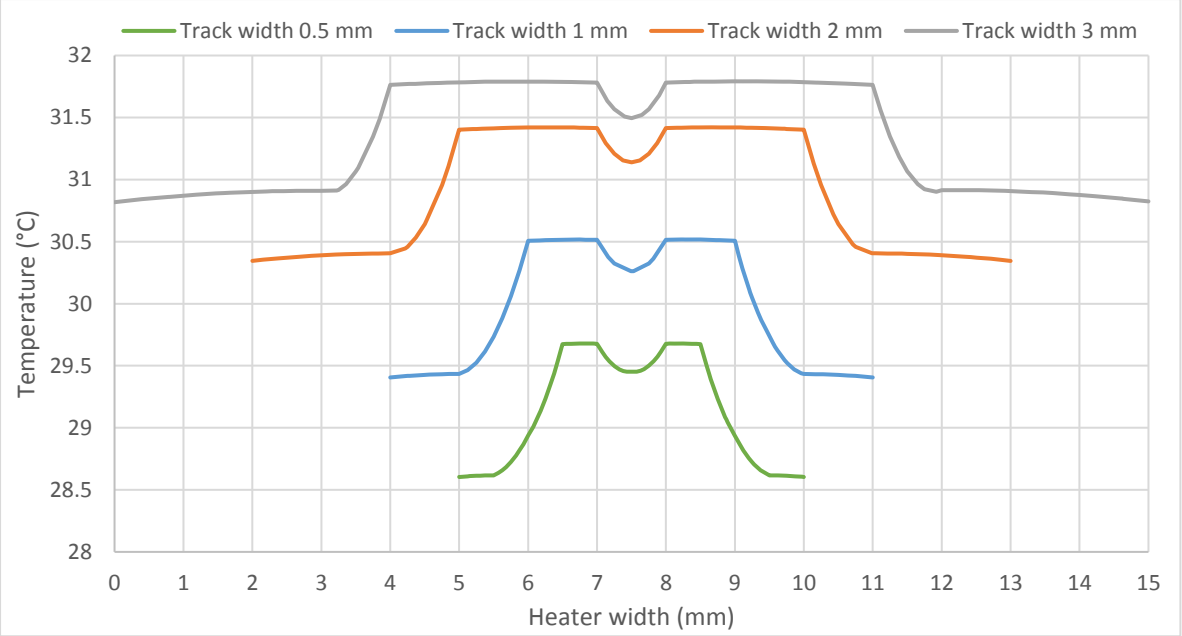

Figure 48: Temperature variation of the heaters with four different track widths along a straight line

The graphs in figure 48 shows the temperature across the entire width of the four heaters; the temperature is relatively constant on the tracks whereas it varies in the gap between the tracks. The four heaters show similar temperature variation across the heater widths. The difference between the highest and lowest temperature points on the graphs is around 1 °C for all four heaters. The results show that the track width does not have a significant impact on the uniformity of temperature distribution of the heaters.

Wider tracks increased the area of the silver track on the heater by the same factor as the increment in track widths because the overall track length is the same. Due to different sizes of the four heaters, the amount of silver required to fabricate the heaters is evaluated by analysing the area of silver track per unit fabrication area of the heater. Table 16 below shows the area of the heaters covered in silver and the ratio of area of silver tracks to fabrication area for the four heaters.

Track width of the heaters (mm)	Area of silver tracks (mm^2)	Area of silver tracks /Fabrication area
0.5	61.5	0.410
1	123	0.586
2	246	0.745
3	369	0.820

Table 16: Heater area coved in silver and the ratio of silver track area to fabrication area of the four heaters simulated with track widths 0.5 mm, 1 mm, 2mm and 3mm

The results in table 16 and figure 47 show that heaters with narrower tracks require less silver per unit area than wider tracks to produce a comparable temperature output. The heaters with 3 mm, 2 mm and 1 mm track widths required 100%, 82% and 43% more silver per unit fabrication area than the 0.5mm tracks respectively. The demerit of using narrower silver tracks is that a heater design will require a larger number of track lines to fill a fixed fabrication area, which increases the number of gaps between the tracks leading to more frequent variation across the heater width. Therefore, it can be concluded that the track width influences a trade-off between the temperature variation in a heater and the cost of fabrication of a heater design, determined by the amount of silver required to fabricate it.

Based on the results 1 mm track width provides a good combination of temperature variation and amount of silver used per unit area in a heater design. For a fixed fabrication area a 1 mm track width will produce fewer gaps between the tracks compared to 0.5 mm track width and use significantly lesser silver than both 2 mm and 3 mm track width designs.

4.2.4.2 Gap between the heater track lines

Four meander heaters with a track line gap of 0.5 mm, 1 mm, 2mm and 3 mm were simulated in COMSOL to assess the impact of the gap on the heater output. Track width, track layout, input power per unit fabrication area and thickness of the silver tracks were kept the same for the four heaters. The track length increases from 91 mm – 96 mm as the track line gap is increased for the four heaters. The values of the fixed parameters are shown in table 17 below.

Parameter	Value
Thickness of silver tracks (µm)	20
Track width (mm)	1
Input power per unit fabrication area (mW)	1

Table 17: Fabrication parameters kept constant for the gap variation tests

Figure 49 shows the temperature distribution of the four meander heaters with 0.5mm, 1 mm, 2 mm and 3 mm track line gap. Figure 50 shows the graphs of temperature variation for the four heaters along a straight line drawn at length 15 mm across the heater width.

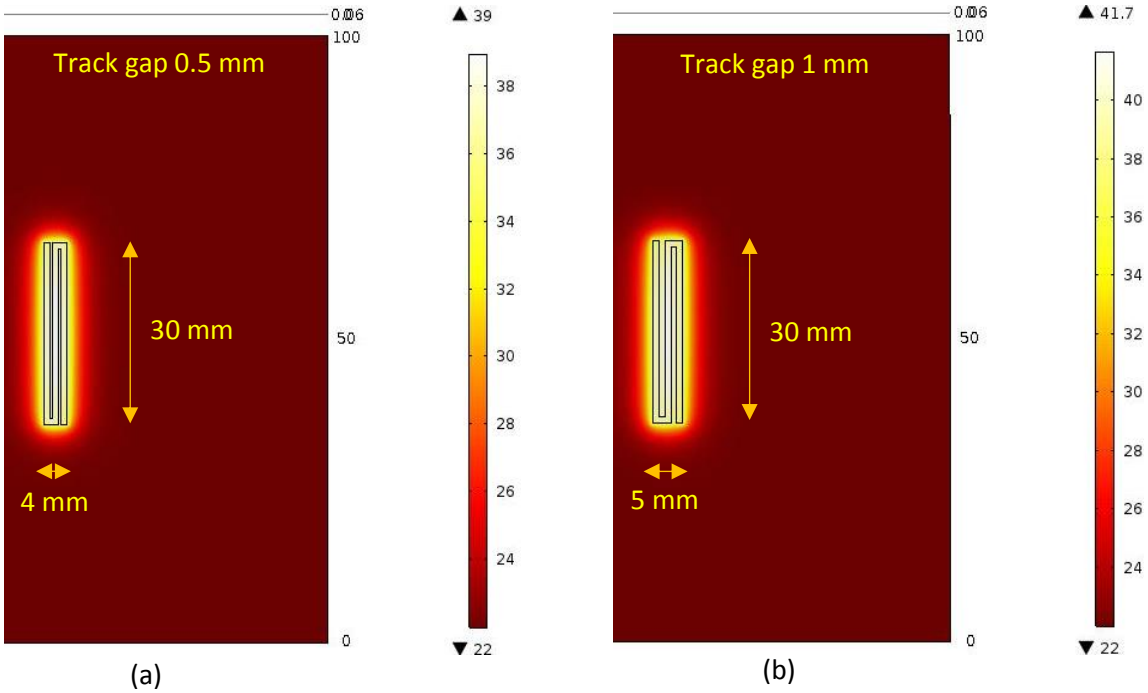

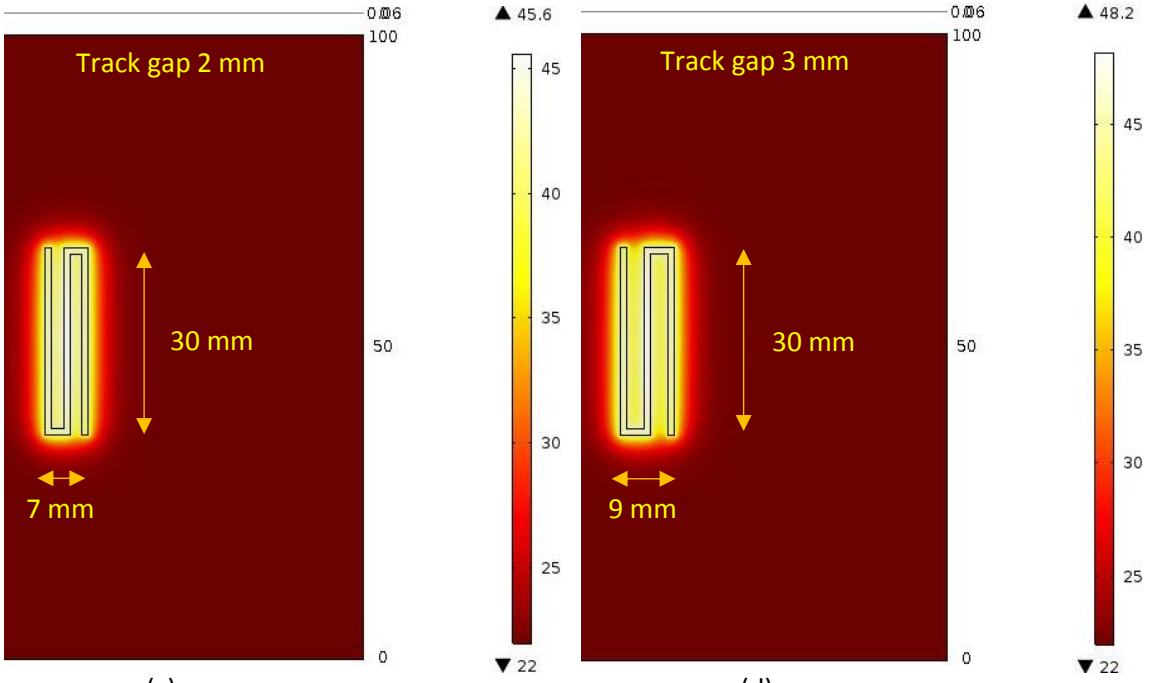

Figure 49: Temperature distribution of four heaters with track loop gap (a) 0.5 mm (b) 1 mm (c) 2 mm (d) 3 mm

The temperature distribution of the heaters show that, as the track line gap increases, the peak temperatures achieved by the heaters also increase. The heaters with track line gaps of 0.5 mm, 1 mm, 2 mm and 3mm achieved peak temperatures of 39°C, 41.7°C, 45.6°C and 48.2°C respectively. The temperature increase can be attributed to the higher input power, which corresponds to the area of each heater. If the same input power was applied to all four heaters, the heater with 0.5 mm gap would achieve the highest temperature because the thermal energy would be distributed to a smaller area.

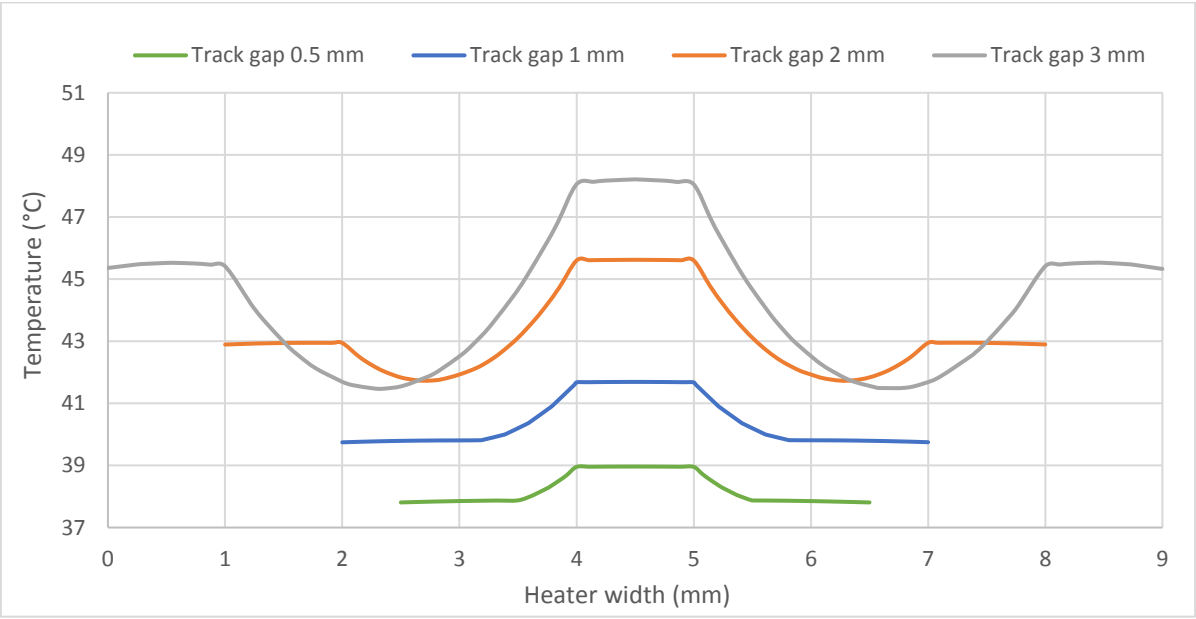

Figure 50: Temperature variation of four heaters with track loop gaps 0.5 mm, 1 mm, 2mm and 3mm across the heater widths

The temperature variation graphs show that the overall temperature variation in the heater output increases with an increase in the track line gap. The track lines are represented in the graphs by flat regions whereas the gaps are represented by slopes and curves. Larger track line gaps increased the magnitude and degree of the temperature variation and the shape of the graphs representing the gaps changes from slopes to parabolas. The magnitude of variation is judged by the difference in highest and lowest temperature of the heaters. The difference between the lowest and highest temperatures in a 0.5 mm track gap heater is 1.16°C which increases to 1.95°C for a 1 mm track gap heater, 3.89°C for a 2 mm track gap heater and 6.74°C for a 3 mm track gap heater.

All four heaters use about the same amount of silver ink however the silver tracks are distributed over different areas on the substrates. The amount of silver used in the four heater configurations is compared using the area of silver per unit fabrication area of the heaters. Table 18 below shows the area of silver track and area of silver per unit fabrication area in the four simulated heaters.

Gap between heater tracks (mm)	Area of silver track configuration (mm^2)	Area of silver track configuration /Fabrication area
0.5	91	0.758
1	92	0.613
2	94	0.448
3	96	0.356

Table 18: Silver track area and the ratio of silver track area to fabrication area of the four heaters simulated with tack gap 0.5 mm, 1 mm, 2 mm and 3 mm

The results show that the amount of silver used per unit area decreases as the gap between the tracks is increased. Silver used per unit area decreased by about 53 % as the track gap is increased from 0.5 mm to 3 mm. It is ideal to fabricate a heater with no gap between the track lines for minimal variation, however a large amount of silver per unit area would be required to cover the entire area raising the cost of fabrication. Increasing the gap between the track lines reduces the fabrication cost however it increases the magnitude of the temperature variation so a compromise has to be made between the two.

The results of the tests show that a 1 mm gap between tracks in a meander pattern provides a good combination of temperature variation and cost of fabrication. The heater with 1 mm gap used about 19.1 % less silver per unit area than the 0.5 mm track gap heater and produced lower magnitude variation than the 2 mm and 3 mm track gap heaters when judged by the difference of highest and lowest temperature produced by the heaters.

4.2.4.3 Variation in the geometrical layout of the heater

The geometrical layout of a silver track heater can be varied by arranging the track in a meander or spiral pattern and by aligning the track either along the length or width of the fabrication area. This section investigates the impact of varying the heater geometrical layout on its output by simulating three heaters using the COMSOL model. Two heaters were simulated to compare the output of a meander pattern heater with a spiral pattern; the third heater was simulated to assess the impact of changing the spatial orientation of the track arrangement. The three heaters were designed in the same fabrication area of 270 mm^2 with the length fixed to 30 mm and width fixed to 9 mm. Other parameters that affect the heater output (the input power, thickness of the tracks, gap between the track line and track width) are all kept constant. Table 19 presents the parameters kept constant for the tests.

Parameter	Value
Thickness of silver tracks (µm)	20
Track width (mm)	1
Gap between tracks (mm)	1
Input power (W)	0.18

Table 19: Parameters kept constant for the geometrical variation simulation tests

Figure 51 shows the temperature distribution of a meander and a spiral patterned heater and figure 52 shows temperature variation within the two heaters along a straight line drawn at length 15 mm across the heater width.

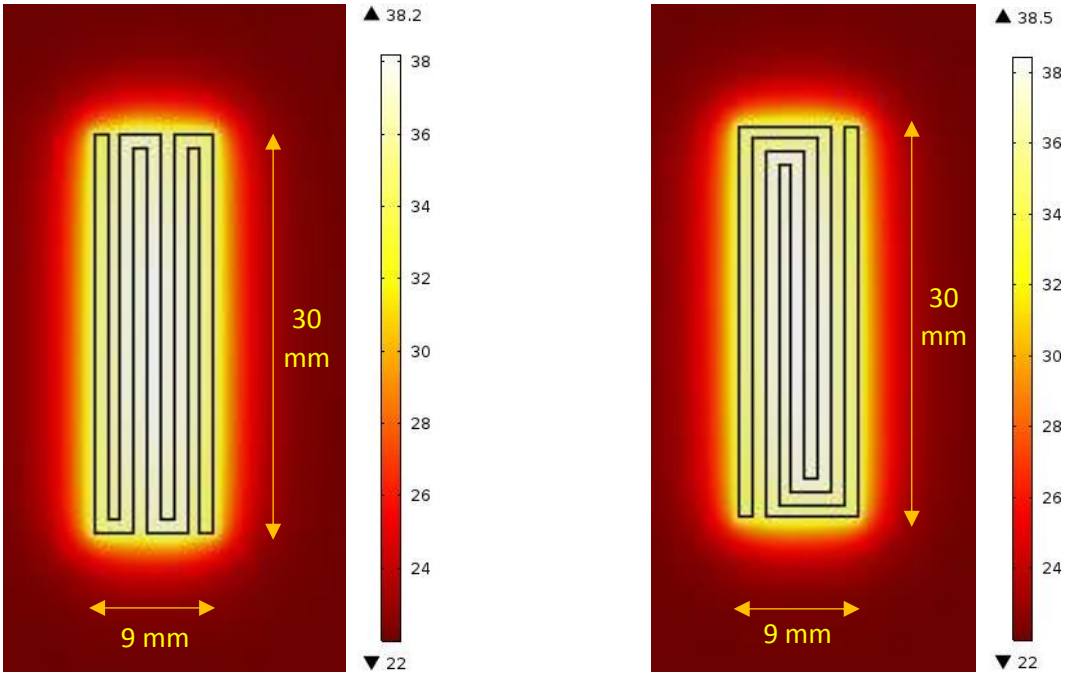

(a) (b)

Figure 51: Temperature distribution of (a) meander patterned heater and its equivalent (b) spiral pattern heater

The two heaters achieved similar temperature distributions, the peak temperature region, within both the heaters, is located at the centre of the heaters. The spiral pattern heater, for the same input power and amount of silver used, produced a 0.3°C higher peak temperature than the meander pattern heater.

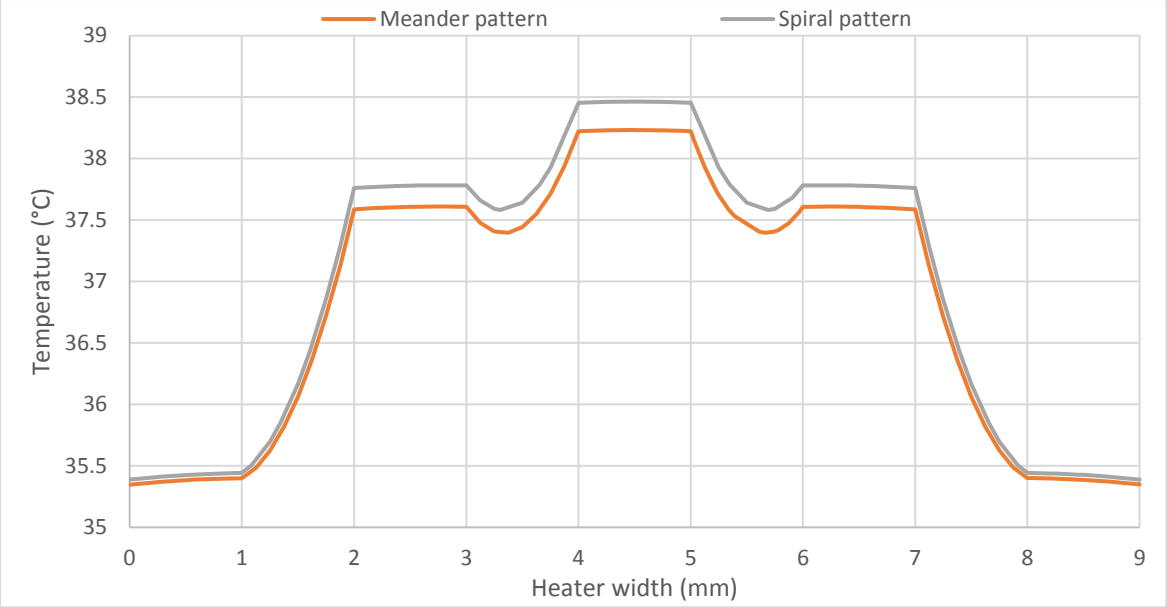

Figure 52: Temperature variation across equivalent meander and spiral pattern heaters width along the straight line drawn at length 15 mm

The shape of the temperature variation graph for the two heaters is the same although the meander pattern heater produced a slightly lower variation when judged by the difference between highest and lowest temperatures. The maximum temperature difference produced by the meander heater is 2.88°C and spiral heater is 3.07°C. The meander pattern heater is easier to design when compared to a spiral heater as a meander pattern can be considered modular. Individual silver track lines can be added or removed from a meander pattern to adapt to an increase or decrease in fabrication area whereas a spiral pattern has to be completely redesigned.

A second meander heater design consisting of track lines laid out along the width of the fabrication area was simulated in COMSOL. Figure 53 shows the temperature distribution of the heater and figure 54 presents the temperature variation graph of the heater across its length along a straight line drawn at width 4.5 mm. As the spatial orientation of the tracks in the heater design has changed, almost all the temperature variation occurs across the heater length. The track arrangement covered a 29 mm length instead of 30 mm as adding another track to the design required a 2 mm increase in fabrication area.

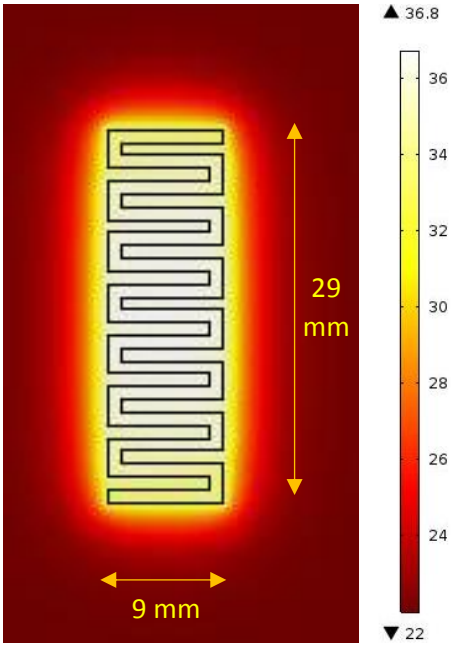

Figure 53: Temperature distribution of a meander heater design with tracks aligned along the width of the fabrication area

Figure 53 shows that the change in the spatial orientation of the meander design reduced the length of the tracks but increased their frequency. The temperature distribution of a higher track frequency meander heater has the same shape as the lower frequency meander design (figure 51 (a)). For the same input power and fabrication area the higher frequency meander heater produced a maximum temperature of 36.8°C which is 1.4°C lower than the lower frequency meander heater.

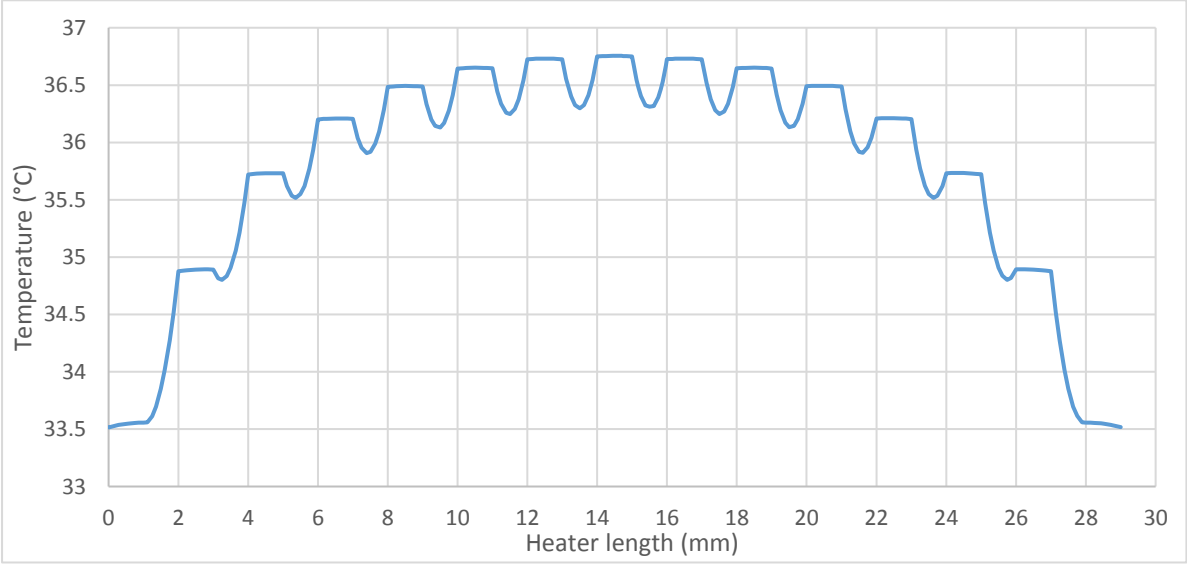

Figure 54: Temperature variation across the length of the meander heater design with tracks laid out along the width of the fabrication area

Figure 54 shows that the high frequency heater has a higher degree of temperature variation than the low frequency meander due to larger number of gaps between the tracks. The magnitude of variation is 3.24°C which is 0.36°C higher than the lower frequency meander heater, judged by the difference between the highest and lowest temperature achieved by the heaters.

Comparison of the low frequency meander with the high frequency meander shows that for the same input power and track width the heaters produce comparable peak temperatures and magnitude of temperature variation. However, the high frequency heater has more gaps between the track lines, which produces more frequent changes in temperature than the low frequency heater therefore producing a less uniform output. It can be concluded that for a rectangular fabrication area it is better to print the meander pattern with tracks along the heater length (low frequency) than width (high frequency) as it produces a more uniform temperature output.

The heater arrangement of a meander pattern with 1 mm wide tracks and 1 mm gap between tracks can be used as a basic configuration to design heaters in various shapes. As examples two heaters were designed in COMSOL to produce circular and triangular temperature profiles. Figure 55 below shows heaters with circular and triangular shaped temperature profiles.

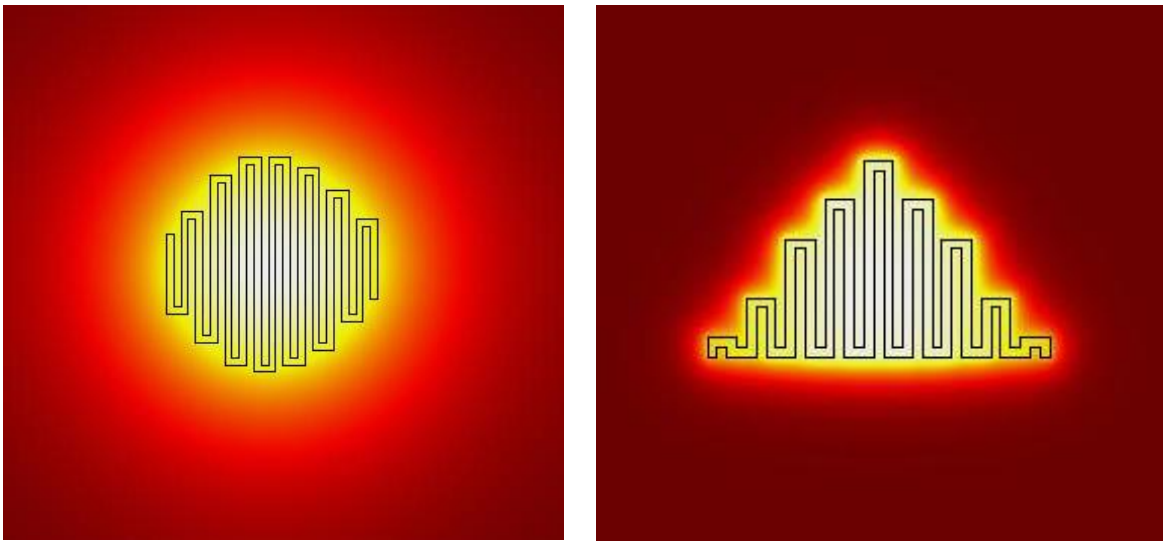

(a) (b)

Figure 55: (a) Circular and (b) triangular temperature profiles of heaters achieved using meander pattern, 1 mm wide track and 1 mm track gap

4.2.5 Heater design template for dispenser printing tests

This section summarises the results of the heater design simulation tests to derive a set of general rules for designing a track heater. It also presents a heater design based on the specific results from the simulation tests as a template to characterise dispenser printed heaters. The following presents the general rules for designing a track based heater.

- Track width in a heater design influences the temperature variation and the amount of silver used. Wider tracks produce lower variation use more silver because there are fewer gaps between the tracks.
- The gaps between the tracks affects the magnitude of temperature variation of a heater and the amount of silver used to fabricate the heater. A larger gap would produce a higher magnitude variation and use less silver.
- In a rectangular fabrication area, heater tracks laid out along the longer side of the fabrication area will produce a lower temperature variation than if the tracks are fabricated along the shorter side of the area.

The specific results from the simulation tests showed that a meander pattern with a combination of 1 mm track width and gap provided a suitable compromise between temperature variation and the cost of fabrication, judged by the amount of silver used. Therefore, the heater template for printing tests

was designed in a 30 mm x 31 mm fabrication area using a meander pattern with 1 mm track width and gap. The thickness of the tracks, 20µm, was chosen to match the resistance of the printed heaters presented in section 4.3.1. 1.27 W of input power is supplied to the heater in the simulation. Figure 56 below shows temperature distribution of the test heater and figure 57 shows the temperature variation of the heater across its 31 mm width at steady state. The variation is measured along a straight line drawn at 15 mm length.

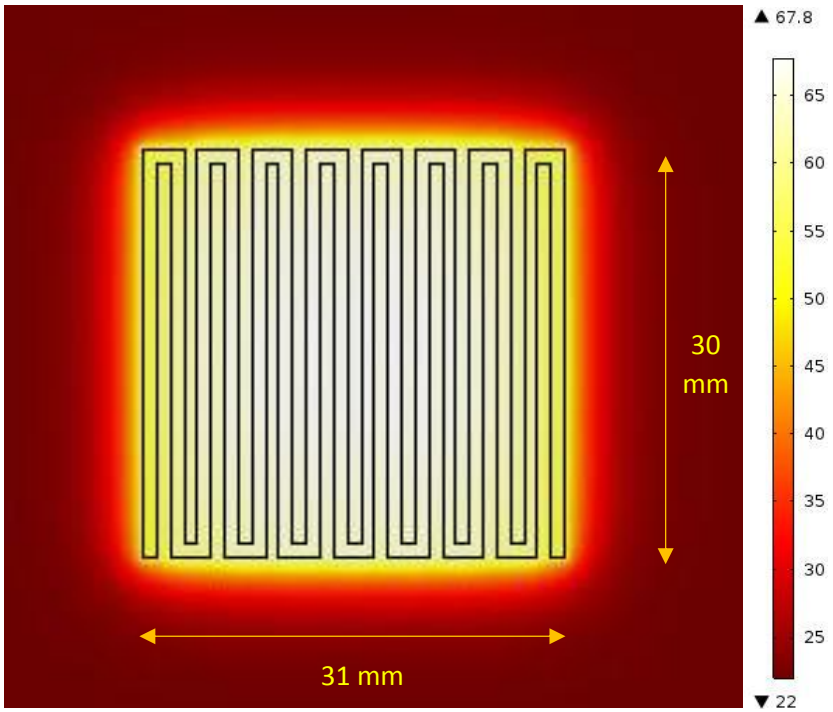

Figure 56: Temperature distribution of the simulated test heater

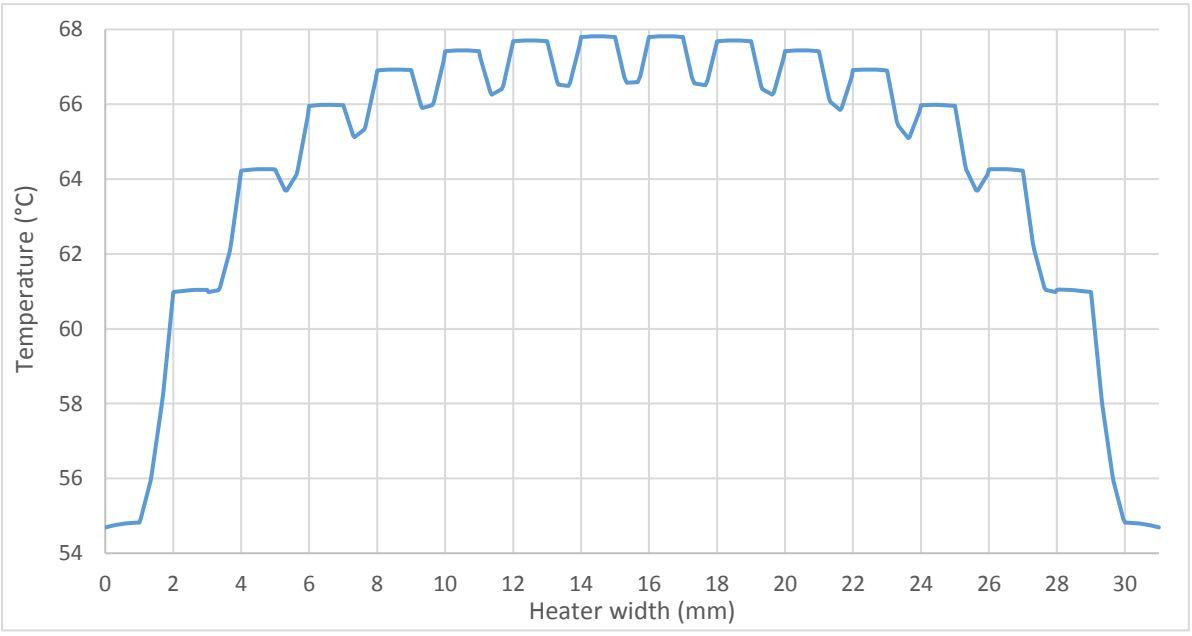

Figure 57: Temperature variation across the heater width measured along a straight line drawn at length 15 mm

The temperature distribution of the heater shows that it achieved a peak temperature of 67.8°C.The temperature variation graph of the heater shows that there is a significant amount of variation in the

heater. The difference between the highest and lowest temperature in the graph is 13.1°C. Most of the temperature variation is found at ends of the heater width. Ideally a heater would have no temperature variation however it cannot be entirely avoided in a meander design due to the gaps between track lines.

4.3 Printing and characterisation of dispenser printed heaters

This section describes dispenser printing of the track heaters using the design template presented in section 4.2.5. It details characterisation of the printed heaters in terms of temperature distribution and temperature variation across the width. The output of the printed heaters is compared with the output of the simulated test heater. Printing and characterisation of carbon heaters which offers an alternative to silver-based heaters is also presented. This section also discusses formulation of custom conductive inks for dispenser printing heaters and presents a test heater fabricated using one of the formulated inks. Finally, it details the concept of selectively heating parts of a track heater and presents approaches to achieve it. Selective heating ensures that, in a printed electronic circuit consisting of a complex network of electrical interconnections, only heater specific tracks produce heat.

4.3.1 Dispenser printed silver ink heaters

The heater design described in section 4.2.5 was dispenser printed on Kapton and polyester cotton 65/35 blend fabric. DuPont 5000 silver ink was used for printing the heater, using the settings in table table 8. DuPont 5018 interface ink was printed on the fabric using the print settings in table 11. A 35 mm x 35 mm interface print was dispensed first on the fabric to provide a smooth platform for the subsequent silver layer. Figure 58 below shows the test heaters dispenser printed on Kapton and the fabric.

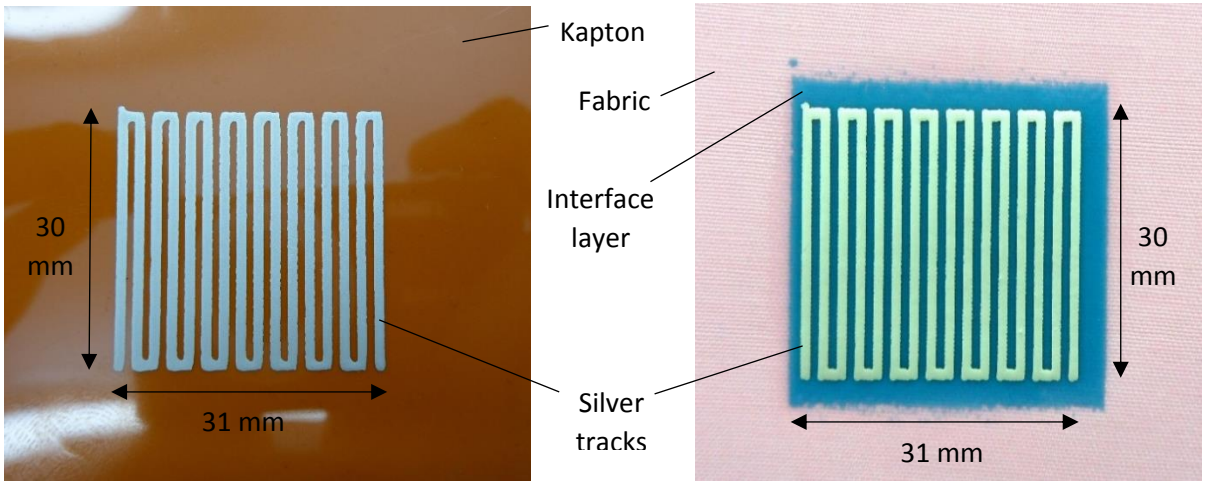

Figure 58: Dispenser printed test heaters printed on (a) Kapton and (b) interface layer on fabric

The resistance achieved by the Kapton and fabric heaters was 6.01 Ω and 5.97 Ω respectively. The heaters were characterised in terms of temperature distribution and temperature variation across the width of the heaters. The temperature distribution was measured by supplying 1.27 W power to the heaters and taking their thermal image after 300 seconds using a Testo 875 thermal imager. The thermal image was further processed in Testo IRSoft software to obtain the temperature variation profile of the heater across its width. Similar to the simulation tests, a straight line was drawn at the mid-point of the heater length across its width to obtain temperature variation data. Figure 59 shows the temperature distribution of the Kapton and the fabric heaters.

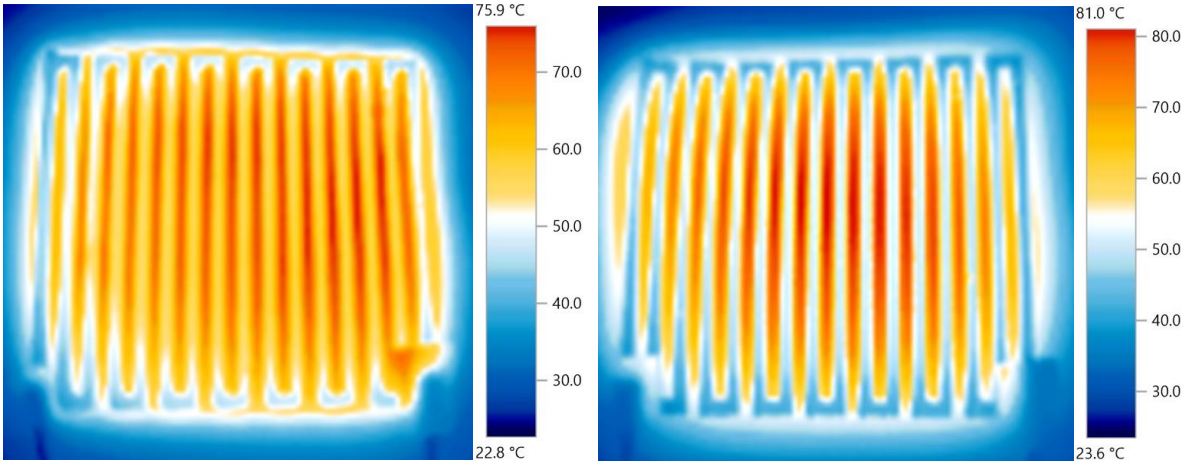

(a) (b)

Figure 59: Temperature distribution of dispenser printed heater on (a) Kapton and (b) interface layer on fabric at steady state

The temperature distribution shows that the Kapton and the fabric heaters achieved a peak temperature of 75.9°C and 81.0°C respectively. The heat distribution in both the heaters is uneven, it is less uneven in Kapton heater than the fabric heater. The highest temperatures in Kapton heater, 70.9°C-75.9°C, are distributed in a broader area compared to the highest temperatures, 75°C-81°C, in the fabric heater. The uneven heat distribution shows that the heaters have non-uniform resistance distribution, as for the same input current the regions of printed tracks with higher resistance produce higher temperature and vice versa. The non-uniform resistance distribution is caused by non-uniform thickness of the printed silver meander track, as other factors which affect the resistance such as length, width and resistivity of the silver ink are same for the entire silver meander track. The thickness variation in the printed track is caused by the variation in the gap between the printing nozzle and the substrate (nozzle height), as discussed in section 3.6. The nozzle height variation can be caused by the variation in the thickness of alumina tiles to which the substrates are glued for dispenser printing and the expected thickness variation in the interface prints, shown in table 12. The region in the middle of the fabric silver track has a higher resistance than any part of the Kapton track which causes the fabric heater to reach a higher temperature than the Kapton heater.

The silver track surfaces are at a lower temperature than the temperature in the gap between the track lines. The peak temperature difference between the tracks and the track gaps is 15°C for the Kapton heater and 27°C for the fabric heater; the higher temperature difference in the fabric heater is caused by the higher resistance region of the heater. The silver tracks are at a lower temperature to the gaps because of slow heat flow within the silver track due to the thermal properties of the printed silver ink as explained in section 4.2.3. Figure 60 below shows the temperature variation in the two heaters measured along a straight line drawn across the heater width.

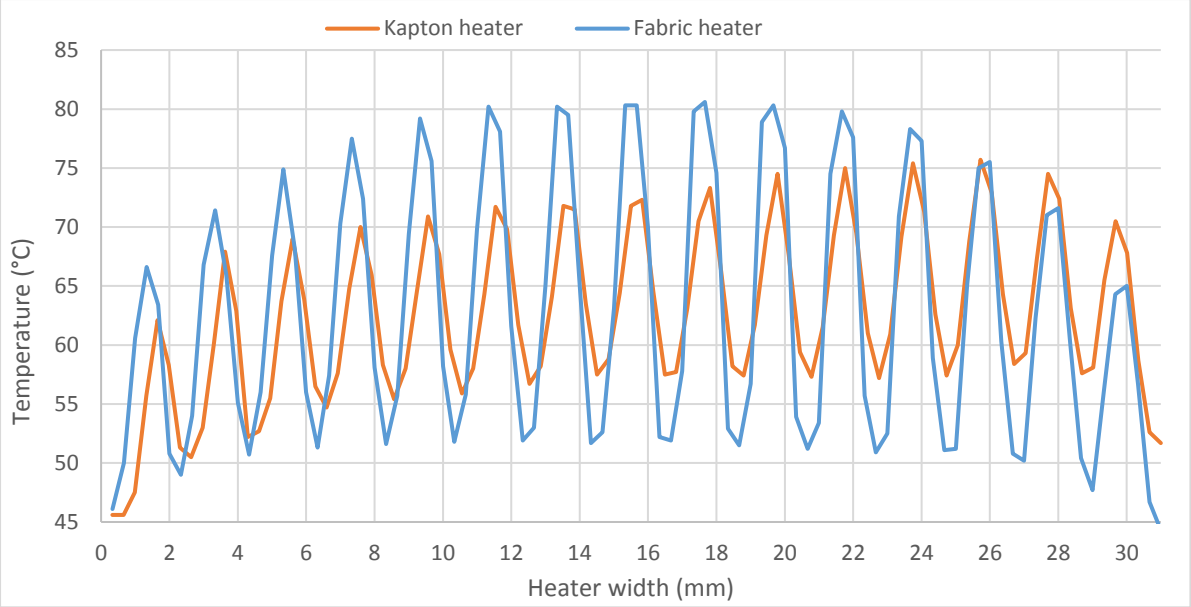

Figure 60: Temperature variation of printed heaters on Kapton and fabric across the heater width

The temperature variation graphs of Kapton and fabric heaters have a similar shape. The troughs represent the tracks and the peaks represent gaps between the track lines. The magnitude of the temperature variation is higher in the fabric heater output, 36.3°C than the Kapton heater, 30.1°C as judged by the difference between highest and lowest temperatures in the graph. The higher variation magnitude of the fabric heater can be attributed to the higher resistance region in the middle of the fabric heater. The higher resistance region attains a higher temperature than the rest of the fabric heater and the Kapton heater, therefore increasing the gap between highest and lowest temperatures of the fabric heater. The peaks and troughs of the variation graph for Kapton heater rises across the width of the heater which is reflective of its uneven temperature distribution.

Comparison of the simulated and printed heaters shows that the printed heaters achieved higher temperatures than the simulated heater for the same input power. The comparison however is unfair as the heat distribution of the printed heaters is uneven and varies significantly within the heaters. Printed heaters have a significantly higher temperature variation across the heater widths than the simulated heater. The simulated heater produced a highest temperature difference of 13.1°C across its width which is much lower than 30.1°C produced by the Kapton heater and 36.3°C by the fabric heater. The difference in temperature variation between printed and simulated heaters is caused by the non-uniform resistance distribution and the difference in the thermal properties of printed silver ink and the simulated pure silver tracks.

The results show that the thickness uniformity of the printed silver path can significantly affect the output of a printed heater as it correlates with the temperature variation; more uniform thickness leads to lower temperature variation. Despite the high temperature variation, the printed heaters can be used for active actuation of thermochromic fabrics by ensuring that the lowest temperature achieved by the heater is raised higher than the activation temperature of the thermochromic layer. The temperature variation in the heater output is expected to be lower once the thermochromic layer is printed over the heater as the heater track will not be exposed to the air. The heat lost from the track will be transferred to the thermochromic layer instead of the air.

A disadvantage of silver ink as the constituent material for the printed heaters is that the resistivity of the ink is low which produces a low resistance for the printed silver track heater. Low resistance track

heaters may not be suitable for wearable applications as a small voltage across heater terminals would produce a high current in the heater which make it more likely to cause dangerous electric shocks. As an example 5 V applied to the printed silver heaters would produce a current of 0.83 A.

4.3.2 Dispenser printed carbon ink heaters

Carbon in the form of DuPont 7102 carbon ink is used as an alternative constituent material for printing heaters. DuPont 7102 is a high resistivity carbon ink which satisfies the requirement of a low curing temperature ink with dispenser printable viscosity. A low curing temperature ensures the curing process does not damage the polyester cotton 65/35 blend fabric. This section details printing and characterisation of dispenser printed carbon heaters. It also compares the output of the carbon heaters with the printed silver heaters. Table 20 below shows properties of the carbon ink.

Resistivity (Ω.m)	$5.08 – 7.62 \times 10^{-4}$
Viscosity (Pa.S)	60 - 125
Curing Temperature (°C)	120
Curing Time (mins)	5-6

Table 20: Properties of DuPont 7102 carbon ink

First, a number of printing tests were carried out to identify dispenser printer settings for printing the carbon ink. The aim of the tests was to determine a set of printer settings which allowed the carbon ink to completely fill the designated print area. Table 21 below shows the dispenser printer settings used for printing the carbon ink on Kapton and the interface on the fabric.

Pressure (kPa)	90.0
Dispense Time (ms)	25
X-resolution (mm)	0.40
Y-resolution (mm)	0.40
Nozzle Height (µm)	100
Vacuum (kPa)	0.10
Speed (mm/s)	1

Table 21: Dispenser printer settings for printing DuPont 7102 carbon ink

A set of ten 30 mm x 2.5 mm carbon tracks was dispenser printed on Kapton and interface on fabric to determine the resistivity of the printed carbon ink. The resistivity of the printed tracks was calculated using equation 3. The resistance of the printed tracks was measured using Wayne Kerr 6500 B precision impedance analyser and the thickness of the tracks was measured using a Mitutoyo micrometre. Figure 61 shows four carbon tracks dispenser printed on Kapton and the interface on fabric. Table 22 below shows the average resistivity of the printed carbon ink achieved on Kapton and the interface on fabric along with ±1 standard deviation.

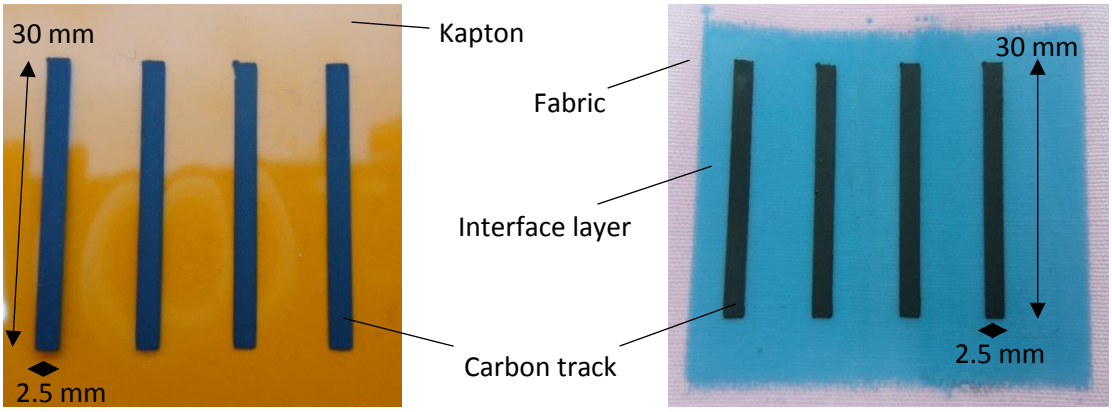

Figure 61: Carbon tracks dispenser printed on (a) Kapton and (b) Interface layer on fabric

Substrate	*Kapton*	*Interface layer on fabric*
Avg. Resistivity (Ω.m)	7.50×10^{-04}	1.10×10^{-03}
±1 Standard deviation	9.94×10^{-05}	2.84×10^{-04}

Table 22: Average resistivity of the dispenser printed carbon ink on Kapton and the interface on fabric

The results show that the resistivity value of the printed ink on Kapton lies in the range provided in table 20. The resistivity value achieved on the interface is higher than Kapton and the expected resistivity range in table 20. The variation in the resistivity value is also higher on the interface on fabric compared to Kapton. The higher resistivity value and variation is caused by non-uniform resistance distribution of the carbon tracks which can be attributed to higher thickness variation within the printed tracks. The printed tracks produce non-uniform printed structures due to the nozzle height variation as discussed in sections 3.6 and 3.8.

Carbon heaters were printed on Kapton and the interface on fabric using the test heater design, presented in section 4.2.5. A 35 mm x 35 mm interface layer was printed first on the fabric surface to reduce the fabric surface variation followed by the carbon layer which was printed using the settings presented in table 21. Figure 62 below shows the carbon heaters printed on Kapton and on the interface layer on fabric.

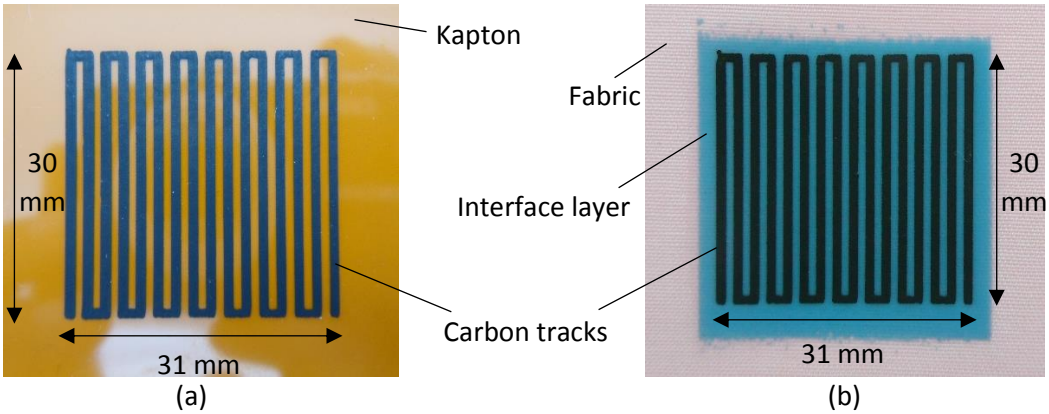

Figure 62: Carbon ink heaters dispenser printed on (a) Kapton and (b) interface on fabric

The heaters were characterised in terms of temperature distribution and temperature variation across the heater width. The variation was measured along a straight line drawn at the midpoint of the heater

length. The carbon heater printed on Kapton produced a resistance of 16.34 kΩ whereas the heater printed on fabric produced 36.89 kΩ resistance. The difference in resistance occurs due to the difference in the thickness of the printed tracks. The carbon tracks on average were 19.2 µm thick on Kapton and 16.4 µm thick on the interface on fabric. The difference in thickness was a result of difference in nozzle height set up.

An electric current of 5 mA was passed through the two heaters and a thermal image was taken after 300 seconds to assess the temperature distribution and the temperature variation of the two heaters. The carbon heaters have very high resistances so a high voltage power supply was required to actuate the heaters. Figure 63 below shows the temperature distribution of the two heaters.

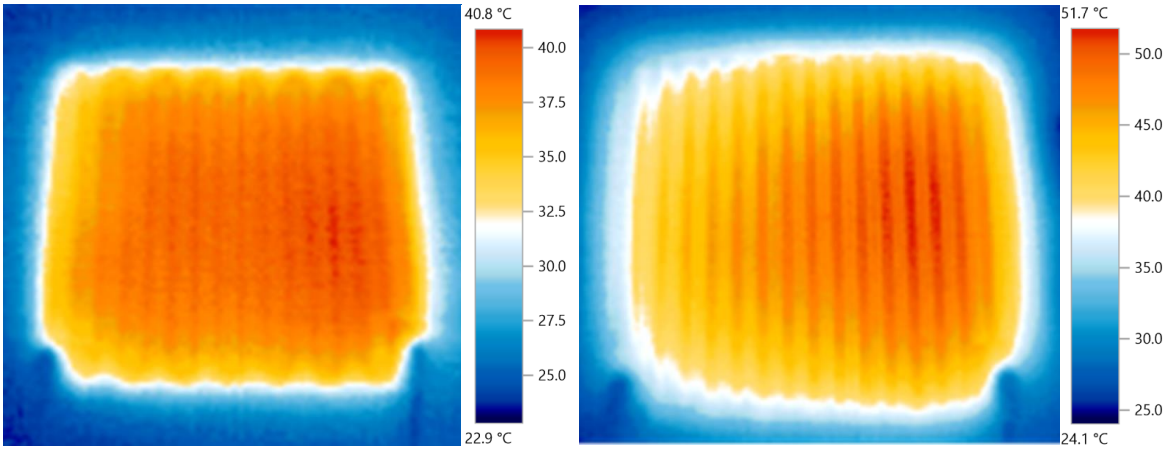

(a) (b)

Figure 63: Temperature distribution of dispenser printed carbon heater on (a) Kapton and (b) interface on fabric

The peak temperature produced by the Kapton heater is 40.8°C and the fabric heater is 51.7°C. The Kapton heater produced fairly uniform temperature distribution whereas fabric heater produced an uneven heat distribution. The highest temperature region in the fabric heater is located on the right side of the thermal image and is represented by the red colour. This suggests that the resistance distribution in the fabric heater is non-uniform. The non-uniform resistance is caused by the non-uniform thickness of the printed conductive tracks as discussed in section 4.3.1. The fabric heater produced a higher temperature than the Kapton heater due to the higher input power. The power supplied to the Kapton heater was 0.41 W and the power supplied to the fabric heater was 0.92 W. Figure 64 shows the temperature variation graphs of the two dispenser printed carbon heaters.

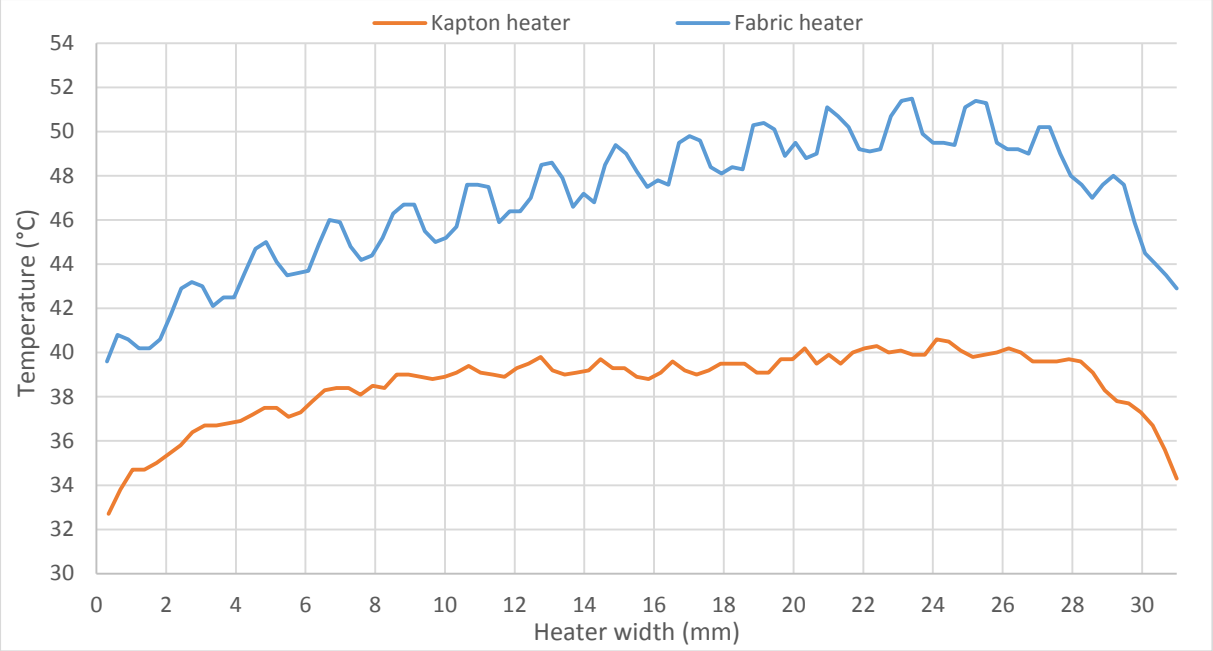

Figure 64: Temperature variation graph of dispenser printed carbon heaters on Kapton and fabric across the heater widths

The results show that the overall temperature variation is relatively low in both carbon heaters although it is higher in the fabric heater than the Kapton heater. The highest temperature difference is 11.9°C in the fabric heater and 7.9°C in the Kapton heater. The Kapton heater has a fairly uniform heat distribution, hence its temperature variation graph is almost symmetrical. The fabric heater has an uneven temperature distribution with a higher temperature region towards the right of the heater which is reflected in the graph. The temperature variation in the gap between two consecutive tracks is around 1°C for the Kapton heater and 2°C for the fabric heater.

Comparison of the carbon heaters with the printed silver heaters shows that the carbon heaters produced improved output. The carbon heaters produced more uniform temperature distribution and lower temperature variation graphs than the printed silver heaters. The highest temperature difference in the carbon heaters is 7.9°C for the Kapton and 11.9°C for the fabric heater which is much lower than 30.1°C for the Kapton silver heater and 36.3°C for the fabric silver heater. Unlike the printed silver tracks, the temperature difference between the carbon track surfaces and the surrounding substrate is very low, 1-2°C, although the carbon track surfaces are at a lower temperature than their surrounding substrate. This shows that the heat transfer rate within the carbon tracks is faster than the heat transfer rate within the silver tracks.

The carbon heaters produced significantly higher resistance than the silver heaters for the same track arrangement. The very high resistance of the carbon heaters limits the choice of suitable power sources for them. For a fixed input power a carbon heater pattern will require a considerably higher voltage for actuation than the same patterned silver heater. As an example, an input power of 0.41W requires 82 V for the carbon Kapton heater (16.34 kΩ) and 1.57 V for the silver Kapton heater (6.01Ω). This makes carbon heaters less suitable for wearable and battery powered applications as batteries are not suitable power sources for them. Another disadvantage of the carbon heaters is that their output is more prone to temperature variation than the silver heaters. Carbon ink has high resistivity, so a small thickness variation in a carbon track will produce a higher magnitude resistance variation than a silver track. The higher magnitude resistance variation will translate into a higher magnitude temperature variation in a heater.

4.3.3 Formulation of custom conductive inks for printing heaters

This section discusses formulation of custom conductive inks for dispenser printing of heaters. DuPont 5000 silver and DuPont 7102 carbon inks offer limited choice of electrical resistivity for printing heaters, which causes a heater design to attain either low or high resistance. The aim of the ink formulation is to provide inks which offer a range of resistivity values between that of silver and carbon inks. All parameters that affect the resistance of a printed heater can be controlled during the design stage with the exception of resistivity of the constituent material. The range of inks offer control of the resistivity of the material constituting the printed tracks. For a fixed input power, the resistance of a heater directly affects the amount of electric current that passes through the heater tracks and influences the choice of power source for a heater. DuPont 7102 carbon ink was mixed with DuPont 5000 silver ink in five different proportions to provide the range of ink. The low curing temperatures and dispenser printer compatible viscosity range makes the two inks suitable as constituents of the custom formulations.

The carbon ink was mixed with the silver ink in the proportions of 20%, 40%, 60%, 70% and 80% by mass. The contents of the five formulations were mixed using a SpeedMixer DAC 150.1 FVZ. Five 30 mm x 2.5 mm tracks of each of the ink formulations were dispenser printed on Kapton and interface on fabric for resistivity measurement of the inks. The resistivity of the inks was calculated using the measured resistance and thickness of the printed tracks using equation 4. The print settings were identified using numerous printing tests and previous experience of dispenser printing. The formulation consisting of 20% carbon ink and 80% silver ink could not be printed as the ink separated after mixing. Table 23 below shows dispenser printer settings for the four printed inks. Figure 65 shows the bar chart of calculated average electrical resistivity of the silver, custom formulations and the carbon ink on Kapton and the interface on fabric. The error bars in the chart represent ±1 standard deviation in the average resistivity values of the inks.

% Carbon ink in the formulation	**40**	**60**	**70**	**80**
Pressure (kPa)	70.0	80.0	90.0	
Dispense Time (ms)	20	25	25	
X-resolution (mm)	0.5	0.5	0.4	
Y-resolution (mm)	0.4	0.4	0.4	
Nozzle Height (µm)	150	100	100	
Vacuum (kPa)	0.10	0.10	0.10	
Speed (mm/s)	1	1	1	

Table 23: Dispenser printer settings for custom conductive ink formulations

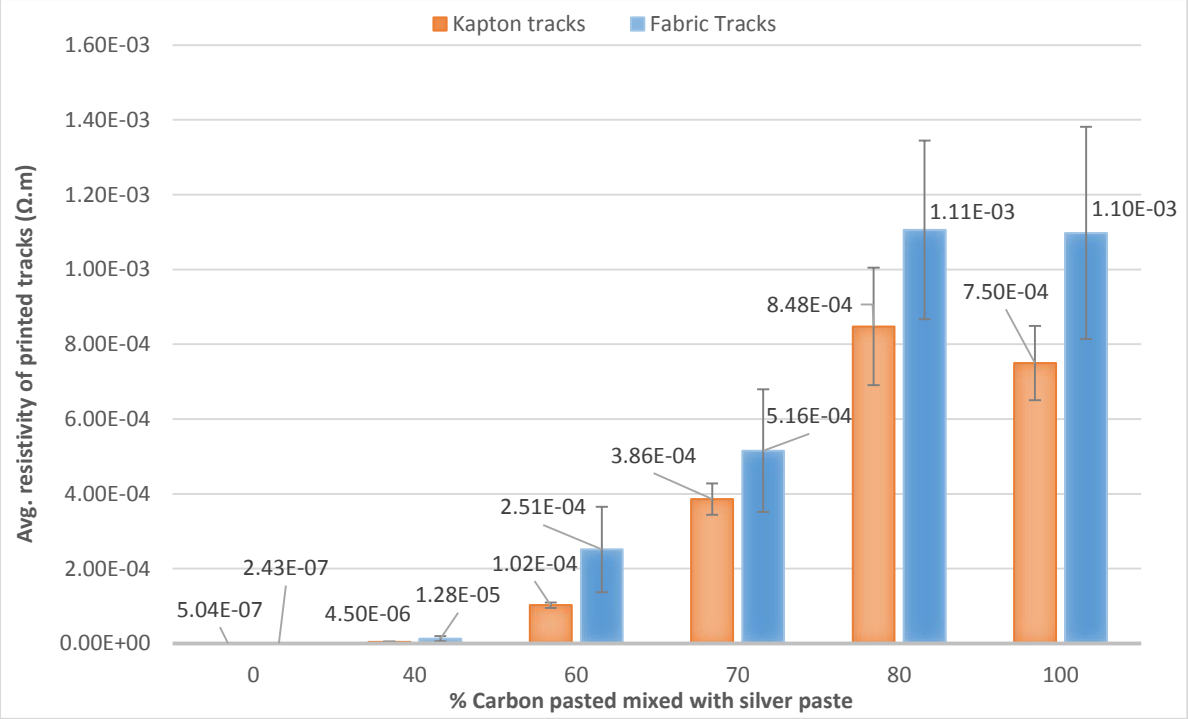

Figure 65: Average resistivity and variation of silver ink, custom formulations and carbon ink on Kapton and interface on fabric

The results show that the resistivity of the printed inks increases as the proportion of carbon ink mixed with silver ink is increased. The resistivity of 80% carbon formulation matched the resistivity of carbon ink which suggests that the silver ink doesn't have any effect on the resistivity of the formulations above 80% of carbon ink. The average resistivity, and variation in the resistivity values, is higher for tracks printed on the interface on fabric compared to Kapton. This is because thickness variation and surface variation within the interface on the fabric is higher than Kapton. The resistance variation within the tracks is reflected in the chart by the variation in the average resistivity values. The proportions of carbon mixed with silver can be varied between 40% and 80% to formulate inks which would produce printed resistivity values in the range of 4.50 $x10^{-06}$ – 1.11 x 10^{-03} Ω.m.

The range of resistivity offered by the custom formulations allows a designer to vary the resistance of an application specific heater design. As an example, the test heater presented in section 4.2.5 was printed on Kapton and the interface on fabric using the 60% carbon formulation and its output is compared to the silver and the carbon heaters. The interface layer was printed first on the fabric measuring 36 mm x 40 mm followed by the conductive ink. Figure 66 shows the dispenser printed heaters printed on Kapton and fabric using a custom formulation consisting of 60% carbon ink and 40% silver ink.

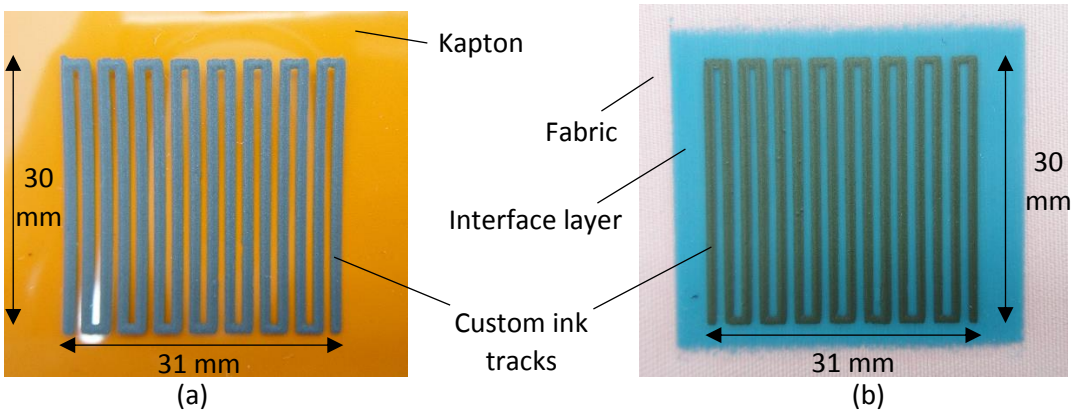

Figure 66: Heaters dispenser printed using 60% carbon ink formulation on (a) Kapton and (b) interface on fabric

The resistance of the Kapton heater was 1.9 kΩ and that of the fabric heater was 7.2 kΩ. The difference in resistance is caused by the difference in thickness of the printed tracks. The two heaters were supplied with 1.44 W and 1.62 W of electrical power respectively and thermally imaged after 300 seconds. Figure 67 below shows temperature distribution of the two heaters.

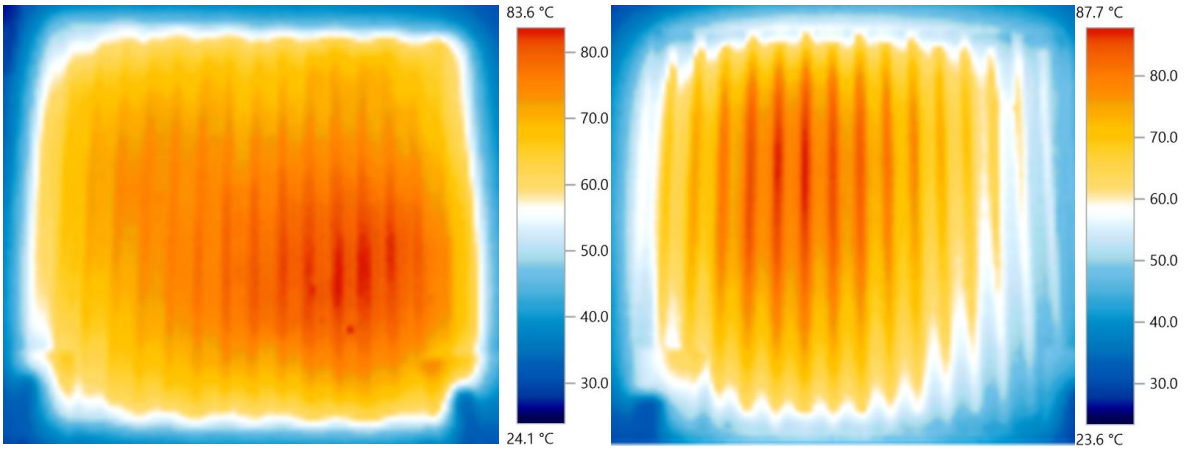

Figure 67: Temperature distribution of 60% carbon formulation heater printed on (a) Kapton and (b) interface on fabric

The temperature distribution of the two heaters shows that both the heaters have uneven heat distribution. The Kapton heater produced a much more uniform temperature distribution compared to the fabric heater. The Kapton heater produced a peak temperature of 83.6°C and the fabric heater produced a peak temperature of 87.7°C. The highest temperature region of the Kapton heater is located around the bottom right of the heater and for fabric heater it is located around the top left of the heater. The uneven temperature distribution is caused by the resistance variation in the heater, which is produced by non-uniform thickness of the printed track. Figure 68 shows the temperature variation of the two heaters measured across the width of the heaters using the thermal image.

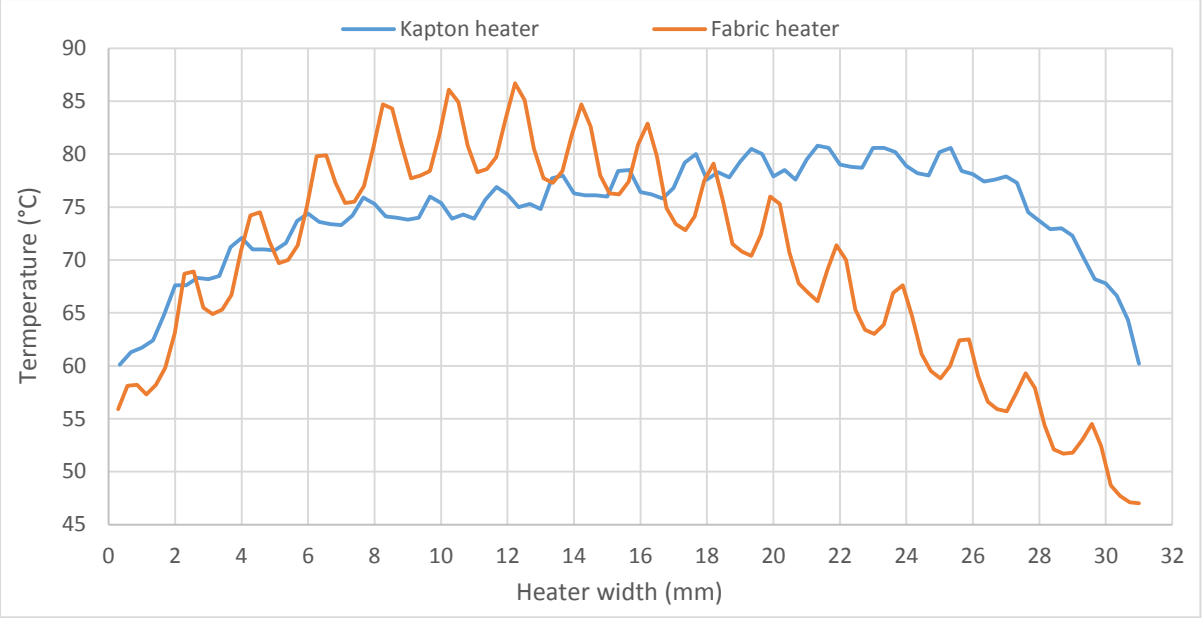

Figure 68: Temperature variation across the dispenser printed custom formulation heaters printed on (a) Kapton and (b) interface on fabric

The temperature variation graph shows that the Kapton heater has a lower variation than the fabric heater. The difference between the highest and lowest temperatures in the Kapton heater is 20.7°C and in the fabric heater it is 39.7°C. Uneven resistance distribution caused by the non-uniform thickness of the tracks is a major contributing factor to the higher temperature difference of the fabric heater. The temperature distribution of the heater shown in figure 67 shows that the tracks are at lower temperature than the gap between the tracks. It is represented in the temperature variation graph in figure 68 as the regular crests and troughs. The temperature of the tracks is 3°C lower than the temperature between the track lines for the Kapton heater and around 8°C for the fabric heater. It is higher in the fabric heater because the interface loses heat at a lower rate than Kapton causing it to retain a higher temperature at the steady state as previously explained in section 4.2.3.2.

The output of the 60% carbon formulation heater is better than the silver heater and inferior to the 100% carbon heater when judged by the temperature variation within the heaters. Among the Kapton heaters, the carbon ink heater produced a temperature variation of 1°C in the track gap which rises to 3°C for the 60% carbon formulation heater and around 15°C for the silver heater. For the fabric heaters, the temperature variation in the track gap is 3°C for the carbon heater, 8°C for the 60% carbon formulation heater and around 27°C for the silver heater.

The common fabrication issue for all the heaters is the variation in the gap between the printing nozzle and substrate. It must be noted that, for a thermochromic device, a layer of thermochromic ink would be printed over the heaters which will affect the dynamics of heat transfer. The temperature variation in the heaters may not be noticeable to the same extent as in the thermal images when a thermochromic device changes colour.

4.3.4 Selective heating within a conductive track arrangement

The temperature distribution in a track heater can be controlled to selectively heat specific regions within the heater. Selective heating can be used to ensure that, in a printed electronic circuit consisting of a complex network of electrical interconnections, only heater specific tracks produce heat. In context of smart fabric devices, selective heating can be used to connect conductive tracks dedicated to a heater to electrical interconnections common to other sensors and actuators in the

device. This section discusses the theory of selective heating, methods of achieving localised/selective heating and fabrication of heaters that produce selectively heated regions.

In a track heater, heat generation due to joule heating depends on the electrical resistance of the track arrangement and the electrical current passing through it as shown in equation 1. A conductive track can be considered as a chain of small resistors arranged in a series circuit. According to circuit theory, the electric current is constant throughout a series circuit. For a track heater, regions of higher resistance will receive a higher proportion of the input electrical energy as the resistance factor in the equation $P = I^2R$ would be higher for the same magnitude of current. The magnitude of current passing through a conductive track depends on the overall resistance of the track and the potential difference applied across its terminals. The higher resistance regions in a track heater would generate more heat than the rest of the track and achieve a higher temperature region.

An arrangement of conductive track can be designed to produce different electrical resistances at different locations. The resistance of a track is governed by the resistivity of the constituent material, the length of the track, the width of the track and the thickness of the track. These factors can be manipulated to produce pre-selected resistances at specific spots in a heater and therefore selectively/preferentially heat parts of a conductive track arrangement. The resistivity of the constituent material of a conductive track can only be altered by using multiple materials. The following presents methods of achieving localised heating in a conductive track arrangement using a single conductive ink and also using multiple conductive inks.

4.3.4.1 Selective heating using a single conductive ink

Selective heating using a single conductive ink can be achieved by varying the length, width and thickness of the printed conductive track arrangement. One or more of these parameters can be varied at specific locations in a heater to produce regions of higher/lower resistance. Three heaters were dispenser printed to demonstrate selective heating due to variation of the length, width and thickness in the conductive tracks. The three heaters were printed using silver ink on the interface on fabric. Figure 69 shows the three dispenser printed heaters, their physical dimensions, and the resistances of different sections of the heater.

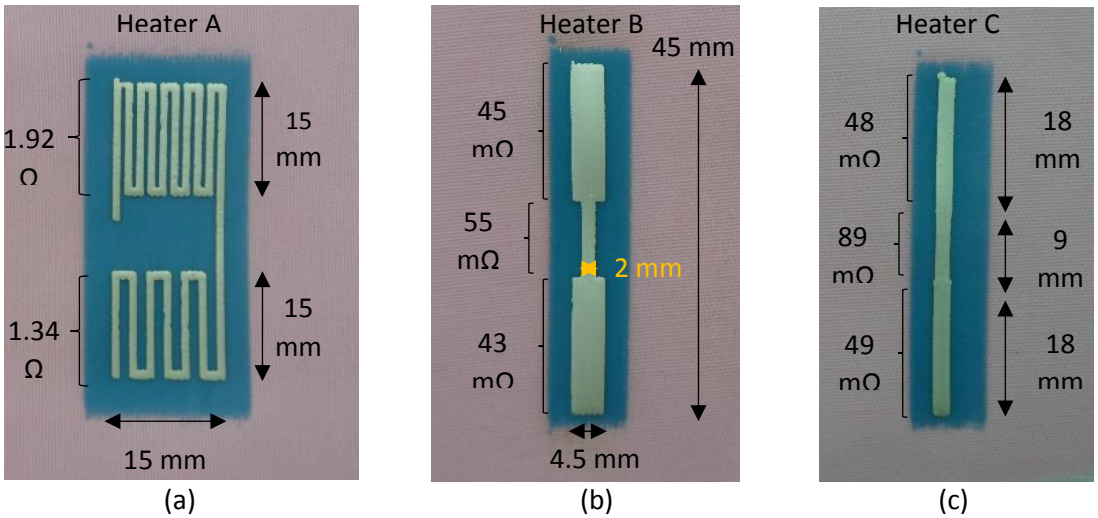

(a) (b) (c)

Figure 69: Heaters dispenser printed to demonstrate selective heating due to (a) length, (b) width and (c) thickness variation

Heater A is designed to produce a region of higher resistance by varying the length of the conductive track. The top half is printed with a narrower gap between the tracks compared to the bottom half to

increase length of the tracks. The top half of the heater has 0.58 Ω higher resistance than the bottom half. The width and thickness of the tracks were kept same for the entire heater design.

Region of higher resistance in heater B is created by varying the width of the conductive track constituting the heater. The middle section of the conductive track was printed 2.5 mm narrower than the rest of the track as shown in figure 69(b). The variation in width produced a resistance difference of about 12 mΩ between the higher and lower resistance regions. The resistance difference is very small because the wider regions of the track are longer than the narrower region.

Heater C is designed to produce a region of higher resistance by varying the thickness of the conductive track constituting the heater. The middle section of the heater consists of 1 layer of silver ink whereas the top and bottom sections each consist of 4 layers of silver ink printed using the same settings. The middle section is a quarter of thickness of the top and bottom sections. The resistance of the middle section is about 41 mΩ higher than the other two sections.

Figure 70 presents the thermal images of the three heaters showing the temperature distribution within the three heaters.

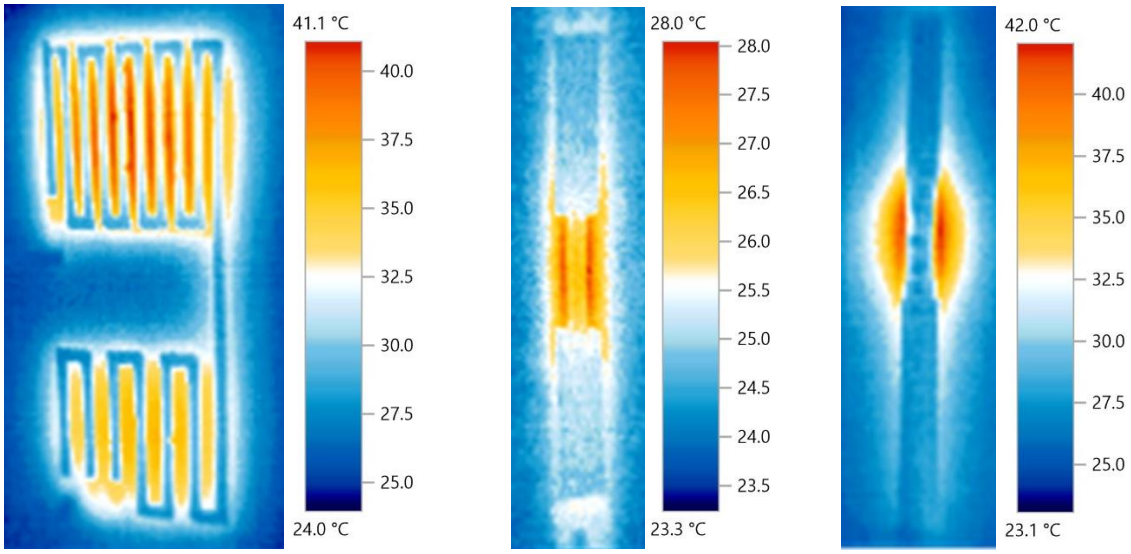

(a) (b) (c)

Figure 70: Temperature distribution of the three heaters printed to demonstrate selective heating

The results show that the highest temperature generated in the three heaters is distributed in the highest resistance region of the heaters. The temperature distribution of heater A shows that the top half of the heater produced a higher temperature with a broader heat spread compared to the bottom half of the heater. The temperature distribution of heaters B and C shows a peak temperature concentrated in the middle section of the heaters which are highest resistance regions.

4.3.4.2 Selective heating using multiple conductive inks

High resistance regions in a conductive track arrangement of uniform physical dimensions can be created by varying the resistivity of the constituent material of the tracks. Resistivity can be varied by using multiple materials to fabricate a track heater. Two heaters were dispenser printed using silver ink, 40% and 60% carbon formulations to demonstrate selective heating using multiple materials. The average resistivity of printed silver ink on interface on fabric is 2.43 $x10^{-07}$ Ω.m. The average resistivity of the printed 40% and 60% carbon formulation is 1.28 $x10^{-05}$ Ω.m and 2.51 x 10^{-04} Ω.m respectively. Figure 71 shows the two dispenser printed heaters on the interface on fabric. Silver ink was printed

using the print settings in table 8. 40 % and 60% carbon formulations were printed using the print settings in table 23.

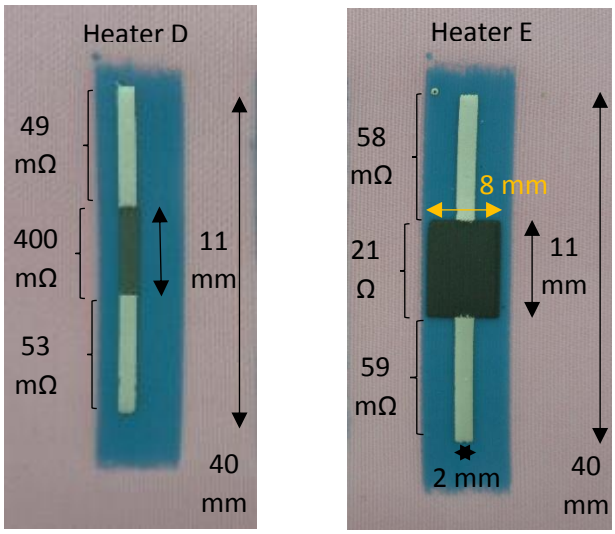

Figure 71: Heaters dispenser printed to demonstrate selective heating using multiple inks

Heater D consists of a 40 mm x 2 mm track; higher resistance region in heater D is produced by printing 11 mm of the 40 mm track using the 40 % carbon formulation. Heater E track consists of 11 mm x 8 mm of 60 % carbon formulation sandwiched between 29 mm x 2 mm of silver ink. Heater E is printed to show that the heat spread is larger if the higher resistance region is spread over a larger area. The two tracks are divided into three sections: a custom formulation section which is grey/dark grey in colour and two silver sections. The corresponding resistances of each section is labelled in figure 71. Figure 72 shows the temperature distribution of the two heaters.

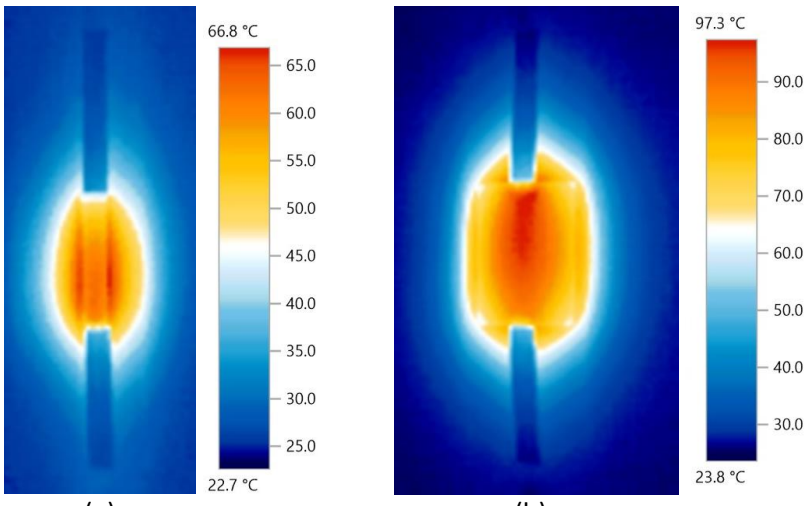

Figure 72: Temperature distribution of (a) heater D and (b) heater E printed to demonstrate selective heating using multiple inks

The results show that the highest temperature regions in the heaters correspond with the highest resistance regions. The heat spread of heater E is much broader than the heat spread of heater D since it covers the entire area of the printed 60% carbon formulation.

4.4 Discussion

In the context of this research the dispenser printed fabric heaters are used for the actuation of thermochromic materials on fabric. In a wider context, applications of fabric heaters include medical use to aid in the recovery from injuries [78], active warming garments for comfort [79], antibacterial applications for hospital bedding [74] and for heated seats in the automotive industry. The heater model and fabrication details of the dispenser printed heaters can be used to design fabric heaters to suit the requirements of these multiple application areas.

There are very few examples of printed heaters in general and printed heaters on fabrics in particular in the literature [74,80]. The examples use screen printing for fabrication and do not evaluate the design parameters of the heaters. Dispenser printing offers a greater design freedom than screen printing as discussed in chapter 3. The model and evaluation of heater fabrication parameters presented in this chapter offers new knowledge for designing fabric heaters.

4.5 Conclusions

This chapter presented the development of a COMSOL model for simulating the dispenser printed track heaters. The model was validated by comparing the temperature distribution and the time temperature relationship of the simulated heaters with the printed equivalent. The highest difference between the peak temperatures of the printed and simulated heaters was 2°C. The model was found to be a reasonable approximation of the printed heaters and a useful design tool for predicting the temperature output of a heater design.

The COMSOL model was used to simulate various track heater configurations to investigate the effect of track width, the gap between the meander track lines and the variation in geometric pattern on the heater output. The simulated heater configurations were evaluated in terms of the temperature distribution, the temperature variation across the width of the heaters and the amount of silver used in fabricating the heaters. The following general design rules were derived for a fixed fabrication area from the results of the simulation tests.

- Wider tracks produce lower temperature variation in a heater and use more silver because there are fewer gaps between the track lines.
- A larger gap between the tracks produces a higher temperature variation and uses less silver because there are fewer tracks.
- In a rectangular fabrication area, heater tracks laid out along the longer side of the fabrication area will produce a lower temperature variation than if the tracks are fabricated along the shorter side of the area.

Specific results from the simulation tests were used for designing and simulating a test heater for printing tests. A meander pattern with a 1 mm track width and 1 mm gap between the track lines were selected as the preferred design parameters for the test heater as this combination provides a good compromise between the temperature variation in the heater output and the amount of silver used for fabricating the heater. It was also demonstrated that the preferred design parameters could be used for designing heaters with different shaped heat profiles such as circular and triangular heat profiles.

The test heater design was dispenser printed on Kapton and polyester cotton 65/35 fabric using DuPont 5000 silver ink; the heaters achieved 6.01 Ω and 5.97 Ω resistance on Kapton and the interface on fabric respectively. The heaters were characterised in terms of temperature distribution and temperature variation across the heater width. The printed heaters produced much higher temperature variation compared to the simulated silver heaters. The temperature variation in the

track gaps was found to be around 1.8°C for the simulated heater, 15°C for the silver heater printed on Kapton and 27°C for the silver heater printed on fabric. The surfaces of the printed silver tracks were at a lower temperature than the rest of the tracks due to difference in thermal properties of simulated and printed silver.

Carbon, in the form of DuPont 7102 ink, was used as an alternative constituent material for the printed heaters on Kapton and interface on fabric. The carbon heaters produced much higher resistance than the silver heaters; 16.34 kΩ and 36.89 kΩ for carbon heaters printed on Kapton and fabric respectively. The carbon heaters, when characterised, produced a significantly better output than silver heaters as the temperature variation between the tracks reduced to 1°C for the Kapton heater and 3°C for the fabric heater.

The silver and carbon inks offered limited resistivity options of 2.43-3.44 x 10^{-7} Ω.m and 0.284-1.10 x 10^{-3} Ω.m for the fabrication of heaters respectively. Four custom conductive inks were formulated by mixing the carbon ink with the silver ink in the range of 20% - 80% to provide a broader range of resistivity options. The mixture of 20% carbon ink and 80% silver ink separated after mixing and was deemed unsuitable for printing. The inks offered a printed resistivity in the range of 4.50 x 10^{-06} – 1.11 x 10^{-03} Ω.m. The range of resistivity allows a designer to control the resistance of an application specific heater to make it suitable for a specific power source. The test heater design was printed using a formulation consisting of 60% carbon ink and 40% silver ink to demonstrate the impact of ink resistivity on an application specific heater design. The heater produced a value 1.6 kΩ on Kapton and 7.2 kΩ on fabric. The temperature variation in the heaters was found to be better than silver and inferior to carbon. The variation in the gap between the tracks was 3°C for a Kapton heater and 8°C for a fabric heater.

The variation in the gap between the nozzle height and the substrate during the printing process is found to be a major issue when dispenser printing heaters. It produced non-uniform thicknesses in printed heater tracks which led to a non-uniform temperature distribution. The output of all the heaters was affected by nozzle height variation; however the fabric heaters were affected more than the Kapton heaters which was reflected in the higher temperature variation of the fabric heaters. The interface on fabric has a higher combined surface and thickness variation than the Kapton which causes the fabric heaters to produce higher temperature variation. Although all the heaters had temperature variation in their output, the heat was spread in a sufficiently broad area for the heaters to be used for thermochromic devices. The noticeable temperature variation of heaters is likely to be less in a thermochromic device than the thermal images because the thermochromic layer printed over a heater will change the thermal dynamics. The thermochromic devices will be actuated by raising the input power of the heater till the lowest temperature of the heater is sufficiently above the actuation temperature of the thermochromic layer.

This chapter also demonstrated that, by designing higher resistance regions in a track heater, specific parts of it can be selectively heated. Resistance variation within a track heater can be designed by varying one or more of: resistivity of the constituent material, length, width and thickness of the tracks. Varying the resistivity of a track requires the use of more than one material as resistivity is a material property. Selective heating can enable a printed heater to share the electrical interconnections of a printed electronic circuit with other components without heating the interconnections.

Chapter 5 DISPENSER PRINTED ACTIVELY ACTUATED THERMOCHROMIC DEVICES ON FABRICS

5.1 Introduction

This chapter details development of thermochromic inks, and fabrication of dispenser printed thermochromic devices on fabric. The ink development covers material selection, ink formulation and optimisation. The fabrication of thermochromic devices include details of design layout and dispenser printing. The devices are characterised in terms of power requirements and rate of colour change. A range of devices are presented to demonstrate various colour changing effects such as multiple colour changes and sequential activation of thermochromic prints in a single device. This chapter also presents demonstrator applications of the thermochromic devices consisting of a shutter display, a matrix display, a 7-segment display and a proximity sensor controlled thermochromic device on fabric.

5.2 Development of thermochromic inks

This section discusses development of dispenser printable thermochromic inks using commercially available materials. The aim of the ink development is to formulate a black thermochromic ink which is opaque below its activation temperature and transparent above it. As part of the CREATIF project which has funded this research, the thermochromic demonstrator was required to conceal an inkjet printed image below a black thermochromic layer, the image is revealed when the thermochromic layer is heated and returns to its opaque state when the heat is removed. This section describes the selection of the relevant materials and testing to identify the formulations which fulfil these requirements. It presents methods of characterisation of the formulated inks and analysis of the optimum thermochromic inks.

5.2.1 Material selection for the ink development

An extensive market survey was carried out to identify the commercially available thermochromic materials and suitable suppliers; the materials are available in the following four formats.

- **Thermochromic powder**: Microcapsules containing constituents of the thermochromic leuco dye.
- **Thermochromic slurry**: Formulated by dispersing thermochromic powder in an aqueous solution.
- **Ready to use thermochromic inks**: Thermochromic pigments (powder or slurry) combined with a substrate appropriate binder, inks may also contain additives and solvents. Designed for specific printing processes and substrates, such as screen printing and plastic films.
- **Thermochromic master batch**: Thermochromic powder is blended with a master batch. A master batch is a concentrated mixture of pigments encapsulated in a carrier resin. It is supplied in a pellet form which is suitable for use in plastic applications.

Of these options, only the master batch was deemed unsuitable for the ink development. Most of the identified suppliers were unsuitable because of factors such as a large minimum order quantity, irreversibly colour change, materials that change from one colour to another instead of transparent and materials not suitable for fabrics. Colour changing products ltd, UK [81] and new colour chemical co. ltd, China [82] were chosen as the suitable suppliers for the thermochromic slurries and powder respectively. They offer thermochromic materials in flexible quantities, in a range of activation temperatures and colours. Ready to use thermochromic inks were sourced from 'UNICO INKS' Belgium and Kilabitzzz, UK. These inks are compatible with fabrics, turn transparent when heated above their

activation temperatures and are suitable for screen printing. As the dispenser printing process is able to print a broader range of ink viscosities than screen printing, an ink suitable for screen printing can also be dispenser printed.

A series of initial tests were carried out to observe the output of thermochromic materials. The tests consisted of formulating thermochromic inks by combining chameleon thermochromic slurry [81] with transparent, opaque and coloured binders, and printing them on fabric. The tests provided the following conclusions.

- Inks with a white opaque binder exhibit the colour of its constituent thermochromic pigment before colour change and turn white after activation.
- Inks with a transparent binder display the colour of its constituent thermochromic pigment before colour change and turn translucent after activation.
- Mixing thermochromic pigment with a coloured binder creates colour blends which change to the binder colour after activation.
- Inks containing multiple thermochromic pigments with different activation temperatures provided a range of colour changes. The activation temperatures of the individual pigments were not affected in the mixture.

The results of initial tests highlighted the need for a transparent binder for the development of thermochromic inks which turn transparent when actuated. A suitable binder for the ink development was required to be screen printable, compatible with fabrics, transparent, flexible and having a low curing temperatures <180° C. The following table presents the six commercially available binders identified for the ink development.

Binder	Curing conditions
AS 100 aqua screen clear binder (AS) [83]	160°C for 4 minutes
Adva print fabric medium (AP) [84]	140°C for 4 minutes
Chromazone textile binder (CH) [85]	160°C for 2 minutes
Screentec tprint t2000 transparent base (ST) [86]	150°C for 15 seconds
Speedball transparent base (SB) [87]	80°C for 2 minutes
Fabinks-IF-UV-1004	UV radiation 2000mW/cm^2 for 60 seconds

Table 24: The six identified binders for the ink development along with their curing conditions

Fabinks-IF-UV-1004 dielectric ink was developed at University of Southampton for overcoming fabric surface variation. However, it was deemed suitable for the ink development because it is flexible, transparent, dispenser printable, and provides good adhesion to a range of surfaces including the polyester cotton 65/35 fabric. The advantage of UV curable binder over the heat curable binders is that it is faster to cure and it does not produce fumes of volatile solvents during the curing process.

5.2.2 Thermochromic ink formulation trials

A thermochromic ink formulation in this section is defined as a combination of thermochromic pigments and a fabric binder. The aim of the formulation trials is to identify the formulations which change from a black opaque state to a transparent/translucent state. The trials consist of varying the following four parameters:

- Type of thermochromic materials: Thermochromic powder or slurry
- The binders
- Concentration of thermochromic pigments in an ink
- Print thickness

31°C activation temperature chameleon black thermochromic slurry, 38°C activation temperature black thermochromic powder supplied by 'New Colour Chemical' ltd and following three ready to use inks were used in the trials; 45°C magenta Chromotex CR [88], 44°C blue UV AQ CR [89] and 30°C black Zuperpaint pro [90]. The formulation trails were carried out in four stages; first stage tested formulations consisting of thermochromic slurry, the second stage tested thermochromic powder formulations, the third stage tested UV curable formulations and the final stage tested ready to use inks.

Figure 73 shows a flowchart representing the format of the formulation trials. A total of thirty eight formulations were tested including five UV curable formulations and three ready to use inks. The thermochromic slurry and powder were mixed with each of the five binders individually to formulate thermochromic inks. The concentration of the slurry in the formulations was varied between 10-50 % whereas the powder concentration in the formulations was varied between 1-10%. As an example the arrows in figure 73 show the combination to form 10% AS slurry formulation. The ready to use inks did not require a binder and could be printed directly on the fabric substrate. The UV curable formulations were only formed using the thermochromic powder and therefore are not included in the flowchart. The UV curable formulations were tested in a range 1-20% to achieve suitable opacity and transparency levels.

Each formulation was printed over an area of fabric marked by a pen, the mark was used to assess the opacity of the print before colour change and its transparency after colour change. A formulation was tested by dispenser printing four 1x1 cm samples over marked areas on the fabric. The first sample of each formulation was printed using the dispenser printer settings, determined by preliminary trials for each ink that produced the thinnest complete print. Printing pressure was increased for each subsequent sample thus increasing thickness across the four prints. Each print was empirically assessed to determine if the print could successfully conceal and reveal the pen mark underneath it. The prints were heated using a hot plate to a temperature higher than their activation temperatures to ensure prints had completely changed colour for transparency assessment. In addition to opacity and transparency, the colour strength of the thermochromic prints was also assessed, it was measured using a Photoshop based method detailed in section 5.2.2.1. This sample size and approach produced clearly identifiable trends and contained distinguishable optimum prints. The thickness of the prints was measured down to 0.001 mm with an error of ±0.005 mm using a Mitutoyo micrometer. Each measurement consisted of an average of three readings. The tests identified these key points:

- The suitable thermochromic formulations in terms of opacity and transparency.
- The print thickness of the suitable formulations which achieved the required opacity and transparency.
- The printer settings for the suitable formulations to achieve the required thickness.

The most suitable formulations were characterised and further analysed which is discussed in section 5.2.3.

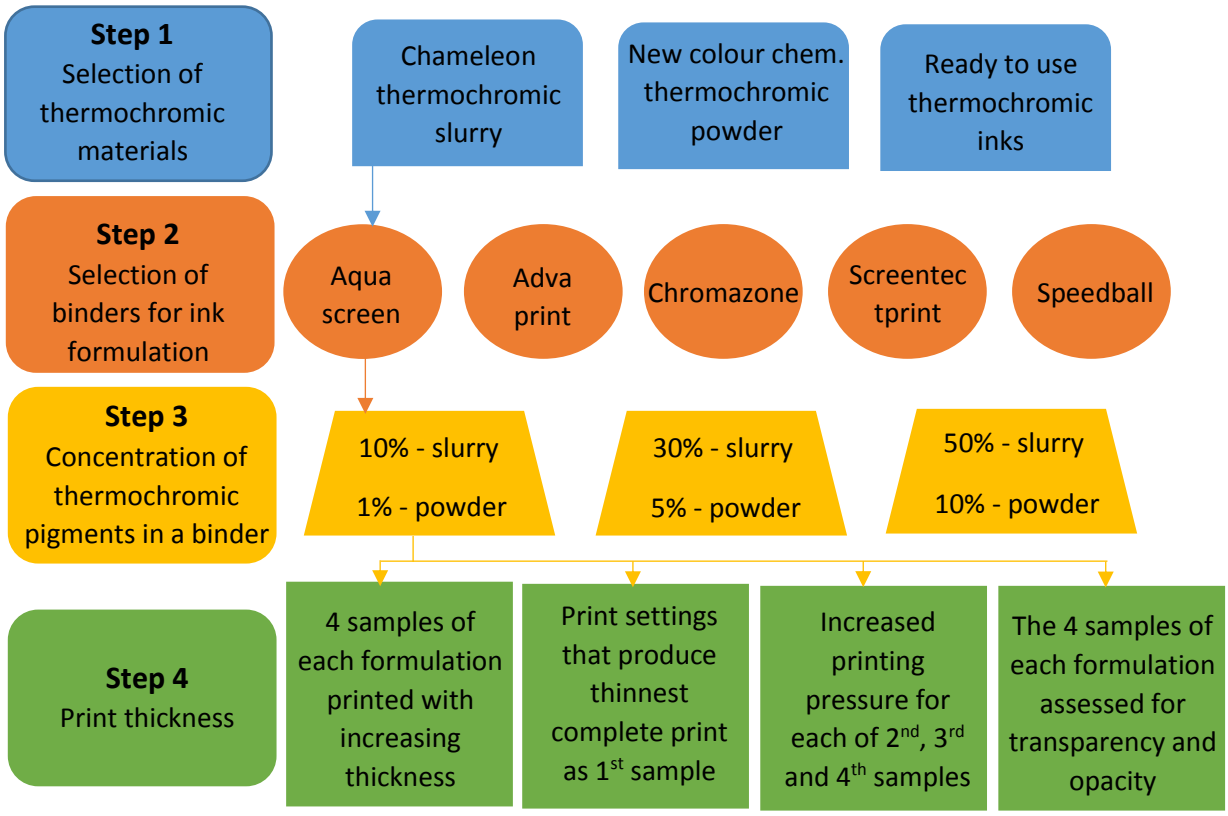

Figure 73: Flowchart detailing the format of thermochromic formulation trials

5.2.2.1 Colour strength comparison method

A colour strength comparison method based on Corel Photo-Paint x6 software is devised to evaluate the thermochromic prints. RGB colour model where three primary colours red, green and blue are additively combined together in varying intensities to produce wide array of colours is used for the evaluation. Thermochromic formulations use black coloured pigment so a scale, shown in figure 74, is derived from the software for comparison of black colour concentration in a print. The scale shows the output of varying concentrations of black colour in a sample.

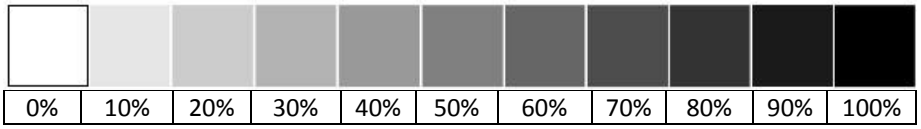

Figure 74: Black colour concentration scale

Table 25 shows the combination of intensity levels of the three primary colours which produce the colour outputs shown in the scale.

Black colour concentration	**0%**	**10 %**	**20%**	**30%**	**40%**	**50%**	**60%**	**70%**	**80%**	**90%**	**100%**
Red intensity level	255	230	204	179	153	128	102	77	51	26	0
Green intensity level	255	230	204	179	153	128	102	77	51	26	0
Blue intensity level	255	230	204	179	153	128	102	77	51	26	0

Table 25: Primary colour intensity values in RGB model that produces concentrations of black colours between 0 and 100 %

Each printed sample is photographed using a Samsung PL221 16 megapixels digital camera in a photo box which ensures as close as possible identical illumination conditions. The photograph is then imported in the Corel photo-paint software and the colour of the print is analysed for average intensity levels of red, green and blue channels. The intensity values of RGB are compared with table 25 to establish black colour concentration in the print.

5.2.2.2 Results of thermochromic ink formulation trials

Most of the slurry formulation prints were able to conceal the pen mark, however all those that concealed the mark were not able to reveal it upon heating. Generally, increase in slurry concentration and the thickness of the prints resulted in higher opacity and lower transparency. Figure 75 below compares the fifteen slurry based formulations by combined mean RGB value of four prints within each formulation. The higher the mean RGB value the lower the black colour strength and vice versa.

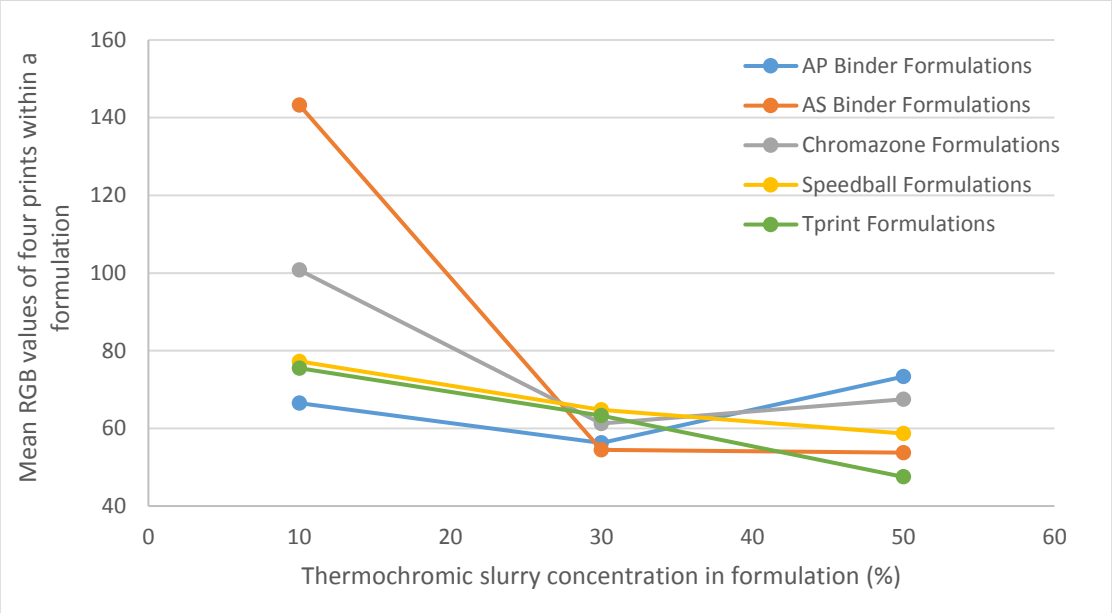

Figure 75: Comparison of the black colour concentration of the 10%, 30% and 50% formulations of each of the five binders

The results show that AS, tprint and speedball binder formulation prints produce better colour strength as the slurry concentration increases in the formulation. Chromazone and AP binder formulation prints produce higher black colour strength with 30% slurry than the 50% slurry prints. Although generally the black colour strength of the prints increased with an increase in print thickness for a formulation, the increase in most of the cases was very small.

Increase in slurry concentration increased cracking in the prints for all the binders. Cracking shows that the dried ink does not have sufficient adhesion and is easily rubbed off the surface of the fabric. The slurries when exposed to air dry within 10 seconds, this made the ink formulations susceptible to blocking the printing nozzles during and immediately after printing which lead to incomplete prints. A method of avoiding incomplete prints was to use a fresh nozzle for each print. Print 3 of the chromazone binder formulation containing 30% thermochromic slurry (CH-30-print 3), 70µm thick, is the best print for slurry based formulations. The print showed no surface cracking, bleeding and is able to completely conceal and reveal the pen marking as shown in figure 76.

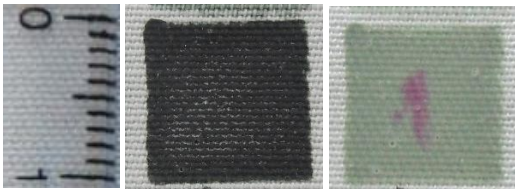

(a) (b)

Figure 76: CH 30 – print 3 at a temperature of (a) 30°C (b) at 36°C

All of the powder based inks resulted in good levels of transparency with all revealing the pen marks. A majority of the prints were however unable to conceal the pen marks before colour change. Increase in powder concentration and print thickness improved the opacity and colour strength of the prints. Figure 77 below compares the fifteen powder based formulations by the combined mean RGB values of the four prints of each formulation. Higher RGB values represent lower black colour strength and vice versa.

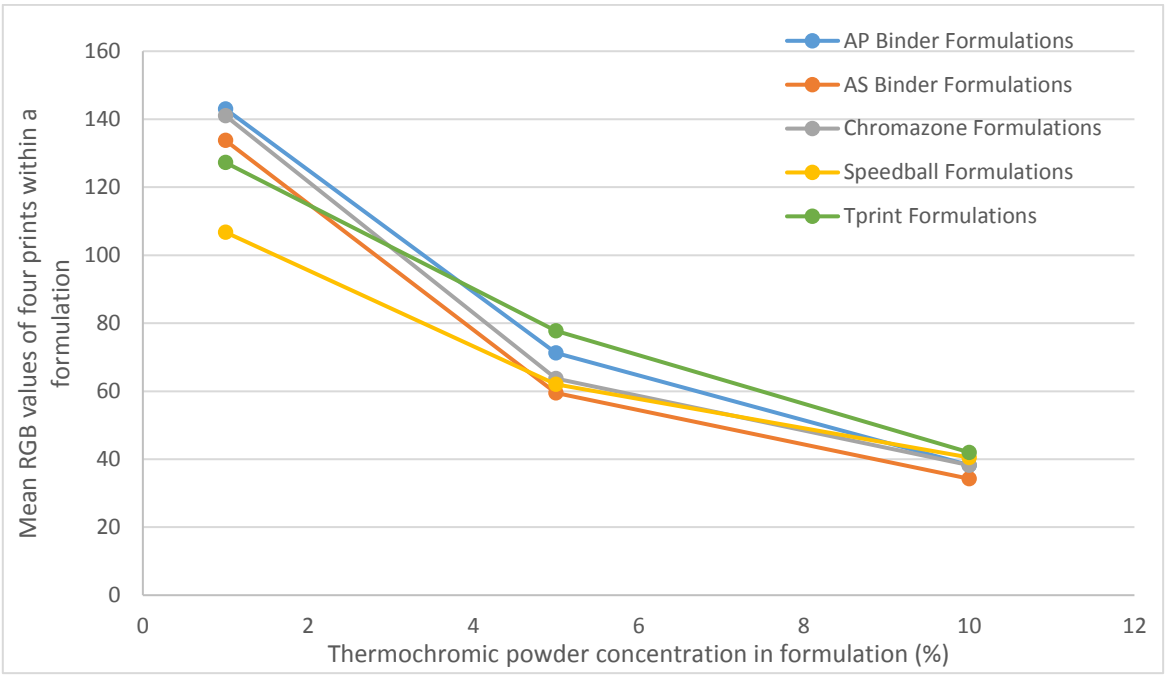

Figure 77: Comparison of the black colour concentration of the 1%, 5% and 10% formulations of each of the five binders

The results show that increasing the thermochromic powder content increases the black colour strength of the prints. The increased black strength of the prints is steeper as the powder content is increased from 1% to 5% compared to 5% to 10%. Powder based formulations did not show any surface cracking. Thermochromic ink consisting of the chromazone binder and 10% powder produced a 42 µm thick optimum print, CH-10-print 3. It shows good colour strength, is able to completely conceal the pen mark and reveal it when heated above 44°C, as shown in figure 78.

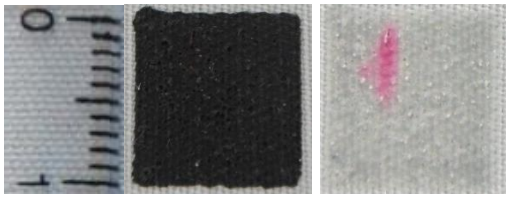

(a) (b)

Figure 78: CH 10 – print 3 at a temperature of (a) 38°C (b) at 44°C

The three commercial thermochromic inks tested showed similar general trends to the bespoke thermochromic inks. Thicker prints showed improved opacity and reduced transparency. The inks did not offer any additional advantages over the bespoke inks so have not been used further in this research.

The prints of powder based formulations showed better transparency, no surface cracking and did not cause nozzle blockages, therefore the UV curable thermochromic inks were only formulated using thermochromic powder. The results showed that the UV curable thermochromic inks provided good printability and adhesion to the fabrics. They followed the same trend as before; increasing powder concentration and print thickness increased opacity and colour strength. All the prints of UV curable inks showed very good transparency; all were able to completely reveal the pen mark. However, only the formulations with 20% powder concentration were able to conceal the pen mark. The thinner prints of inks <50 µm produced a matt surface whereas the thicker prints produced glossy surface as the thicker prints start to overcome the roughness of the fabric. FB-20-print 3 is the optimum fabink-UV-IF-1004 based print as it produces a consistent glossy surface, black concentration of 90-100 % with a comparatively modest thickness of 90 µm. Figure 79 below shows the print before and after colour change.

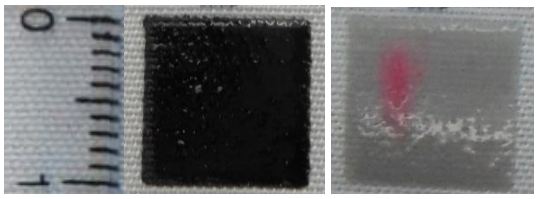

(a) (b)

Figure 79: FB-20-3 print at a temperature (a) below 38°C (b) above 44° C

5.2.3 Characterisation and analysis of the most suitable thermochromic ink formulations

This section presents characterisation and analysis of the three shortlisted thermochromic formulations as the most suitable for an approach where a coloured layer is revealed from underneath a black thermochromic layer on a fabric. The three shortlisted formulations are listed below.

- CH-30 – 70% Chromazone binder, 30% 'chameleon' black slurry
- CH-10 – 90% Chromazone binder, 10% 'New color chemical' black thermochromic powder
- FB-20 – 80% Fabink-UV-IF-1004 ink, 20% 'New color chemical' black thermochromic powder

They were selected for exhibiting better combined opacity, transparency and colour strength properties than other formulations. Table 26 shows the viscosity, thicknesses, RGB intensity values and black colour concentration for the optimum prints of each formulation. The inks were freshly formulated for the viscosity measurements. The contents of the formulations were mixed using a SpeedMixer DAC 150.1 FVZ; first mix was performed at 1000 rpm for 1 minute and the second mix at 3000 rpm for 1 minute to ensure thorough mixing. Viscosity of the inks was measured using a Brookfield CAP1000+ viscometer at 10 rpm and 25°C. Viscosity for CH-30 and CH-10 was measured using spindle 1 whereas viscosity of FB-20 was measured using spindle 2; these are the spindles recommended by Brookfield.

Formulation	Optimum Print Thickness (µm) ± 5 µm	Viscosity (Pa.s)	RGB Intensity Values	Black Colour Concentration (%)
CH-30	70	1.98	51	80
CH-10	42	2.32	35	80-90
FB-20	90	14.32	14	90-100

Table 26: Thickness, viscosity and colour strength of optimum prints of shortlisted formulations

Table 27 shows the dispenser printer settings used to print the optimum print for the three formulations.

Formulation	Pressure (kPa)	Dispensing Time (ms)	X-Resolution (mm)	Y-Resolution (mm)	Speed (mm/s)	Vacuum (kPa)	Nozzle Height (µm)
CH-30	15	15	0.4	0.2	1	1.0	100
CH-10	35	15	0.4	0.2	1	1.0	150
FB-20	80	20	0.4	0.2	1	0.5	100

Table 27: Dispenser printer settings for optimum prints of shortlisted formulations

The RGB intensity values indicate that the FB-20 formulation produces the strongest colour strength followed by CH-10 and CH-30 respectively. The dispenser printer settings of the prints correlate with the viscosity of the inks as FB-20 is printed with the highest pressure and dispensing time followed by CH-10 and CH-30 respectively.

5.2.3.1 Opacity and transparency assessment of the shortlisted formulations

The transparency and opacity of the printed inks so far in this work has been assessed subjectively using a pen mark. This section presents a quantitative assessment of opacity and transparency of the three shortlisted formulations.

The three formulations were printed in 1x1 cm dimensions on indium tin oxide coated polyester sheets [91] (ITO films) using the dispenser printer settings for the most suitable prints. ITO films are transparent conductive films which were used as heaters to obtain colour change in the prints. The opacity and transparency was assessed by analysing transmission of light through the printed thermochromic samples before and after the colour change. An arrangement of Ocean Optics USB 2000 spectrometer, tungsten halogen lamp and a closure lid was used for the assessment, shown in figure 80. The spectrometer was calibrated by covering the setup by the closure lid to eliminate the background light and inputting the lamp light as a reference spectrum using Ocean View 1.5.0 software. Subsequently, the lamp was switched off and with the closure lid covering the setup, the background spectrum was measured by the spectrometer to eliminate any background light.

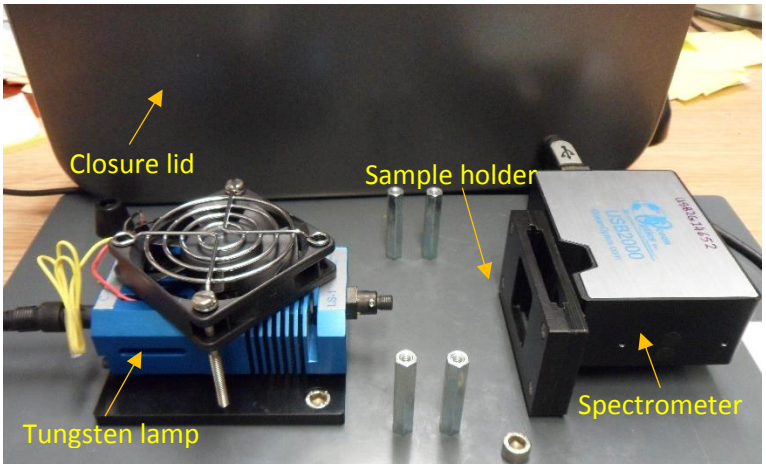

Figure 80: Spectrometer equipment used for opacity and transparency assessment of the thermochromic prints

The bare ITO film was first assessed for transparency, its transmittance was analysed in the visible light range of 380nm to 700nm as shown in figure 81.

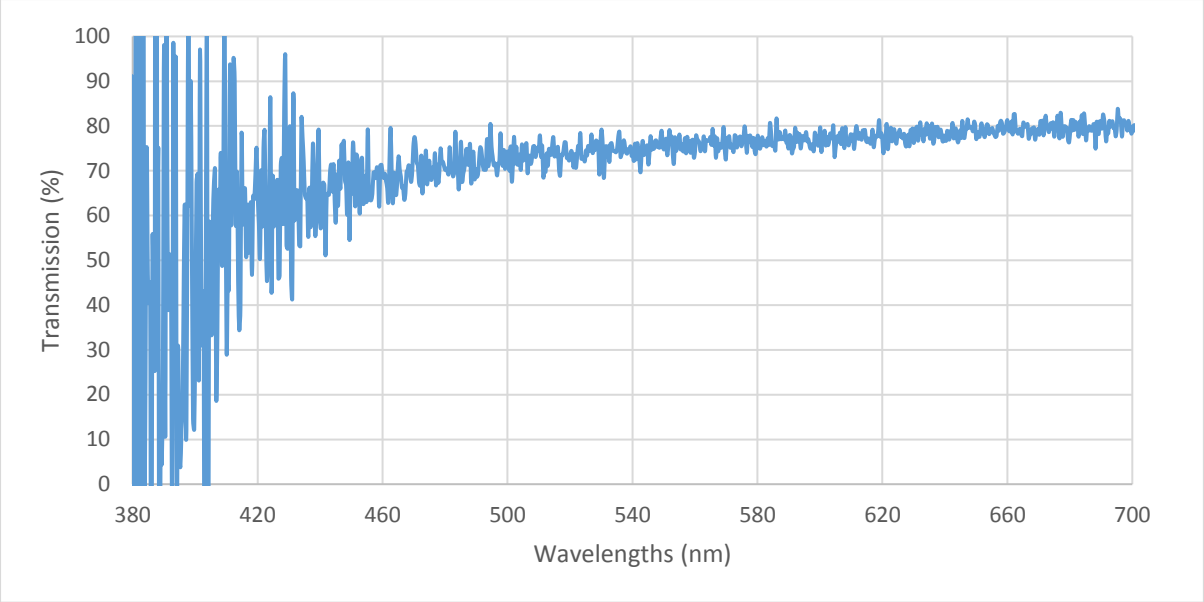

Figure 81: Transmittance graph of ITO film in visible spectrum

Transmittance can be regarded as a direct measure of transparency and opacity with higher transmittance corresponding to higher transparency and lower opacity and vice versa. It can be seen from the graph that the ITO film produced a transparency level of 70 to 80 % in the visible spectrum with improvement in transparency at higher wavelengths in the visible spectrum.

Opacity of the prints was assessed by measuring the transmittance of the prints before colour change. A 10 x 10 cm ITO sheet containing the three printed thermochromic formulations was cut into 3.5 x 1.5 cm pieces to allow each print to be placed in the sample holder. The spectrometer was calibrated before each measurement to eliminate background spectrum as before. The samples were each placed in the sample holder and the experiment was covered using the opaque lid whilst taking measurements to avoid any external interference. The transmittance graph of the three thermochromic samples before colour change is presented in figure 82.

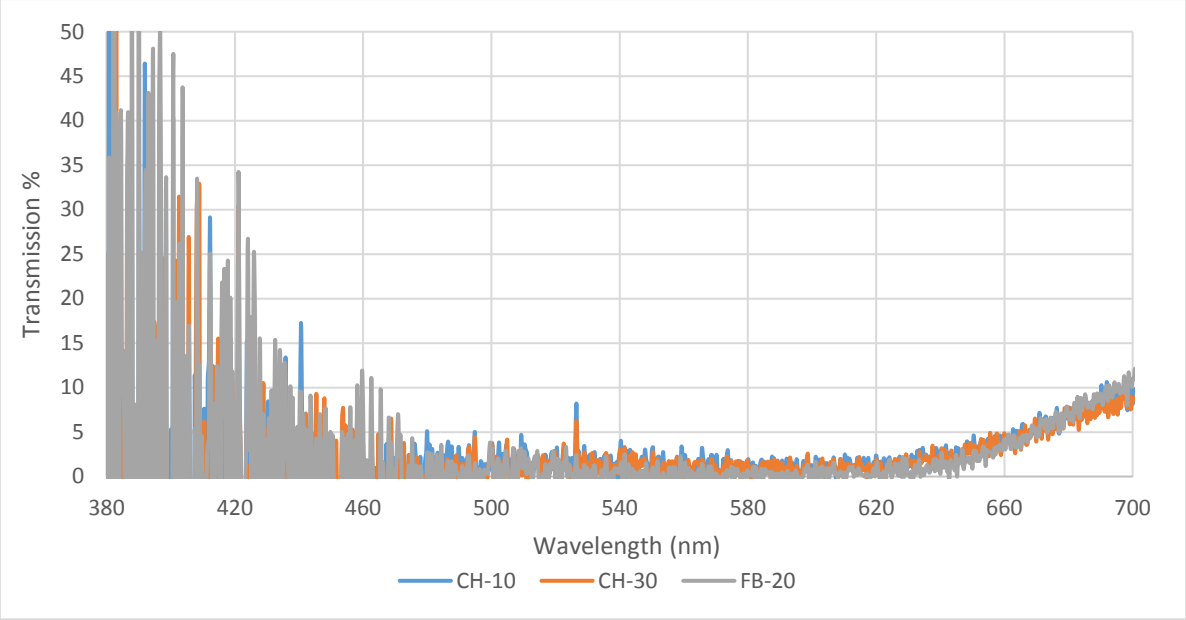

Figure 82: Transmittance graph of CH-10, CH-30 and FB-20 thermochromic formulations in visible spectrum before colour change.

The transmission percentage shows a high variation in the wavelength range of 380 nm to 450 nm which makes it difficult to analyse the opacity of the prints in that region. The high variation is introduced by the ITO sheet, it can also be observed in the transmittance graph of ITO sheet. The transmission percentage shows very small variation between 0 to 5 % in the region of 450 to 650 nm after which there is a rise of 10% in transmission between 650 nm to 700 nm.

The voltage applied across the pieces of ITO sheet did not result in any electric current through the sheet due to very high resistance of the ITO layer. The prints were therefore heated using a Xytronic 850D hot air SMD rework station. The spectrometer was recalibrated, the prints were placed in the holder and heated by blowing 105°C hot air using the rework station on the prints by slightly lifting the lid. The hot air was blown at the prints for 40 seconds; the prints changed colour within the first 5 seconds. The additional 35 seconds ensured that the prints reached a higher temperature than their activation temperature and would not change colour immediately upon removal of the heat source. The heat source was removed, the lid was closed and a measurement was taken. The measurement took about 4 seconds which is sufficient to obtain a reading before the material cooled enough to start changing colour again. Three measurements were taken and averaged for each formulation to produce the transmittance graph of the prints after colour change shown in figure 83.

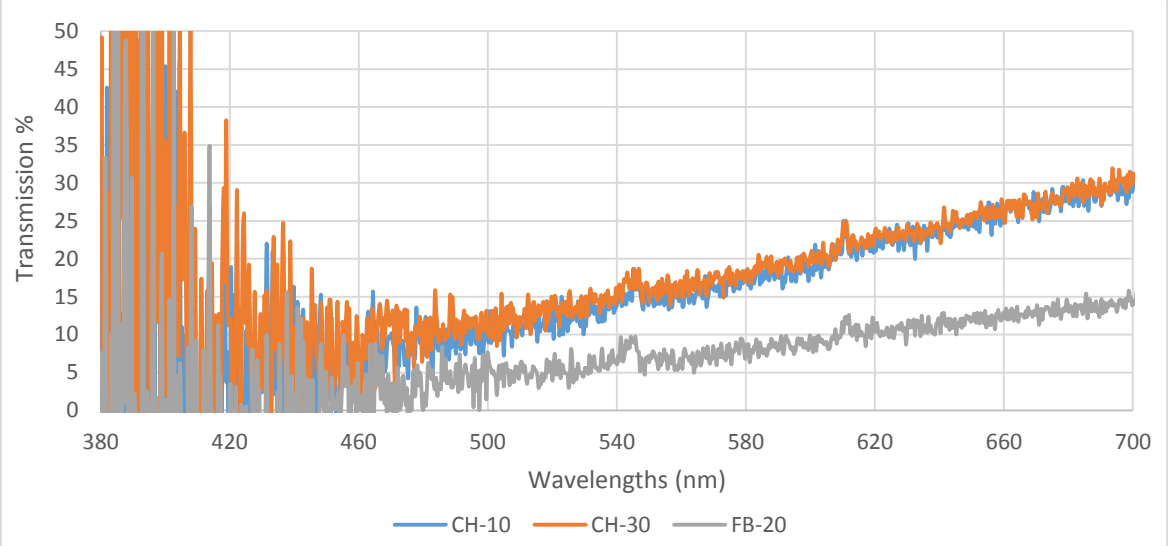

Figure 83: Transmittance graph of CH-10, CH-30 and FB-20 thermochromic formulations in visible spectrum after colour change

Figure 83 shows the prints retain high variation in transmittance between 380 to 450 nm which makes it difficult to judge the transparency in this range. The transparency of the prints improved at an increasing rate between wavelengths of 450 to 700 nm. CH-10 and CH-30 show very similar transmittance results with peak transmittance of 30% at 700 nm. This can be considered as 50% transparency because ITO films reduce the transparency of the print by 20% at 700 nm. FB-20 comparatively shows poorer transparency as its transmittance increases at a slower rate to CH-10 and CH-30 between 450 nm to 700 nm. The peak transmittance of FB-20 is at 34% after eliminating the effects of the ITO film at 700 nm. Although the data shows that FB-20 showed poorer transparency compared to the other two formulations, the empirical assessment of the transparency of the three inks suggested that their transparency levels are comparable. Unlike CH-30 and CH10 prints, FB-20 prints produce glossy surfaces which may have caused part of the incident light to be reflected off the surface of the print instead of being transmitted through the print leading to a lower peak transmittance value. Figure 84 presents the prints of the three formulations on ITO sheets after complete colour change held over pieces of text to show transparency of the prints. The images in figure 84 also show parts of the text not covered by the prints so the transparency of the prints can be assessed.

a b c

Figure 84: Transparency of the prints of three formulations (a) CH-10, (b) CH-30 and (c) FB-20 respectively

The images show visual representation of 30% and 14% transparency. The transparency levels are sufficient to allow the text to be read. The transparency levels of the print improve when they are printed on the fabric as the effect of the ITO sheets in reducing the transparency is eliminated.

5.2.4 Summary and discussion

The aim of the thermochromic ink development was to develop a dispenser printable ink which was able to change from a black opaque to a transparent state. This work was carried out in three phases where in the first phase suitable materials were identified and sourced. In the second phase, thirty

eight thermochromic ink formulations were tested to identify which are most suitable. The following prints and formulations were shortlisted:

- 70 µm thick print of CH-30, consisting of 70% chromazone textile binder and 0% black 'Chameleon' thermochromic slurry.
- 42 µm thick print of CH-10, consisting of 90% chromazone textile binder and 10% black 'New colour chemical' black thermochromic powder.
- 90 µm thick print of FB-20, consisting of 80% Fabink-IF-UV-1004 ink and 20% black 'New colour chemical' black thermochromic powder

These formulations and print combinations produced better combined opacity, transparency and colour strength compared to the rest. The tests which were carried out in the second phase also showed that certain slurry containing formulations were susceptible to nozzle blockages.

The prints and the three formulations were characterised and analysed in the third phase of the ink development. The three formulations were characterised in terms of viscosity, black colour concentration, opacity and transparency. The results showed that the three formulation and print combinations are sufficiently opaque before colour change. The prints of CH-30 and CH-10 showed a peak transmittance of about 50%; negating the effect of the ITO sheets and FB-20 prints showed a peak transmittance of 34%. Despite the difference in the measured results, the subjective assessment of the transparency of the prints showed that the three formulations produce comparable transparency. The lower transmittance of FB-20 can be attributed to the glossy surface of the prints which has a larger impact on the measured output than the observed output.

The activation temperatures of the three formulations are dependent on the activation temperatures of their constituent thermochromic pigments and can be varied to suit the requirements. CH-30 ink dries out within a minute of exposure to air causing nozzle blockage as soon as the printing is finished. It has shown similar transparency and opacity properties to CH-10 therefore CH-10 is the preferred heat curable thermochromic ink which changes from a black opaque to a transparent state. FB-20 ink is preferred to CH-10 ink for fabricating thermochromic fabrics because, in addition to providing the thermochromic function, it can also encapsulate the conductive tracks when printed over a heater. FB-20 contains 80% Fabinks-UV-IF-1004 interface ink, the UV curable interface ink has been previously shown to be effective as an encapsulation material for silver conductive tracks [92]. Encapsulation provides abrasion resistance and electrical insulation to the printed conductive tracks [92].

Figure 85 subjectively demonstrates the function, opacity and transparency of the FB-20 thermochromic ink. An image, consisting of the colours in the visible spectrum, is inkjet printed on paper. An ITO sheet is then placed over the inkjet image to show the reduction in transparency caused by the ITO sheet. A 2 x 2 cm print of FB-20 is printed on an ITO sheet using the dispenser printer settings presented in table 27. The FB-20 print is placed over the inkjet image to show the opacity of the print, it can be seen in figure 85 (c) that the print completely conceals the inkjet image. The print is heated to a temperature of 45°C to ensure complete colour change has taken place, it can be seen in figure 85 (d) that after colour change all the colours are revealed and can be distinguished.

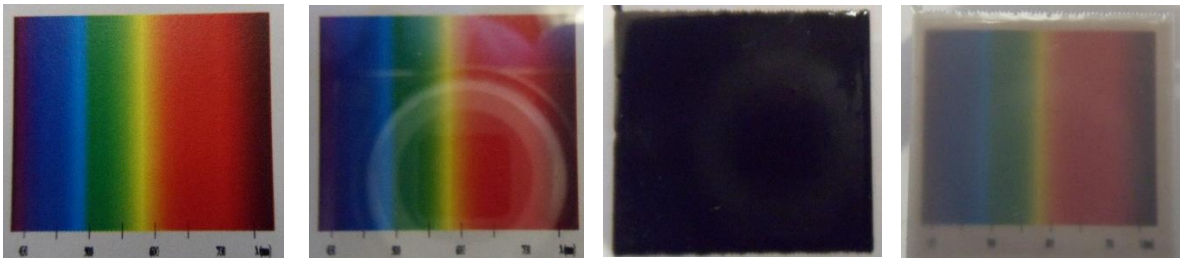

a b c d

Figure 85: (a) Inkjet printed image on paper (b) ITO sheet placed over the inkjet image (c) 2 cm x 2 cm FB-20 print placed over the inkjet image before colour change (d) the inkjet image is revealed after FB-20 print turns transparent

5.3 Fabrication and characterisation of actively controlled thermochromic fabrics

This section details fabrication of actively controlled dispenser printed thermochromic devices on 65% polyester, 35% cotton fabric. It presents three potential layouts of the thermochromic devices, discusses their merits, demerits and the selection of the most suitable layout. The fabricated devices are characterised in terms of their colour change timings. This section presents a comparison of thermochromic devices fabricated using silver and carbon heaters. It discusses the effect of the input electrical power on the performance of thermochromic devices gauged by the colour change timings. It details the impact of activation temperature of the thermochromic pigments on the re-colouration timings of the thermochromic devices. It also demonstrates that the dispenser printing method of fabricating the devices is not limited to polyester cotton 65/35 fabric by fabricating the devices on Kapton and a PVC coated fabric.

5.3.1 Design layouts of the dispenser printed thermochromic devices

An actively controlled thermochromic device consists of three primary elements; a fabric substrate, a heater and a thermochromic layer. The three elements can be arranged in three different fabrication orders presented in figure 86. The three layouts affect the fabrication requirements, functional and aesthetic properties of the thermochromic devices. These factors are important to consider for selecting a device layout to suit an application.

The fabrication requirements are gauged in terms of the fabrication cost, printing time and process requirements such as curing. The functional properties are considered in terms of heating efficiency, flexibility, power requirements and durability. The aesthetic properties judge the visual output of a device in both the actuated and the non-actuated states. The following section presents the fabrication steps, materials, and an assessment of functional and aesthetic properties of the three layouts. It diagrammatically represents the structure of the three layouts of thermochromic devices which include all the elements required for their fabrication. It also presents a table of comparison for the three layouts.

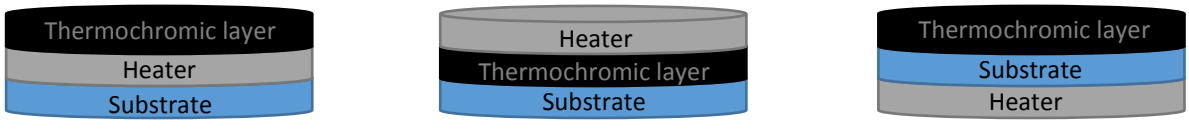

Design layout A Design layout B Design layout C

Figure 86: The three potential layouts of an actively controlled thermochromic device

5.3.1.1 Comparison of the three design layouts of a thermochromic fabric device

The fabrication of a layout A device requires dispenser printing of three materials; an interface layer using DuPont 5018, a heater using DuPont 5000 silver and the FB-20 thermochromic ink on top of the heater. The interface layer is cured first before printing the heater layer, similarly the thermochromic

layer is printed over the cured heater layer. The thermochromic layer in design layout A is able to encapsulate the heater which improves the durability of the device as described earlier. The heater in this layout is sandwiched between the interface and thermochromic layers, as shown in figure 87, which are both dielectric; this arrangement electrically insulates the heater. The heater is in contact with the thermochromic layer which ensures that any generated heat directly conducts to the thermochromic layer. The top layer of the layout is the thermochromic layer which ensures that the colour changing effect can be clearly observed. Aesthetically, this layout is suitable for a majority of applications; it may be less suitable for applications where the thermochromic layer is required to change to a transparent state as that will reveal the printed heater which may not be desirable.

A layout B device requires printing of two materials; the FB-20 ink directly on the fabric surface followed by the heater. The thermochromic layer is cured first before printing the heater layer. It has been shown in chapter 3 that the FB-20 ink can overcome surface roughness therefore layout B does not require an interface layer. The heater in this layout is in contact with the thermochromic layer which ensures the heat is directly conducted to it however one side of the heater is exposed to the air so the heat is also being directly lost to the air; this reduces the heating efficiency of the layout B devices. The thermochromic layer is covered with heater tracks which reduces its visible area; depending on the gap between the heater tracks, the colour change effect may not be clearly observed. Aesthetically, this layout is not suitable for a majority of the applications due to limited visibility of the thermochromic layer. Compared to layout A devices of the same design, the layout B devices are faster to print, less expensive and require less processing because fewer materials are used for its fabrication. The layout B devices are more flexible than layout A devices because they consist of two layers instead of three. The heater in layout B devices is not encapsulated therefore they are less durable than layout A devices. Layout A devices are more heat and power efficient than their equivalent layout B devices because the heaters do not directly lose heat to the air.

A layout C thermochromic device is the most challenging to fabricate as it requires inks to be printed on both surfaces of the fabric. It requires printing of three materials; the FB-20 ink, DuPont 5018 interface ink and DuPont 5000 silver ink. The fabric is prepared for dispenser printing by gluing it to a tile to ensure the fabric doesn't fold or crease during the printing process. The interface layer and the heater are printed on one surface of the fabric, the thermochromic layer is printed on the other. The interface layer is cured before the heater layer is printed. Once one surface of the fabric is printed, the fabric is removed from the tile, flipped and reattached. The unprinted surface has to be marked to align the prints on both sides of the fabric. The heater in this layout is not in direct contact with the thermochromic layer, as shown in figure 87, so the heat is conducted to the thermochromic layer through the interface layer and the fabric. One end of the heater is attached to the interface layer the other end is exposed to the air causing direct heat loss from the heater; this reduces the heating efficiency of the devices. The top layer of layout C devices is the thermochromic layer which ensures that the visibility of the colour changing effects is not affected. Aesthetically, this layout is suitable for a majority of applications especially where the thermochromic layer turns transparent and the heater is desired to be out of view. This layout is not suitable for applications where the thermochromic device is a part of a larger electronic system and the electrical interconnections are required to be fabricated on the same surface as the device. Layout C offers the advantage of keeping the heater out of view over the other two layouts. Layout A and B require fewer fabrication and processing steps than layout C and are therefore faster to fabricate. Layout C devices are more expensive to fabricate than their equivalent layout B devices and cost similar to their equivalent layout A devices when judged by the number of constituent materials. Layout C devices are the least heat and power efficient because they lose heat directly to the air and heat is conducted indirectly to the thermochromic layer. The layout C devices are less flexible than layout B devices and have similar flexibility as layout A

devices when judged by the number of printed layers. These devices are less durable than layout A devices because like the layout B devices the heater is not encapsulated.

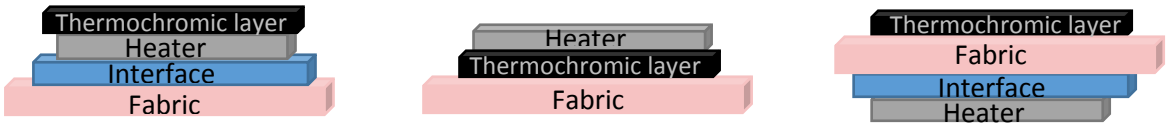

Layout A Layout B Layout C

Figure 87: Schematic of layout A, B and C thermochromic devices

The following table compares the three layouts in terms of fabrication requirements, functional properties and aesthetic properties.

	Layout A	Layout B	Layout C
Fabrication requirements	• Consists of three materials • Fabrication costs higher than layout B and same as layout C • Takes more time to fabricate than layout B and less time than layout C • More processing steps than layout B and less steps than layout C	• Consists of two materials • Least expensive to fabricate • Fastest to fabricate • Requires least processing	• Consists of three materials • Same fabrication cost as layout A and higher cost than layout B • Slowest to fabricate • Requires most processing
Functional properties	• Most power and heat efficient • Most durable • Less flexible than layout B and similar flexibility to layout C	• Lower heat and power efficiency than layout A and higher efficiency than layout C • Less durable than layout A and similar durability to layout C • Most flexible layout	• Least power and heat efficient • Less durable than layout A and similar durability to layout B • Less flexible than layout B and similar flexibility to layout A
Aesthetic properties	• Thermochromic print completely visible • Suitable for majority of applications • Not suitable for applications where the thermochromic ink turns transparent and heater is to be kept out of view	• Thermochromic print covered by heater • Visible thermochromic area may be very small • Not suitable for majority of applications	• Thermochromic print completely visible • Suitable for majority of applications • Not suitable for applications where the thermochromic print and the interconnect is on the same surface

Table 28: Comparison of the three thermochromic layouts

The analysis of the three layouts has shown that although layout B is the cheapest, the fastest to fabricate and requires least processing, it is unsuitable for use in applications because of limited visibility of the thermochromic print. Layout C offers the advantage of keeping the heater out of view for applications where the thermochromic ink turns transparent over layout A. However layout C is least power efficient, requires most processing and is the slowest to fabricate. Layout A is chosen as the preferred design layout for fabricating the thermochromic devices because it offers the following advantages over the other two layouts.

- The heater is encapsulated without printing additional materials improving the durability of the thermochromic devices.
- The heater does not reduce the visible area of the thermochromic print as it is printed underneath the thermochromic layer.
- The heater is in contact with the thermochromic print ensuring the heat is directly conducted to the thermochromic print.
- An additional opaque layer can be printed over the heater to conceal it before printing the thermochromic layer over it to suit the applications which require the heater to be out of view.
- It is the most power efficient layout.

5.3.1.2 Fabrication of the layout A thermochromic fabric devices for characterisation tests

As before, the fabric is first glued to a tile and shaved before printing. A 36 mm x 38 mm interface is dispenser printed first on the fabric in the continuous mode using DuPont 5018 ink and the settings in table 11. Continuous mode is the fastest printing option, it was used to reduce the amount of time the uncured interface deposition remained on the fabric surface which reduced the bleeding of the printing pattern via wicking. It was cured using a Panacol-Elosol UV-P 280 ultraviolet point source with exposure to UV radiation of 2000mW/cm^2 for 60 seconds. The size of the interface print was chosen as a compromise between sufficient fabric coverage and print time. The settings used for printing the interface produced prints with average thickness of 262 µm as mentioned in table 12.

A heater is printed next in the bitmap mode using DuPont 5000 and the settings in table 8; the settings produced an average thickness of 27 µm. The silver was cured at 120°C for 10 mins in a box oven. The heater is printed in bitmap mode because it is the only dispenser printing mode which allows defined patterns. The heater is a meander pattern with 1 mm gap between the tracks and 1 mm track width with contact pads for connecting power. Figure 88 shows the heater design printed on the interface layer on the polyester cotton 65/35 fabric.

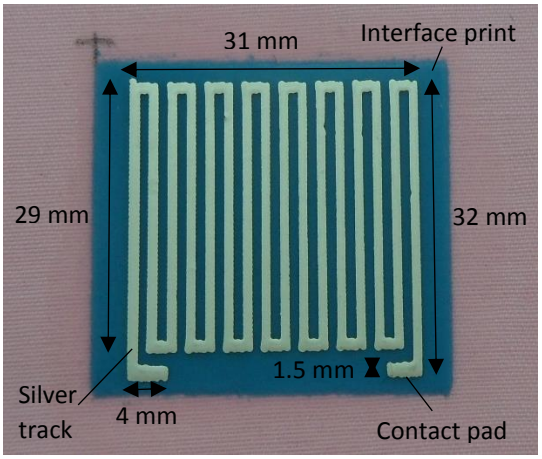

Figure 88: The heater design used for fabrication of thermochromic fabric devices printed on polyester cotton 65/35 fabric

Finally, a 29 mm x 31 mm thermochromic layer is printed over the heater to cover it using the FB-20 ink and the settings presented in table 11; it was also cured using the same process as the interface. The nozzle height was zeroed using the silver tracks as the starting point instead of the interface so that the thermochromic print is thick enough to conceal the heater. The thermochromic layer is printed in continuous mode to speed up the fabrication process. The average thickness of the thermochromic prints was 173 µm and the overall average thickness of the thermochromic device including fabric was 759 µm; averaged from five micrometre measurements. Figure 89 below presents a fabricated thermochromic fabric device before colour change and its schematic of along with the average layer thicknesses.

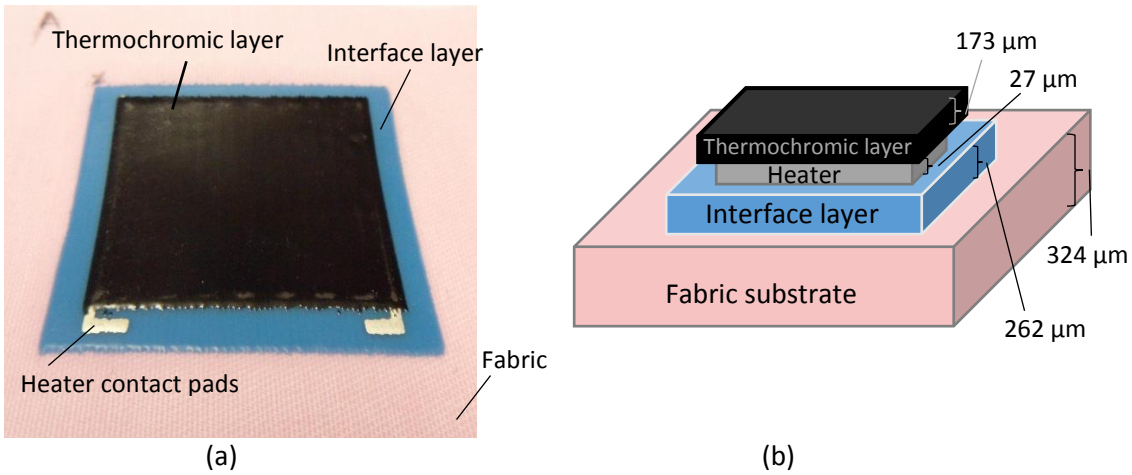

Figure 89: (a) Photo isotropic view of a final printed actively controlled thermochromic fabric device and (b) a schematic with average layer thicknesses

5.3.2 Effect of input power on the actuation response of the thermochromic devices

The actuation response time of a thermochromic fabric device is defined in this thesis as the time taken by the device to complete the colour change from the point of application of input power. The response time is influenced by the input power, environmental temperature, air flow and the thermal properties of the surface or surfaces in contact with the device. This section discusses the effect of input power on actuation response time of a device through experimentation. It also presents a comparison of the carbon and silver heater thermochromic devices.

Six thermochromic devices were fabricated for these experiments using the fabrication steps, inks, heater design and the physical dimensions mentioned in section 5.3.1.2. The FB-20 ink used for the thermochromic layer was formulated with an activation temperature of 33°C. Three of the devices were fabricated using silver heaters and the other three using carbon heaters; the settings for printing the carbon heaters is presented in table 21. The silver heater devices attained resistance values in the range of 4.6 Ω - 5.6 Ω and the carbon heater devices attained resistance values in the range of 13.2 kΩ - 23.8 kΩ. The resistances of the printed heaters varied due to variation in the nozzle height during the printing process as explained in chapter 4.

The heater design shown in figure 88 was simulated using the COMSOL heater model to determine the minimum amount of power required to actuate the thermochromic devices. The target temperature for the heater was set to 38°C which is 5°C higher than the thermochromic ink's activation temperature to ensure the devices complete the colour change. It was found that the simulated heater design required 0.5 W input power to achieve the target temperature.

The input power applied to the devices was varied in the range of 0.5 W to 3W in steps of 0.5 W. Their response time was measured by making videos of the devices as they changed from a coloured to a colourless state. The devices were suspended in air using the retort stand arrangement shown in figure 41 for the tests. Audio references were made in the videos at the point of switching on the power supply to establish the start time. The videos were replayed using Avidemux 2.6.18 software and time stamped markers were placed in the videos at the start point and the complete colour change point to extract the response time of the devices. The software time stamp markers were able to measure time down to 0.01 s. All six devices were tested in the same room at a specific position to ensure the environmental temperature and air flow were the same for all the tests. The room temperature was 22° C, it was regularly monitored using a Keithley 2001 multimeter thermocouple during the testing process. Figure 90 shows the silver and carbon heater thermochromic devices after complete colour change. The wires from the power supply were connected to the contact pads of the heaters using a copper tape to maintain electrical contact.

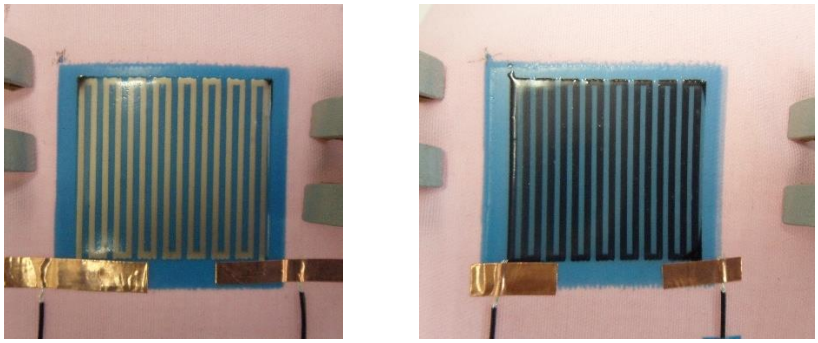

(a) (b)

Figure 90: The thermochromic fabric devices after complete colour change, consisting of (a) silver heater (b) carbon heater

The carbon heater devices were unable to achieve complete colour change at 0.5 W power due to non-uniform heat distribution or hot spots. The hot spots formed due to non-uniform resistance distribution within the heaters caused by the nozzle height variation. Figure 91 presents a carbon device producing incomplete colour change.

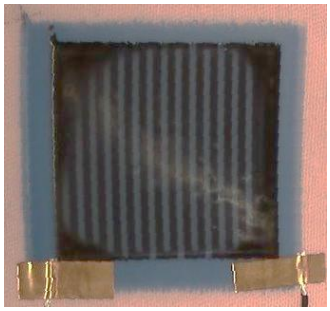

Figure 91: A carbon heater thermochromic fabric device exhibiting partial colour change due to formation of hot spots in the heater

The incomplete colour change was specific to the carbon devices although the heat distribution was non-uniform in both the carbon and the silver heater devices. A carbon track with the same thickness variation and physical dimensions as a silver track would produce a higher resistance difference because the carbon ink has a much higher resistivity compared to the silver ink. The higher resistance difference translates to a higher temperature difference in a heater leading to incomplete colour change. At higher input powers, the rate of heat generation is sufficient for all parts of the device to achieve a temperature higher than or equal 35°C, the temperature at which the device completes the colour change. At 0.5 W the response time of the carbon heater devices was measured to the point after which the devices did not produce further colour change. Figure 92 shows the graph of response time of the thermochromic devices as the applied input power to the devices is increased from 0.5 W to 3 W.

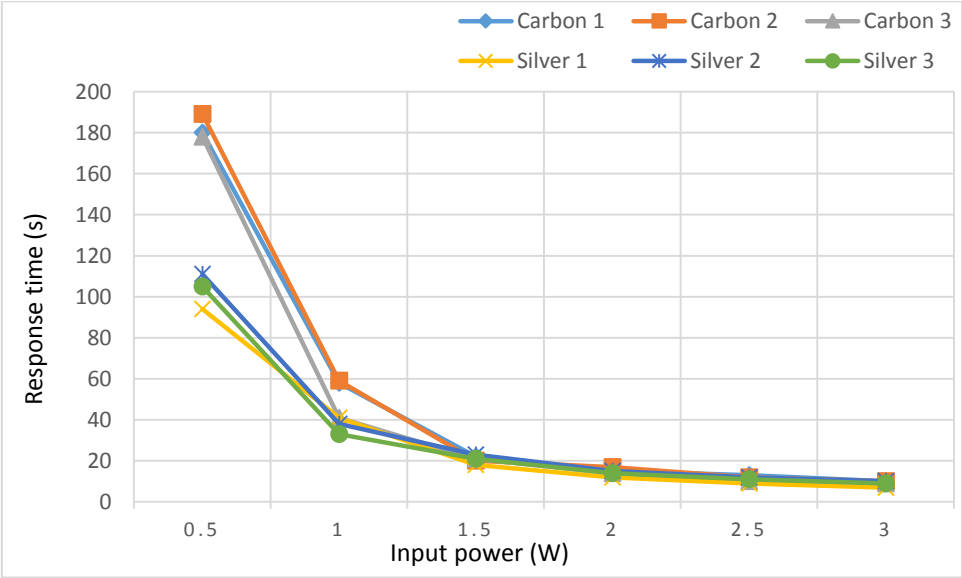

Figure 92: Graph of response time of the six thermochromic devices resulting from the applied input power in the range of 0.5 W to 3 W

The response time graph shows that increasing the input power reduced the response times of the devices. The decrease in the response times is largest from 0.5 W to 1 W, the amount of decrease reduces with each subsequent increase in the input power. The response times of all the devices are very similar for input powers greater than 1.5 W. The variation in the response times of the devices also reduces as the input power increases to 3W as shown in table 29 by the standard deviation of the average response times. Table 29 also shows that a six fold increase in the input power reduced the average actuation response time of the silver devices by 91.6 % and carbon devices by 94.6 %.

	Silver heater thermochromic devices		Carbon heater thermochromic devices	
Input power (W)	**Avg. response time of the devices (s)**	**Std. deviation (s)**	**Avg. response time of the devices (s)**	**Std. deviation (s)**
0.5	103.3	7.0	182.4	4.8
1	37.4	3.3	52.5	8.2
1.5	20.7	2.1	21.0	0.8
2	13.6	1.3	15.3	1.2
2.5	10.8	1.2	11.7	1.2
3	8.7	1.2	9.7	0.5

Table 29: The average response times and variation in the response times of the six devices at input power between 0.5 W to 3 W

The results show that the input power controls the actuation response time of a thermochromic device provided all other parameters are kept constant. There is a trade-off between the input power and actuation response time, higher input power produces faster actuation and vice versa. It was observed that a printed heater producing non-uniform heating can be used to achieve complete colour change although it may require higher input power than a uniform heater of same physical dimensions such as the carbon heater devices.

A specific response time can be selected for a device to suit an application's requirements by using a suitable input power. A suitable input power should be selected by testing the response times of a device in application specific conditions. This is because the room temperature, the air flow, the surfaces a thermochromic device is likely to be in contact with are dynamic factors that can affect the response time of a device. An application specific thermochromic device may be required to change colour and maintain the colourless/second colour state for any time duration. The power consumption of such a device can be managed to achieve a required response time whilst ensuring minimum power consumption. The device can be initially actuated by an input power that achieves the required response time and after complete colour change, the input power to device can be reduced to the minimum required level to maintain colourless/second colour state. This approach minimizes the power consumption compared to the approach where a constant input power is used to achieve the required response time and maintain the colourless state.

Silver heaters are preferred to the carbon heaters for thermochromic devices in this thesis. The carbon ink had a tendency to dry during the printing process which in some cases led to partial nozzle blockages and defective prints. As explained earlier, the carbon heater devices are more susceptible to incomplete colour change due to the high resistivity of the carbon ink. Therefore all of the devices presented in the following sections are fabricated using silver heaters.

5.3.3 Effect of operating temperatures of thermochromic inks on the refresh time of the thermochromic devices

Refresh time of a device can be defined as the time it takes the device to return to its initial/coloured state after actuation. It is measured from the point of cutting off the power to the device to the point where the device returns to its initial state. A thermochromic device returning to its initial state is a passive process affected by the operating temperatures of a device, the environmental temperature, the air flow and the thermal properties of the surfaces in contact with the device. The operating temperatures of a device are a set of temperatures at which its constituent thermochromic ink starts to change colour, completes colour change, starts to revert back to its initial state (re-colouration) and completely reverts back to its initial state (complete re-colouration). This section discusses the effect

of the re-colouration operating temperatures on the refresh times of the thermochromic devices. The operating temperatures of the FB-20 inks can be varied at the formulation stage by selecting the powder with the preferred activation temperatures. The refresh time of thermochromic devices is important to consider from an application point of view as it determines the potential frequency of use of the devices.

Nine devices were fabricated for the assessment of the effect of the operating temperatures on the refresh times of the devices; the fabrication process is presented in section 5.3.1.2. The devices were fabricated in three batches, each consisting of three devices with activation temperatures of 33°C, 43°C and 47°C. The thermochromic inks used for the devices were first tested to determine their operating temperatures. The inks were printed on the fabric in a square shape of 0.5 x 0.5 mm, a Keithley 2001 multimeter thermocouple was attached directly on the prints and a printed heater was placed under the fabric for actuation. The prints were actuated and then the heater was switched off causing the prints to return to their initial/original state. The prints and the thermocouple temperature readings were videoed during the process. The videos were reviewed to extract the operating temperatures of the thermochromic inks using the process described in section 5.3.2; the operating temperatures of the three inks are presented in table 30 below.

	33°C TC ink	**43°C TC ink**	**47°C TC ink**
Start of colour change	33 °C	42.5 °C	47 °C
Complete colour change	35 °C	45 °C	51 °C
Start of re-colouration	33 °C	38 °C	41 °C
Complete re-colouration	31 °C	35 °C	37 °C

Table 30: Operating temperatures of three thermochromic inks with activation temperatures of 33°C, 43°C and 47°C

The operating temperatures of the three inks show the expected thermal hysteresis discussed in chapter 2. The range of operating temperatures of three inks is different because of different compositions; the ink compositions are proprietary.

The devices were tested for refresh times by first heating them to achieve complete colour change and then removing the power to allow the devices to revert back to their initial state; the re-colouration process was videoed with audio references at the point when power was removed. The videos were reviewed to determine the re-colouration times. Like the previous experiments, the devices were suspended in the air using the retort stands, the tests were performed at the same position in the same room and the room temperature was regularly monitored using a thermocouple. The test setup ensured all the factors that affect the re-colouration times of the devices except the operating temperatures and device thicknesses were kept the same. The average thickness of the nine devices excluding the fabric was 435 µm ± 22 µm; thickness of each device was averaged using five measurements. The thickness variation across the devices is very small and therefore does not have any significant influence on the results as shown by the error bars in the refresh time graph. Figure 93 presents the graph of activation temperatures of thermochromic inks vs the refresh time of devices.

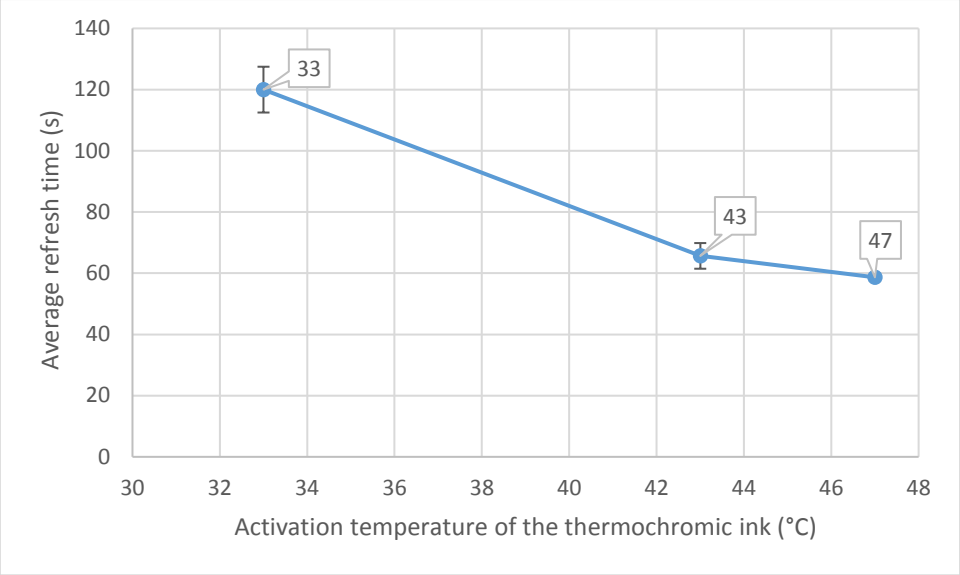

Figure 93: Average refresh times of thermochromic fabric devices consisting of thermochromic inks with 33°C, 43°C and 47°C

The graph shows that the average refresh times of the thermochromic devices decreased as the activation temperatures of the inks increased. The average refresh times decreased from 120 seconds to 65.7 seconds as the activation temperature increased from 33°C to 43°C, a further increase to 47°C reduced the average refresh time to 58.7 seconds. Devices with higher activation temperatures produce higher temperature gradient between the devices and the environment upon completion of colour change. The higher temperature gradient produces a higher heat transfer rate causing the devices to lose heat faster and therefore producing lower refresh times.

The results show that the operating temperatures of a thermochromic ink influences the refresh rate of a thermochromic device; the refresh time of a device limits the frequency of its use in a dynamic application. These findings suggest that a higher activation temperature ink will produce lower refresh times however it will require a higher input power for actuation. There is a trade-off between the input power and the refresh time of a thermochromic fabric device influenced by the activation temperature of the thermochromic ink which must be considered when designing a device for an application.

5.3.4 Fabrication and testing of dispenser printed thermochromic devices on Kapton and Mehler PVC coated fabric

This section demonstrates that the dispenser printed approach of fabricating a thermochromic device is not limited to polyester cotton 65/35 fabric and can be replicated on other substrates. It presents fabrication of the thermochromic devices on Kapton, a standard printed electronics substrate and Mehler Frontlit II Standard FR PVC coated fabric, an architectural fabric.

The fabrication on the two substrates requires printing of two layers; the heater and the thermochromic layer. The two substrates have significantly lower surface variation than polyester cotton fabric as shown in table 13 so they do not require an interface layer. The devices are fabricated in layout A on both substrates using the fabrication steps detailed in section 5.3.1.2. The silver ink was printed on the PVC coated fabric using a different set of dispenser printer settings to Kapton and interface on fabric; the settings are presented in table 14. A 33°C activation temperature thermochromic ink was used for the fabrication of the two devices. The devices were actuated using 0.5W power; their actuation response time and refresh time was measured using the processes and

setups described in section 5.3.2 and 5.3.3 respectively. Figure 94 and figure 95 show thermochromic devices before and after colour change on Kapton and Mehler PVC coated fabric respectively.

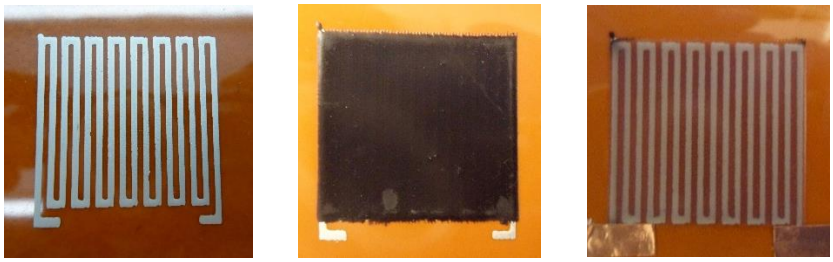

(a) (b) (c)

Figure 94: Dispenser printed (a) heater, dispenser printed actively controlled thermochromic device (b) before colour change and (c) after colour change fabricated on Kapton

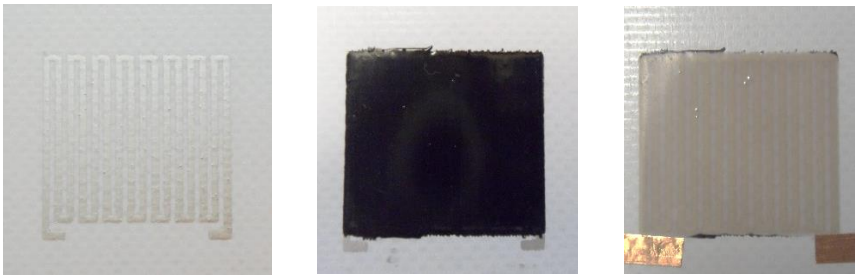

(a) (b) (c)

Figure 95: Dispenser printed (a) heater, dispenser printed actively controlled thermochromic device (b) before colour change and (c) after colour change fabricated on Mehler PVC coated fabric

The Kapton thermochromic device took 36 seconds to achieve complete colour change and 69 seconds to revert back to its initial state after the power was switched off. The actuation response time of the PVC coated fabric was 70 seconds and its refresh time was 82 seconds. This confirms that the colour change timings of the thermochromic devices will vary when printed on different substrates and must be tested before being employed in an application.

The thermochromic devices on the three substrates are flexible which overcomes one of the major limitations of the devices reported in the literature. The flexibility of the devices is demonstrated in figure 96 below by bending them using a 6 mm bend radius and securing them in position with a bulldog clip; the devices in the figure are being actuated.

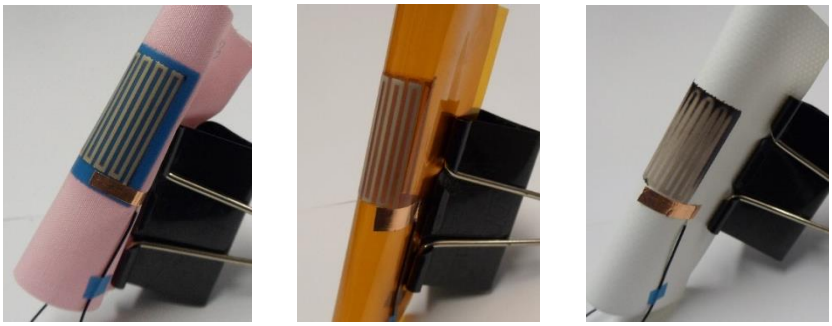

(a) (b) (c)

Figure 96: Dispenser printed thermochromic devices on (a) polyester cotton 65/35 fabric (b) Kapton and (c) Mehler PVC coated fabric being flexed using a bulldog clip

5.3.5 Summary

Section 5.3 presented the details of fabrication of thermochromic devices using the novel dispenser printing approach. It described the structure of the thermochromic devices and discussed the three

potential layouts. The layout A where the heater is printed underneath the thermochromic layer is the optimum layout because it encapsulated and insulated the heater without printing additional materials. It was shown that a heater with non-uniform heat distribution can be used in a thermochromic device to achieve complete colour change.

Actuation response time and the refresh time were highlighted as the two key parameters of a thermochromic device. It was experimentally established that an increase in the input power to a device reduced actuation response time of the devices but only up to a certain power level. Beyond this optimum power, the actuation response would saturate and any improvements would be minor. A comparison of silver and carbon heater thermochromic devices showed that, for same input power, the devices are able to achieve similar response times despite a large difference in the resistance of the silver and carbon devices. It was found that devices fabricated with higher activation temperature thermochromic inks produced lower refresh times. The refresh time of a thermochromic device affects the operating frequency of a thermochromic device and therefore must be considered for each application.

It was shown that the dispenser printing approach of fabricating a thermochromic device is not limited to polyester cotton 65/35 fabric by fabricating the devices on Kapton, a standard printed electronics substrate and Mehler PVC coated fabric, an architectural fabric. It was demonstrated that the devices printed on polyester cotton 65/35 fabric, Kapton and PVC coated fabric are flexible by bending them using a 6 mm bend radius. The devices on Kapton and the Mehler fabric show that the dispenser printed thermochromic devices can be utilised in applications requiring a range of substrates other than the polyester cotton fabric.

5.4 Variation in the colour changing effects of the printed thermochromic devices

All of the thermochromic devices presented in the thesis so far change from a coloured state to a colourless/transparent state. This colour changing effect is embedded in the devices by their constituting thermochromic inks. The ink formulation can be varied to produce other colour change effects such as change from one colour to another and multiple colour changes as explained in section 5.2.1. These colour changing effects enhance the functionality of the thermochromic devices by offering a wider range of colour changing options for applications. For creative applications discussed in the literature review such as a wallpaper and fabric artwork, these effects translate to a broader range of artistic effects. For the discussed sensory indicator applications, they can represent multiple values of a physical quantity such as distance and indicate multiple states of a smart fabric system such as ‘on’, ‘off’ and ‘stand by’. This section demonstrates devices which change from one colour to another, produce multiple colour changes and sequential actuations within a device and details the ink formulation required to achieve them.

The FB-20 ink is modular where Fabinks-IF-1004 ink and the thermochromic pigment are the essential components as the binder and colour changing material. The ink attains the colour and activation temperature of its constituent thermochromic pigment. Multiple colour changes in an FB-20 ink can be achieved by mixing additional components in the ink such as standard coloured fabric pigments and multiple thermochromic pigments. The following subsections present the changes to the standard FB-20 formulation to produce devices which change form one colour to another, exhibit multiple colour changes and sequential actuation within a single thermochromic layer. All the devices presented in this section are fabricated using the steps and dispenser printer settings detailed in section 5.3.1.2.

5.4.1 Thermochromic device which changes from one colour to another

Thermochromic ink which changes from one coloured state to another can be formulated by combining thermochromic pigments with a coloured binder. The FB-20 formulation was altered to achieve this colour change effect by addition of standard dry fabric pigment to the ink. The fabric pigment causes the Fabinks-IF-UV-1004 binder to attain a permanent temperature independent colour. The thermochromic ink that changes from black to red (FB-20-1) was formulated by mixing 19.5% of 33°C black 'new colour chemical' thermochromic powder and 0.5% of red george weil fibrecrafts dry fabric pigment powder [93] with 80% Fabink-IF-UV-1004 ink. The 0.5% proportion of the dry fabric pigment in the ink formulation was recommended by the supplier. The proportion of binder to the powder in this ink is kept the same as FB-20 ink, 80% to 20%, to maintain the printability offered by the FB-20 ink. Before actuation, below 33°C the device exhibits black colour which is a result of subtractive mixture of black and red colour. After actuation, above temperatures of 35°C the device exhibits red colour because the black pigments turn colourless. Figure 97 presents the thermochromic device which changes from black colour to red colour upon actuation.

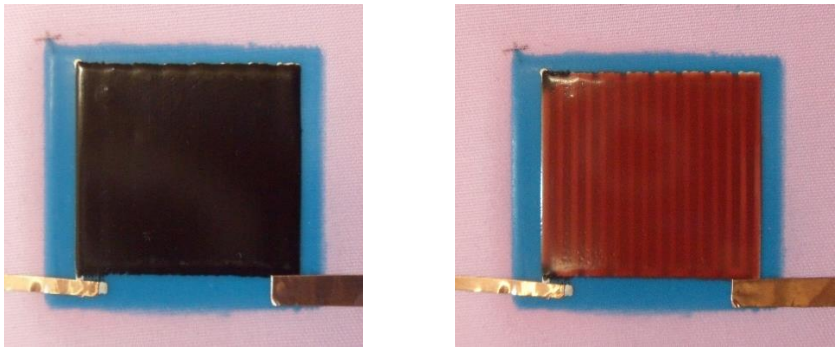

(a) (b)

Figure 97: A thermochromic device exhibiting a colour change from one coloured state to another, (a) the device before actuation displaying black colour and (b) the device after actuation displaying red colour

5.4.2 Thermochromic device which produces multiple colour changes

This section presents a thermochromic device which produces three coloured states and a transparent state upon actuation. The actuation of this device is a three step process where the temperature is increased in each step to produce a colour change. Each actuation step is reversible and can be triggered by varying the input power to the device. The multiple colour changing ink can be formulated by using more than one different coloured thermochromic pigments. The activation temperatures of the individual pigments in the ink are not affected. The colour output of the ink at any temperature displays colour mixtures of all the pigments which are at a lower temperature to their activation temperature.

The multiple colour changing ink was formulated to produce a first step change from black to green, a second step change from green to yellow and a final change from a yellow colour to a transparent state. The ink (FB-20-2) consisted of 6.7% of 33°C black thermochromic powder, 6.6% of 43°C blue thermochromic powder and 6.6% of 47°C yellow thermochromic powder and 80% of Fabinks-IF-UV-1004 binder. The operational temperatures of the three pigments with activation temperature of 33°C, 43°C and 47°C are presented in table 30. Like FB-20-1 the ratio of powder to binder in the FB-20-2 ink is kept the same as the FB-20 ink. Figure 98 shows the multiple colour changing device before and during actuation. It can be seen that the device displays multiple colours, black, green and yellow, at the same time instead of displaying a single colour individually. This is caused by the non-uniform

heat distribution within the heater constituting the device. The temperature variation causes various parts of the device to be actuated to different extents therefore exhibiting different colours.

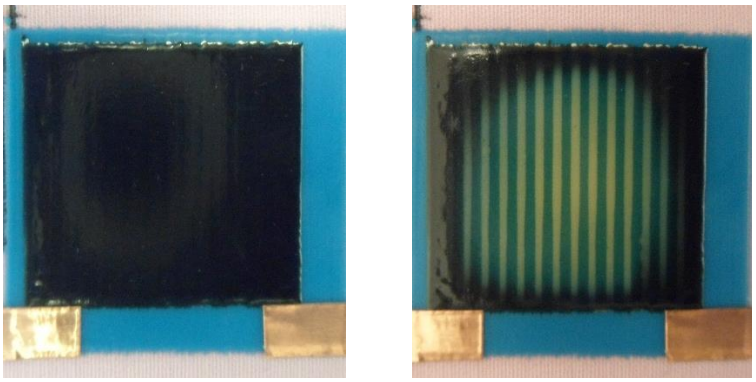

(a) (b)

Figure 98: Thermochromic device which produces multiple colour changes (a) before colour change and (b) during actuation

The device was actuated using a hot plate in the next step to ensure that it heated uniformly and exhibited all the coloured states, shown in figure 99 below. The device displays black colour below 33°C, it displays green colour above 35°C and below 42°C which is a mixture of yellow and blue pigments. Above 45°C and below 47°C, it displays yellow colour as the blue pigments turn colourless. Heating the device above 51°C causes the device to become colourless and transparent. The transparency of device increased at each actuation step because the percentage of coloured thermochromic pigments decreased.

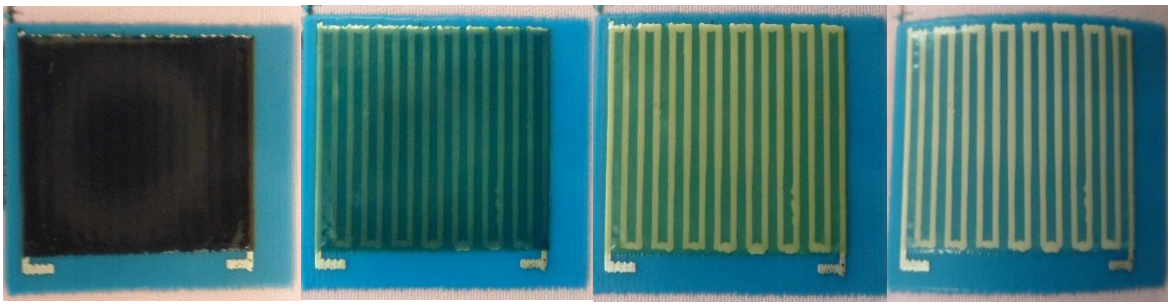

(a) (b) (c) (d)

Figure 99: Thermochromic device being actuated on a hot plate exhibiting multiple colour changes, the device is displaying (a) black colour at 32°C (b) green colour at 37°C (c) yellow colour at 46°C and (d) transparent state at 52°C

A multiple colour changing device requires uniform heating to exhibit all the coloured states individually. Individual coloured states can also be achieved by using thermochromic pigments with a larger actuation temperature difference than the temperature variation in the device. The device can also be used to produce multiple colours at the same time for use in creative applications as shown in figure 98. The FB-20-2 can be formulated to produce a final coloured state instead of transparent state by using standard dry fabric pigment, however the colour of the fabric pigment would mix with the colours of the thermochromic pigments at each actuation step. Therefore, the choice of colours of the thermochromic pigments and the fabric pigments must be carefully considered.

5.4.3 Multiple colour changing device fabricated using a layering approach

This section presents a device which exhibits two coloured states and a transparent state upon actuation. Its actuation process is similar to the previous multiple colour changing device.

The device is fabricated by printing multiple single coloured thermochromic inks over each other in layers. Firstly, a 30 mm x 32 mm layer of dark blue FB-20 ink with an activation temperature of 33°C is printed on the heater followed by a 20 mm x 20 mm layer of yellow FB-20 ink with an activation temperature of 43°C. Figure 100 below shows the multiple colour changing thermochromic device fabricated using the layering approach.

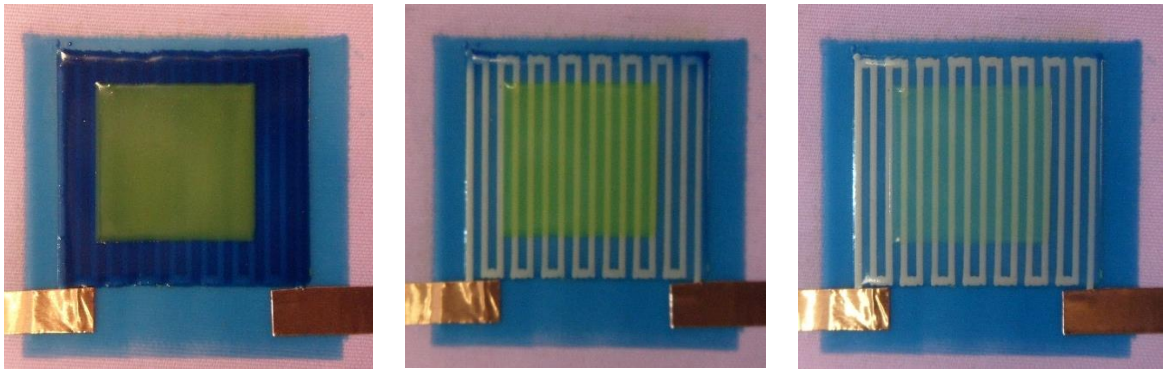

(a) (b) (c)

Figure 100: Multiple colour changing thermochromic device fabricated using a layered approach, (a) initial coloured state, (b) first colour change and (c) final transparent state

The device below 33°C exhibits a combination of dark blue and yellow colour which can be seen in figure 100 (a). The dark blue print turns colourless when the device is heated to a temperature between 35°C and 42.5°C, this constitutes the first actuation step. As the second actuation step, the device is heated to a temperature above 45°C, causing the yellow print to turn colourless and the device to attain a transparent state. The yellow colour produced a more transparent output than the black and dark blue colour as shown in figure 100 (b). The first layer thermochromic ink can be formulated using a coloured binder to produce a coloured state as the final colour change of the device.

Layering thermochromic inks over each other instead of mixing multiple thermochromic pigments reduces colour mixing in the colour output as shown by the devices presented in figure 99 and figure 100. Mixing dark blue and yellow pigments in the figure 99 device produced a green colour whereas layering yellow ink over dark blue ink did not produce green colour. This shows that the layering method can to a large extent preserve the colour of individual thermochromic pigment in a multiple colour changing device. Although it must be noticed that printing a darker coloured thermochromic layer underneath a lighter colour may affect the colour output of the light coloured layer.

5.4.4 Sequential actuation within a single coloured thermochromic device

This section presents a method of fabricating a thermochromic device where parts of the device can be sequentially actuated. Sequential actuation allows a device to produce multiple pattern changes using a single heater which can be used for creative applications. It can be achieved by printing multiple thermochromic inks with different activation temperatures in a single layer. The different parts of the thermochromic layer get electrically actuated in a sequence due to the difference in activation temperatures.

A sequential actuation device was fabricated using three black FB-20 inks with 33°C, 43°C and 47°C activation temperatures. The thermochromic layer is printed in a rectangular shape measuring 31 mm x 32 mm, it consists of four smaller rectangular prints measuring 15.5 cm x 16 cm each; the four smaller rectangles were printed using the three black FB-20 inks. Figure 101 shows the device and the regions printed using each of the three black FB-20 inks. Figure 102 shows the three stages of actuation of the device.

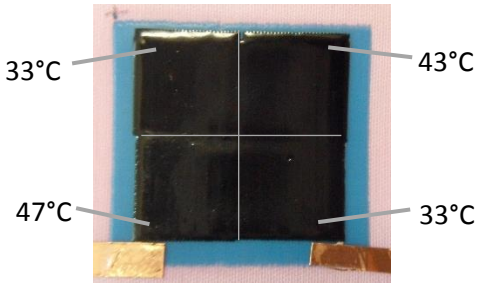

Figure 101: Sequential actuation thermochromic device printed using three thermochromic inks with different activation temperatures before actuation

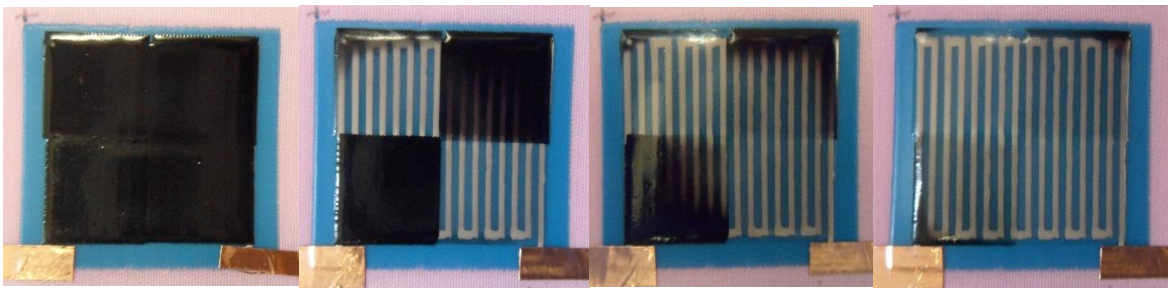

(a) (b) (c) (d)

Figure 102: The stages of the actuation of the sequential actuation thermochromic device, (a) before actuation below 33°C, (b) first actuation step above 35°C and below 42.5°C, (c) second actuation step above 45°C and below 47°C and (d) final actuation step above 51°C

The device is actuated in three steps shown in figure 102 with first one occurring between 35°C and 42.5°C, the second between 45°C and 47°C and the third above 51°C. The heater produced non-uniform heating which caused an overlap especially in the second step causing the 47°C ink rectangle to start colour change before the 43°C rectangle had completed colour change. A uniform heater and a broader range of activation temperatures can produce colour transitions without overlap. The thermochromic inks for the device can by printed in any required arrangement. The number of actuation steps is dictated by the number of thermochromic inks with different activation temperatures. The sequential actuation device can also be fabricated using multiple coloured inks to produce multi-coloured sequential effects.

5.4.5 Summary

Four thermochromic devices which produce a change from one colour to another, multiple colour changes and sequential actuation were demonstrated. It was shown that FB-20 ink formulation can be altered by addition of dry fabric pigments and multiple thermochromic pigments to produce the demonstrated colour changing effects. The colour output of these effects can be varied using different colour blends to those demonstrated. An advantage of layering multiple single colour inks over the use of a multiple colour changing ink is that it reduces the effect of colour mixing in the output. It was generally observed that all the devices required uniform heating to exhibit the four colour changing effects properly. The four demonstrated colour changing effects can be used individually or in combination for smart fabric applications.

5.5 Demonstrator applications of the dispenser printed thermochromic devices

This section presents four demonstrator applications of the dispenser printed thermochromic devices on polyester cotton 65/35 fabric; a shutter display, a matrix display, a 7-segment display and a proximity controlled thermochromic fabric. They show that the dispenser printing approach of fabricating a heater and thermochromic materials on a fabric can be used to produce more complex systems. These applications are not novel and have been previously developed by other researchers

and designers [34,36,94,95,96,97,98]. The previously demonstrated applications use screen printing, coating, weaving conductive yarns, evaporation deposition and Peltier semiconductors as the fabrication methods, have limitations of design freedom, inflexibility and poor integration with the fabrics. Some of the previously developed applications have been fabricated on paper, photo paper and glass substrates [94,95,96] and therefore cannot be compared to applications fabricated on fabrics. The dispenser printed demonstrators improve the previously reported applications by offering the combination of flexibility, design freedom and good integration of heaters with the fabric substrate.

Following are the novel aspects of the four demonstrator applications presented in this section.

- **Fabrication process:** The four demonstrators are the first all printed applications of thermochromic devices on fabric. The interface, heater and the thermochromic materials are all fabricated/deposited on the fabric using dispenser printing.
- **Structure**: The use of a flexible printed heater on the fabric substrate is a novel approach of developing actively controlled thermochromic fabrics.
- **Fabric substrate:** These applications have been fabricated on a commonly used polyester cotton 65/35 fabric.

5.5.1 Actively controlled dispenser printed thermochromic shutter display

A shutter display is a device which is able to exhibit two distinct states; a default and an actuated state. It can be used to communicate preselected information in the form of text and graphics. The two states makes a shutter display suitable for communicating information on specific conditions such as time of the day or a specific output from a sensor. The thermochromic shutter display presented in this section is fabricated to conceal and reveal letters 'TC' in the default/non-actuated and actuated states respectively. The device is electronically controlled via a single heater. Figure 103 presents the schematic of the structure of the shutter display.

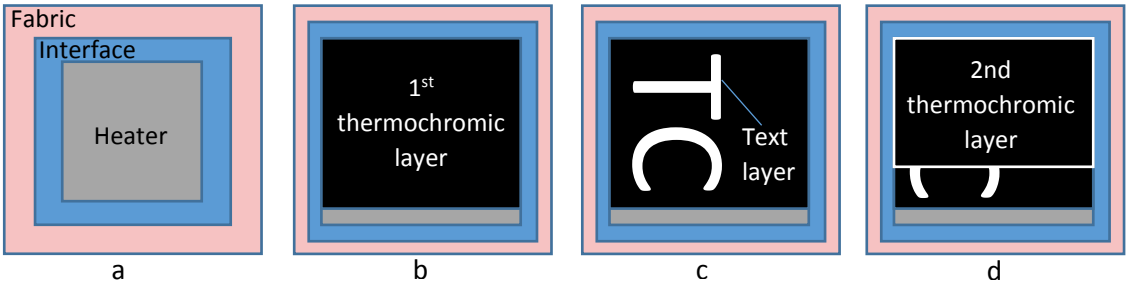

Figure 103: Diagrammatic representation of the structure of the thermochromic shutter display (a) the first three elements of the device (b) first thermochromic layer printed over the heater to hide it (c) the text layer containing a message to be concealed (d) second thermochromic layer to conceal and reveal the message

The shutter display consists of five elements excluding the fabric substrate which are printed in layers; interface layer, heater, first thermochromic layer, a text layer and a second thermochromic layer. The interface layer and the heater were fabricated first using the fabrication steps presented in section 5.3.1.2. The first thermochromic layer is a black FB-20 ink with an activation temperature of 43°C. It is printed over the heater to conceal it and provide a black background for the text layer. The text layer consists of printing letters 'T' and 'C' using white scola fabric paint [99] and settings presented in the table 31; the text layer was printed in bitmap mode. The fabric paint was cured by first allowing it to dry for five minutes and then heating the device at 80°C for 2 minutes. The second thermochromic layer was printed using a 33°C black FB-20 ink to reversibly conceal and reveal the text layer. The two

thermochromic layers were printed using the settings presented in table 11; Figure 104 shows the thermochromic shutter display before, during and after actuation.

Pressure (kPa)	25.0
Dispense Time (ms)	20
X-resolution (mm)	0.40
Y-resolution (mm)	0.20
Nozzle Height (µm)	100
Vacuum (kPa)	0.10
Speed (mm/s)	1

Table 31: Dispenser printer settings used for printing scola fabric paint on the thermochromic layer using bitmap mode

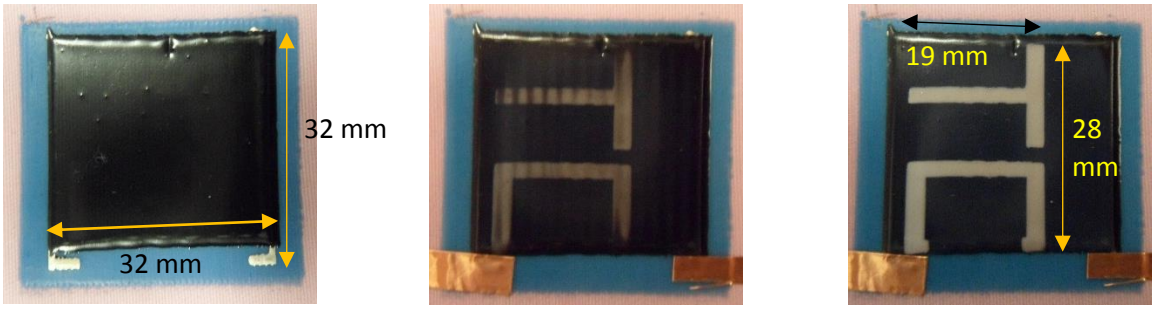

a b c

Figure 104: Dispenser printed thermochromic shutter display (a) initial state before colour change (b) during transition to the actuated state (c) actuated state revealing the text layer

The device heater attained a resistance of 5.17 Ω. The device took 34 seconds to change from its initial state to its actuated state when an input power of 1.39 W was applied and it took 109 seconds to revert back to its initial state. The text layer in the shutter display can be replaced by any other text or image by dispenser printing the required pattern under the final thermochromic layer. Similarly, the size and colours of the text/image can be modified as per the requirement. A disadvantage of the shutter display is that it cannot be used for presenting dynamic information due to a fixed display image.

5.5.2 Actively controlled dispenser printed thermochromic 7-segment display

The 7-segment display consists of seven individually controllable display elements. Different combinations of the display elements can be actuated to represent numbers from 0-9. The numbers on the display can be dynamically changed. The display elements change colour from black to red when actuated. The display is fabricated using five dispenser printed layers; interface layer, carbon heaters, silver interconnects, thermochromic ink and the fabric paint. Figure 105 shows the patterns of carbon ink, silver ink, thermochromic ink and fabric paint used for printing the display. The four inks are patterned on the interface layer on fabric using the bitmap printing mode.

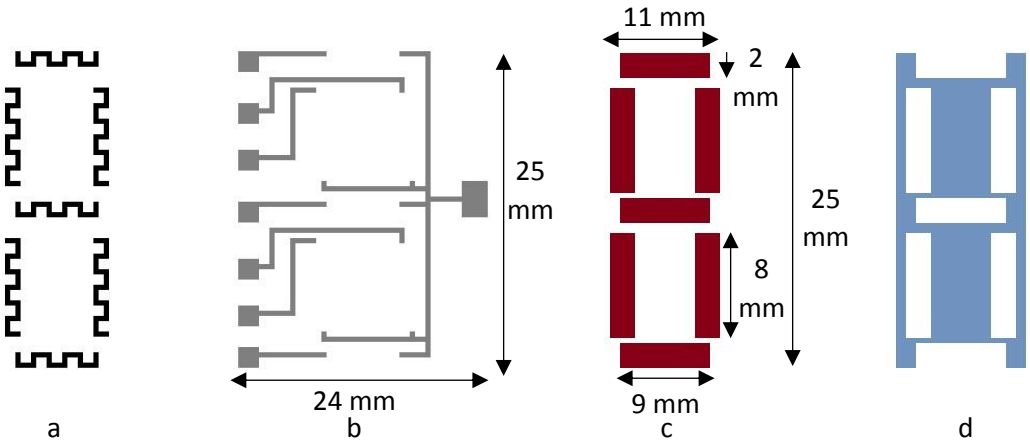

Figure 105: Fabrication steps of the thermochromic 7-segment fabric display; patterns of the (a) carbon ink, (b) silver ink, (c) thermochromic ink and the (d) fabric paint used for the dispenser printing of the 7-segment display

The display was fabricated by dispenser printing the interface layer first on the fabric using the DuPont 5018 ink and the settings presented in table 11. The carbon heaters were printed next using the DuPont 7102 carbon ink and the settings presented in table 21 on the cured interface. Each carbon heater is a meander pattern filling an area of 18 mm^2, the width of the meander track was 0.5 mm. Carbon was selected for the heaters to achieve a higher resistance than the silver interconnections. This ensures that only the carbon tracks produce heat based on the concept of selective heating and a smaller current can be used to actuate the display elements. The seven heaters achieved an average resistance of 642 Ω ± 33 Ω. The resistance variation was caused by the thickness variation which was a result of inconsistent gap between the printing nozzle and the interface.

The silver interconnections were printed next around the uncured carbon heaters using the DuPont 5000 ink and the settings presented in table 8. The low resistivity of the silver ink ensured that the interconnections produced low resistance to reduce the thermal energy losses; the interconnections are 0.5 mm wide. The electrical interconnect was designed to assign each heater an individual contact pad as one terminal and a common contact pad as the other terminal. This allowed individual control of each heaters by connecting and disconnecting power to their respective individual contact pad. The individual silver contact pads were 2 mm x 2 mm and the common contact pad was 3 mm x 2.5 mm in size. The two inks were cured together in box oven at 120°C for 8 minutes. Figure 106 shows the silver and carbon inks printed on the interface layer for the 7-segment display.

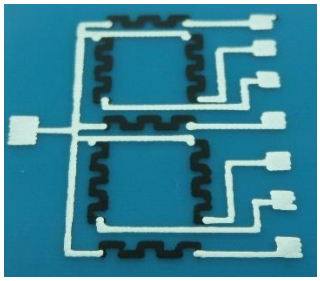

Figure 106: The silver and carbon ink 7-segment display patterns dispenser printed on interface layer

The thermochromic ink is printed next over the carbon heaters. FB-20-1 thermochromic ink with an activation temperature of 33°C presented in section 5.4.1 was used for the display elements, printed using the settings presented in table 32. These settings produced prints with an average thickness of 67 µm; averaged using five measurements. Black scola fabric paint is the final layer printed over the

silver interconnections to conceal them from the view. The thermochromic layer was cured before printing the fabric paint. The fabric paint was printed using the settings presented in table 31, it was cured by first allowing it to dry and then heating the device at 80°C for 2 minutes. Figure 107 shows the dispenser printed thermochromic 7-segment display on polyester cotton 65/35 blend.

Pressure (kPa)	60.0
Dispense Time (ms)	20
X-resolution (mm)	0.50
Y-resolution (mm)	0.40
Nozzle Height (µm)	150
Vacuum (kPa)	1.0
Speed (mm/s)	1

Table 32: Dispenser printer settings used for printing the thermochromic ink for the 7-segment display using bitmap mode

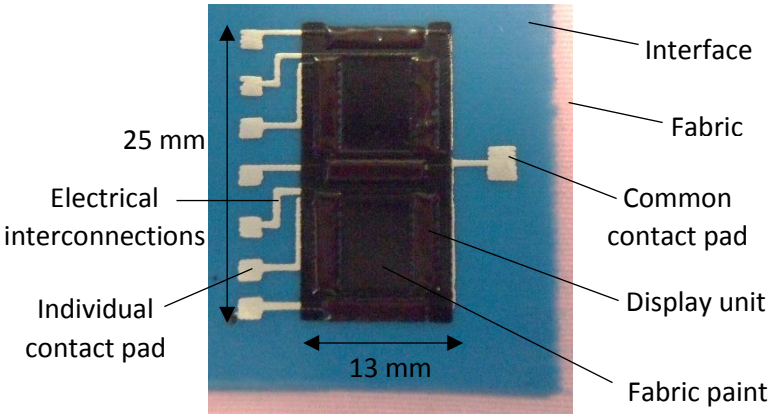

Figure 107: Dispenser printed actively controlled thermochromic 7-segment display

The 7-segment display was actuated to represent all the numbers from 0 to 9 shown in figure 108.

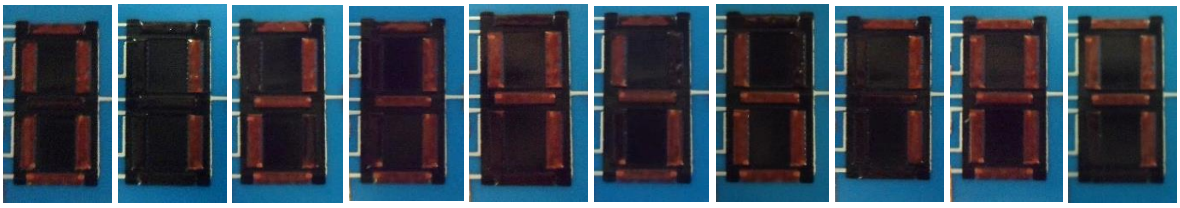

Figure 108: 7-segment display exhibiting numbers from 0-9 by actuating different combinations of the display units

All seven display elements were actuated simultaneously to represent the number 8 by application of 0.3 W of power. It took the seven display elements 17 seconds to change from black colour to the red colour. The device took 47 seconds to revert back to its initial stage. The colour change timings were obtained using the same method as before.

5.5.3 Actively controlled dispenser printed 3 x 3 thermochromic matrix display

The 7-segment display is limited to exhibiting numerical information, it cannot used to display alphabets and graphics. Therefore, a matrix display was fabricated, it consists of nine individually controllable display elements which can be used to present text or graphics; the display elements change from black to red upon actuation.

The matrix display is fabricated using the same five layers and fabrication steps as the 7-segment display. The difference between the two displays in addition to the number of elements is the physical dimensions and the shape of the display elements, heaters and the silver interconnections. Figure 109 presents the patterns of carbon ink, silver ink, thermochromic ink and fabric paint used for dispenser printing the thermochromic matrix display.

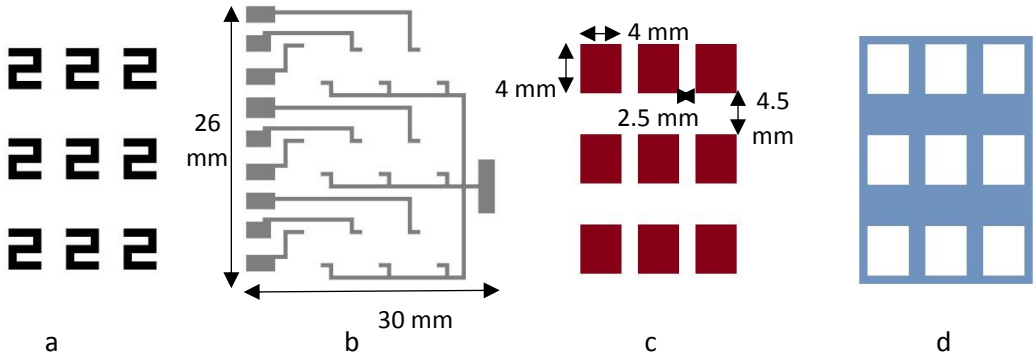

Figure 109: Fabrication steps of the thermochromic 3x3 matrix display; bitmap images used for patterning (a) carbon heaters (b) silver interconnections (c) thermochromic display units and (d) fabric paint for the matrix display

The carbon heaters are in a meander pattern filling an area of 16 mm^2, the width of the meander track was 0.8 mm. The heaters attained an average resistance of 266 Ω ± 15 Ω; the resistance variation is caused due to thickness variation. The silver interconnections are 0.5 mm wide and the contact pads are on average 1.5 mm x 3.5 mm in width and length respectively; the size of the contact pads was varied to allow sufficient room for connecting the power supply wires. The electrical interconnect was designed to assign each heater an individual connect pad as one terminal and a common contact pad as the other. Figure 110 shows the dispenser printed thermochromic matrix display fabricated on polyester cotton 65/35 fabric.

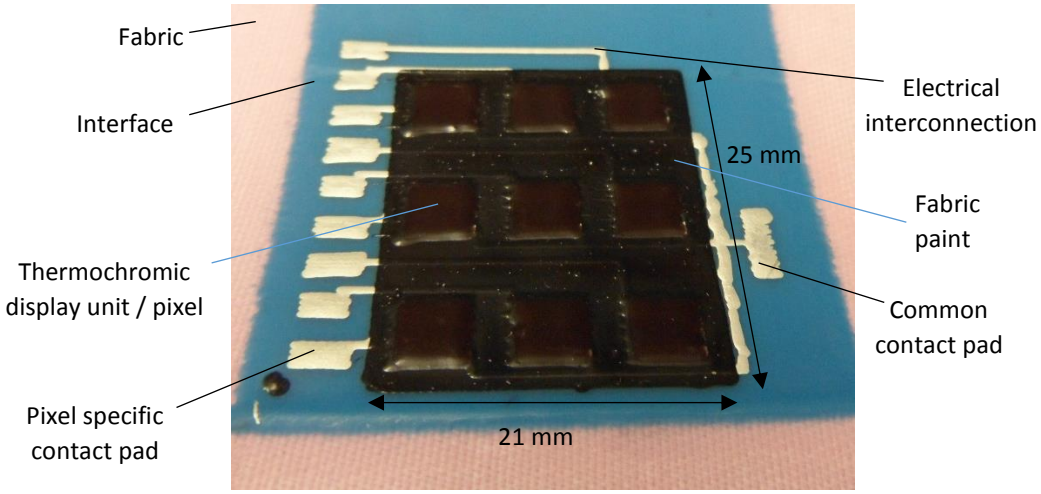

Figure 110: Actively controlled dispenser printed 3x3 thermochromic matrix display

The matrix display was actuated to present all the nine display units and letters A, C, F and T shown in figure 111. The text displayed on the matrix display was chosen to demonstrate different areas of the display active and the ability to isolate individual pixels across the panel. The choice of text and graphics to be displayed on the device was limited by its low-resolution of nine pixels.

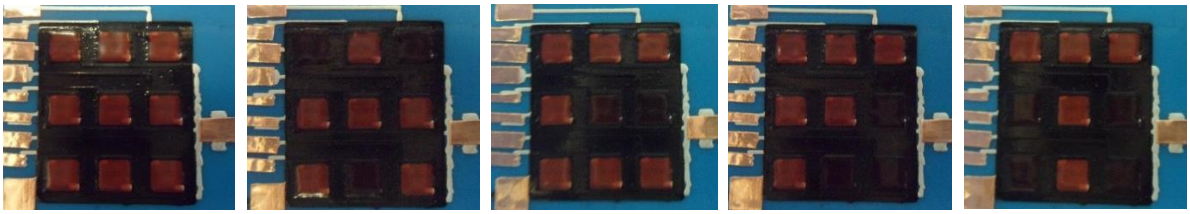

a b c d e

Figure 111: The thermochromic matrix display actuated to present (a) all nine display units, (b) letter A, (c) letter C, (d) letter F and (e) letter T

All nine display units of the device were simultaneously actuated by application of 0.42 W of power. The display units changed colour in 24 seconds and reverted back in 60 seconds when the power was removed. The colour change timings of the device can be varied by varying the input power and the actuation temperature of the thermochromic pigment as explained earlier.

5.5.4 Dispenser printed interactive colour changing smart fabric

The smart fabric is a proximity controlled thermochromic device fabricated on polyester cotton 65/35. A proximity sensor detects the presence or absence of an object without the need of a physical contact. The fabric changes colour in response to the presence of an object in the range of the sensor. The smart fabric demonstrates the use of a thermochromic device as a sensory indicator, in this case for a proximity sensor.

A dispenser printed proximity sensor on the polyester cotton 65/35 fabric was developed at University of Southampton as part of the CREATIF project [65]. It makes use of a printed conductor as the sensing element and is based on capacitive sensing technology. The capacitive sensing technology measures changes in capacitance to detect the presence of objects. The dispenser printed proximity sensor adopts a configuration based on the principle of a parallel plate capacitor where the single conductor acts as one electrode of a capacitor [100]. An approaching object forms the other electrode of the capacitor causing the capacitance between the sensing electrode and the object to increase. The object acts as a virtual earth. The changes in capacitance associated with the presence or absence of the objects is detected by the sensor circuit connected to the proximity sensor. The output of the sensor can be fed into a microcontroller to control an actuator. The sensing element in the form of the printed conductor can be fabricated in various shapes and sizes [65].

The smart fabric was fabricated in three steps. 38 cm x 36cm DuPont 5018 interface layer was dispenser printed first on the fabric followed by the DuPont 5000 silver ink for heater and the proximity sensing element. Figure 112 shows the design and dimensions of the heater and sensing element. The designs were chosen to allow sufficient space for the power supplying wires to be easily connected to the contact pad of the heater and the sensing element. The dimensions of the device was chosen to fit the limits of the current printer.

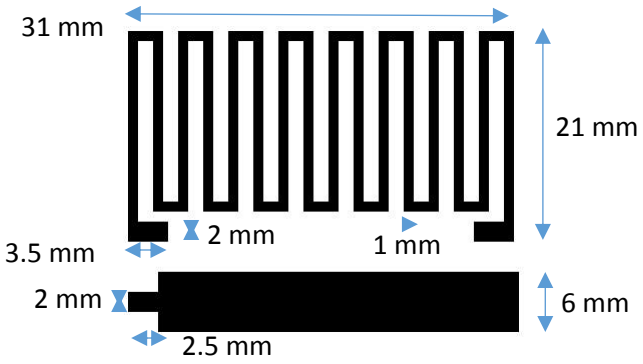

Figure 112: Pattern of the silver ink dispenser printed on the interface layer on fabric for the fabrication of proximity controlled colour changing fabric and the dimensions of the heater and the proximity sensing element

Figure 113 shows the heater and the sensing element dispenser printed on the interface print. The heater was not dispenser printed properly at the first attempt due to nozzle height variation during the printing process, the silver ink was not deposited adequately in some areas in the middle of the heater. Those areas were reprinted causing the silver ink to bleed. The heater attained a resistance of 5.8 Ω.

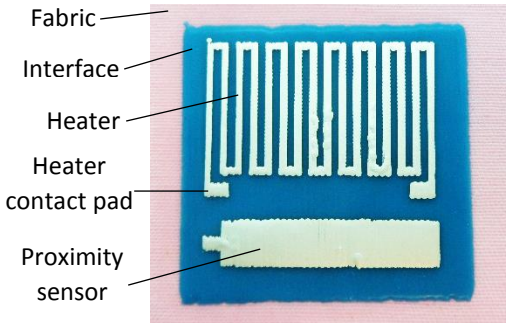

Figure 113: Silver heater and proximity sensing element dispenser printed on interface on polyester cotton 65/35 fabric for the interactive smart fabric

The thermochromic ink was printed next over the heater. The silver ink was cured before the thermochromic ink was printed over the heater. FB-20-2 multiple colour changing ink presented in section 5.4.2 was chosen for the proximity sensor. The ink produces three colour changes with increase in temperature; black to green, green to yellow and yellow to colourless. The ink was selected so that the three colour changes could be used for representing the distance between the proximity sensing conductor and the object triggering the sensor. However, the heater for the proximity sensor produced non-uniform heating and could not achieve the three coloured states individually. All the inks were printed using the same settings as the previous demonstrators. Figure 114 shows the dispenser printed proximity controlled thermochromic fabric.

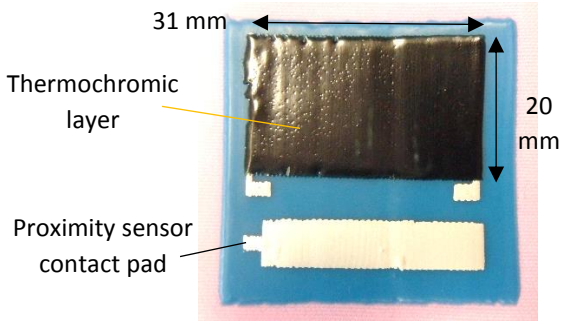

Figure 114: Dispenser printed proximity controlled thermochromic fabric device on polyester cotton 65/35 fabric

The proximity sensor was driven using the MTCH101 proximity sensor IC which is a commercially available single channel proximity detector. The driving circuit for the proximity sensor was developed as part of the CREATIF project [65] and was replicated for controlling the thermochromic device. The output from the IC was fed into an Arduino Uno microcontroller to control the actuation of the thermochromic device. The output signal from the microcontroller was fed into a power transistor which was used as a switch to actuate the device. The transistor was needed to actuate the thermochromic fabric device using a large current which would otherwise damage the microcontroller. The circuit diagram for the setup is presented in figure 116.

The microcontroller was programmed to activate the colour changing fabric as an object approached the sensing conductor. Figure 115 shows the interactive colour changing fabric before actuation, being actuated by a finger approaching the proximity sensor and being actuated by a hand as it comes within the detection range of the sensor. The thermochromic device was actuated by application of 1.08 W of power.

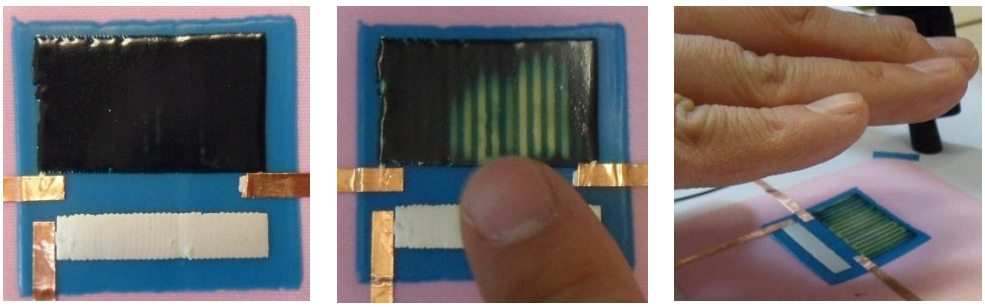

a b c

Figure 115: Dispenser printed proximity controlled thermochromic fabric (a) before being actuated (b) actuated by a finger hovered over the proximity sensor (c) actuated by a hand held over the proximity sensor

The detection distance of the sensor was measured by placing a ruler next to the sensing conductor and moving the hand closer to the conductor in steps of 0.5 cm. It was found that the maximum detection distance of the device was 4 cm for a hand and 3 cm for a finger. The thermochromic device started changing colour within 1 second of the hand triggering the proximity sensor. It took the device 20 seconds to completely change from the initial black colour to yellow/transparent state. The device reverted back to its initial black state in 110 seconds after the hand hovering over the device was removed. The heater produced non-uniform heating which can be seen in figure 115 (b) as the non-uniform colour change.

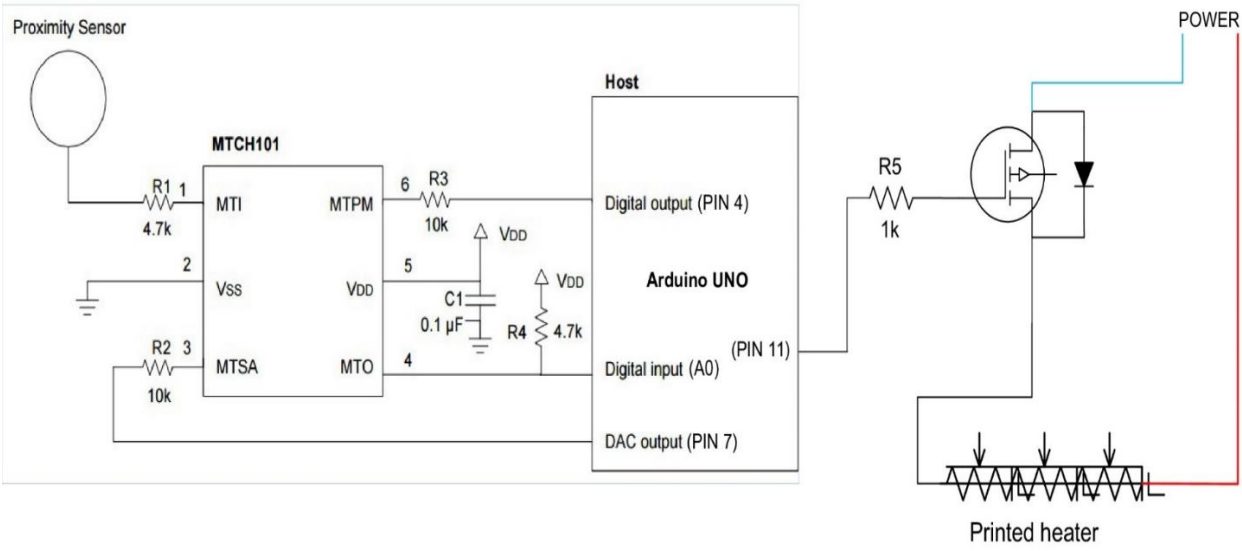

Figure 116: Circuit diagram of the driver circuit of proximity controlled thermochromic fabric

5.5.5 Summary and discussion

The four demonstrated devices of dispenser printed actively controlled thermochromic fabrics highlight the versatility and design freedom of the dispenser printing approach. These devices are quick to fabricate with small lead times, thin < 1 mm, flexible, low cost which make them suitable for a wide range of creative and sensory indicator applications such as posters, wall art, point of sales and fabric artworks. All the displays can be used as indicators for sensors either fabricated on fabric substrates or connected to a fabric substrate such as the proximity sensor. The demonstrated interactive smart fabric can find applications in interactive artworks and displays.

In terms of power requirements all four demonstrators can be operated using a battery. As a specific case, the shutter display requires the highest power compared to the other three demonstrators, 1.39 W. It can be actuated using a 3V battery for more than 25 hours which is determined by the service hour graph of the Duracell CR2 3V battery [101]. The actuation response time of the devices can be improved by applying a higher input power. Similarly, the refresh time can be reduced by using thermochromic inks with higher activation temperatures; a lower refresh time would improve the frequency of use of the displays.

5.6 Conclusions

This chapter has discussed the development of dispenser printable thermochromic inks, the fabrication and characterisation of the actively controlled dispenser printed thermochromic device on polyester cotton 65/35 blend, and has presented four demonstrator applications of the technology.

The ink development consisted of testing thirty eight thermochromic inks formulated using commercially available materials. The FB-20 ink formulation, consisting of 80% Fabink-IF-UV-1004 binder and 20% black ‘New colour chemical’ thermochromic powder was found to be the most suitable thermochromic ink. It is a UV curable formulation, a 90 µm print of the ink produced a black colour concentration between 90-100 %. The print was opaque before colour change and produced a peak transmittance value of 34% after colour change. It was shown that the ink was able to completely conceal and reveal all the colours in the visible spectrum as targeted. It was also shown that the FB-20 ink formulation can be changed to produce other colour changing effects such as a change from one colour to another and multiple colour changes. The addition of common colour pigments to the FB-20 formulation produced an ink which changed from one colour to another and the addition of

multiple thermochromic pigments to the FB-20 formulation produced an ink which exhibited multiple colour changes.

The fabrication of actively actuated thermochromic devices was detailed in terms of the device layout, inks, printing modes and settings. The layout where the thermochromic layer is printed over the heater layer is found to be the most suitable as it encapsulates and insulates the heater without the need to print an encapsulation layer. It is shown that the dispenser printed thermochromic technology is compatible with a range of substrates by printing the devices on a breathable commonly used polyester cotton 65/35 fabric, a PVC coated fabric and a traditional printed electronics substrate, Kapton. The flexibility of the devices was demonstrated by first bending the devices around a 6 mm radius and then actuating them. It was shown that multiple colour changing devices can be produced by layering single colour thermochromic inks. This approach reduced colour mixing between individual colours compared to printing a multiple colour changing ink. It was demonstrated that parts of single coloured thermochromic device can be sequentially actuated by printing multiple inks with different activation temperatures. These colour changing effects enhance the functionality of the devices by offering more features for creative smart textile applications such as wall art, fabric artworks and interactive displays.

The thermochromic devices were characterised in terms of actuation response times and the refresh times. It was found that the response time of the device can be controlled by the input electric power. A higher input power reduces the response time for a device although only up to a specific power beyond which the improvement in the response time is minor. The refresh times of the devices were found to be influenced by the operational temperatures of the thermochromic materials constituting the device. A device with a higher actuation temperature reverted back to its initial state faster than a device with a lower actuation temperature; the fabrication parameters and environmental conditions were the same for the tested devices. The refresh time influences the frequency of use of the device in an application.

Four demonstrator applications of the thermochromic devices on polyester cotton 65/35 were achieved in the form of a shutter display, a matrix display, a 7-segment display and an interactive colour changing fabric. These devices can used for creative applications such as posters, wallpapers and fabric artworks. They can also be linked to sensors in smart fabric systems for use as indicators as shown by the interactive colour changing fabrics. They can be scaled up or down to suit the requirements of an application. The four demonstrator devices can be powered using batteries which makes them portable. They are not suitable for applications which require fast refresh rates.

CHAPTER 6 CONCLUSIONS & FUTURE WORK

This chapter concludes the thesis by summarising the research carried out and discusses the impact of the results for the fabric applications of printed thermochromic technology. It also presents future work suggestions for the research work presented in this thesis.

6.1 Conclusions

The literature review showed that the actively actuated thermochromic devices on fabrics find applications in three areas; creative, sensory indicator and display applications. The state of the art devices have been fabricated using at least two different fabrication methods each of which requires the relevant knowledge, expertise and equipment. The thermochromic materials have been applied using screen printing or coating. The heaters have consisted of one of the following technologies; conductive yarns, conductive threads, printed circuit boards, flexible heat sink, Peltier semiconductors, coated and commercial heaters. It is shown that the state of the art thermochromic fabrics have one or more of the following four major limitations by virtue of the heater technology used.

- Inflexibility - PCB and Peltier semiconductor heaters
- Limited design freedom - conductive yarns, Peltier elements and coated heaters
- Poor integration with fabrics – PCB, Peltier semiconductors and commercial heaters
- Unreliability – conductive thread and flexible heat sink heaters.

A majority of the devices reported in the literature do not provide sufficient technical information to analyse the actuation technologies. This study has developed actively actuated all dispenser printed thermochromic devices which overcome the limitations of the existing methods by offering a combination of flexibility, design freedom, good integration with fabrics and reliability. It reduces the technical barriers by using dispenser printing as a sole method for fabrication and provides comprehensive technical information about fabrication and characterisation of the devices.

Dispenser printing is a direct-write process, novel for printing active and functional materials on fabrics. It offers features of custom patterning, rapid prototyping and ability to print multi-layered and multi-material structures which have been utilised for fabrication of thermochromic devices. It can print a broader range of ink viscosities (1 mPa.s – 100 Pa.s) than its competing technologies, inkjet printing (1 m - 20 mPa.s) and screen printing (1 – 10 Pa.s) which translates to a wider array of printable materials. It offers a greater design freedom than screen printing as it does not require a physical template for custom patterning of an ink.

The thermochromic devices are printed on polyester cotton 65/35 blend as the fabric substrate. It is a commonly used fabric with a high surface variation, it produced an Sa value of 34 µm and a peak to peak variation of 270 µm. The optimisation and printing of materials on polyester cotton 65/35 can be replicated on surfaces with similar or lower surface variation which allows the dispenser printed thermochromic technology to be used on a wide range of substrates.

It was experimentally demonstrated that a high surface variation of a substrate leads to geometrically inconsistent conductive tracks because the ink conforms to the surface structure. Geometrical inconsistency leads to non-uniform resistance distribution within the conductors and a high overall resistance. The resistance distribution of the printed conductors was analysed by passing electrical current through the conductor and taking a thermal image, which is a novel method; regions of higher resistance produced higher temperature. A dispenser printable method of overcoming the surface

variation by printing an interface layer on the fabric surface was investigated. Four interface inks, DuPont 5018, Electra EFV4/4965, Fabinks-IF-UV-1004 and FB-20, were found to be suitable for reducing the surface variation. The optimised dispenser printing of these inks reduced the fabric surface variation by more than 95%. It is shown that the improvement in surface variation translated to improvement in printed conductors as the resistivity of the conductive tracks on the interface surfaces was 90% lower than the tracks on fabric surface. The tracks printed directly on the fabric surface required three times more silver ink to produce similar resistance to the four interface surfaces and Kapton. Printing the interface layer between the fabric and the conductive tracks improved their performance and reduced the cost of fabrication by using less silver ink. Improved printing of conductive tracks produced more uniform heat distribution which is essential to printed heaters. In the wider context, printed tracks are fundamental to smart fabrics with electronic functionality as electrical interconnections, so improvement in track printing produces interconnections with lower resistance; lower resistance interconnects reduce the power loss in a device.

A COMSOL model of track heaters was developed as a tool to visualise and determine the output of heater configurations. Simulations of heater designs showed that a meander pattern with 1 mm track width and 1 mm track gap are the most suitable fabrication parameters as they provide a good compromise between the temperature variation in the heater output and the amount of ink used to fabricate a heater design. It was demonstrated that these fabrication parameters can be used to fabricate different shaped heat profiles such as triangular and circular profiles. The two commercially available inks used for dispenser printing heaters, DuPont 5000 silver ink and DuPont 7102 carbon ink offered limited resistivity options, 2.43×10^{-7} Ω.m and 1.10×10^{-3} Ω.m. For an application specific heater design, the resistivity of a conductive ink determines the resistance of a heater, which is an important factor in selection of a suitable power supply for the heater. Four custom conductive inks were formulated to increase the available resistivity range to 2.43×10^{-7} Ω.m – 1.11×10^{-03} Ω.m. Heaters were dispenser printed on both the polyester cotton 65/35 fabric and Kapton. Printed heaters produced a higher temperature variation than their equivalent simulated heaters due to variation in the thickness of the heater tracks. The thickness variation was caused by variation in the gap between the printing nozzle and the substrate. The current dispenser printer does not have a mechanism to measure and maintain the nozzle height which a limitation of the printer. It was shown that parts of a conductive track can be selectively heated by creating regions of higher resistance. Selective heating can be produced by either varying the physical dimensions of a single material heater or by printing a heater using multiple materials of different resistivity. Selective heating allows a heater to share electrical interconnections with multiple components without heating the interconnections.

The dispenser printed track heaters offer complete design freedom as all the fabrication parameters of a track heater can be varied such as the size, shape, pattern and the resistivity of the conductive inks. The heaters are flexible and printed directly on the fabric and therefore overcome the limitations of the heating technologies for thermochromic fabrics reported in the literature. In a wider context, fabric heaters find applications in medical, garments and automotive industry. The COMSOL model and the fabrication details of the dispenser printed heaters can be used to fabricate heaters for the multiple application areas. The development of heaters reported in this study including the model adds new information to the field of printed heaters.

A UV curable thermochromic ink which turns from black to transparent was achieved. The ink consists of 80% Fabink-IF-UV-1004 binder and 20% black ‘New colour chemical’ thermochromic powder. A 90 µm print of the ink produced a black colour concentration of 90-100 % before colour change and a peak transmittance value of 34% after colour change. The print was able to completely conceal and reveal all the colours of the visible spectrum. It was shown that addition of a common coloured

pigment to the FB-20 ink formulation achieved a change from one colour to another and the addition of multiple thermochromic pigments produced multiple colour changes. These colour changing effects increase the options available for thermochromic fabric applications especially creative applications.

The actively actuated thermochromic devices were fabricated on three different substrates, polyester cotton 65/35 fabric, a PVC coated fabric and Kapton, which shows that the dispenser printed thermochromic technology is not limited to fabrics. The devices were bent around a 6 mm radius and actuated to demonstrate their flexibility. The thermochromic devices on fabrics were characterised in terms of actuation response time and refresh time. It is shown that increasing the input power to a device reduces its actuation response time up to a certain power after which the change in response time is minor. The activation temperature of thermochromic pigments affects the refresh time of a device; higher activation temperature devices produced lower refresh times. Refresh time influences the frequency of use a thermochromic device. Multiple colour changing devices achieved by printing multiple single coloured thermochromic inks was demonstrated. This approach produced less colour mixing than the approach of printing a multi-colour changing ink. A thermochromic layer can be sequentially actuated by printing the layer using single coloured inks with different actuation temperatures. A shutter display, a 7-segment display, a matrix display and an interactive smart fabric are the four demonstrator applications of the dispenser printed thermochromic devices which show that the technology can be used to fabricate complicated thermochromic systems. The demonstrator applications show also that dispenser printed thermochromic devices can be fabricated in different shapes and sizes to suit an application. The interactive smart fabric, shutter and matrix display can be used in all three application areas of thermochromic devices because they can be used for communicating both artistic expressions and data. Their potential applications include fabric artworks, point of sale displays, information posters and a fabric sensor controlled display. The 7-segment display can be used as a sensory indicator to communicate numerical information for a smart fabric system incorporating sensors such as proximity and strain sensors.

The dispenser printed thermochromic technology is less compatible with applications which require high refresh rates due to temperature dependent actuation. The process of heating the thermochromic devices causes a time delay; it is shown that this time delay can be reduced by increasing the input power however after a certain input power the change in time delay is very small. The re-colouration of a thermochromic device also introduces a time delay. The re-colouration is a passive process dependent on the temperature gradient between the environment and the device. These time delays cannot be entirely avoided as they are inherent to the thermochromic technology. They limit the frequency of use of a thermochromic device. As the thermochromic technology is temperature dependent, a specific thermochromic device may not be suitable for all weather conditions and environments. A change in ambient temperature will cause a shift in power requirements, actuation response and refresh times of a thermochromic device. If the ambient temperature is higher than the activation temperature of a thermochromic device, it will maintain an actuated state and will not be able to produce colour change.

The dispenser printed thermochromic technology offers complete design freedom as the thermochromic materials and heater can be laid out in any pattern on a wide range of substrates. It is a versatile technology that produces flexible devices overcoming the limitations of the existing thermochromic devices. The development of dispenser printed thermochromic technology offers a comprehensive guideline for the adoption of this technology in fabric applications. It has reduced technical barriers to the use of thermochromic technology by reducing the fabrication requirements and providing detailed technical knowledge. The dispenser printed thermochromic technology will

improve the existing applications and is expected to pave way for a wider adoption of thermochromic technology in fabrics.

6.2 Future work

- Improvement in the dispenser printer hardware and software:
  A limitation of the current dispenser printer is that it cannot measure and maintain the gap between the printing nozzle and the substrate. This leads to temperature variation in the heater output. The printer can be improved by incorporating a displacement sensor in the printer setup which is compatible with a range of substrates including fabrics. This will improve the heater output and the performance of thermochromic fabrics.
  Another limitation of the printer is that it cannot print patterns whilst continuously dispensing an ink. An upgrade of the printer stages and software to incorporate continuous pattern dispensing can significantly reduce the time it takes the printer to fabricate the thermochromic devices.

- Fabrication and characterisation of the three layouts of thermochromic devices:
  The three layouts of dispenser printed thermochromic devices can be further analysed by fabricating and characterising them. They can be compared with each other in terms of power requirements for achieving similar performance, actuation response times with fixed input power, refresh times in the same environment and power efficiency. It will provide a better insight into the differences between the three layouts and experimentally validate the comparison made in this work.

- Liquid crystal thermochromic materials:
  Thermochromic liquid crystals are able to produce all the colours in the visible spectrum in response to a temperature change. They offer an alternative option to the commonly available leuco dyes. Liquid crystal materials can be tested for fabricating thermochromic devices. They can achieve multiple colour changes and multiple colours in a device. An important requirement for precise colour changes using liquid crystals is to have a uniform heater which would require improvement in the current dispenser printer.

- Transparent conductive inks:
  Transparent conductive inks can be explored as a potential option for fabricating heaters for thermochromic devices. This will offer the advantage of reducing the impact of the heaters on the visual output of devices.

References

1. R M Christie, S Robertson, S Taylor. (2007). Design Concepts for a Temperature-sensitive Environment Using Thermochromic Colour Change. *Colour: Design and Creativity*. 5, 1-11.

2. Berglin, Lena. (2013). *Smart Textiles and Wearable Technology - A study of smart textiles in fashion and clothing*. A report within the Baltic Fashion Project, published by the Swedish School of Textiles, University of Borås.

3. Cherenack, K., and van Pieterson, L. (2012). Smart textiles: challenges and opportunities. *Journal of Applied Physics*, *112*(9), 091301.

4. Magenes, G., Curone, D., Caldani, L., and Secco, E. L. (2010, September). Fire fighters and rescuers monitoring through wearable sensors: The ProeTEX project. In *Conf Proc IEEE Eng Med Biol Soc* (pp. 3594-3597).

5. VivoSense Life shirt system smart fabric - http://vivonoetics.com/products/sensors/lifeshirt/. last accessed on 09/10/2017.

6. Vieroth, R., Loher, T., Seckel, M., Dils, C., Kallmayer, C., Ostmann, A., and Reichl, H. (2009, September). Stretchable circuit board technology and application. In *Wearable Computers, 2009. ISWC'09. International Symposium on* (pp. 33-36). IEEE.

7. Schwarz, A., Van Langenhove, L., Guermonprez, P., and Deguillemont, D. (2010). A roadmap on smart textiles. *Textile progress*, *42*(2), 99-180.

8. Bamfield, P., and Hutchings, M. G. (Eds.). (2010). *Chromic phenomena: technological applications of colour chemistry*. Royal Society of Chemistry.

9. Day, J. H. (1968). Thermochromism of inorganic compounds. *Chemical Reviews*, *68*(6), 649-657.

10. Day, J. H. (1963). Thermochromism. *Chemical Reviews*, *63*(1), 65-80.

11. Robertson, S. (2011). *An investigation of the design potential of thermochromic textiles used with electronic heat-profiling circuitry* PhD, Heriot-Watt University.

12. Peiris, R. L. (2013). *Development of an Integrated, Programmable, Non-Emissive Textile Display Material*. PhD. National University of Singapore.

13. Aitken, D., Burkinshaw, S. M., Griffiths, J., and Towns, A. D. (1996). Textile applications of thermochromic systems. *Review of Progress in Coloration and Related Topics*, *26*(1), 1-8.

14. MacLaren, D. C., and White, M. A. (2003). Competition between dye–developer and solvent–developer interactions in a reversible thermochromic system. *Journal of Materials Chemistry*, *13*(7), 1701-1704.

15. MacLaren, D. C., and White, M. A. (2003). Dye–developer interactions in the crystal violet lactone–lauryl gallate binary system: implications for thermochromism. *Journal of Materials Chemistry*, *13*(7), 1695-1700.

16. Olikrom smart pigments - supplier for thermochromic pigments - http://olikrom.com/en/olikrom-products/thermochromic-pigments-ink-paint-heat-sensitive/ last accessed on 24/07/2017.

17. Temperature hysteresis graph of a commercial thermochromic pigment - http://www.tmchallcrest.com/how-it-works/thermochromic last accessed on 24/07/2017.

18. Kulčar, R., Friškovec, M., Gunde, M. K., and Knešaurek, N. (2011). Dynamic colorimetric properties of mixed thermochromic printing inks. *Coloration Technology*, *127*(6), 411-417.

19. Parsley, M. (1991). The Hallcrest handbook of thermochromic liquid crystal technology. *Hallcrest, Glenview*.

20. Information acquired through private correspondence with LCR Hallcrest Ltd.

21. Thermometry industrial applications of thermochromic pigments - http://www.lcrhallcrest.com/pdfs/labels-reversible/Literature/Labels-RE-Digitemp-SalesLit.pdf last accessed on 08/08/2017.

22. Final Report, Sunlight Responsive Thermochromic Window System, Pleotint LLC, 2006, www.osti.gov/energycitations/servlets/purl/894091-FRpWuI/894091.PDF. last accessed on 08/08/2017.

23. Colour changing products ltd. – supplier of thermochromic materials - http://www.colourchanging.co.uk/ last accessed on 08/08/2017.

24. Heat-Activated Paint for Colour-Changing Interior Designs - http://dornob.com/heat-actived-paint-for-color-changing-interior-designs/ last accessed on 08/08/2017.

25. Global Technacolour commercially available t-shirts - https://www.amazon.co.uk/Global-Technacolour-Hypercolour-Colour-Change/dp/B00AE8U4ZYlast accessed on 08/08/2017.

26. Ferrara, M., and Bengisu, M. (2014). *Materials that Change Color: Smart Materials, Intelligent Design*. Springer.

27. Berzowska, J. (2004, August). Very slowly animating textiles: shimmering flower. In *ACM SIGGRAPH 2004 Sketches* (p. 34). ACM.

28. Worbin, L. (2010). *Designing dynamic textile patterns*. PhD. Chalmers University of Technology.

29. Blip thermochromic fabric artwork by Maggie Orth - http://www.maggieorth.com/art_Blip.html last accessed on 22/08/2017.

30. Landin, H., and Worbin, L. (2005). The Fabrication Bag An Accessory To A Mobile Phone. *Ambience 05*.

31. Teh, J. K. S., Cheok, A. D., Peiris, R. L., Choi, Y., Thuong, V., and Lai, S. (2008, June). Huggy Pajama: a mobile parent and child hugging communication system. In *Proceedings of the 7th international conference on Interaction design and children* (pp. 250-257). ACM.

32. Ferrara, M., and Bengisu, M. (2014). Intelligent design with chromogenic materials. *JAIC-Journal of the International Colour Association*, *13*.

33. Peiris, R. L., Cheok, A. D., Teh, J. K. S., Fernando, O. N. N., Yingqian, W., Lim, A. and Tharakan, M. (2009, August). AmbiKraf: an embedded non-emissive and fast changing wearable display. In *ACM SIGGRAPH 2009 Emerging Technologies* (p. 1). ACM.

34. Wakita, A., and Shibutani, M. (2006, June). Mosaic textile: wearable ambient display with non-emissive color-changing modules. In *Proceedings of the 2006 ACM SIGCHI international conference on Advances in computer entertainment technology* (p. 48). ACM.

35. Electronically controllable, visually dynamic textile, fabric or flexible substrate patent http://www.google.com/patents/US20030224155 last accessed on 18/08/2017.

36. Berzowska, J., and Bromley, M. (2007). Soft computation through conductive textiles. In *Proceedings of the International Foundation of Fashion Technology Institutes Conference* (pp. 12-15).

37. Chen, H. J., and Huang, L. H. (2015). An investigation of the design potential of thermochromic home textiles used with electric heating techniques. *Mathematical Problems in Engineering*, *2015*.

38. Berzowska, J. (2005, April). Memory rich clothing: second skins that communicate physical memory. In *Proceedings of the 5th conference on Creativity and cognition* (pp. 32-40). ACM.

39. Huang, G., Liu, L., Wang, R., Zhang, J., Sun, X., and Peng, H. (2016). Smart color-changing textile with high contrast based on a single-sided conductive fabric. *Journal of Materials Chemistry C*, *4*(32), 7589-7594.

40. Electronics fluid dispensing equipment article by Fishman Corporation - http://www.fishmancorp.com/solutions/electronic/ last accessed on 03/08/2017.

41. Hon, K. K. B., Li, L., and Hutchings, I. M. (2008). Direct writing technology—advances and developments. *CIRP Annals-Manufacturing Technology*, *57*(2), 601-620.

42. Ho, C. C., Steingart, D., Salminent, J., Sin, W., Rantala, T., Evans, J., and Wright, P. (2006). Dispenser printed electrochemical capacitors for power management of millimeter scale lithium ion polymer microbatteries for wireless sensors. In *6th international workshop on micro and nanotechnology for power generation and energy conversion applications (PowerMEMS 2006), Berkeley, CA,* 219-222.

43. Steingart, D., Ho, C. C., Salminen, J., Evans, J. W., and Wright, P. K. (2007). Dispenser printing of solid polymer-ionic liquid electrolytes for lithium ion cells. In *Polymers and Adhesives in Microelectronics and Photonics, 2007. Polytronic 2007, IEEE,* 261-264.

44. Ho, C. C., Evans, J. W., and Wright, P. K. (2010). Direct write dispenser printing of a zinc microbattery with an ionic liquid gel electrolyte. *Journal of Micromechanics and Microengineering*, *20*(10), 104009.

45. Li, B., Clark, P. A., and Church, K. H. (2007, January). Robust direct-write dispensing tool and solutions for micro/meso-scale manufacturing and packaging. In *ASME 2007 International*

Manufacturing Science And Engineering Conference. American Society of Mechanical Engineers. 715-721.

46. Chen, A., Madan, D., Wright, P. K., and Evans, J. W. (2011). Dispenser-printed planar thick-film thermoelectric energy generators. *Journal of Micromechanics and Microengineering*, *21*(10), 104006.

47. Wang, Z., Chen, A., Winslow, R., Madan, D., Juang, R. C., Nill, M., Evans, J.W. and Wright, P. K. (2012). Integration of dispenser-printed ultra-low-voltage thermoelectric and energy storage devices. *Journal of Micromechanics and Microengineering*, *22*(9), 094001.

48. Wright, P. K., Dornfeld, D. A., Chen, A., Ho, C. C., and Evans, J. W. (2010). Dispenser printing for prototyping microscale devices. *Transactions of NAMRI/SME*, *38*.

49. Miller, L. M., Chen, A., Wright, P. K., and Evans, J. (2010). Resonance frequency modification of MEMS vibration energy harvesters using dispenser-printed proof mass. *Technical Digest PowerMEMS 2010 (Leuven, Belgium, 1–3 December)*, 411-4.

50. Leland, E. S., Wright, P. K., and White, R. M. (2009). A MEMS AC current sensor for residential and commercial electricity end-use monitoring. *Journal of Micromechanics and Microengineering*, *19*(9), 094018.

51. Sun, K., Wei, T. S., Ahn, B. Y., Seo, J. Y., Dillon, S. J., and Lewis, J. A. (2013). 3D Printing of Interdigitated Li-Ion Microbattery Architectures. *Advanced Materials*, *25*(33), 4539-4543.

52. Ahn, B. Y., Walker, S. B., Slimmer, S. C., Russo, A., Gupta, A., Kranz, S., and Lewis, J. A. (2011). Panar and three-dimensional printing of conductive inks. *Journal of visualized experiments: JoVE*, (58).

53. Ahn, B. Y., Lorang, D. J., and Lewis, J. A. (2011). Transparent conductive grids via direct writing of silver nanoparticle inks. *Nanoscale*, *3*(7), 2700-2702.

54. YeopáAhn, B. (2010). Direct-write assembly of microperiodic planar and spanning ITO microelectrodes. *Chemical Communications*, *46*(38), 7118-7120.

55. Adams, J. J., Duoss, E. B., Malkowski, T. F., Motala, M. J., Ahn, B. Y., Nuzzo, R. G., and Lewis, J. A. (2011). Conformal Printing of Electrically Small Antennas on Three-Dimensional Surfaces. *Advanced Materials*, *23*(11), 1335-1340.

56. Sun, L., Parker, S. T., Syoji, D., Wang, X., Lewis, J. A., and Kaplan, D. L. (2012). Direct-Write Assembly of 3D Silk/Hydroxyapatite Scaffolds for Bone Co-Cultures. *Advanced healthcare materials*, *1*(6), 729-735.

57. Muth, J. T., Vogt, D. M., Truby, R. L., Mengüç, Y., Kolesky, D. B., Wood, R. J., and Lewis, J. A. (2014). Embedded 3D printing of strain sensors within highly stretchable elastomers. *Advanced Materials*, *26*(36), 6307-6312.

58. Compton, B. G., and Lewis, J. A. (2014). 3D-Printing of Lightweight Cellular Composites. *Advanced Materials*, *26*(34), 5930-5935.

59. Hitachi Industiral Continuous Inkjet Printing

http://www.hitachi-america.us/ice/inkjetprinters/products/principles/ last accessed on 03/08/2017.

60. Hakola, L. (2005). Benefits of inkjet printing for printed electronics. Pira Printed Electronics London.

61. Parashkov, R., Becker, E., Riedl, T., Johannes, H., and Kowalsky, W. (2005). Large area electronics using printing methods. *Proceedings of the IEEE*, *93*(7), 1321-1329.

62. Sridhar.A, Blaudeck.T, Baumann.R. Inkjet Printing as a Key Enabling Technology for Printed Electronics. Material Matters Vol. 6 Article 1.

63. Lewis, J. A., and Gratson, G. M. (2004). Direct writing in three dimensions. *Materials Today*, *7*(7), 32-39.

64. Industrial screen printing - http://www.gwent.org/gem_screen_printing.html#principle last accessed on 03/08/2017

65. Wei, Y., Torah, R., Li, Y., and Tudor, J. (2015, April). Dispenser printed proximity sensor on fabric for creative smart fabric applications. In *Design, Test, Integration and Packaging of MEMS/MOEMS (DTIP), 2015 Symposium on* (pp. 1-4). IEEE.

66. Dispsner printing stages -SGSP Series http://www.global-optosigma.com/en/page_pdf/SGSP26-(XY).pdf last accessed on 03/08/2017.

67. Nordson Ultimus V high precision dispenser manual - http://www.nordson.com/en/divisions/efd/products/fluid-dispensing-systems/ultimus-v-high-precision-dispenser last accessed on 03/08/2017.

68. Li, B., Clark, P. A., and Church, K. H. (2007, January). Robust direct-write dispensing tool and solutions for micro/meso-scale manufacturing and packaging. In *ASME 2007 International Manufacturing Science And Engineering Conference* (pp. 715-721). American Society of Mechanical Engineers.

69. Datasheet LM 10 micro laser displacement sensor. https://www.panasonic-electric-works.com/pew/es/downloads/ds_lm10_en.pdf last accessed 03/08/2017.

70. Alicona Infinite focus IFM Manual, IFM 2.1.5 EN 30.06.2008. Manual obtained through private correspondence.

71. Tafesse, M. (2015). Surface Metrology and the National Science Foundation (Doctoral dissertation, Worcester Polytechnic Institute).

72. Bollero, A., Andrés, M., Garcia, C., Abajo, J. D., and Gutiérrez, M. T. (2009). Morphological, electrical and optical properties of sputtered Mo thin films on flexible substrates. *Physica status solidi. A, Applied research*, *206*(3), 540.

73. Karaguzel, B., Merritt, C. R., Kang, T., Wilson, J. M., Nagle, H. T., Grant, E., and Pourdeyhimi, B. (2009). Flexible, durable printed electrical circuits. *The Journal of The Textile Institute*, *100*(1), 1-9.

74. Torah, R., Yang, Kai, Beeby, S.P. and Tudor, M.J. (2012) Screen-printed multilayer meander heater on polyester cotton At *88th Textile Institute World Conference, Malaysia*. *15 - 17 May 2012.*

75. Komolafe, A. O., Torah, R. N., Yang, K., Tudor, J., and Beeby, S. P. (2015). Durability of screen printed electrical interconnections on woven textiles. In *Electronic Components and Technology Conference (ECTC), 2015 IEEE 65th* (pp. 1142-1147). IEEE.

76. Suh, M., Carroll, K. E., Grant, E., and Oxenham, W. (2013). Effect of fabric substrate and coating material on the quality of conductive printing. *Journal of the Textile Institute*, *104*(2), 213-222.

77. MICROFLEX EU funded research project - http://microflex.ecs.soton.ac.uk/home.html last accessed on 03/08/2017.

78. Poboroniuc, M. S., Curteza, A., Cretu, V., and Macovei, L. (2014, October). Designing wearable textile structures with embeded conductive yarns and testing their heating properties. In *Electrical and Power Engineering (EPE), 2014 International Conference and Exposition on* (pp. 778-783). IEEE.

79. Hao, L., Yi, Z., Li, C., Li, X., Yuxiu, W., and Yan, G. (2012). Development and characterization of flexible heating fabric based on conductive filaments. *Measurement*, *45*(7), 1855-1865.

80. He, X., He, R., Lan, Q., Wu, W., Duan, F., Xiao, J. and Liu, J. (2017). Screen-Printed Fabrication of PEDOT: PSS/Silver Nanowire Composite Films for Transparent Heaters. *Materials*, *10*(3), 220.

81. Colour changing products thermochromic ink starter pack - https://colourchanging.co.uk/collections/thermochromic/products/colour-changing-ink-paint-thermochromic-ink-paint-trial-beginner-pack-can-be-used-on-paper-board-textiles last accessed on 09/10/2017.

82. Thermochromic pigments supplier New Colour Chemical - http://newcolorchem.com/default.php?action=pro&fl=Thermochromic^^pigment last accessed on 09/10/2017.

83. Clear Binder (AS 100) technical data sheet obtained through private correspondence.

84. AP Screen/Block printing system data sheet obtained through private correspondence.

85. Chromazone Textile Binder data sheet obtained through private correspondence.

86. Screentec Tprint T2000 Transparent Base datasheet - http://www.schleiper.com/onlinecatalogue/series/8393-screentec-tprint-t2000-transparant-medium?lang=nl last accessed on 09/10/2017.

87. Speedball Transparent Base data sheet obtained through private correspondence.

88. Chromotex CR data sheet obtained through private correspondence.

89 . Thermochromic Ink AQ CR and UV AQ CR data sheet obtained through private correspondence.

90. Zuperpaint - Thermochromic temperature colour change paint - http://glowinthedarkshop.co.uk/thermochromic/ last accessed on 09/10/2017.

91. Transparent ITO Coated Film http://www.gwent.org/gem_data_sheets/polymer_systems_products/electroluminescent_display_materials/ito_film_f2071018d1.pdf last accessed on 09/10/2017.

92. Yang, K., Torah, R., Wei, Y., Beeby, S., and Tudor, J. (2013). Waterproof and durable screen printed silver conductive tracks on textiles. *Textile Research Journal*, *83*(19), 2023-2031.

93. Dry fabric pigments - http://www.georgeweil.com/ProductGroup.aspx?Menu=1&Level1=81&Level2=1190&Level3=0&PID=6733 last accessed on 09/10/2017.

94. Heo, K. C., Son, P. K., Sohn, Y., Yi, J., Kwon, J. H., and Gwag, J. S. (2013). A Reflective Display Based on Thermochromic Pigment. *Molecular Crystals and Liquid Crystals*, *584*(1), 87-93.

95. Siegel, A. C., Phillips, S. T., Wiley, B. J., and Whitesides, G. M. (2009). Thin, lightweight, foldable thermochromic displays on paper. *Lab on a Chip*, *9*(19), 2775-2781.

96. Shin, H., Yoon, B., Park, I. S., and Kim, J. M. (2014). An electrothermochromic paper display based on colorimetrically reversible polydiacetylenes. *Nanotechnology*, *25*(9), 094011.

97. Peiris, R. L., Tharakan, M. J., Fernando, N., and Chrok, A. D. (2011, October). Ambikraf: A nonemissive fabric display for fast changing textile animation. In *Embedded and Ubiquitous Computing (EUC), 2011 IFIP 9th International Conference on* (pp. 221-228). IEEE.

98. Southee, D. J., Hay, G. I., Evans, P. S., & Harrison, D. J. (2008). Flexible dot-matrix display manufacture by offset lithography. *Proceedings of the Institution of Mechanical Engineers, Part B: Journal of Engineering Manufacture*, *222*(8), 943-948.

99. Scola fabric paint - http://www.rapidonline.com/education/scola-fabric-paint-standard-colours-6-x-150ml-bottles-06-8554 last accessed on 09/10/2017.

100. Wei, Y., Torah, R., Li, Y., and Tudor, J. (2016). Dispenser printed capacitive proximity sensor on fabric for applications in the creative industries. *Sensors and Actuators A: Physical*, *247*, 239-246.

101. Duracell 3 V battery datasheet - http://docs-europe.electrocomponents.com/webdocs/1265/0900766b81265659.pdf last accessed on 09/10/2017.